2021

# Analysis Of Host Factors Involved In Regulating Hiv-1-Induced Syncytium Formation

Emily Elizabeth Whitaker
*University of Vermont*

# ANALYSIS OF HOST FACTORS INVOLVED IN REGULATING HIV-1-INDUCED SYNCYTIUM FORMATION

A Dissertation Presented

by

Emily E. Whitaker

to

The Faculty of the Graduate College

Of

The University of Vermont

In Partial Fulfilment of the Requirements
for the Degree of Doctor of Philosophy
Specializing in Cellular, Molecular and Biomedical Sciences

October, 2021

Defense Date: August 16th, 2021
Dissertation Examination Committee:

Markus Thali, Ph.D., Advisor
Dimitry N. Krementsov, Ph.D., Chairperson
Jason W. Botten, Ph.D.
Jonathan E. Boyson, Ph.D.
Julie A. Dragon, Ph.D.
Cynthia J. Forehand, Ph.D., Dean of the Graduate College

## ABSTRACT

Human Immunodeficiency Virus type 1 (HIV-1) is a retrovirus and the causative agent of Acquired Immunodeficiency Syndrome (AIDS). HIV-1 can spread through multiple modes of transmission including cell-to-cell transmission between $CD4^+$ T cells at a transient junction known as the virological synapse (VS). The VS forms upon HIV-1 Envelope (Env) on the surface of an infected (producer) cell binding CD4 on an uninfected (target) cell. While the VS typically resolves with complete cell separation and transfer of virus particles, Env can occasionally facilitate cell-cell fusion at this site, forming a multinucleated infected cell (syncytium). Excessive syncytium formation is prevented by viral and host factors, though this subpopulation of infected cells can still comprise ~20% of all infected cells *in vivo*. T cell-based syncytia detected *in vivo* are unique from mononucleated infected cells as they contain 2-4 nuclei, can have an elongated morphology, and appear highly motile. Despite such significant presence of syncytia, little is known about how these multinucleated infected entities contribute to HIV-1 spread and pathogenesis.

During cell-to-cell transmission at the VS, viral and host factors are enriched at this site to support virus spread (reviewed in Chapter 2). This thesis focused on fusion inhibitory factors HIV-1 Gag and several host proteins, including tetraspanins, ezrin, and EWI-2. We determined that EWI-2 is recruited specifically to the producer cell side of the VS (the presynapse) where it inhibits HIV-1-induced cell-cell fusion in a dose-dependent manner (Chapter 3). Although both EWI-2 and tetraspanins are typically downregulated upon infection, both tetraspanin CD81 and EWI-2 surface levels are partially restored on HIV-1-induced $CD4^+$ primary T cell-based syncytia compared to mononucleated infected cells.

We sought to determine whether target cells influence the surface profile upon fusion and whether the altered protein levels are maintained for the lifetime of a syncytium (Chapter 4). We demonstrated that EWI-2 surface levels on syncytia correlate with levels of the target cell population, suggesting that EWI-2 brought along by target cells at least partially restores surface expression in syncytia. Further, we determined that newly formed, "young" syncytia, have higher levels of EWI-2 than older ones, suggesting that downregulation of EWI-2 continues in syncytia. We expect that higher levels of EWI-2 on young syncytia will render them less susceptible to continued cell-cell fusion than mononucleated infected cells and may also reduce virus particle infectivity. This will be tested by analysis of a purified syncytia population to measure fusogenicity and particle infectivity relative to fusogenicity and particle infectivity of mononucleated infected cells. Those data will be included in a future manuscript.

Collectively, the work presented in this dissertation has furthered our understanding of HIV-1-induced cell-cell fusion regulation and allowed us to characterize distinct differences in protein expression between syncytia and mononucleated infected cells. These findings open the door to future investigations aimed at understanding how syncytia contribute to virus transmission and pathogenesis.

## CITATIONS

Material from this dissertation has been published in the following form:

Whitaker, E.E., Matheson, N.J., Perlee, S., Munson, P.B., Symeonides, M., Thali, M.. (2019). EWI-2 Inhibits Cell-Cell Fusion at the HIV-1 Virological Presynapse. Viruses, 11, 1082; doi:10.3390/v11121082.

## ACKNOWLEDGEMENTS

I want to thank my husband, friends, family, colleagues, and mentors for all of their help.

To my husband, friends, and family – You've all supported me, lifted my spirits, and believed in me when I wasn't sure I was cut out for graduate school. Many of you visited me in Vermont, and even came to see the Thali lab space – which meant the world to me. A special shout out to my parents and brother - you shaped who I am today and were always great company on the phone during my walks to and from lab. To my husband Charm - Thank you for cheering me on every step of the way, I'm so happy to be jumping into this next stage of our lives together!

There are many people at UVM who enriched my experience during graduate school. You'll be missed, and I hope our paths cross again in the future. A big thank you to the Ward lab for frequent troubleshooting advice and for being great lab neighbors and friends. To all of the members of the Thali lab I've had a chance to work with - Thank you for collaborating on ideas, helping out in a pinch, and making the lab a fun place to be. To our postdoc Mel, thank you for training me in the lab, brainstorming, and always knowing where to find any hard-to-locate item in the lab. To the students I've mentored (Megna, Danielle, Ethan, and Elise), I was inspired by your enthusiasm, curiosity, and perseverance. Thank you for learning alongside me through journal clubs, new experiments, and weekly meetings. I'm grateful to have worked with you all and I'll take the lessons I've learned while working with each of you with me for years to come.

A huge thank you to my thesis committee and my instructors at UVM You've all challenged me to be a better scientist, educator, and to think more broadly when I get a bit lost in the weeds. The members of my committee helped me immensely by sharing their perspectives, providing advice and guidance, and instilling a stronger sense of confidence in myself and my work. To Drs. Janet Murray and Rebecca Guy, you were both outstanding examples of the type of educator I aspire to be. Thank you for taking extra time to help me grow as a teacher.

To my advisor Markus - thank you for always keeping an open door to facilitate frequent exchange of ideas or catch-up chats, for fostering my independence, and for always considering the big picture of the questions we're tackling. You have been a kind and patient mentor and I have greatly appreciated your support through the years. I'm sure we'll stay in touch – and hopefully have a chance to grab a cup of coffee together in the future!

-Emily

# TABLE OF CONTENTS

## LIST OF FIGURES

# CHAPTER 1 : INTRODUCTION

## 1.1. Abstract

Human immunodeficiency virus type 1 (HIV-1) has infected millions of individuals around the world and is the causative agent of acquired immunodeficiency syndrome (AIDS). Given that we don't yet have a cure for this virus, HIV-1 infection is a lifelong condition for an individual. Continued investigation into how this virus replicates and spreads may uncover novel therapeutic targets to help manage or even eliminate the virus. HIV-1 can spread through multiple modes of transmission, including cell-to-cell transmission at the virological synapse (VS). The work presented in this dissertation focuses on fusion regulation at the VS during cell-to-cell transmission of HIV-1. Further, our data indicate that multinucleated infected cells (syncytia), which form upon HIV-1-induced cell-cell fusion, have unique characteristics compared to mononucleated infected cells. Should future investigations find that syncytia differentially contribute to virus spread, these infected entities could be an intriguing target for novel therapeutic development.

## 1.2. HIV-1 Origins & Disease Progression

Human immunodeficiency virus types 1 and 2 (HIV-1 and HIV-2) are primate lentiviruses and the causative agents of acquired immunodeficiency syndrome (AIDS).

HIV-1 strains comprise the majority of infections around the world, with group M being responsible for the HIV-1 pandemic and the focus of this dissertation. HIV-1 M

(hereafter referred to only as "HIV-1") originated as a result of zoonotic transmission of a strain of chimpanzee (cpz) Simian Immunodeficiency Virus ($SIV_{cpz}$) carried by the chimpanzee subspecies *Pan troglodytes troglodytes* ($SIV_{PTT}$) [1,2] (and reviewed in [3]). While some primate lentiviruses, such as natural SIV infections in sooty mangabeys and African green monkeys ($SIV_{smm}$ and $SIV_{agm}$, respectively) are non-pathogenic in their natural hosts, $SIV_{cpz}$ and HIV-1 can be pathogenic in humans and chimpanzees and can lead to the development of AIDS [4-7].

HIV-1 primarily infects $CD4^+$ T cells and can be transmitted to a new host upon mucosal or percutaneous exposure to virus-containing bodily fluids. During virus transmission to a new host, an individual is exposed to numerous virus variants from the infected donor (reviewed in [8-10]). Shortly after exposure, there is a bottleneck where one virus variant emerges as the predominant virus present in the new host known as the Transmitted/Founder (T/F) virus [8-10]. During the early phase of infection, the virus replicates exponentially (until reaching peak viraemia ~3-4 weeks after infection) , spreads systemically, and establishes a reservoir of latently infected cells (reviewed in [11-14]). During this period, the host generates an immune response against the virus that helps control viraemia, though modulation of the infected cell by viral accessory proteins and rapid virus evolution can help infected cells and free virus particles evade immune detection [11,15]. Chronic infection is associated with a period of clinical latency where the infected individual appears asymptomatic but is still producing virus [13]. Over the course of disease progression, in untreated individuals, HIV-1 infection leads to chronic immune activation and exhaustion as well as severe depletion of CD4+ T cells, thus

impairing the host's ability to counteract secondary infections and eventually leading to the development of AIDS [16,17].

Since the beginning of the HIV-1 pandemic, an enormous amount of work has been done to investigate how this virus replicates and spreads as well as to understand the host response to infection. Not only do we now have a better understanding of viral replication and transmission, but this work has also led to the development of therapeutics and shed light on potential strategies to eliminate infection within a host. Continued investigation into the biology of HIV-1, modes of virus transmission, and the heterogeneity of the infected cell population could allow for the development of novel therapeutics and/or treatment strategies to manage, and perhaps even eliminate, virus within a host.

### 1.3. HIV-1 Replication Cycle

A mature virus particle is composed of a host-derived lipid bilayer/envelope that is decorated by the viral Envelope (Env) glycoprotein (a trimer of non-covalently associated Env surface and transmembrane subunit, gp120/gp41, heterodimers [18]) (reviewed in [19]) and contains Matrix (MA) protein associated with the inner leaflet of the lipid bilayer (for a review and schematic representation of structural protein distribution in viral particles, see [20] Figure 3). Within the particle is a cone-shaped core made up of viral Capsid (CA) protein lattice that surrounds 2 copies of the positive-sense, single strand RNA genome bound by the viral Nucleocapsid (NC) protein [20]. Virus-encoded proteins also present in the core include Reverse transcriptase (RT), Integrase (IN), Vif, and Vpr [21-25].

When a free mature virus particle that encounters an uninfected target cell it can initiate a new round of infection upon Env-mediated fusion with the target cell. The Env surface subunit gp120 contains the receptor (CD4) and co-receptor (either chemokine receptor CCR5 or CXCR4) binding domains [26]. Sequential gp120 binding to CD4 and then the coreceptor induces conformational changes in Env necessary for exposure of the Env fusion peptide (reviewed in [27]). Each gp41 subunit within the Env trimer contains a hydrophobic fusion peptide and two alpha-helical heptad repeat regions (HR1 and HR2) [26] which together help facilitate fusion. Specifically, the exposed gp41 fusion peptides are inserted into the plasma membrane (PM) of the target cell followed by folding of the HR1 and HR2 subunits into a hairpin structure which brings the viral envelope and PM in close proximity to promote fusion between the two lipid bilayers (reviewed in [28]).

Viral envelope and target cell PM fusion allows the viral core to be released into the cytoplasm of the cell. While the viral core is being transported to the nucleus along microtubules [29], RT is reverse transcribing the viral RNA genome to double-stranded DNA. The RT is extremely error prone (comparison of RT error rates in recent review [30]), thus contributing to the relatively high mutation rate of HIV-1 that can help this virus overcome selective pressures and promote overall viral heterogeneity [31]. Prior to reliable and efficient intracellular labeling/visualization of CA, it was thought that uncoating of the viral core and reverse transcription were likely completed prior to nuclear entry and that the core did not enter the nucleus [32]. However, recent studies have shown that uncoating of the viral core and completion of reverse transcription occur *after* nuclear entry [33-35] and that intact cores can even enter the nucleus [36,37] (see [38] for a recent commentary)!

Upon entry into the nucleus, host factors help target IN and viral DNA to sites of active transcription away from the nuclear periphery [39-41]. IN directs exposed 3' OH groups in the long terminal repeat sequences (LTR) flanking either end of the viral DNA to the host DNA to facilitate integration by strand transfer [40,42]. Initial transcription from the integrated provirus is dependent on host transcription factors, allowing for the production of "early" viral proteins (Tat, Rev, and Nef). Tat and Rev can then drive viral gene expression (by Tat) and export positive-sense viral mRNA encoding "late" viral proteins (Gag/GagPol, Vif, Vpr, Vpu, and Env) and transport the full-length RNA genome to the cytoplasm (by Rev) [43,44]. Viral accessory proteins Nef, Vpu, Vpr, and Vif help establish an environment in the infected cell to support production of new infectious virus particles and continued virus spread [15,45-49].

Both Env and Gag are produced as precursors and require maturation by proteolytic cleavage for production of infectious virus particles. Newly synthesized Env precursor (gp160) is cleaved in the Golgi by a host protease into gp120 and gp41 (which associate by noncovalent interactions to form a gp120-gp41 heterodimer [18]), generating mature Env [26]. Once trafficked to the PM, Env is recycled into endosomes before being trafficked back to the PM – a process that is predicted to prevent excessive Env-induced cell-cell fusion by reducing Env at the PM and is implicated in supporting Env incorporation into virus particles [50,51]. The Gag precursor polyprotein contains MA, CA, NC, and p6 domains (and 2 spacer peptides). The GagPol precursor protein is generated as a result of a programmed ribosomal frameshift in the Gag transcript [52]. GagPol polyproteins contains MA, CA, NC, and p6 (like the Gag precursor) as well as RT,

IN, and Protease (PR) (encoded by Pol) [53]. Gag precursors rely on the MA domain for localization to the inner leaflet of the PM (reviewed in [53-55]) in preparation for particle assembly.

Assembly of new virus particles occurs at the PM and is driven by the immature Gag precursor polyprotein. The MA domain of the precursor promotes incorporation of Env into viral particles through MA interactions with Env-CT and also traps Env in a non-fusogenic state [56-64]. Further, the NC domain binds the viral RNA genome to ensure incorporation into new particles (reviewed in [65,66]). Gag accumulation at the PM drives viral budding and the p6 domain is required for viral release [67,68] as it binds host Endosomal Sorting Complex Required for Transport (ESCRT) machinery [69-71] which are recruited to complete the budding process, thus allowing particles to be released into the extracellular milieu (reviewed in [72,73]). Dimerization of PR monomers upon particle budding and/or release forms the active protease which mediates PR release from the GagPol precursor by autocatalysis [74], at which point PR can cleave the Gag and GagPol polyprotein precursors into the individual proteins to form a mature virus particle (reviewed in [75]). Additionally, cleavage of the Gag precursor releases Env from its trapped state allowing for increased diffusion within the lipid envelope and Env can now facilitate fusion upon CD4 binding to initiate a new round of infection [76,77].

### 1.4. HIV-1-induced cell-cell fusion

HIV-1 can induce the formation of multinucleated infected cells (syncytia). HIV-1-induced syncytia include both large, macrophage-based syncytia [78,79] and small (2-4

nuclei), T cell-based syncytia [80-83], and HIV-1 is likely also responsible for the giant, multinucleated infected cells detected in the brains of AIDS patients [84]. Small T cell-based syncytia (hereafter referred to only as "syncytia") present *in vivo*, while anecdotally reported in infected individuals [85], have only been recognized recently [80,82,83], as they had previously been thought to only be *in vitro* cell culture artifacts [86]. Whether these syncytia contribute to virus spread remains unknown.

HIV-1-induced syncytia formation is facilitated by the viral fusogen Env at the virological synapse (VS). The VS is a transient cellular junction between and infected cell and an uninfected cell that allows for HIV-1 cell-to-cell transmission. The VS forms when Env on the surface of an infected cell binds CD4 on the surface of an uninfected T cell [87,88] (and reviewed in greater detail in Chapter 2). As Env is fusogenic at neutral pH, VS formation could result in fusion of the producer and infected cell membranes, forming a syncytium. However, HIV-1-induced cell-cell fusion is largely prevented by both viral (Gag) and host (ezrin, tetraspanins, and recently identified EWI-2) fusion inhibitory factors [61,89-91] (as will be discussed further in Chapter 2). Despite these fusion inhibitory mechanisms, T cell-based syncytia have still been detected *in vivo* and can comprise ~20% of infected cells in the lymph nodes of humanized mice [80,82,83,85].

T cell-based syncytia detected in humanized mice during early infection can have an elongated, multilobed morphology and remain small as they have only been shown to contain up to 4 nuclei, with most syncytia only containing 2 nuclei [80,81]. Intriguingly, syncytia have also been shown to be capable of releasing "clouds" of virus particles and can transfer virus particles to uninfected cells upon cell-cell contact [81]. Collectively,

these studies suggest that syncytia likely play a yet-to-be determined role in viral spread within a host, including the potential to contribute to transmission at a VS. T cell-based syncytia have even been shown to have increased levels of fusion inhibitory host proteins EWI-2 and CD81 compared to mononucleated infected cells [91], indicating that syncytia may be *less* likely to undergo cell-cell fusion than other infected cells. We propose that the same fusion inhibitory machinery already implicated in fusion inhibition at the HIV-1 VS helps to maintain the relatively small size of T cell-based syncytia seen during early infection [81], therefore preventing indefinite growth (i.e. additional cell-cell fusion) of these infected entities.

### 1.5. EWI family protein EWI-2 (IGSF8)

EWI proteins are a subfamily of the immunoglobulin super family (IGSF) comprised of 4 members, EWI-F (CD9P-1/FPRP/PTGFRN), EWI-2 (IGSF8/PGRL), EWI-3 (IGSF3), and EWI-101 (CD101/IGSF2). EWI proteins have an extracellular Gln-Trp-Ile (E-W-I) motif and share 23-35% amino acid similarity [92]. Members of the EWI subfamily, EWI-F and EWI-2 are both interacting partners of tetraspanins CD9 (TSPAN29/MIC3) and CD81 (TSPAN28) [92,93], and EWI-3 was also recently shown to interact with tetraspanin CD231 (TSPAN7/TM4SF2) [94]. Tetraspanins are a family of 4-pass transmembrane proteins and are involved in numerous membrane processes. Tetraspanins can organize membrane microdomains (TEMs) or tetraspanin "webs" that can be comprised of a diverse network of proteins, including EWI-F and EWI-2 (reviewed in [95-97]). The interactions of EWI family members EWI-F and EWI-2 with tetraspanins

CD9 and CD81 have been robustly characterized and the functions of these EWI family proteins are frequently linked to those of tetraspanins [92,98-103]. Like tetraspanins, EWI-F and EWI-2 are implicated in a variety of processes at the PM including cell migration, signaling, synapse formation, cell-cell fusion, and regulating the lifecycle of several pathogens [91,99-101,104-110].

EWI-2 is a 70-kDa protein composed of 4 extracellular Ig domains and a short (10 AA), highly basic cytoplasmic tail. EWI-2 contains 3 sites of *N*-glycosylation in its extracellular domain [99] and EWI-2 is also subject to palmitoylation of two membrane-proximal cysteine residues ($Cys^{604}$ and $Cys^{605}$) [99,111]. Palmitoylation of the EWI-2 cytoplasmic tail influences EWI-2 interactions with phosphatidylinositol phosphates (PIPs) and is necessary for efficient interactions with both CD9 and CD81 [99,111]. EWI-2 can be cleaved by a yet-to-be determined protease to yield a 55 kDa product that lacks the N-terminal Ig domain (ie. EWI-2 "without its N-terminus" or EWI-2wint) which is also an interacting partner of CD9 and CD81 [109]. EWI-2 and/or EWI-2wint can influence TEM composition in the PM which is shown to impact a diverse array of cellular processes including cancer cell metastasis [105,107,112] and hepatitis C virus entry [99,100,109,110,113-116]. Further, EWI-2 has been shown to regulate HIV-1 induced cell-cell fusion alongside previously described fusion inhibitory tetraspanins interacting partners [91,117], suggesting that EWI-2 may also influence TEM composition/distribution in HIV-1-infected cells.

## 1.6. Dissertation Overview

The work presented in this dissertation has added a new perspective on the field of HIV-1 cell-to-cell transmission (Chapter 2, review in preparation), increased our understanding of fusion inhibition at the VS (Chapter 3), and described mechanisms of protein modulation for HIV-1-induced syncytia (Chapter 4). By discussing recent advancements in the field of HIV-1 cell-to-cell transmission at the VS and highlighting still unanswered questions (Chapter 2), we hope our review will serve as a resource for understanding the dynamic nature of the VS and provide direction for future investigations. Our work enhanced the field's understanding of factors which promote efficient cell-to-cell transmission by identifying EWI-2 as a novel inhibitor of HIV-1-induced cell-cell fusion which is recruited exclusively to the producer cell side of the synapse (the presynapse; Chapter 3). Intriguingly, our single cell analysis of infected cells by quantitative microscopy revealed that HIV-1-induced syncytia have higher levels of fusion inhibitory EWI-2 and CD81 than mononucleated infected cells (Chapter 3). This unique feature of multinucleated infected cells was further investigated and allowed us to determine that EWI-2 levels on syncytia depend on the levels of previously unfused target cells and can be modulated over time after fusion (Chapter 4, to be included in a future manuscript). We are excited as this work advances the field of cell-to-cell transmission through our investigations of HIV-1-induced cell-cell fusion regulation, including how multinucleated infected cells differ from mononucleated infected cells. Further, this work has provided the foundation for continued investigations aimed at understanding the

mechanisms of EWI-2-mediated fusion inhibition and the role of HIV-1-induced syncytia in virus spread (as proposed in Chapter 5).

## 1.7. References


1. Gao, F.; Bailes, E.; Robertson, D.L.; Chen, Y.; Rodenburg, C.M.; Michael, S.F.; Cummins, L.B.; Arthur, L.O.; Peeters, M.; Shaw, G.M., et al. Origin of HIV-1 in the chimpanzee Pan troglodytes troglodytes. *Nature* **1999**, *397*, 436-441, doi:10.1038/17130.

2. Keele, B.F.; Van Heuverswyn, F.; Li, Y.; Bailes, E.; Takehisa, J.; Santiago, M.L.; Bibollet-Ruche, F.; Chen, Y.; Wain, L.V.; Liegeois, F., et al. Chimpanzee reservoirs of pandemic and nonpandemic HIV-1. *Science* **2006**, *313*, 523-526, doi:10.1126/science.1126531.

3. Sharp, P.M.; Hahn, B.H. The evolution of HIV-1 and the origin of AIDS. *Philos Trans R Soc Lond B Biol Sci* **2010**, *365*, 2487-2494, doi:10.1098/rstb.2010.0031.

4. Sodora, D.L.; Silvestri, G. Immune activation and AIDS pathogenesis. *Aids* **2008**, *22*, 439-446, doi:10.1097/QAD.0b013e3282f2dbe7.

5. Silvestri, G. Immunity in natural SIV infections. *J Intern Med* **2009**, *265*, 97-109, doi:10.1111/j.1365-2796.2008.02049.x.

6. Keele, B.F.; Jones, J.H.; Terio, K.A.; Estes, J.D.; Rudicell, R.S.; Wilson, M.L.; Li, Y.; Learn, G.H.; Beasley, T.M.; Schumacher-Stankey, J., et al. Increased mortality and AIDS-like immunopathology in wild chimpanzees infected with SIVcpz. *Nature* **2009**, *460*, 515-519, doi:10.1038/nature08200.

7. Etienne, L.; Nerrienet, E.; LeBreton, M.; Bibila, G.T.; Foupouapouognigni, Y.; Rousset, D.; Nana, A.; Djoko, C.F.; Tamoufe, U.; Aghokeng, A.F., et al. Characterization of a new simian immunodeficiency virus strain in a naturally infected Pan troglodytes troglodytes chimpanzee with AIDS related symptoms. *Retrovirology* **2011**, *8*, 4, doi:10.1186/1742-4690-8-4.

8. Shaw, G.M.; Hunter, E. HIV transmission. *Cold Spring Harb Perspect Med* **2012**, *2*, doi:10.1101/cshperspect.a006965.

9. Joseph, S.B.; Swanstrom, R.; Kashuba, A.D.; Cohen, M.S. Bottlenecks in HIV-1 transmission: insights from the study of founder viruses. *Nat Rev Microbiol* **2015**, *13*, 414-425, doi:10.1038/nrmicro3471.

10. Kariuki, S.M.; Selhorst, P.; Ariën, K.K.; Dorfman, J.R. The HIV-1 transmission bottleneck. *Retrovirology* **2017**, *14*, 22, doi:10.1186/s12977-017-0343-8.

11. McMichael, A.J.; Borrow, P.; Tomaras, G.D.; Goonetilleke, N.; Haynes, B.F. The immune response during acute HIV-1 infection: clues for vaccine development. *Nat Rev Immunol* **2010**, *10*, 11-23, doi:10.1038/nri2674.

12. Cohen, M.S.; Shaw, G.M.; McMichael, A.J.; Haynes, B.F. Acute HIV-1 Infection. *N Engl J Med* **2011**, *364*, 1943-1954, doi:10.1056/NEJMra1011874.

13. Swanstrom, R.; Coffin, J. HIV-1 pathogenesis: the virus. *Cold Spring Harb Perspect Med* **2012**, *2*, a007443, doi:10.1101/cshperspect.a007443.

14. Vanhamel, J.; Bruggemans, A.; Debyser, Z. Establishment of latent HIV-1 reservoirs: what do we really know? *J Virus Erad* **2019**, *5*, 3-9.

15. Sugden, S.M.; Bego, M.G.; Pham, T.N.; Cohen É, A. Remodeling of the Host Cell Plasma Membrane by HIV-1 Nef and Vpu: A Strategy to Ensure Viral Fitness and Persistence. *Viruses* **2016**, *8*, 67, doi:10.3390/v8030067.

16. Okoye, A.A.; Picker, L.J. CD4(+) T-cell depletion in HIV infection: mechanisms of immunological failure. *Immunol Rev* **2013**, *254*, 54-64, doi:10.1111/imr.12066.

17. Vidya Vijayan, K.K.; Karthigeyan, K.P.; Tripathi, S.P.; Hanna, L.E. Pathophysiology of CD4+ T-Cell Depletion in HIV-1 and HIV-2 Infections. *Front Immunol* **2017**, *8*, 580, doi:10.3389/fimmu.2017.00580.

18. Kowalski, M.; Potz, J.; Basiripour, L.; Dorfman, T.; Goh, W.C.; Terwilliger, E.; Dayton, A.; Rosen, C.; Haseltine, W.; Sodroski, J. Functional regions of the envelope glycoprotein of human immunodeficiency virus type 1. *Science* **1987**, *237*, 1351-1355, doi:10.1126/science.3629244.

19. Xiao, T.; Cai, Y.; Chen, B. HIV-1 Entry and Membrane Fusion Inhibitors. *Viruses* **2021**, *13*, doi:10.3390/v13050735.

20. Briggs, J.A.; Kräusslich, H.G. The molecular architecture of HIV. *J Mol Biol* **2011**, *410*, 491-500, doi:10.1016/j.jmb.2011.04.021.

21. Toccafondi, E.; Lener, D.; Negroni, M. HIV-1 Capsid Core: A Bullet to the Heart of the Target Cell. *Front Microbiol* **2021**, *12*, 652486, doi:10.3389/fmicb.2021.652486.

22. Elliott, J.L.; Kutluay, S.B. Going beyond Integration: The Emerging Role of HIV-1 Integrase in Virion Morphogenesis. *Viruses* **2020**, *12*, doi:10.3390/v12091005.

23. Liu, H.; Wu, X.; Newman, M.; Shaw, G.M.; Hahn, B.H.; Kappes, J.C. The Vif protein of human and simian immunodeficiency viruses is packaged into virions and associates with viral core structures. *J Virol* **1995**, *69*, 7630-7638, doi:10.1128/jvi.69.12.7630-7638.1995.

24. Kogan, M.; Rappaport, J. HIV-1 accessory protein Vpr: relevance in the pathogenesis of HIV and potential for therapeutic intervention. *Retrovirology* **2011**, *8*, 25, doi:10.1186/1742-4690-8-25.

25. Khan, M.A.; Aberham, C.; Kao, S.; Akari, H.; Gorelick, R.; Bour, S.; Strebel, K. Human immunodeficiency virus type 1 Vif protein is packaged into the nucleoprotein complex through an interaction with viral genomic RNA. *J Virol* **2001**, *75*, 7252-7265, doi:10.1128/jvi.75.16.7252-7265.2001.

26. Checkley, M.A.; Luttge, B.G.; Freed, E.O. HIV-1 envelope glycoprotein biosynthesis, trafficking, and incorporation. *J Mol Biol* **2011**, *410*, 582-608, doi:10.1016/j.jmb.2011.04.042.

27. Munro, J.B.; Mothes, W. Structure and Dynamics of the Native HIV-1 Env Trimer. *J Virol* **2015**, *89*, 5752-5755, doi:10.1128/jvi.03187-14.

28. Chen, B. Molecular Mechanism of HIV-1 Entry. *Trends Microbiol* **2019**, *27*, 878-891, doi:10.1016/j.tim.2019.06.002.

29. Naghavi, M.H. HIV-1 capsid exploitation of the host microtubule cytoskeleton during early infection. *Retrovirology* **2021**, *18*, 19, doi:10.1186/s12977-021-00563-3.

30. Yeo, J.Y.; Goh, G.R.; Su, C.T.; Gan, S.K. The Determination of HIV-1 RT Mutation Rate, Its Possible Allosteric Effects, and Its Implications on Drug Resistance. *Viruses* **2020**, *12*, doi:10.3390/v12030297.

31. Cuevas, J.M.; Geller, R.; Garijo, R.; López-Aldeguer, J.; Sanjuán, R. Extremely High Mutation Rate of HIV-1 In Vivo. *PLoS Biol* **2015**, *13*, e1002251, doi:10.1371/journal.pbio.1002251.

32. Arhel, N. Revisiting HIV-1 uncoating. *Retrovirology* **2010**, *7*, 96, doi:10.1186/1742-4690-7-96.

33. Burdick, R.C.; Li, C.; Munshi, M.; Rawson, J.M.O.; Nagashima, K.; Hu, W.S.; Pathak, V.K. HIV-1 uncoats in the nucleus near sites of integration. *Proc Natl Acad Sci U S A* **2020**, *117*, 5486-5493, doi:10.1073/pnas.1920631117.

34. Dharan, A.; Bachmann, N.; Talley, S.; Zwikelmaier, V.; Campbell, E.M. Nuclear pore blockade reveals that HIV-1 completes reverse transcription and uncoating in the nucleus. *Nat Microbiol* **2020**, *5*, 1088-1095, doi:10.1038/s41564-020-0735-8.

35. Francis, A.C.; Marin, M.; Prellberg, M.J.; Palermino-Rowland, K.; Melikyan, G.B. HIV-1 Uncoating and Nuclear Import Precede the Completion of Reverse Transcription in Cell Lines and in Primary Macrophages. *Viruses* **2020**, *12*, doi:10.3390/v12111234.

36. Zila, V.; Margiotta, E.; Turoňová, B.; Müller, T.G.; Zimmerli, C.E.; Mattei, S.; Allegretti, M.; Börner, K.; Rada, J.; Müller, B., et al. Cone-shaped HIV-1 capsids are transported through intact nuclear pores. *Cell* **2021**, *184*, 1032-1046.e1018, doi:10.1016/j.cell.2021.01.025.

37. Müller, T.G.; Zila, V.; Peters, K.; Schifferdecker, S.; Stanic, M.; Lucic, B.; Laketa, V.; Lusic, M.; Müller, B.; Kräusslich, H.G. HIV-1 uncoating by release of viral cDNA from capsid-like structures in the nucleus of infected cells. *Elife* **2021**, *10*, doi:10.7554/eLife.64776.

38. Bedwell, G.J.; Engelman, A.N. You can keep your coat on. *Elife* **2021**, *10*, doi:10.7554/eLife.69887.

39. Schröder, A.R.; Shinn, P.; Chen, H.; Berry, C.; Ecker, J.R.; Bushman, F. HIV-1 integration in the human genome favors active genes and local hotspots. *Cell* **2002**, *110*, 521-529, doi:10.1016/s0092-8674(02)00864-4.

40. Lusic, M.; Siliciano, R.F. Nuclear landscape of HIV-1 infection and integration. *Nat Rev Microbiol* **2017**, *15*, 69-82, doi:10.1038/nrmicro.2016.162.

41. Achuthan, V.; Perreira, J.M.; Sowd, G.A.; Puray-Chavez, M.; McDougall, W.M.; Paulucci-Holthauzen, A.; Wu, X.; Fadel, H.J.; Poeschla, E.M.; Multani, A.S., et al. Capsid-CPSF6 Interaction Licenses Nuclear HIV-1 Trafficking to Sites of Viral DNA Integration. *Cell Host Microbe* **2018**, *24*, 392-404.e398, doi:10.1016/j.chom.2018.08.002.

42. Engelman, A.N.; Singh, P.K. Cellular and molecular mechanisms of HIV-1 integration targeting. *Cellular and molecular life sciences : CMLS* **2018**, *75*, 2491-2507, doi:10.1007/s00018-018-2772-5.

43. Wu, Y. HIV-1 gene expression: lessons from provirus and non-integrated DNA. *Retrovirology* **2004**, *1*, 13, doi:10.1186/1742-4690-1-13.

44. Karn, J.; Stoltzfus, C.M. Transcriptional and posttranscriptional regulation of HIV-1 gene expression. *Cold Spring Harb Perspect Med* **2012**, *2*, a006916, doi:10.1101/cshperspect.a006916.

45. Malim, M.H.; Emerman, M. HIV-1 accessory proteins--ensuring viral survival in a hostile environment. *Cell Host Microbe* **2008**, *3*, 388-398, doi:10.1016/j.chom.2008.04.008.

46. He, J.; Choe, S.; Walker, R.; Di Marzio, P.; Morgan, D.O.; Landau, N.R. Human immunodeficiency virus type 1 viral protein R (Vpr) arrests cells in the G2 phase of the cell cycle by inhibiting p34cdc2 activity. *J Virol* **1995**, *69*, 6705-6711, doi:10.1128/jvi.69.11.6705-6711.1995.

47. Re, F.; Braaten, D.; Franke, E.K.; Luban, J. Human immunodeficiency virus type 1 Vpr arrests the cell cycle in G2 by inhibiting the activation of p34cdc2-cyclin B. *J Virol* **1995**, *69*, 6859-6864, doi:10.1128/jvi.69.11.6859-6864.1995.

48. Ospina Stella, A.; Turville, S. All-Round Manipulation of the Actin Cytoskeleton by HIV. *Viruses* **2018**, *10*, doi:10.3390/v10020063.

49. Greenwood, E.J.D.; Williamson, J.C.; Sienkiewicz, A.; Naamati, A.; Matheson, N.J.; Lehner, P.J. Promiscuous Targeting of Cellular Proteins by Vpr Drives Systems-Level Proteomic Remodeling in HIV-1 Infection. *Cell Rep* **2019**, *27*, 1579-1596.e1577, doi:10.1016/j.celrep.2019.04.025.

50. Rowell, J.F.; Stanhope, P.E.; Siliciano, R.F. Endocytosis of endogenously synthesized HIV-1 envelope protein. Mechanism and role in processing for association with class II MHC. *J Immunol* **1995**, *155*, 473-488.

51. Kirschman, J.; Qi, M.; Ding, L.; Hammonds, J.; Dienger-Stambaugh, K.; Wang, J.J.; Lapierre, L.A.; Goldenring, J.R.; Spearman, P. HIV-1 Envelope Glycoprotein Trafficking through the Endosomal Recycling Compartment Is Required for Particle Incorporation. *J Virol* **2018**, *92*, doi:10.1128/jvi.01893-17.

52. Jacks, T.; Power, M.D.; Masiarz, F.R.; Luciw, P.A.; Barr, P.J.; Varmus, H.E. Characterization of ribosomal frameshifting in HIV-1 gag-pol expression. *Nature* **1988**, *331*, 280-283, doi:10.1038/331280a0.

53. Freed, E.O. HIV-1 assembly, release and maturation. *Nat Rev Microbiol* **2015**, *13*, 484-496, doi:10.1038/nrmicro3490.

54. Bussienne, C.; Marquet, R.; Paillart, J.C.; Bernacchi, S. Post-Translational Modifications of Retroviral HIV-1 Gag Precursors: An Overview of Their Biological Role. *Int J Mol Sci* **2021**, *22*, doi:10.3390/ijms22062871.

55. Chukkapalli, V.; Ono, A. Molecular determinants that regulate plasma membrane association of HIV-1 Gag. *J Mol Biol* **2011**, *410*, 512-524, doi:10.1016/j.jmb.2011.04.015.

56. Freed, E.O.; Martin, M.A. Domains of the human immunodeficiency virus type 1 matrix and gp41 cytoplasmic tail required for envelope incorporation into virions. *J Virol* **1996**, *70*, 341-351, doi:10.1128/jvi.70.1.341-351.1996.

57. Wyma, D.J.; Kotov, A.; Aiken, C. Evidence for a stable interaction of gp41 with Pr55(Gag) in immature human immunodeficiency virus type 1 particles. *J Virol* **2000**, *74*, 9381-9387, doi:10.1128/jvi.74.20.9381-9387.2000.

58. Murakami, T.; Freed, E.O. Genetic evidence for an interaction between human immunodeficiency virus type 1 matrix and alpha-helix 2 of the gp41 cytoplasmic tail. *J Virol* **2000**, *74*, 3548-3554, doi:10.1128/jvi.74.8.3548-3554.2000.

59. Alfadhli, A.; Staubus, A.O.; Tedbury, P.R.; Novikova, M.; Freed, E.O.; Barklis, E. Analysis of HIV-1 Matrix-Envelope Cytoplasmic Tail Interactions. *J Virol* **2019**, *93*, doi:10.1128/jvi.01079-19.

60. Pezeshkian, N.; Groves, N.S.; van Engelenburg, S.B. Single-molecule imaging of HIV-1 envelope glycoprotein dynamics and Gag lattice association exposes

determinants responsible for virus incorporation. *Proc Natl Acad Sci U S A* **2019**, *116*, 25269-25277, doi:10.1073/pnas.1910008116.

61. Roy, N.H.; Chan, J.; Lambelé, M.; Thali, M. Clustering and mobility of HIV-1 Env at viral assembly sites predict its propensity to induce cell-cell fusion. *J Virol* **2013**, *87*, 7516-7525, doi:10.1128/jvi.00790-13.

62. Tedbury, P.R.; Freed, E.O. The cytoplasmic tail of retroviral envelope glycoproteins. *Prog Mol Biol Transl Sci* **2015**, *129*, 253-284, doi:10.1016/bs.pmbts.2014.10.009.

63. Qu, K.; Ke, Z.; Zila, V.; Anders-Osswein, M.; Glass, B.; Mucksch, F.; Muller, R.; Schultz, C.; Muller, B.; Krausslich, H.G., et al. Maturation of the matrix and viral membrane of HIV-1. *Science* **2021**, *373*, 700-704, doi:10.1126/science.abe6821.

64. Hikichi, Y.; Freed, E.O. Maturation of HIV-1. *Science* **2021**, *373*, 621-622, doi:10.1126/science.abj9075.

65. Levin, J.G.; Mitra, M.; Mascarenhas, A.; Musier-Forsyth, K. Role of HIV-1 nucleocapsid protein in HIV-1 reverse transcription. *RNA Biol* **2010**, *7*, 754-774, doi:10.4161/rna.7.6.14115.

66. Mouhand, A.; Pasi, M.; Catala, M.; Zargarian, L.; Belfetmi, A.; Barraud, P.; Mauffret, O.; Tisné, C. Overview of the Nucleic-Acid Binding Properties of the HIV-1 Nucleocapsid Protein in Its Different Maturation States. *Viruses* **2020**, *12*, doi:10.3390/v12101109.

67. Göttlinger, H.G.; Dorfman, T.; Sodroski, J.G.; Haseltine, W.A. Effect of mutations affecting the p6 gag protein on human immunodeficiency virus particle release. *Proc Natl Acad Sci U S A* **1991**, *88*, 3195-3199, doi:10.1073/pnas.88.8.3195.

68. Huang, M.; Orenstein, J.M.; Martin, M.A.; Freed, E.O. p6Gag is required for particle production from full-length human immunodeficiency virus type 1 molecular clones expressing protease. *J Virol* **1995**, *69*, 6810-6818, doi:10.1128/jvi.69.11.6810-6818.1995.

69. Martin-Serrano, J.; Zang, T.; Bieniasz, P.D. HIV-1 and Ebola virus encode small peptide motifs that recruit Tsg101 to sites of particle assembly to facilitate egress. *Nat Med* **2001**, *7*, 1313-1319, doi:10.1038/nm1201-1313.

70. VerPlank, L.; Bouamr, F.; LaGrassa, T.J.; Agresta, B.; Kikonyogo, A.; Leis, J.; Carter, C.A. Tsg101, a homologue of ubiquitin-conjugating (E2) enzymes, binds the L domain in HIV type 1 Pr55(Gag). *Proc Natl Acad Sci U S A* **2001**, *98*, 7724-7729, doi:10.1073/pnas.131059198.

71. Strack, B.; Calistri, A.; Craig, S.; Popova, E.; Göttlinger, H.G. AIP1/ALIX is a binding partner for HIV-1 p6 and EIAV p9 functioning in virus budding. *Cell* **2003**, *114*, 689-699, doi:10.1016/s0092-8674(03)00653-6.

72. Votteler, J.; Sundquist, W.I. Virus budding and the ESCRT pathway. *Cell Host Microbe* **2013**, *14*, 232-241, doi:10.1016/j.chom.2013.08.012.

73. Rose, K.M. When in Need of an ESCRT: The Nature of Virus Assembly Sites Suggests Mechanistic Parallels between Nuclear Virus Egress and Retroviral Budding. *Viruses* **2021**, *13*, doi:10.3390/v13061138.

74. Debouck, C.; Gorniak, J.G.; Strickler, J.E.; Meek, T.D.; Metcalf, B.W.; Rosenberg, M. Human immunodeficiency virus protease expressed in Escherichia coli exhibits autoprocessing and specific maturation of the gag precursor. *Proc Natl Acad Sci U S A* **1987**, *84*, 8903-8906, doi:10.1073/pnas.84.24.8903.

75. Konvalinka, J.; Kräusslich, H.G.; Müller, B. Retroviral proteases and their roles in virion maturation. *Virology* **2015**, *479-480*, 403-417, doi:10.1016/j.virol.2015.03.021.

76. Jiang, J.; Aiken, C. Maturation-dependent human immunodeficiency virus type 1 particle fusion requires a carboxyl-terminal region of the gp41 cytoplasmic tail. *J Virol* **2007**, *81*, 9999-10008, doi:10.1128/jvi.00592-07.

77. Chojnacki, J.; Waithe, D.; Carravilla, P.; Huarte, N.; Galiani, S.; Enderlein, J.; Eggeling, C. Envelope glycoprotein mobility on HIV-1 particles depends on the virus maturation state. *Nat Commun* **2017**, *8*, 545, doi:10.1038/s41467-017-00515-6.

78. Orenstein, J.M.; Wahl, S.M. The macrophage origin of the HIV-expressing multinucleated giant cells in hyperplastic tonsils and adenoids. *Ultrastruct Pathol* **1999**, *23*, 79-91, doi:10.1080/019131299281734.

79. Dargent, J.L.; Lespagnard, L.; Kornreich, A.; Hermans, P.; Clumeck, N.; Verhest, A. HIV-associated multinucleated giant cells in lymphoid tissue of the Waldeyer's ring: a detailed study. *Mod Pathol* **2000**, *13*, 1293-1299, doi:10.1038/modpathol.3880237.

80. Murooka, T.T.; Deruaz, M.; Marangoni, F.; Vrbanac, V.D.; Seung, E.; von Andrian, U.H.; Tager, A.M.; Luster, A.D.; Mempel, T.R. HIV-infected T cells are migratory vehicles for viral dissemination. *Nature* **2012**, *490*, 283-287, doi:10.1038/nature11398.

81. Symeonides, M.; Murooka, T.T.; Bellfy, L.N.; Roy, N.H.; Mempel, T.R.; Thali, M. HIV-1-Induced Small T Cell Syncytia Can Transfer Virus Particles to Target Cells through Transient Contacts. *Viruses* **2015**, *7*, 6590-6603, doi:10.3390/v7122959.

82. Law, K.M.; Komarova, N.L.; Yewdall, A.W.; Lee, R.K.; Herrera, O.L.; Wodarz, D.; Chen, B.K. In Vivo HIV-1 Cell-to-Cell Transmission Promotes Multicopy Micro-compartmentalized Infection. *Cell Rep* **2016**, *15*, 2771-2783, doi:10.1016/j.celrep.2016.05.059.

83. Ventura, J.D.; Beloor, J.; Allen, E.; Zhang, T.; Haugh, K.A.; Uchil, P.D.; Ochsenbauer, C.; Kieffer, C.; Kumar, P.; Hope, T.J., et al. Longitudinal bioluminescent imaging of HIV-1 infection during antiretroviral therapy and treatment interruption in humanized mice. *PLoS Pathog* **2019**, *15*, e1008161, doi:10.1371/journal.ppat.1008161.

84. Wiley, C.A.; Schrier, R.D.; Nelson, J.A.; Lampert, P.W.; Oldstone, M.B. Cellular localization of human immunodeficiency virus infection within the brains of acquired immune deficiency syndrome patients. *Proc Natl Acad Sci U S A* **1986**, *83*, 7089-7093, doi:10.1073/pnas.83.18.7089.

85. Orenstein, J.M. In vivo cytolysis and fusion of human immunodeficiency virus type 1-infected lymphocytes in lymphoid tissue. *J Infect Dis* **2000**, *182*, 338-342, doi:10.1086/315640.

86. Compton, A.A.; Schwartz, O. They Might Be Giants: Does Syncytium Formation Sink or Spread HIV Infection? *PLoS Pathog* **2017**, *13*, e1006099, doi:10.1371/journal.ppat.1006099.

87. Jolly, C.; Kashefi, K.; Hollinshead, M.; Sattentau, Q.J. HIV-1 cell to cell transfer across an Env-induced, actin-dependent synapse. *J Exp Med* **2004**, *199*, 283-293, doi:10.1084/jem.20030648.

88. Jolly, C.; Sattentau, Q.J. Retroviral spread by induction of virological synapses. *Traffic* **2004**, *5*, 643-650, doi:10.1111/j.1600-0854.2004.00209.x.

89. Krementsov, D.N.; Weng, J.; Lambele, M.; Roy, N.H.; Thali, M. Tetraspanins regulate cell-to-cell transmission of HIV-1. *Retrovirology* **2009**, *6*, 64, doi:10.1186/1742-4690-6-64.

90. Roy, N.H.; Lambelé, M.; Chan, J.; Symeonides, M.; Thali, M. Ezrin is a component of the HIV-1 virological presynapse and contributes to the inhibition of cell-cell fusion. *J Virol* **2014**, *88*, 7645-7658, doi:10.1128/jvi.00550-14.

91. Whitaker, E.E.; Matheson, N.J.; Perlee, S.; Munson, P.B.; Symeonides, M.; Thali, M. EWI-2 Inhibits Cell-Cell Fusion at the HIV-1 Virological Presynapse. *Viruses* **2019**, *11*, doi:10.3390/v11121082.

92. Stipp, C.S.; Kolesnikova, T.V.; Hemler, M.E. EWI-2 is a major CD9 and CD81 partner and member of a novel Ig protein subfamily. *J Biol Chem* **2001**, *276*, 40545-40554, doi:10.1074/jbc.M107338200.

93. Stipp, C.S.; Orlicky, D.; Hemler, M.E. FPRP, a major, highly stoichiometric, highly specific CD81- and CD9-associated protein. *J Biol Chem* **2001**, *276*, 4853-4862, doi:10.1074/jbc.M009859200.

94. Usardi, A.; Iyer, K.; Sigoillot, S.M.; Dusonchet, A.; Selimi, F. The immunoglobulin-like superfamily member IGSF3 is a developmentally regulated protein that controls neuronal morphogenesis. *Dev Neurobiol* **2017**, *77*, 75-92, doi:10.1002/dneu.22412.

95. Hemler, M.E. Tetraspanin functions and associated microdomains. *Nat Rev Mol Cell Biol* **2005**, *6*, 801-811, doi:10.1038/nrm1736.

96. Le Naour, F.; André, M.; Boucheix, C.; Rubinstein, E. Membrane microdomains and proteomics: lessons from tetraspanin microdomains and comparison with lipid rafts. *Proteomics* **2006**, *6*, 6447-6454, doi:10.1002/pmic.200600282.

97. Yáñez-Mó, M.; Barreiro, O.; Gordon-Alonso, M.; Sala-Valdés, M.; Sánchez-Madrid, F. Tetraspanin-enriched microdomains: a functional unit in cell plasma membranes. *Trends Cell Biol* **2009**, *19*, 434-446, doi:10.1016/j.tcb.2009.06.004.

98. Gordón-Alonso, M.; Sala-Valdés, M.; Rocha-Perugini, V.; Pérez-Hernández, D.; López-Martín, S.; Ursa, A.; Alvarez, S.; Kolesnikova, T.V.; Vázquez, J.; Sánchez-Madrid, F., et al. EWI-2 association with α-actinin regulates T cell immune synapses and HIV viral infection. *J Immunol* **2012**, *189*, 689-700, doi:10.4049/jimmunol.1103708.

99. Montpellier, C.; Tews, B.A.; Poitrimole, J.; Rocha-Perugini, V.; D'Arienzo, V.; Potel, J.; Zhang, X.A.; Rubinstein, E.; Dubuisson, J.; Cocquerel, L. Interacting regions of CD81 and two of its partners, EWI-2 and EWI-2wint, and their effect on hepatitis C virus infection. *J Biol Chem* **2011**, *286*, 13954-13965, doi:10.1074/jbc.M111.220103.

100. Potel, J.; Rassam, P.; Montpellier, C.; Kaestner, L.; Werkmeister, E.; Tews, B.A.; Couturier, C.; Popescu, C.I.; Baumert, T.F.; Rubinstein, E., et al. EWI-2wint promotes CD81 clustering that abrogates Hepatitis C Virus entry. *Cellular microbiology* **2013**, *15*, 1234-1252, doi:10.1111/cmi.12112.

101. Charrin, S.; Yalaoui, S.; Bartosch, B.; Cocquerel, L.; Franetich, J.F.; Boucheix, C.; Mazier, D.; Rubinstein, E.; Silvie, O. The Ig domain protein CD9P-1 down-regulates CD81 ability to support Plasmodium yoelii infection. *J Biol Chem* **2009**, *284*, 31572-31578, doi:10.1074/jbc.M109.057927.

102. Charrin, S.; Le Naour, F.; Labas, V.; Billard, M.; Le Caer, J.P.; Emile, J.F.; Petit, M.A.; Boucheix, C.; Rubinstein, E. EWI-2 is a new component of the tetraspanin web in hepatocytes and lymphoid cells. *Biochem J* **2003**, *373*, 409-421, doi:10.1042/bj20030343.

103. Umeda, R.; Satouh, Y.; Takemoto, M.; Nakada-Nakura, Y.; Liu, K.; Yokoyama, T.; Shirouzu, M.; Iwata, S.; Nomura, N.; Sato, K., et al. Structural insights into tetraspanin CD9 function. *Nat Commun* **2020**, *11*, 1606, doi:10.1038/s41467-020-15459-7.

104. Sala-Valdés, M.; Ursa, A.; Charrin, S.; Rubinstein, E.; Hemler, M.E.; Sánchez-Madrid, F.; Yáñez-Mó, M. EWI-2 and EWI-F link the tetraspanin web to the actin cytoskeleton through their direct association with ezrin-radixin-moesin proteins. *J Biol Chem* **2006**, *281*, 19665-19675, doi:10.1074/jbc.M602116200.

105. Kolesnikova, T.V.; Kazarov, A.R.; Lemieux, M.E.; Lafleur, M.A.; Kesari, S.; Kung, A.L.; Hemler, M.E. Glioblastoma inhibition by cell surface immunoglobulin protein EWI-2, in vitro and in vivo. *Neoplasia* **2009**, *11*, 77-86, 74p following 86, doi:10.1593/neo.81180.

106. Gordon-Alonso, M.; Sala-Valdes, M.; Rocha-Perugini, V.; Perez-Hernandez, D.; Lopez-Martin, S.; Ursa, A.; Alvarez, S.; Kolesnikova, T.V.; Vazquez, J.; Sanchez-Madrid, F., et al. EWI-2 association with alpha-actinin regulates T cell immune synapses and HIV viral infection. *J Immunol* **2012**, *189*, 689-700, doi:10.4049/jimmunol.1103708.

107. Wang, H.X.; Sharma, C.; Knoblich, K.; Granter, S.R.; Hemler, M.E. EWI-2 negatively regulates TGF-β signaling leading to altered melanoma growth and metastasis. *Cell research* **2015**, *25*, 370-385, doi:10.1038/cr.2015.17.

108. Charrin, S.; Latil, M.; Soave, S.; Polesskaya, A.; Chrétien, F.; Boucheix, C.; Rubinstein, E. Normal muscle regeneration requires tight control of muscle cell fusion by tetraspanins CD9 and CD81. *Nat Commun* **2013**, *4*, 1674, doi:10.1038/ncomms2675.

109. Rocha-Perugini, V.; Montpellier, C.; Delgrange, D.; Wychowski, C.; Helle, F.; Pillez, A.; Drobecq, H.; Le Naour, F.; Charrin, S.; Levy, S., et al. The CD81 partner EWI-2wint inhibits hepatitis C virus entry. *PloS one* **2008**, *3*, e1866, doi:10.1371/journal.pone.0001866.

110. Schuster, C.; Baumert, T.F. EWI-2wint--a host cell factor inhibiting hepatitis C virus entry. *Journal of hepatology* **2009**, *50*, 222-224, doi:10.1016/j.jhep.2008.10.009.

111. He, B.; Zhang, Y.H.; Richardson, M.M.; Zhang, J.S.; Rubinstein, E.; Zhang, X.A. Differential functions of phospholipid binding and palmitoylation of tumour suppressor EWI2/PGRL. *Biochem J* **2011**, *437*, 399-411, doi:10.1042/bj20101381.

112. Wang, H.X.; Li, Q.; Sharma, C.; Knoblich, K.; Hemler, M.E. Tetraspanin protein contributions to cancer. *Biochemical Society transactions* **2011**, *39*, 547-552, doi:10.1042/bst0390547.

113. Dahmane, S.; Rubinstein, E.; Milhiet, P.E. Viruses and tetraspanins: lessons from single molecule approaches. *Viruses* **2014**, *6*, 1992-2011, doi:10.3390/v6051992.

114. Samreen, B.; Khaliq, S.; Ashfaq, U.A.; Khan, M.; Afzal, N.; Shahzad, M.A.; Riaz, S.; Jahan, S. Hepatitis C virus entry: role of host and viral factors. *Infection, genetics and evolution : journal of molecular epidemiology and evolutionary genetics in infectious diseases* **2012**, *12*, 1699-1709, doi:10.1016/j.meegid.2012.07.010.

115. Dubuisson, J.; Helle, F.; Cocquerel, L. Early steps of the hepatitis C virus life cycle. *Cellular microbiology* **2008**, *10*, 821-827, doi:10.1111/j.1462-5822.2007.01107.x.

116. Helle, F.; Dubuisson, J. Hepatitis C virus entry into host cells. *Cellular and molecular life sciences : CMLS* **2008**, *65*, 100-112, doi:10.1007/s00018-007-7291-8.

117. Weng, J.; Krementsov, D.N.; Khurana, S.; Roy, N.H.; Thali, M. Formation of syncytia is repressed by tetraspanins in human immunodeficiency virus type 1-producing cells. *J Virol* **2009**, *83*, 7467-7474, doi:10.1128/jvi.00163-09

# CHAPTER 2 : SYSTEMS SUPPORTING EFFICIENT T CELL-TO-T CELL TRANSMISSION AT THE HIV-1 VIROLOGICAL SYNAPSE

Emily E. Whitaker [1,2], Menelaos Symeonides [1], Elise Courtney [1], Markus Thali [1,2]

[1] Department of Microbiology and Molecular Genetics, University of Vermont, Burlington, VT 05405, USA

[2] Graduate Program in Cellular, Molecular, and Biomedical Sciences, University of Vermont, Burlington, VT 05405, USA

## 2.1. Abstract

Cell-to-cell transmission is an efficient mode of HIV-1 spread that is unique from cell-free transmission as it relies on the formation of a transient junction between HIV-1-infected cells and uninfected target cells known as a virological synapse (VS). Extensive remodeling in both cells engaged at the contact results in polarization of viral and host factors to the VS. Upon formation of the VS, virus particles can be transferred to the uninfected target cell to facilitate a new round of infection, and ultimately the VS typically resolves with complete cell separation. Therefore, protein organization at the VS is tightly regulated to ensure transfer of virus particles to target cells and complete cell separation. This review will focus on cell-to-cell transmission between T cells and aims to summarize advancements in our understanding of VS structure, emphasize the contribution of fusion regulation to ensuring continued spread, signaling events, and temporal dynamics at the synapse.

## 2.2. Defining HIV-1 Cell-to-Cell Transmission

With this review, we will discuss recent developments in the field of human immunodeficiency virus type 1 (HIV-1) cell-to-cell transmission between $CD4^+$ T cells at the virological synapse (VS; named for its similarity to the immunological synapse/IS [1,2]). We will not include a figure depicting a schematic representation of transmission at the VS in this review as this could give the impression that the VS is a singular, fixed junction and would be in contrast with our increased understanding that the VS is actually a multiform, dynamic cellular junction. This review will complement recent reviews of HIV-1 transmission upon cell-cell contact and lentiviral cell-to-cell spread [3-7], while

adding a resource for HIV-1 transmission at the VS which is focused on features that support efficient transmission including T cell VS structure, fusion regulation (our group's area of expertise), signaling, and temporal events supporting efficient cell-to-cell spread.

Human immunodeficiency virus type 1 (HIV-1) can spread through multiple modes of transmission, including cell-free and cell-to-cell transmission which both ultimately require the release of free virus particles. What distinguishes cell-to-cell from cell-free transmission is that cell-to-cell transmission is dependent on transfer of virus particles at a transient cellular junction between an infected T (producer) cell and an uninfected $CD4^+$ T (target) cell known as the virological synapse (VS) [8] (as also defined previously [3]). The VS forms upon HIV-1 Envelope (Env) on the surface of a producer cell binding its receptor CD4 on the surface of a target cell [8], leading to rapid polarization of viral and host factors to the contact site. While the producer-target cells are engaged at the VS, newly produced virus particles can bud from the surface of the producer cell in a polarized manner near the target cell. The released virus particles can then enter the target cell engaged at the VS to initiate a new round of infection [9].

### 2.3. VS Structure, Composition, and Organization

Since the HIV-1 VS was first described [8], a substantial number of studies conducted *in vitro* have enhanced our understanding of the structure and composition of the VS. The VS is a cellular structure formed upon Env-CD4-mediated contact between opposing producer and target cell membranes where both viral and host factors are typically rapidly polarized to support efficient cell-to-cell transmission. Although factors which have been shown to support cell-to-cell transmission are typically present at the VS,

it is also clear that the VS is a dynamic structure for which a single version likely does not exist, but rather multiple, dynamic variations of this junction could support virus transmission.

Studies from multiple groups demonstrated that contact between the producer and target cell at the VS does not appear to be a continuous contact between the two cell membranes, but rather multiple points of membrane contact across the synapse [8,10]. Early studies using transmission electron microscopy and three-dimensional (3D) electron tomography documented that the VS is comprised of multiple CD4-positive membrane contacts across the synapse [8] and has a remarkably porous structure, composed of open, cell-free zones between the distinct membrane contact sites [10]. Further, free virus particles were frequently seen within the open zones between cell contact points [10]. A more recent investigation of the structure of the VS utilized homotypic producer:target cell co-cultures of either Jurkat or primary $CD4^+$ T cells to visualize the VS by focused ion beam scanning electron microscopy (FIB-SEM), which allowed for 3D reconstruction of the synapse of whole embedded samples imaged in sequential <50 nm slices, revealed important distinctions between cell line (Jurkat) and primary T cell-based VS structures [11]. While both Jurkat and primary T cell-based synapses had distinguishable membrane protrusions, primary T cells appeared to form closer contacts than those between Jurkat cells, and virus budded from the synapse periphery of primary T cells rather than near the synapse center as was shown for Jurkat cells [11]. Such close membrane contacts between cells at primary T cell-based synapses were also documented by another group [12]. Correlative fluorescence and electron microscopy further documented that cell-to-cell transmission mediated by both Jurkat and primary T cell producer cells can result in the

transfer of virus particles which appeared to be present at both the target cell surface and within endosomes [12]. Overall, these studies demonstrate that close membrane contacts at the VS support transfer of virus upon release of free particles in close proximity to target cells.

A frequently observed feature of the VS is robust polarization of host and viral factors to both the producer and target cell sides of the contact interface (the pre- and postsynapse, respectively) upon Env-CD4-mediated cell-cell contact [13,14]. Redistribution of viral and host factors upon Env-CD4 contact to form the VS requires dynamic cytoskeletal rearrangements [8,15]. A prominent pattern of VS organization is that the Env receptor CD4 and coreceptors are recruited exclusively to the postsynapse [8] while the hallmark distinguishing the presynapse is, unsurprisingly, prominent enrichment of viral proteins including structural proteins Env and Gag, which are likely accompanied by a high concentration of copies of the viral genome for assembly of new virus particles (as suggested in [16] and reviewed in [7]). Cellular organelles, namely the microtubule organizing complex (MTOC) and mitochondria, are also found to polarize to the presynapse [14,15]. Additionally, it was recently demonstrated that the host factor EWI-2 (IGSF8), which supports cell-to-cell transmission by inhibiting excessive Env-mediated cell-cell fusion that could impede efficient virus spread (as will be discussed in more detail below), is also enriched exclusively at the presynapse [17]. Host factors found to be enriched at both sides of the synapse include adhesion molecule LFA-1 [8] and ICAM binding partners (ICAM-1 and -3, specifically) [18]. LFA-1 contributes to the formation of a stable VS as depletion from either target or producer cells impairs synapse formation [18,19]. Interestingly, engagement of LFA-1 on producer cells also induced signaling

events in HIV-1-infected cells that support polarization of both viral (Gag and Env) and cellular factors to the presynapse [19]. Together, this work establishes that there is polarization and distinct organization of host and viral factors at the producer-target cell sides of the VS.

Collectively, these studies establish that VS formation can lead to robust, organized polarization of host and viral factors to the contact interface to support cellular contacts which allow virus to be released in close proximity to a target cell [8,10,11] thus ultimately allowing for transfer of particles [12].

### 2.4. Fusion Inhibition at the VS

Historically, virus transfer at Env-mediated infected-uninfected cell contacts that can occur *without cell-cell fusion* has long been speculated to contribute to overall virus transmission [20] thus identifying fusion inhibition at such cellular junctions as an important regulatory system for promoting continued virus spread. Specifically, mechanisms that efficiently inhibit fusion are necessary as Env, which is fusogenic at neutral pH, could trigger fusion of the producer and target cell membranes upon Env-CD4 binding at the VS which would form a multinucleated HIV-1 infected cell (or syncytium; plural syncytia). Uncontrolled cell-cell fusion resulting in the formation of large, multinucleated infected entities would likely be detrimental to virus spread as it would reduce the number of producer cells available to independently contribute to spread (i.e. because they would have fused with the target cell rather than becoming a new and independent infected entity), and potentially causing increased cytopathic effects (as seen *in vitro* [21]). Cultures containing many large syncytia have even been shown to produce

less infectious particles than cultures with few or no large syncytia, owing to insufficient packaging of GagPol into particles [22]. Therefore, fusion regulation at the VS is necessary to ensure efficient transmission and continued virus spread.

Relatively recent studies have determined that cell-cell fusion at the VS can be prevented by both viral (Gag) and host (ezrin, EWI-2, and tetraspanin family members) fusion inhibitory factors which are enriched at the VS. However, HIV-1-induced T cell-based syncytia can still form, including shortly after infection *in vivo* (documented in infected humanized mice [23-25]). HIV-1-induced syncytia observed *in vivo* remain small (2-4 nuclei) [26], indicating that multinucleated HIV-1 infected T cells are also themselves subject to mechanisms that inhibit cell-cell fusion. The presence of small syncytia suggests that the recruitment and organization of these fusion inhibitory factors at the VS is likely variable as these proteins are not always able to prevent HIV-1-induced cell-cell fusion. Preventing excessive HIV-1-induced cell-cell fusion, including after a small syncytium has already formed, likely promotes virus spread by supporting an exponential increase in the number of infected entities via cell-to-cell transmission at the VS rather than the formation of one, large (many nuclei) infected entity.

Cytoplasmic Gag polyprotein (p55) is largely considered the primary inhibitor of HIV-1-induced cell-cell fusion at the VS. Gag inhibits syncytium formation by trapping Env in a non-fusogenic state at the infected cell surface [27]. Gag traps Env through an association with the Env cytoplasmic tail (EnvCT), as demonstrated by CT-truncated Env having strikingly smaller Gag-associated clusters at the plasma membrane (PM), which correlated with increased Env-mediated cell-cell fusion [27]. In agreement with this model, truncation of the EnvCT results in reduced Gag recruitment to the VS [28]. Trapping of

Env by Gag is relieved upon maturation by protease-mediated cleavage of the Gag precursor into the viral structural components matrix (MA/p17), capsid (CA/p24), nucleocapsid (NC/p7) and p6 (for a review of Gag maturation, see [29]) in newly assembled and released virions, thus allowing Env to facilitate fusion/entry of the particle into the target cell [30-33]. In addition to Gag-mediated fusion inhibition, rapid Env recycling from the PM by endocytosis is required for efficient Env incorporation into virus particles [34,35] and likely also prevents excessive cell-cell fusion with neighboring target cells by keeping Env expression at the producer cell surface relatively low [36]. Together, Gag-mediated Env trapping and Env recycling contribute to potent inhibition of HIV-1-induced cell-cell fusion.

In addition to viral factor-mediated fusion inhibition, excessive fusion at the VS is also prevented by several host fusion inhibitory factors. Specifically, a previously defined complex of interacting partners (ezrin, EWI-2, and tetraspanins [37-40]) were all shown to be enriched at the VS and inhibit HIV-1-induced syncytium formation [17,41,42]. Ezrin likely inhibits excessive syncytium formation through actin bundling when in its active/phosphorylated form (p-ezrin) [41]. Indeed, actin remodeling is known to restrict expansion of fusion pores once membrane fusion has been initiated by several viral fusogens [43,44]. Further, dynamic actin remodeling is in fact required for HIV-1 Env-induced fusion [45]. Intriguingly, ezrin knockdown reduced overall cellular F-actin levels and also resulted in decreased enrichment of tetraspanin CD81 to the VS [41], suggesting that this network of fusion inhibitory proteins is highly connected and at least partially dependent on interaction(s) with other host fusion inhibitory partner proteins. EWI-2 inhibits HIV-1-induced cell-cell fusion at the producer cell side of the VS (the presynapse)

in a dose-dependent manner [17], similar to tetraspanins [42]. Though it is not yet known *how* EWI-2 inhibits cell-cell fusion, it is interesting to speculate that EWI-2, which contains 4 extracellular immunoglobulin domains [40], might prevent fusion by steric hinderance (i.e. keeping the two membranes apart) or by influencing the composition and organization of fusion inhibitory tetraspanin clusters/microdomains at the presynapse (as has been demonstrated in other cellular contexts [46-48]). Tetraspanins inhibit HIV-1-induced cell-cell fusion at a post-hemifusion stage [49], indicating that this family of host proteins may inhibit fusion as a "back up" to Gag-mediated restriction of Env-induced membrane fusion and therefore may only be necessary once Env has already initiated the fusion process. Further, it was recently demonstrated that the fusion inhibitory tetraspanin CD63 interacts directly with Env via the CD63 large extracellular loop (LEL) region [50]. It is intriguing to speculate that the LEL region of CD63 (and possibly other tetraspanins as well) might be a molecular determinant for tetraspanin-mediated inhibition of Env-induced cell-cell fusion, however this has not yet been tested. In addition to tetraspanins inhibiting cell-cell fusion at the VS, it is well-documented that tetraspanin incorporation into virus particles reduces particle infectivity [51-53]. Presumably, virus particles budding from the VS where tetraspanins are enriched could have increased incorporation of these host proteins, which would therefore be expected to decrease particle infectivity. This suggests a compromise where preventing cell-cell fusion at the VS is more critical for optimal virus spread than releasing highly infectious particles in this context, specifically because particles released at the VS are in very close proximity to the target cell and are released in high concentrations – potentially increasing the likelihood of establishing a new, productive infection.

Enrichment of both viral and host fusion inhibitory factors to the VS promotes efficient cell-to-cell transmission by restricting excessive HIV-1-induced syncytium formation, thus supporting exponential virus spread. It should be noted that efficacy of cell-cell fusion inhibition by these factors at the VS is variable, indicating that fusion inhibitory factor enrichment and/or overall organization at the VS is likely also variable. Additional data highlighting the importance of fusion regulation in viral spread is demonstrated in recent studies which identified decreased Env fusogenicity as a viral-evasion strategy when subjected to pressure from host restriction factors (APOBEC3G) [22], antiviral drugs or mutations to other viral proteins (p6 and Integrase) which typically impair particle infectivity [54]. These studies, combined with the identification of several fusion inhibitory factors, support the idea that robust fusion inhibition at this site may even *enhance* virus spread overall by extending the "window" for which virus can be transferred to the target cell without cell-cell fusion occurring.

### 2.5. T Cell Receptor Signaling

It has long been understood that infected-uninfected cell contact induces signaling necessary for cellular reorganization to form the VS and support efficient cell-to-cell transmission. Intriguingly, much of the reorganization and polarization at the infected:uninfected cell contact site upon VS formation parallels what has also been observed upon TCR-stimulation at the IS, including translocation of mitochondria and localized calcium flux [14,55,56]. A recent report enhanced our understanding of signaling events taking place at the VS by documenting that non-canonical and antigen-independent T cell receptor (TCR) signaling occurs upon infected-uninfected cell contact during HIV-

1 cell-to-cell transmission [57]. This finding supports previous reports indicating that TCR-like signaling events might be taking place during cell-to-cell transmission by demonstrating that host proteins known to be involved in T cell signaling during IS formation (LFA-1, ZAP-70) are also implicated in cell signaling upon Env-CD4-mediated cell-cell contact [19,58,59] and can positively contribute to efficient cell-to-cell transmission of HIV-1. However, ZAP-70 appears to also contribute to the viral replication cycle in a CD3-independent manner [3]. Additionally, lipid bilayers containing only gp120 and ICAM-1 (used as a minimal "producer cell" membrane) appeared to induce TCR-mediated signaling events in the target cell as well [59]. In further support of TCR-mediated signaling promoting efficient cell-to-cell transmission, CD3 knockdown in HIV-1-infected producer cells decreased cell-to-cell virus spread [57].

Intriguingly, it has been suggested that TCR-CD3-mediated signaling during HIV-1 cell-to-cell transmission may contribute to the virulence of this virus. Specifically, there is differential modulation of CD3 surface expression by the viral accessory protein Nef encoded by pathogenic (i.e. viruses which induce robust $CD4^+$ T cell depletion) and non-pathogenic primate lentiviruses [60]. For example, the Nef encoded by pathogenic lentiviruses such as the chimpanzee Simian Immunodeficiency Virus ($SIV_{CPZ}$) and HIV-1 typically do not downregulate CD3 upon infection, whereas Nef encoded by several non-pathogenic (in their respective natural hosts) strains of SIV, including $SIV_{SMM}$, can downregulate CD3 [60]. It is hypothesized that a lack of Nef-mediated CD3 downregulation enhances viral pathogenicity by inducing T cell activation [60], and possibly also by enhancing cell-to-cell transmission, as has indeed been demonstrated *in vitro* by targeted mutagenesis of HIV-1 Nef which impaired or restored CD3 modulation

[61]. Infected cells expressing a CD3-downregulating Nef variant produced less infectious particles than those from infected cells where Nef did not downregulate CD3 [61] which is somewhat in contrast with the previous findings that CD3 knockdown in infected producer cells did not affect particle infectivity [57]. Collectively, these studies indicate that Nef-mediated downregulation (or lack thereof) of CD3 influences the pathogenicity of primate lentivirus infection.

Overall, these studies support the idea that the presence of CD3 on infected cells allows for antigen-independent TCR-mediated signaling events at the VS, which may support polarization of viral and host factors to this contact site and also appear to promote efficient cell-to-cell transmission and increased viral pathogenicity (as previously described [61]).

### 2.6. Temporal Dynamics of Cell-to-Cell Transmission

For efficient cell-to-cell transmission, viral and host factors rapidly polarize to an Env-mediated producer-target cell contact site (the VS) to support assembly and release of virus particles, ultimately followed by complete cell-separation. Advancements in labeling HIV-1-infected cells by engineering virus strains to encode a fluorescent reporter or viral protein(s) bearing a fluorescent tag(s), facilitated investigating cell-to-cell transmission by live-cell imaging both *in vitro* and *in vivo*. Notably, the introduction of stable fluorescent tags to Gag and (more recently) Env in full-length virus strains allowed for clear microscopic visualization of VS formation, transfer of virus particles, and establishment of a new infection as a result of cell-to-cell transmission [9,62], as well as monitoring by flow cytometry [63,64]. Live-cell imaging studies, paired with analysis of the kinetics of viral

and host factor polarization to the VS in fixed cells, have greatly enhanced our understanding of the molecular determinants and temporal regulation which support VS formation and efficient cell-to-cell transmission.

Live-cell imaging of cells infected with a virus strain encoding both fluorescent protein-tagged Gag and Env revealed increased complexity of protein polarization to the VS [62], specifically that Env is transiently enriched at the synapse, and that recruitment of Env and Gag to the synapse occurs sequentially [62]. Briefly, Env was shown to be increasingly enriched at the presynapse over time beginning shortly after producer-target cell contact, but preceding Gag enrichment, and Env enrichment at the contact site eventually decreased while Gag remained [62]. The finding that there is dynamic and sequential recruitment of Env and Gag to the synapse complements the earlier finding that Gag polarization to the VS depends on the presence of both the EnvCT and the MA domain of Gag, regions which were subsequently shown to directly interact [65]. These studies collectively suggest that direct Gag-Env interactions upon initial Env enrichment at the VS might trigger further Gag recruitment to this site. Further, temporally organized protein enrichment to the VS likely extends to proteins recruited to Gag-enriched microdomains and to the VS, such as tetraspanins [66], which we predict are likely also enriched downstream of the formation of Env puncta at the VS as was seen for Gag [62]. Collectively, these studies suggest that, upon initial Env-CD4-mediated cell-cell contact, outside-in EnvCT-mediated signaling triggers subsequent polarization of Gag (and possibly additional proteins) to the VS.

However, the EnvCT is not required for polarization of all factors known to be enriched at the VS, such as the microtubule organizing center (MTOC), which is recruited

upon LFA-1 engagement in a manner that is independent of the EnvCT [19]. Further, LFA-1-induced signaling is predicted to contribute to re-localization of intracellular Env to the presynapse [19]. Taken together, we propose that during early VS formation there is likely (brief) temporal separation between factors recruited to the contact site that parallels the temporal dynamics seen for Env and Gag. Briefly, we predict that the temporal enrichment pattern of factors which are recruited in an EnvCT-independent manner would more closely reflect that of Env, while factors that depend on both the EnvCT and Gag would more closely reflect Gag enrichment patterns. However, we would like to note that this proposed system for temporal regulation of protein polarization to the VS is likely an *additional* element contributing to organized and robust polarization at the synapse, rather than an oversimplified model for all recruitment to the VS. We do not expect that this pattern could sufficiently describe the temporal enrichment patterns of *all* viral and cellular factors, for which it has been previously suggested that polarization to the HIV-1 VS depends on a combination of several different recruitment mechanisms [13].

Given that the VS is a transient junction between producer and target cells, efforts to characterize the duration of these dynamic contacts can advance our understanding of the conditions necessary for efficient cell-to-cell transmission. HIV-1 encoding GFP-labeled Gag ($Gag^{iGFP}$)[9] has been extremely valuable for delineating events taking place during cell-to-cell transmission using 2D culture systems and could be useful to apply in a 3D environment that is more similar to what infected cells would be expected to experience in tissue. One study that embedded $Gag^{iGFP}$ infected cells in a 3D extracellular matrix demonstrated that this culture system allows for visualization of virus transfer upon cell-cell contact and recapitulates infected cell morphologies documented by in situ imaging of

infected humanized mice [23] including that of small (2-4 nuclei) T cell-based syncytia [26], thus offering an alternative system for studying *in vitro* cell-to-cell spread by live-cell imaging. Indeed, cultures of primary T cells embedded in 3D collagen matrices were recently used to quantify the duration of infected-uninfected cell contacts, presumably at Env-dependent synapses, though this study did not use a fluorescently-labeled Gag or Env strain [67]. This investigation demonstrated that relatively short (25 min) contacts were sufficient to support continued virus spread under the particular environmental/3D culture conditions tested [67]. This finding implies that a 3D environment potentially alters the total duration of these transient contacts compared to a 2D environment where more robust, longer-lived synapses have been documented (separate reports documenting polarization at the synapse lasting 38-44 min [14] and cell-cell contacts with an average duration of 82 min [9]). Further, if the short-lived contacts observed between cells embedded in a 3D extracellular matrix are indeed VSs, the relatively short contact time between infected and uninfected T cells is seemingly analogous to previously described short-term IS-like events of actively migrating T cells termed "immunological kinapses" [68-71]. However, determining whether short-lived cell conjugates are indeed VS mediated contacts that can support cell-to-cell transmission will need to be further investigated using markers to confidently identify the VS. This 3D culture system for monitoring virus spread and which can be used to investigate VS dynamics may reveal potential new phenomena, such as short-lived contacts that appear to contribute to viral spread and which had not previously been recorded for HIV-1 infected cells by live-cell imaging of 2D cultures which typically captured robust, relatively longer-lasting synapses.

Together, these studies demonstrate that protein organization at the VS is dynamically and temporally regulated while also helping to capture the potential breadth of VS duration through visualization of both short and long-lived contacts that likely collectively contribute to efficient cell-to-cell spread *in vivo* depending on the environmental context.

## 2.7. Perspectives

HIV-1 cell-to-cell transmission has been an active area of investigation over the last few decades and has historically been suggested to be a high priority for continued HIV-1 research, even before the VS was first described [20]. However, we have observed that there is often a lack of clarity surrounding how cell-to-cell transmission differs from cell-free transmission. As such, we provided our current working definition of cell-to-cell transmission – productive infection that relies on virus transfer at the VS upon Env-CD4-mediated cell-cell contact – as a means to ground this review and potentially future conversations regarding this distinct mode of transmission.

We would like to expand on our definition of cell-to-cell transmission outlined above to help dispel lingering confusions regarding scenarios that might be mistaken for cell-to-cell transmission events. The key distinction between cell-free and cell-to-cell transmission lies in the spatiotemporal relationship between producer and target cell. During cell-free transmission, producer and target cell may be quite distant from each other, and the time elapsed between particle release and uptake could be relatively long. In contrast, during cell-to-cell transmission, the producer and target cell are kept directly apposed as a result of VS formation, and the virus transfer event which leads to productive

infection of the target cell occurs while the cells are still engaged in the VS. A particular case should be considered: a producer and target cell may be physically in contact, but Env-CD4 ligation may not have occurred and thus no VS is established, yet particles released by that producer cell may still be taken up by that target cell, resulting in successful infection. For the sake of simplicity, we would consider that to be a cell-free transmission event. In other words, we assume that cell-to-cell transmission also implies VS formation. Another instance of virus spread to consider is that of virus transfer at a dendritic cell (DC)-mediated cell-cell contact known as the infectious synapse. A DC can capture cell-free virus particles, without becoming productively infected, and release these captured particles in close proximity to a target cell upon DC-target cell contact. Although the infectious synapse and the VS share similar features as have been previously documented at the IS [1,2,72], DCs themselves are not infected nor does the infectious synapse formation between DC and target CD4+ T cells require Env-CD4 ligation [73], unlike the VS. Thus, while we do consider transfer at the infectious synapse to be a system that contributes to efficient virus spread, it is not cell-to-cell transmission. Further it should also be clearly stated here that we do not consider cell-cell fusion to be a form cell-to-cell transmission, nor a transmission event at all. By definition, virus transmission is the infection of a susceptible target cell by a virus. In contrast, cell-cell fusion merely involves the virus-dependent "absorption" of a target cell into the already-infected cell and is thus a process that both begins with and results in a single infected entity. A possible case where cell-cell fusion could be seen as a transmission event is if the resulting syncytium could then "divide" (presumably not by mitosis, but by simple fission) and if both "daughter cells" are then independently capable of onward virus transmission. However, this has not

been observed in the case of retroviruses, nor for any virus-induced cell-cell fusion process, to our knowledge. Together, we hope that this description has helped clarify the definition of HIV-1 cell-to-cell transmission (based on our current knowledge) and can thus be used for continued productive discussions and investigations regarding this mode of transmission including our perspectives on the direction(s) we would be eager to see the field move toward in the future.

Collectively, efforts by several groups have greatly enhanced our understanding of cell-to-cell transmission at the VS. While *in vitro* studies have been crucial for building a deeper appreciation of the necessary regulatory factors and events for cell-to-cell transmission under the conditions tested, relatively little is known regarding the significance of cell-to-cell transmission *in vivo* and will likely be a prominent focus for future investigations. Recent studies documenting the presence of HIV-1-induced syncytia *in vivo* by live-cell imaging of infected humanized mice [23,24] strongly suggest that cell-to-cell transmission likely occurs *in vivo*, given that syncytia form as a result of Env-induced cell-cell fusion at the VS, though productive infection following cell-to-cell transmission has yet to be demonstrated *in vivo*. Some efforts have been made to try to systematically analyze the relative efficiency and contribution of cell-to-cell transmission using *in vitro* [7,10,74-76] and *in silico* approaches [67,77,78]. These studies, combined with data demonstrating that migratory infected cells are the primary drivers of systemic virus spread including during the acute phase of infection [23,79,80] are often used to claim that cell-to-cell transmission is more efficient than cell-free and the dominant mode of spread *in vivo*. However, we would like to acknowledge that it is now clear that *in vitro* systems may not recapitulate the nuances of transmission *in vivo* (e.g. the identification of

cell-free virus particle "clouds" released from producer cells [26,81,82] as well as the high density of target cells present in tissue) that would be necessary to compare cell-to-cell to cell-free transmission. These potential limitations of *in vitro* analyses further complicate *in silico* modeling (based on conclusions from *in vitro* data) aiming to demonstrate how virus transmission may occur *in vivo*. Therefore, it is challenging to make claims regarding potential differences in efficiency and/or relative contributions to spread between cell-free and cell-to-cell transmission. As such, we hope that the conversation might shift toward one that is more inclusive by acknowledging how *both* modes likely play a significant role in overall virus spread *in vivo*. Here, we would like to also offer a perspective on how apparent distinctions between cell-to-cell and cell-free transmission might allow these two modes to differentially contribute to spread and suggest what still needs to be done to conclusively demonstrate whether cell-to-cell transmission does indeed play a role *in vivo*.

Although at this time it is difficult to compare the efficiency and contribution of cell-to-cell versus cell-free transmission, we can investigate whether host proteins, viral mutations, or alterations to environmental conditions differentially impact free virus particles (i.e. infectivity and release) and cell-to-cell transmission. For example, the host protein BST-2/tetherin is frequently described as a "restriction factor" as it inhibits efficient release of free virus particles [83,84]. However, the role of BST-2 in cell-to-cell transmission remains more controversial as BST-2 has actually been shown to *promote* efficient transmission at the VS [85] thus potentially demonstrating how host proteins might differentially influence stages of the viral replication cycle/modes of virus spread, though this phenomenon may be restricted to certain conditions (reviewed in [86]). Another prominent example of host proteins with differential influence on virus spread are members

of the tetraspanin family. Our group and others have demonstrated that increased incorporation of tetraspanins into virus particles reduces particle infectivity [51-53]. At the same time, tetraspanins do not strictly impair virus spread as these transmembrane proteins also promote efficient cell-to-cell transmission by inhibiting excessive HIV-1-induced cell-cell fusion at the VS [42,52]. We propose that additional factors which may have been exclusively studied for their influence on particle infectivity and release should be investigated for their role in cell-to-cell spread, such as recently described restriction factors PSGL-1 and CD43 (as suggested previously [87]). Such differential influence on free virus particles and cell-to-cell transmission at the VS are particularly intriguing as they support the idea that multiple modes of transmission collectively promote optimal virus spread by allowing efficient transmission in a variety of environmental contexts.

## 2.8. Conclusions

An extensive amount of work over the years has enhanced our understanding of cell-to-cell transmission at the VS. These efforts have characterized the VS structure and composition, as well as revealed the dynamic, multiform nature of this junction – including even the ability of infected cells to form multiple synapses with target cells at once (polysynapses) [88]! Further, it has also been demonstrated that cell-to-cell transmission can contribute to the infection of resting primary T cells and facilitate multicopy infection, indicating potential roles for cell-to-cell transmission in establishing a cellular reservoir and promoting viral heterogeneity and evolution [24,89-92] (and for a recent review of cell-to-cell transmission in latent infection see [6]). These advancements will fuel continued investigations into how cell-to-cell transmission could contribute to virus spread.

Future studies aimed at establishing that VSs form *in vivo*, which should be possible using our currently available resources, will greatly increase confidence that cell-to-cell transmission contributes to virus spread alongside cell-free infection *in vivo*. Although not currently feasible using animal models nor in natural human infection, we encourage that continued efforts are made to document the occurrence of cell-to-cell transmission *in vivo* using yet-to-be developed technologies that could increase the duration of live-cell imaging to effectively track the fate of a target cell upon virus transfer at a VS, or a labeling system that could allow for distinction between cells infected by cell-free and cell-to-cell transmission. Overall, cell-to-cell transmission at the VS is a unique mode of virus transmission that contributes to virus spread alongside other modes of transmission.

## 2.9. References


1. Jolly, C.; Sattentau, Q.J. Retroviral spread by induction of virological synapses. *Traffic* **2004**, *5*, 643-650, doi:10.1111/j.1600-0854.2004.00209.x.

2. Bangham, C.R.M. The immune control and cell-to-cell spread of human T-lymphotropic virus type 1. *J Gen Virol* **2003**, *84*, 3177-3189, doi:10.1099/vir.0.19334-0.

3. Alvarez, R.A.; Barría, M.I.; Chen, B.K. Unique features of HIV-1 spread through T cell virological synapses. *PLoS Pathog* **2014**, *10*, e1004513, doi:10.1371/journal.ppat.1004513.

4. Law, K.M.; Satija, N.; Esposito, A.M.; Chen, B.K. Cell-to-Cell Spread of HIV and Viral Pathogenesis. *Adv Virus Res* **2016**, *95*, 43-85, doi:10.1016/bs.aivir.2016.03.001.

5. Bracq, L.; Xie, M.; Benichou, S.; Bouchet, J. Mechanisms for Cell-to-Cell Transmission of HIV-1. *Front Immunol* **2018**, *9*, 260, doi:10.3389/fimmu.2018.00260.

6. Pedro, K.D.; Henderson, A.J.; Agosto, L.M. Mechanisms of HIV-1 cell-to-cell transmission and the establishment of the latent reservoir. *Virus Res* **2019**, *265*, 115-121, doi:10.1016/j.virusres.2019.03.014.

7. Zhong, P.; Agosto, L.M.; Munro, J.B.; Mothes, W. Cell-to-cell transmission of viruses. *Curr Opin Virol* **2013**, *3*, 44-50, doi:10.1016/j.coviro.2012.11.004.

8. Jolly, C.; Kashefi, K.; Hollinshead, M.; Sattentau, Q.J. HIV-1 cell to cell transfer across an Env-induced, actin-dependent synapse. *J Exp Med* **2004**, *199*, 283-293, doi:10.1084/jem.20030648.

9. Hübner, W.; McNerney, G.P.; Chen, P.; Dale, B.M.; Gordon, R.E.; Chuang, F.Y.; Li, X.D.; Asmuth, D.M.; Huser, T.; Chen, B.K. Quantitative 3D video microscopy of HIV transfer across T cell virological synapses. *Science* **2009**, *323*, 1743-1747, doi:10.1126/science.1167525.

10. Martin, N.; Welsch, S.; Jolly, C.; Briggs, J.A.; Vaux, D.; Sattentau, Q.J. Virological synapse-mediated spread of human immunodeficiency virus type 1 between T cells is sensitive to entry inhibition. *Journal of virology* **2010**, *84*, 3516-3527, doi:10.1128/jvi.02651-09.

11. Do, T.; Murphy, G.; Earl, L.A.; Del Prete, G.Q.; Grandinetti, G.; Li, G.H.; Estes, J.D.; Rao, P.; Trubey, C.M.; Thomas, J., et al. Three-dimensional imaging of HIV-1 virological synapses reveals membrane architectures involved in virus

transmission. *Journal of virology* **2014**, *88*, 10327-10339, doi:10.1128/jvi.00788-14.

12. Wang, L.; Eng, E.T.; Law, K.; Gordon, R.E.; Rice, W.J.; Chen, B.K. Visualization of HIV T Cell Virological Synapses and Virus-Containing Compartments by Three-Dimensional Correlative Light and Electron Microscopy. *Journal of virology* **2017**, *91*, doi:10.1128/jvi.01605-16.

13. Jolly, C. T cell polarization at the virological synapse. *Viruses* **2010**, *2*, 1261-1278, doi:10.3390/v2061261.

14. Groppelli, E.; Starling, S.; Jolly, C. Contact-induced mitochondrial polarization supports HIV-1 virological synapse formation. *Journal of virology* **2015**, *89*, 14-24, doi:10.1128/jvi.02425-14.

15. Jolly, C.; Welsch, S.; Michor, S.; Sattentau, Q.J. The regulated secretory pathway in CD4(+) T cells contributes to human immunodeficiency virus type-1 cell-to-cell spread at the virological synapse. *PLoS Pathog* **2011**, *7*, e1002226, doi:10.1371/journal.ppat.1002226.

16. Zhong, P.; Agosto, L.M.; Ilinskaya, A.; Dorjbal, B.; Truong, R.; Derse, D.; Uchil, P.D.; Heidecker, G.; Mothes, W. Cell-to-cell transmission can overcome multiple donor and target cell barriers imposed on cell-free HIV. *PLoS One* **2013**, *8*, e53138, doi:10.1371/journal.pone.0053138.

17. Whitaker, E.E.; Matheson, N.J.; Perlee, S.; Munson, P.B.; Symeonides, M.; Thali, M. EWI-2 Inhibits Cell-Cell Fusion at the HIV-1 Virological Presynapse. *Viruses* **2019**, *11*, doi:10.3390/v11121082.

18. Jolly, C.; Mitar, I.; Sattentau, Q.J. Adhesion molecule interactions facilitate human immunodeficiency virus type 1-induced virological synapse formation between T cells. *Journal of virology* **2007**, *81*, 13916-13921, doi:10.1128/jvi.01585-07.

19. Starling, S.; Jolly, C. LFA-1 Engagement Triggers T Cell Polarization at the HIV-1 Virological Synapse. *Journal of virology* **2016**, *90*, 9841-9854, doi:10.1128/jvi.01152-16.

20. Phillips, D.M. The role of cell-to-cell transmission in HIV infection. *Aids* **1994**, *8*, 719-731, doi:10.1097/00002030-199406000-00001.

21. Montefiori, D.C.; Mitchell, W.M. Persistent coinfection of T lymphocytes with HTLV-II and HIV and the role of syncytium formation in HIV-induced cytopathic effect. *Virology* **1987**, *160*, 372-378, doi:10.1016/0042-6822(87)90008-0.

22. Ikeda, T.; Symeonides, M.; Albin, J.S.; Li, M.; Thali, M.; Harris, R.S. HIV-1 adaptation studies reveal a novel Env-mediated homeostasis mechanism for

evading lethal hypermutation by APOBEC3G. *PLoS Pathog* **2018**, *14*, e1007010, doi:10.1371/journal.ppat.1007010.

23. Murooka, T.T.; Deruaz, M.; Marangoni, F.; Vrbanac, V.D.; Seung, E.; von Andrian, U.H.; Tager, A.M.; Luster, A.D.; Mempel, T.R. HIV-infected T cells are migratory vehicles for viral dissemination. *Nature* **2012**, *490*, 283-287, doi:10.1038/nature11398.

24. Law, K.M.; Komarova, N.L.; Yewdall, A.W.; Lee, R.K.; Herrera, O.L.; Wodarz, D.; Chen, B.K. In Vivo HIV-1 Cell-to-Cell Transmission Promotes Multicopy Micro-compartmentalized Infection. *Cell Rep* **2016**, *15*, 2771-2783, doi:10.1016/j.celrep.2016.05.059.

25. Ventura, J.D.; Beloor, J.; Allen, E.; Zhang, T.; Haugh, K.A.; Uchil, P.D.; Ochsenbauer, C.; Kieffer, C.; Kumar, P.; Hope, T.J., et al. Longitudinal bioluminescent imaging of HIV-1 infection during antiretroviral therapy and treatment interruption in humanized mice. *PLoS Pathog* **2019**, *15*, e1008161, doi:10.1371/journal.ppat.1008161.

26. Symeonides, M.; Murooka, T.T.; Bellfy, L.N.; Roy, N.H.; Mempel, T.R.; Thali, M. HIV-1-Induced Small T Cell Syncytia Can Transfer Virus Particles to Target Cells through Transient Contacts. *Viruses* **2015**, *7*, 6590-6603, doi:10.3390/v7122959.

27. Roy, N.H.; Chan, J.; Lambelé, M.; Thali, M. Clustering and mobility of HIV-1 Env at viral assembly sites predict its propensity to induce cell-cell fusion. *Journal of virology* **2013**, *87*, 7516-7525, doi:10.1128/jvi.00790-13.

28. Gardiner, J.C.; Mauer, E.J.; Sherer, N.M. HIV-1 Gag, Envelope, and Extracellular Determinants Cooperate To Regulate the Stability and Turnover of Virological Synapses. *Journal of virology* **2016**, *90*, 6583-6597, doi:10.1128/jvi.00600-16.

29. Freed, E.O. HIV-1 assembly, release and maturation. *Nat Rev Microbiol* **2015**, *13*, 484-496, doi:10.1038/nrmicro3490.

30. Murakami, T.; Ablan, S.; Freed, E.O.; Tanaka, Y. Regulation of human immunodeficiency virus type 1 Env-mediated membrane fusion by viral protease activity. *Journal of virology* **2004**, *78*, 1026-1031, doi:10.1128/jvi.78.2.1026-1031.2004.

31. Wyma, D.J.; Jiang, J.; Shi, J.; Zhou, J.; Lineberger, J.E.; Miller, M.D.; Aiken, C. Coupling of human immunodeficiency virus type 1 fusion to virion maturation: a novel role of the gp41 cytoplasmic tail. *Journal of virology* **2004**, *78*, 3429-3435, doi:10.1128/jvi.78.7.3429-3435.2004.

32. Jiang, J.; Aiken, C. Maturation-dependent human immunodeficiency virus type 1 particle fusion requires a carboxyl-terminal region of the gp41 cytoplasmic tail. *Journal of virology* **2007**, *81*, 9999-10008, doi:10.1128/jvi.00592-07.

33. Chojnacki, J.; Staudt, T.; Glass, B.; Bingen, P.; Engelhardt, J.; Anders, M.; Schneider, J.; Müller, B.; Hell, S.W.; Kräusslich, H.G. Maturation-dependent HIV-1 surface protein redistribution revealed by fluorescence nanoscopy. *Science* **2012**, *338*, 524-528, doi:10.1126/science.1226359.

34. Rowell, J.F.; Stanhope, P.E.; Siliciano, R.F. Endocytosis of endogenously synthesized HIV-1 envelope protein. Mechanism and role in processing for association with class II MHC. *J Immunol* **1995**, *155*, 473-488.

35. Kirschman, J.; Qi, M.; Ding, L.; Hammonds, J.; Dienger-Stambaugh, K.; Wang, J.J.; Lapierre, L.A.; Goldenring, J.R.; Spearman, P. HIV-1 Envelope Glycoprotein Trafficking through the Endosomal Recycling Compartment Is Required for Particle Incorporation. *Journal of virology* **2018**, *92*, doi:10.1128/jvi.01893-17.

36. Berlioz-Torrent, C.; Shacklett, B.L.; Erdtmann, L.; Delamarre, L.; Bouchaert, I.; Sonigo, P.; Dokhelar, M.C.; Benarous, R. Interactions of the cytoplasmic domains of human and simian retroviral transmembrane proteins with components of the clathrin adaptor complexes modulate intracellular and cell surface expression of envelope glycoproteins. *Journal of virology* **1999**, *73*, 1350-1361, doi:10.1128/jvi.73.2.1350-1361.1999.

37. Sala-Valdés, M.; Ursa, A.; Charrin, S.; Rubinstein, E.; Hemler, M.E.; Sánchez-Madrid, F.; Yáñez-Mó, M. EWI-2 and EWI-F link the tetraspanin web to the actin cytoskeleton through their direct association with ezrin-radixin-moesin proteins. *J Biol Chem* **2006**, *281*, 19665-19675, doi:10.1074/jbc.M602116200.

38. Charrin, S.; Le Naour, F.; Labas, V.; Billard, M.; Le Caer, J.P.; Emile, J.F.; Petit, M.A.; Boucheix, C.; Rubinstein, E. EWI-2 is a new component of the tetraspanin web in hepatocytes and lymphoid cells. *Biochem J* **2003**, *373*, 409-421, doi:10.1042/bj20030343.

39. Montpellier, C.; Tews, B.A.; Poitrimole, J.; Rocha-Perugini, V.; D'Arienzo, V.; Potel, J.; Zhang, X.A.; Rubinstein, E.; Dubuisson, J.; Cocquerel, L. Interacting regions of CD81 and two of its partners, EWI-2 and EWI-2wint, and their effect on hepatitis C virus infection. *J Biol Chem* **2011**, *286*, 13954-13965, doi:10.1074/jbc.M111.220103.

40. Stipp, C.S.; Kolesnikova, T.V.; Hemler, M.E. EWI-2 is a major CD9 and CD81 partner and member of a novel Ig protein subfamily. *J Biol Chem* **2001**, *276*, 40545-40554, doi:10.1074/jbc.M107338200.

41. Roy, N.H.; Lambelé, M.; Chan, J.; Symeonides, M.; Thali, M. Ezrin is a component of the HIV-1 virological presynapse and contributes to the inhibition of cell-cell fusion. *Journal of virology* **2014**, *88*, 7645-7658, doi:10.1128/jvi.00550-14.

42. Weng, J.; Krementsov, D.N.; Khurana, S.; Roy, N.H.; Thali, M. Formation of syncytia is repressed by tetraspanins in human immunodeficiency virus type 1-

producing cells. *Journal of virology* **2009**, *83*, 7467-7474, doi:10.1128/jvi.00163-09.

43. Chen, A.; Leikina, E.; Melikov, K.; Podbilewicz, B.; Kozlov, M.M.; Chernomordik, L.V. Fusion-pore expansion during syncytium formation is restricted by an actin network. *J Cell Sci* **2008**, *121*, 3619-3628, doi:10.1242/jcs.032169.

44. Wurth, M.A.; Schowalter, R.M.; Smith, E.C.; Moncman, C.L.; Dutch, R.E.; McCann, R.O. The actin cytoskeleton inhibits pore expansion during PIV5 fusion protein-promoted cell-cell fusion. *Virology* **2010**, *404*, 117-126, doi:10.1016/j.virol.2010.04.024.

45. Pontow, S.E.; Heyden, N.V.; Wei, S.; Ratner, L. Actin cytoskeletal reorganizations and coreceptor-mediated activation of rac during human immunodeficiency virus-induced cell fusion. *Journal of virology* **2004**, *78*, 7138-7147, doi:10.1128/jvi.78.13.7138-7147.2004.

46. Kolesnikova, T.V.; Kazarov, A.R.; Lemieux, M.E.; Lafleur, M.A.; Kesari, S.; Kung, A.L.; Hemler, M.E. Glioblastoma inhibition by cell surface immunoglobulin protein EWI-2, in vitro and in vivo. *Neoplasia* **2009**, *11*, 77-86, 74p following 86, doi:10.1593/neo.81180.

47. Wang, H.X.; Hemler, M.E. Novel impact of EWI-2, CD9, and CD81 on TGF-β signaling in melanoma. *Mol Cell Oncol* **2015**, *2*, doi:10.1080/23723556.2015.1030536.

48. Wang, H.X.; Sharma, C.; Knoblich, K.; Granter, S.R.; Hemler, M.E. EWI-2 negatively regulates TGF-β signaling leading to altered melanoma growth and metastasis. *Cell Res* **2015**, *25*, 370-385, doi:10.1038/cr.2015.17.

49. Symeonides, M.; Lambele, M.; Roy, N.H.; Thali, M. Evidence showing that tetraspanins inhibit HIV-1-induced cell-cell fusion at a post-hemifusion stage. *Viruses* **2014**, *6*, 1078-1090, doi:10.3390/v6031078.

50. Ivanusic, D.; Madela, K.; Bannert, N.; Denner, J. The large extracellular loop of CD63 interacts with gp41 of HIV-1 and is essential for establishing the virological synapse. *Sci Rep* **2021**, *11*, 10011, doi:10.1038/s41598-021-89523-7.

51. Sato, K.; Aoki, J.; Misawa, N.; Daikoku, E.; Sano, K.; Tanaka, Y.; Koyanagi, Y. Modulation of human immunodeficiency virus type 1 infectivity through incorporation of tetraspanin proteins. *Journal of virology* **2008**, *82*, 1021-1033, doi:10.1128/jvi.01044-07.

52. Krementsov, D.N.; Weng, J.; Lambele, M.; Roy, N.H.; Thali, M. Tetraspanins regulate cell-to-cell transmission of HIV-1. *Retrovirology* **2009**, *6*, 64, doi:10.1186/1742-4690-6-64.

53. Lambelé, M.; Koppensteiner, H.; Symeonides, M.; Roy, N.H.; Chan, J.; Schindler, M.; Thali, M. Vpu is the main determinant for tetraspanin downregulation in HIV-1-infected cells. *Journal of virology* **2015**, *89*, 3247-3255, doi:10.1128/jvi.03719-14.

54. Van Duyne, R.; Kuo, L.S.; Pham, P.; Fujii, K.; Freed, E.O. Mutations in the HIV-1 envelope glycoprotein can broadly rescue blocks at multiple steps in the virus replication cycle. *Proc Natl Acad Sci U S A* **2019**, *116*, 9040-9049, doi:10.1073/pnas.1820333116.

55. Quintana, A.; Schwindling, C.; Wenning, A.S.; Becherer, U.; Rettig, J.; Schwarz, E.C.; Hoth, M. T cell activation requires mitochondrial translocation to the immunological synapse. *Proc Natl Acad Sci U S A* **2007**, *104*, 14418-14423, doi:10.1073/pnas.0703126104.

56. Trebak, M.; Kinet, J.P. Calcium signalling in T cells. *Nat Rev Immunol* **2019**, *19*, 154-169, doi:10.1038/s41577-018-0110-7.

57. Len, A.C.L.; Starling, S.; Shivkumar, M.; Jolly, C. HIV-1 Activates T Cell Signaling Independently of Antigen to Drive Viral Spread. *Cell Rep* **2017**, *18*, 1062-1074, doi:10.1016/j.celrep.2016.12.057.

58. Sol-Foulon, N.; Sourisseau, M.; Porrot, F.; Thoulouze, M.I.; Trouillet, C.; Nobile, C.; Blanchet, F.; di Bartolo, V.; Noraz, N.; Taylor, N., et al. ZAP-70 kinase regulates HIV cell-to-cell spread and virological synapse formation. *Embo j* **2007**, *26*, 516-526, doi:10.1038/sj.emboj.7601509.

59. Vasiliver-Shamis, G.; Cho, M.W.; Hioe, C.E.; Dustin, M.L. Human immunodeficiency virus type 1 envelope gp120-induced partial T-cell receptor signaling creates an F-actin-depleted zone in the virological synapse. *Journal of virology* **2009**, *83*, 11341-11355, doi:10.1128/jvi.01440-09.

60. Schindler, M.; Münch, J.; Kutsch, O.; Li, H.; Santiago, M.L.; Bibollet-Ruche, F.; Müller-Trutwin, M.C.; Novembre, F.J.; Peeters, M.; Courgnaud, V., et al. Nef-mediated suppression of T cell activation was lost in a lentiviral lineage that gave rise to HIV-1. *Cell* **2006**, *125*, 1055-1067, doi:10.1016/j.cell.2006.04.033.

61. Mesner, D.; Hotter, D.; Kirchhoff, F.; Jolly, C. Loss of Nef-mediated CD3 down-regulation in the HIV-1 lineage increases viral infectivity and spread. *Proc Natl Acad Sci U S A* **2020**, *117*, 7382-7391, doi:10.1073/pnas.1921135117.

62. Wang, L.; Izadmehr, S.; Kamau, E.; Kong, X.P.; Chen, B.K. Sequential trafficking of Env and Gag to HIV-1 T cell virological synapses revealed by live imaging. *Retrovirology* **2019**, *16*, 2, doi:10.1186/s12977-019-0464-3.

63. Dale, B.M.; McNerney, G.P.; Hübner, W.; Huser, T.R.; Chen, B.K. Tracking and quantitation of fluorescent HIV during cell-to-cell transmission. *Methods* **2011**, *53*, 20-26, doi:10.1016/j.ymeth.2010.06.018.

64. Durham, N.D.; Chen, B.K. Measuring T Cell-to-T Cell HIV-1 Transfer, Viral Fusion, and Infection Using Flow Cytometry. *Methods Mol Biol* **2016**, *1354*, 21-38, doi:10.1007/978-1-4939-3046-3_2.

65. Alfadhli, A.; Staubus, A.O.; Tedbury, P.R.; Novikova, M.; Freed, E.O.; Barklis, E. Analysis of HIV-1 Matrix-Envelope Cytoplasmic Tail Interactions. *Journal of virology* **2019**, *93*, doi:10.1128/jvi.01079-19.

66. Krementsov, D.N.; Rassam, P.; Margeat, E.; Roy, N.H.; Schneider-Schaulies, J.; Milhiet, P.E.; Thali, M. HIV-1 assembly differentially alters dynamics and partitioning of tetraspanins and raft components. *Traffic* **2010**, *11*, 1401-1414, doi:10.1111/j.1600-0854.2010.01111.x.

67. Imle, A.; Kumberger, P.; Schnellbächer, N.D.; Fehr, J.; Carrillo-Bustamante, P.; Ales, J.; Schmidt, P.; Ritter, C.; Godinez, W.J.; Müller, B., et al. Experimental and computational analyses reveal that environmental restrictions shape HIV-1 spread in 3D cultures. *Nat Commun* **2019**, *10*, 2144, doi:10.1038/s41467-019-09879-3.

68. Dustin, M.L. Cell adhesion molecules and actin cytoskeleton at immune synapses and kinapses. *Curr Opin Cell Biol* **2007**, *19*, 529-533, doi:10.1016/j.ceb.2007.08.003.

69. Dustin, M.L. T-cell activation through immunological synapses and kinapses. *Immunol Rev* **2008**, *221*, 77-89, doi:10.1111/j.1600-065X.2008.00589.x.

70. Friedman, R.S.; Beemiller, P.; Sorensen, C.M.; Jacobelli, J.; Krummel, M.F. Real-time analysis of T cell receptors in naive cells in vitro and in vivo reveals flexibility in synapse and signaling dynamics. *J Exp Med* **2010**, *207*, 2733-2749, doi:10.1084/jem.20091201.

71. Mayya, V.; Judokusumo, E.; Abu Shah, E.; Peel, C.G.; Neiswanger, W.; Depoil, D.; Blair, D.A.; Wiggins, C.H.; Kam, L.C.; Dustin, M.L. Durable Interactions of T Cells with T Cell Receptor Stimuli in the Absence of a Stable Immunological Synapse. *Cell Rep* **2018**, *22*, 340-349, doi:10.1016/j.celrep.2017.12.052.

72. McDonald, D.; Wu, L.; Bohks, S.M.; KewalRamani, V.N.; Unutmaz, D.; Hope, T.J. Recruitment of HIV and its receptors to dendritic cell-T cell junctions. *Science* **2003**, *300*, 1295-1297, doi:10.1126/science.1084238.

73. Rodriguez-Plata, M.T.; Puigdomènech, I.; Izquierdo-Useros, N.; Puertas, M.C.; Carrillo, J.; Erkizia, I.; Clotet, B.; Blanco, J.; Martinez-Picado, J. The infectious synapse formed between mature dendritic cells and CD4(+) T cells is independent

of the presence of the HIV-1 envelope glycoprotein. *Retrovirology* **2013**, *10*, 42, doi:10.1186/1742-4690-10-42.

74. Dimitrov, D.S.; Willey, R.L.; Sato, H.; Chang, L.J.; Blumenthal, R.; Martin, M.A. Quantitation of human immunodeficiency virus type 1 infection kinetics. *Journal of virology* **1993**, *67*, 2182-2190, doi:10.1128/jvi.67.4.2182-2190.1993.

75. Chen, P.; Hübner, W.; Spinelli, M.A.; Chen, B.K. Predominant mode of human immunodeficiency virus transfer between T cells is mediated by sustained Env-dependent neutralization-resistant virological synapses. *Journal of virology* **2007**, *81*, 12582-12595, doi:10.1128/jvi.00381-07.

76. Sourisseau, M.; Sol-Foulon, N.; Porrot, F.; Blanchet, F.; Schwartz, O. Inefficient human immunodeficiency virus replication in mobile lymphocytes. *Journal of virology* **2007**, *81*, 1000-1012, doi:10.1128/jvi.01629-06.

77. Komarova, N.L.; Anghelina, D.; Voznesensky, I.; Trinité, B.; Levy, D.N.; Wodarz, D. Relative contribution of free-virus and synaptic transmission to the spread of HIV-1 through target cell populations. *Biol Lett* **2013**, *9*, 20121049, doi:10.1098/rsbl.2012.1049.

78. Zhang, C.; Zhou, S.; Groppelli, E.; Pellegrino, P.; Williams, I.; Borrow, P.; Chain, B.M.; Jolly, C. Hybrid spreading mechanisms and T cell activation shape the dynamics of HIV-1 infection. *PLoS Comput Biol* **2015**, *11*, e1004179, doi:10.1371/journal.pcbi.1004179.

79. Deruaz, M.; Murooka, T.T.; Ji, S.; Gavin, M.A.; Vrbanac, V.D.; Lieberman, J.; Tager, A.M.; Mempel, T.R.; Luster, A.D. Chemoattractant-mediated leukocyte trafficking enables HIV dissemination from the genital mucosa. *JCI Insight* **2017**, *2*, e88533, doi:10.1172/jci.insight.88533.

80. Usmani, S.M.; Murooka, T.T.; Deruaz, M.; Koh, W.H.; Sharaf, R.R.; Di Pilato, M.; Power, K.A.; Lopez, P.; Hnatiuk, R.; Vrbanac, V.D., et al. HIV-1 Balances the Fitness Costs and Benefits of Disrupting the Host Cell Actin Cytoskeleton Early after Mucosal Transmission. *Cell Host Microbe* **2019**, *25*, 73-86.e75, doi:10.1016/j.chom.2018.12.008.

81. Ladinsky, M.S.; Kieffer, C.; Olson, G.; Deruaz, M.; Vrbanac, V.; Tager, A.M.; Kwon, D.S.; Bjorkman, P.J. Electron tomography of HIV-1 infection in gut-associated lymphoid tissue. *PLoS Pathog* **2014**, *10*, e1003899, doi:10.1371/journal.ppat.1003899.

82. Kieffer, C.; Ladinsky, M.S.; Ninh, A.; Galimidi, R.P.; Bjorkman, P.J. Longitudinal imaging of HIV-1 spread in humanized mice with parallel 3D immunofluorescence and electron tomography. *Elife* **2017**, *6*, doi:10.7554/eLife.23282.

83. Neil, S.J.; Zang, T.; Bieniasz, P.D. Tetherin inhibits retrovirus release and is antagonized by HIV-1 Vpu. *Nature* **2008**, *451*, 425-430, doi:10.1038/nature06553.

84. Van Damme, N.; Goff, D.; Katsura, C.; Jorgenson, R.L.; Mitchell, R.; Johnson, M.C.; Stephens, E.B.; Guatelli, J. The interferon-induced protein BST-2 restricts HIV-1 release and is downregulated from the cell surface by the viral Vpu protein. *Cell Host Microbe* **2008**, *3*, 245-252, doi:10.1016/j.chom.2008.03.001.

85. Jolly, C.; Booth, N.J.; Neil, S.J. Cell-cell spread of human immunodeficiency virus type 1 overcomes tetherin/BST-2-mediated restriction in T cells. *Journal of virology* **2010**, *84*, 12185-12199, doi:10.1128/jvi.01447-10.

86. Dale, B.M.; Alvarez, R.A.; Chen, B.K. Mechanisms of enhanced HIV spread through T-cell virological synapses. *Immunol Rev* **2013**, *251*, 113-124, doi:10.1111/imr.12022.

87. Murakami, T.; Carmona, N.; Ono, A. Virion-incorporated PSGL-1 and CD43 inhibit both cell-free infection and transinfection of HIV-1 by preventing virus-cell binding. *Proc Natl Acad Sci U S A* **2020**, *117*, 8055-8063, doi:10.1073/pnas.1916055117.

88. Rudnicka, D.; Feldmann, J.; Porrot, F.; Wietgrefe, S.; Guadagnini, S.; Prévost, M.C.; Estaquier, J.; Haase, A.T.; Sol-Foulon, N.; Schwartz, O. Simultaneous cell-to-cell transmission of human immunodeficiency virus to multiple targets through polysynapses. *Journal of virology* **2009**, *83*, 6234-6246, doi:10.1128/jvi.00282-09.

89. Del Portillo, A.; Tripodi, J.; Najfeld, V.; Wodarz, D.; Levy, D.N.; Chen, B.K. Multiploid inheritance of HIV-1 during cell-to-cell infection. *Journal of virology* **2011**, *85*, 7169-7176, doi:10.1128/jvi.00231-11.

90. Agosto, L.M.; Herring, M.B.; Mothes, W.; Henderson, A.J. HIV-1-Infected CD4+ T Cells Facilitate Latent Infection of Resting CD4+ T Cells through Cell-Cell Contact. *Cell Rep* **2018**, *24*, 2088-2100, doi:10.1016/j.celrep.2018.07.079.

91. Kreger, J.; Komarova, N.L.; Wodarz, D. Effect of synaptic cell-to-cell transmission and recombination on the evolution of double mutants in HIV. *J R Soc Interface* **2020**, *17*, 20190832, doi:10.1098/rsif.2019.0832.

92. Kreger, J.; Garcia, J.; Zhang, H.; Komarova, N.L.; Wodarz, D.; Levy, D.N. Quantifying the dynamics of viral recombination during free virus and cell-to-cell transmission in HIV-1 infection. *Virus Evol* **2021**, *7*, veab026, doi:10.1093/ve/veab026.

# CHAPTER 3 : EWI-2 INHIBITS CELL-CELL FUSION AT THE HIV-1 VIROLOGICAL PRESYNAPSE

Emily E. Whitaker [1,2], Nicholas J. Matheson [3,4], Sarah Perlee [1,†] , Phillip B. Munson [2,5,‡], Menelaos Symeonides [1,2,§] and Markus Thali [1,2,§]

[1] Department of Microbiology and Molecular Genetics, University of Vermont, Burlington, VT 05405, USA

[2] Graduate Program in Cellular, Molecular, and Biomedical Sciences, University of Vermont, Burlington, VT 05405, USA

[3] Department of Medicine, University of Cambridge, Cambridge CB2 0QQ, UK

[4] Cambridge Institute for Therapeutic Immunology and Infectious Disease (CITIID), University of Cambridge, Cambridge CB2 0AW, UK

[5] Department of Pathology and Laboratory Medicine, University of Vermont, Burlington,VT 05405, USA

† Current affiliation: Memorial Sloan Kettering Cancer Center, Louis V. Gerstner, Jr. Graduate School of Biomedical Sciences, New York, NY 10065, USA.

‡ Current affiliation: Massachusetts General Hospital, Cutaneous Biology Research Center, Charlestown, MA 02129, USA.

§ Co-senior authors.

## 3.1 Abstract

Cell-to-cell transfer of virus particles at the Env-dependent virological synapse (VS) is a highly efficient mode of HIV-1 transmission. While cell–cell fusion could be triggered at the VS, leading to the formation of syncytia and preventing exponential growth of the infected cell population, this is strongly inhibited by both viral (Gag) and host (ezrin and tetraspanins) proteins. Here, we identify EWI-2, a protein that was previously shown to associate with ezrin and tetraspanins, as a host factor that contributes to the inhibition of Env-mediated cell–cell fusion. Using quantitative fluorescence microscopy, shRNA knockdowns, and cell–cell fusion assays, we show that EWI-2 accumulates at the presynaptic terminal (i.e., the producer cell side of the VS), where it contributes to the fusion-preventing activities of the other viral and cellular components. We also find that EWI-2, like tetraspanins, is downregulated upon HIV-1 infection, most likely by Vpu. Despite the strong inhibition of fusion at the VS, T cell-based syncytia do form *in vivo* and in physiologically relevant culture systems, but they remain small. In regard to that, we demonstrate that EWI-2 and CD81 levels are restored on the surface of syncytia, where they (presumably) continue to act as fusion inhibitors. This study documents a new role for EWI-2 as an inhibitor of HIV-1-induced cell–cell fusion and provides novel insight into how syncytia are prevented from fusing indefinitely.

## 3.2 Introduction

HIV-1 spreads between T cells primarily through two modes of transmission: the release of cell-free virus particles followed by their uptake by (more or less distantly located) cells expressing the viral receptor/co-receptor, and the cell-to-cell transmission of

particles to an adjacent cell via the virological synapse (VS), i.e., when infected and uninfected cells transiently align. The formation of the HIV-1 VS is initiated by the viral envelope glycoprotein (Env) on the surface of productively infected cells binding to its receptor, CD4, on target T cells [1] and is followed by the polarization of Gag at the cell–cell contact site [1,2]. Virus particles are then released in high concentrations towards the target cell [3], facilitating efficient infection while also possibly shielding virus particles from some neutralizing antibodies ([4] and recently reviewed in [5]). Indeed, as demonstrated in a recent study using physiologically relevant cell culture systems [6], it is possible that virus that is not released in close proximity to a target cell is rapidly inactivated, emphasizing the importance of VS-mediated transmission. However, given that Env is fusogenic at neutral pH, it would seem likely at first that VS-mediated contacts should frequently result in cell–cell fusion, thus forming a multinucleated infected cell (syncytium). While we now know that small, T cell-based syncytia arise early in HIV-1 infection and can spread the virus by cell–cell contact [7–12], the majority of infected T cells observed in lymphoid tissue are mononucleated, documenting that most HIV-1 VSs ultimately result in complete cell separation and the generation of a new, productively infected cell. This is likely due to tight regulation at the VS that acts to prevent excessive syncytium formation (reviewed in [13,14]).

Multiple independent studies have identified viral and host functions which, together, prevent excessive HIV-1-induced cell–cell fusion at the VS. Firstly, Env is rapidly downregulated from the surface of infected cells in the absence of Gag [15,16]. Secondly, upon Gag multimerization at the plasma membrane, Env is trapped by immature Gag through Env's cytoplasmic tail and maintained in a poorly fusogenic state [17]. This

trapping by Gag ends only after Env's incorporation into virus particles when Gag precursor gets cleaved, i.e., upon maturation [18–21]. The residual fusion activity of Gag-trapped Env on infected cells has been shown to be inhibited by several host membrane proteins that accumulate at the producer cell side of the VS, including tetraspanins and phosphorylated ezrin (p-ezrin) [22–24]. Tetraspanins inhibit HIV-1-induced cell–cell fusion at a post-hemifusion stage [23], while ezrin is implicated in F-actin organization and the recruitment of the tetraspanin CD81 to the VS [24]. It remains unclear how and whether these protein functions are coordinated, though based on other cell–cell fusion regulation paradigms (discussed below), additional host proteins are likely required to mediate the efficient inhibition of HIV-1-induced fusion by tetraspanins and ezrin.

EWI-F (CD9P-1/FPRP) is an immunoglobulin superfamily (IgSF) member and partner of tetraspanins CD9 and CD81 [25]. EWI-F was shown to be a potent inhibitor of cell–cell fusion in myoblasts, where EWI-F knockout resulted in more frequent fusion than CD9/CD81 double knockout [26]. However, EWI-F is poorly expressed in T cells [27], the primary host cell type for HIV-1. A related protein, EWI-2 (IGSF8/PGRL) [28,29], which also associates with tetraspanins and is expressed in T cells [25,27], has been documented to play a role in hepatitis C virus (HCV) entry [30,31] and T cell immunological synapse (IS) formation [32]. The latter study also suggested that EWI-2 has a yet undetermined involvement in HIV-1 particle production [32]. Furthermore, both EWI-F and EWI-2 interact with ezrin to organize the cytoskeleton in concert with tetraspanins [27]. EWI-2 thus lies at the nexus of tetraspanins, ezrin, and the actin cytoskeleton (which can also inhibit cell–cell fusion) [33].

## 3.3 Materials and Methods

### *3.3.1. Cell Lines and Cell Culture*

The following cells were obtained through the NIH AIDS Reagent Program (Germantown, MD, USA), Division of AIDS, NIAID, NIH: HeLa cells from Dr. Richard Axel [34], TZM-bl cells from Dr. John C. Kappes, Dr. Xiaoyun Wu, and Tranzyme Inc. [35–39], CEM.NKR CCR5+Luc+ (CEM-luc) cells from Dr. John Moore and Dr. Catherine Spenlehauer [40,41], CEM-T4 cells from Dr. J.P. Jacobs [42], and CEM-SS cells from Dr. Peter L. Nara [34,43,44].

HEK 293T, HeLa, and TZM-bl cells were maintained in Dulbecco's Modification of Eagle's Medium (DMEM) (Corning, Corning, NY, USA, Cat. #10-017-CV) containing 10% fetal bovine serum (FBS; Corning, Corning, NY, USA, Cat. #35-010-CV) and antibiotics (100 units/mL penicillin and 100 µg/mL streptomycin; Invitrogen, Carlsbad, CA, USA). CEM-luc cells were maintained in RPMI 1640 medium (Corning, Corning, NY, USA, Cat. #10-104-CV) supplemented with 10% FBS and 0.8 mg/mL geneticin sulfate (G418). CEM2n, a kind gift from R. Harris [45], and CEM-SS cells were maintained in RPMI medium supplemented with 10% FBS and antibiotics.

Human primary blood mononuclear cells (PBMCs) were isolated as buffy coats from the whole blood of healthy donors by Ficoll density centrifugation. $CD4^+$ T cells were enriched from PBMCs by negative selection using the MACS $CD4^+$ T Cell Isolation Kit (Miltenyi Biotec, Auburn, CA, USA, Cat. #130-096-533) or the EasySep Human $CD4^+$ T Cell Isolation Kit (STEMCELL Technologies, Vancouver, BC, Canada, Cat. #17952) according to manufacturer's instructions. Primary $CD4^+$ T cells were activated in RPMI containing 10% FBS, 50 units/mL IL-2, antibiotics, and 5 µg/mL phytohemagglutinin.

After 48 h of activation, cells were washed and subsequently maintained and expanded in the same medium but without phytohemagglutinin. Cells were used for infections at 4–7 days post isolation.

*3.3.2. Antibodies*

Mouse monoclonal antibody (mAb) to EWI-2 (8A12) was a kind gift from Dr. Eric Rubinstein [25]. Mouse mAb to HIV-1 p24 (AG3.0) was obtained through the NIH AIDS Reagent Program (Germantown, MD, USA), Division of AIDS, NIAID, NIH, from Dr. Jonathan Allan [46]. Rabbit antiserum to HIV-1 p6 was a kind gift from David E. Ott. Rabbit polyclonal antibody (pAb) to HIV-1 p24 was obtained from Advanced Biotechnologies (Eldersburg, MD, USA, Cat. #13-203-000). Secondary antibodies were as follows: Alexa Fluor 488-conjugated donkey pAb to mouse IgG (#A21202), Alexa Fluor 488-conjugated donkey pAb to rabbit IgG (Cat. #A21206), Alexa Fluor 594-conjugated donkey pAb to mouse IgG (Cat. #R37115), Alexa Fluor 594-conjugated donkey pAb to rabbit IgG (Cat. #A21207), Alexa Fluor 647-conjugated donkey pAb to mouse IgG (Cat. #A31571), and Alexa Fluor 647-conjugated goat pAb to mouse IgG (Cat. #A21235), all from Invitrogen (Carlsbad, CA, USA). Zenon labeling of primary antibodies with either Alexa Fluor 488 or Alexa Fluor 594 was carried out using Zenon Labeling Kits according to the manufacturer's instructions (Molecular Probes, Eugene, OR, USA, Cat. #Z25002 and #Z25007).

*3.3.3. Plasmids and Virus Strains*

Respectively, pcDNA3, pCDNA3.1, and pCMV SPORT6 (Invitrogen, Carlsbad, CA, USA) were vectors for EWI-2, CD81, and L6 overexpression (EWI-2 was a kind gift from Dr. Eric Rubinstein; Université Paris-Sud, Villejuif, France). Proviral plasmids pNL4-3 and pNL4-3 ΔEnv (KFS) were kind gifts from Dr. Eric Freed (National Cancer Institute, Frederick, MD, USA) [47]. NL4-3-derived fluorescent protein-tagged proviral plasmids pNL-sfGI, pNL-sfGI ΔEnv, pNL-CI, and pNL-CI ΔEnv [10] were kind gifts from Dr. Benjamin Chen (Mount Sinai School of Medicine, New York, NY, USA). Vesicular stomatitis virus glycoprotein (VSV-G) was used to pseudotype viral stocks produced in HEK 293T cells. The lentiviral vector FG12 [48], previously modified to include a puromycin resistance cassette [24], was further modified to remove the GFP reporter cassette by digestion with AfeI and PshAI and subsequent blunt-end relegation.

*3.3.4. Virus Stocks and Infections*

VSV-G-pseudotyped virus stocks of NL4-3, NL4-3 ΔEnv, NL-sfGI, NL-CI, and NL-CI ΔEnv were produced in HEK 293T cells transfected with the proviral plasmid and pVSV-G (at 17:3 ratio) using calcium phosphate precipitation. For shRNA encoding lentiviruses, shEWI-2 and shScramble, stocks were produced in HEK 293T cells transfected with FG12-shRNA vector, ΔR8.2 packaging vector, and pVSV-G (at a ratio of 3:7:1. Supernatants were harvested 2 days after transfection, cleared by centrifugation at 2000 rcf for 10 min, filtered, and stored at −80 ˚C.

To infect CEM2n cells by spinoculation, two million cells were incubated with RPMI/10% FBS containing 90 µL of virus stock (resulting in ~3% of the cells being infected) or medium alone (for uninfected controls), for 20 min at 37 ˚C, followed by centrifugation at 1200 rcf for 2 h at 37 ˚C.

Cell pellets were allowed to recover at 37 ˚C for 15 min, centrifuged at 300 rcf for 2 min, and resuspended in fresh RPMI/10% FBS. Cells were incubated at 37 ˚C, the medium was refreshed 2 days post infection, and the cells were used 1 day later for all subsequent experiments.

To infect primary $CD4^+$ T cells, 1 or 2 million cells were incubated in RPMI/10% FBS/IL-2 containing 200 or 400 µL of virus, respectively, and spinoculated as described above. Cells were resuspended in fresh RPMI/10% FBS/PS/IL-2 and incubated at 37 ˚C/5% $CO_2$. Cells were used 2-3 days post infection for all subsequent experiments.

To infect CEM-SS cells by shaking, one or two million cells suspended in $CO_2$-independent medium (Gibco, Grand Island, NY, USA, Cat #18045088) supplemented with 10% FBS were mixed with VSV-G-pseudotyped virus stocks and shaken at 220 rpm for 2 h at 37 ˚C. Cells were then washed and plated in fresh RPMI/10% FBS, and used for experiments as described. For CEM-SS infection by spinoculation, the procedure was performed as described above with some modifications; one or two million cells were incubated in RPMI/10% FBS containing 40–50 µL (analyzing surface expression and post-synapse enrichment, respectively) of virus stock or medium alone (for uninfected controls). Following spinoculation, cells were incubated at 37 ˚C for 2 days before being used for subsequent experiments.

*3.3.5. Imaging and Quantification of EWI-2 Accumulation at the VS*

CEM-SS and primary $CD4^+$ T cells were infected by shaking or spinoculation, respectively, with VSV-G-pseudotyped WT or ΔEnv virus then treated as follows: For CEM-SS cells, two days post infection, uninfected CEM-SS target cells were labeled with CMAC (Invitrogen, Carlsbad, CA, USA) according to manufacturer's instructions, mixed with infected cells at a 1:1 or 1:2 ratio (infected:target), seeded onto the microwell of a 35 mm glass-bottom dish (MatTek Corporation, Ashland, MA, USA, Cat. #P35G-1.5-14-C) coated with poly-L-Lysine (Trevigen, Gaithersburg, MD, USA), and incubated at 37° C for 3 to 4.5 h. Cells were then chilled on ice and surface-labeled with 1:200 mouse anti-EWI-2 mAb in RPMI/10% FBS for 45 min at 4 °C. Surface-labeled cells were fixed with 4% PFA in PBS at 4 °C for 10 min, and blocked and permeabilized overnight with 1% BSA and 0.2% Triton X-100 in PBS (block/perm buffer). All CEM-SS conditions were labeled with Alexa Fluor 647-conjugated anti-mouse secondary pAb in block/perm buffer at 1:500 dilution. Cells were subsequently stained with Alexa Fluor 594 Zenon-labeled anti-p24 AG3.0 mouse mAb and fixed again with 4% PFA in PBS. Cells were kept in PBS for imaging.

For primary cells, uninfected cells were mixed with infected cells at a 1:1 ratio (infected:target), seeded onto 8-well glass-bottom plates (CellVis, Mountain View, CA, USA, Cat. #C8-1.5H-N) coated with 1:10 poly-L-Lysine in double-distilled water ($ddH_2O$), and incubated for 2 to 2.5 h at 37 °C. Cells were surface-labeled for EWI-2 and fixed as above, then blocked and permeabilized with block/perm buffer for 10 min. Cells were then labeled with a mixture of rabbit anti-p24 and anti-p6 antibodies, each at 1:1000

dilution, in PBS with 1% BSA (block) for 45 min. Subsequently, cells were labeled with Alexa Fluor-conjugated secondary pAbs as indicated. Cells were kept in PBS for imaging.

To visualize the only producer cell-associated EWI-2 at the VS, 10,000 target TZM-bl cells (which have nearly-undetectable levels of EWI-2) were seeded onto 8-well glass-bottom plates coated with 1:10 poly-L-Lysine in $ddH_2O$. The next day, those TZM-bl cells were labeled with CMAC at 1:250 dilution in serum-free DMEM, and then co-cultured with 150,000 CEM-SS cells (either uninfected or infected with NL-CI or NL-CI ΔEnv 2 days prior as described above) per well for 2.5 h at 37 ˚C in RPMI/10% FBS. The cells were then surface-labeled with 1:200 mouse anti-EWI-2 mAb in RPMI/10% FBS on ice for 45 min. Cells were subsequently fixed with 4% PFA in PBS and permeabilized with block/perm for 10 min. After permeabilization, the cells were labeled using a mixture of rabbit anti-p24 and anti-p6 antibodies, each at 1:1000 dilution, in block for 45 min. Cells were subsequently labeled using Alexa Fluor-conjugated secondary pAbs (anti-mouse-Alexa Fluor 647 and anti-rabbit-Alexa Fluor 488) each at 1:500 in block for 45 min. Cells were kept in PBS for imaging.

To visualize only target cell-associated EWI-2 at the VS, HeLa producer cells (which have nearly-undetectable levels of EWI-2) were plated (10,000 cells per well) in 8-well glass-bottom plates coated with 1:10 poly-L-Lysine in $ddH_2O$. Twenty-four hours later, cells were transfected with NL-sfGI, NL-sfGI ΔEnv, or empty vector, using FuGENE6 transfection reagent at a ratio of 3:1 (FuGENE6:DNA) according to manufacturer's instructions (Promega, Madison, WI, USA, Cat. #E2691). Twenty-four hours post-transfection, 100,000–150,000 uninfected CEM-SS cells (labeled with CMAC at a 1:250 dilution in serum-free RPMI) were added to form VSs with provirus-transfected

HeLa cells. After 2-2.5 h of coculture, cells were surface-labeled with 1:200 mouse anti-EWI-2 mAb in RPMI/10% FBS for 45 min at 4 ˚C. Surface-labeled cells were fixed with 4% PFA in PBS at 4 ˚C for 10 min, and then incubated with block/perm for 10 min, before labeling with a mixture of rabbit anti-p24 and anti-p6 antibodies, each at 1:1000 dilution, in block for 45 min. Subsequently, cells were labeled with secondary pAbs (anti-mouse-Alexa Fluor 647 and anti-rabbit-Alexa Fluor 594), each at 1:500 in block. Cells were kept in PBS for imaging.

Images were acquired on a DeltaVision epifluorescence microscope (GE/Applied Precision, Issaquah, WA, USA) with an Olympus IX-70 base using an Olympus 60× PlanApo 1.42 NA objective and equipped with a CoolSNAP HQ CCD camera (Photometrics, Tucson, AZ, USA). Images were imported into Fiji Version 2.0.0-rc-69/1.52p [49] for analysis following deconvolution and cropping using Softworx software (GE Healthcare Bio-Sciences, Pittsburgh, PA, USA). The VS was identified using the Gag channel and the level of EWI-2 accumulation was determined by measuring its signal intensity at the VS. For ΔEnv controls, cell–cell contacts were identified using the differential interference contrast (DIC) channel and treated analogous to a VS. The EWI-2-associated signal intensity at non-contact sites was determined by manually outlining the surface of the cell, excluding any regions that were in contact with an adjacent cell, and calculating the mean EWI-2 intensity within the selected area. To determine the level of enrichment at the VS (or cell–cell contact for ΔEnv controls), an “unbiased” approach was applied to account for the EWI-2 signal contributed by both the target and producer cell at each VS/contact. Enrichment was calculated as the EWI-2 signal intensity at the

VS/contact divided by the sum of the EWI-2 signal at non-contact sites of the producer and target cell in that particular VS/contact.

### *3.3.6. Proteomic Analysis of EWI-2 Levels in HIV-1 Infected Cells*

To identify HIV-1-dependent changes in the abundance of total EWI-2, we re-analysed data from two previous studies [50,51]. In brief, primary human $CD4^+$ T cells were infected with pNL4-3-ΔEnv-Nef-P2A-SBP-ΔLNGFR (HIV-AFMACS) at MOI≤0.5, enriched by antibody-free magnetic cell sorting (AFMACS) [52] and analysed 48 h after infection [51]. CEM-T4 T cells were infected with pNL4-3-ΔEnv-EGFP at MOI=1.5 and analysed 48 h after infection [50]. TMT-labeled tryptic peptides from whole cell lysates were subjected to off-line high pH reversed-phase (HpRP)-HPLC fractionation and analysed using an Orbitrap Fusion Tribrid mass spectrometer (ThermoFisher Scientific, Waltham, MA, USA) coupled to a Dionex UltiMate 3000 UHPLC (Thermo Scientific, Waltham, MA, USA). Details of sample processing and data analysis have been previously described [50,51] and proteomic data from primary human $CD4^+$ T cells are available from the ProteomeX-change Consortium using dataset identifier PXD012263 (http://proteomecentral.proteomexchange.org).

To characterise HIV-1-dependent changes in the abundance of plasma membrane EWI-2, we re-analysed data from a previous study [53]. In brief, for the TMT-based time course experiment, CEM-T4 T cells were infected with pNL4-3-ΔEnv-EGFP at MOI=10 and analysed at the indicated time points after infection. For the SILAC-based single time point experiments, cells were pre-labeled with light, medium or heavy lysine and arginine and either infected with WT or Vpu-/Nef-deficient pNL4-3-ΔEnv-EGFP at MOI=10 and

analysed 72 h after infection, or transduced with GFP or Vpu/Nef and selected with puromycin. Sialylated cell surface glycoproteins were enriched by selective aminooxy-biotinylation followed by immunoaffinity purification using streptavidin-conjugated beads (plasma membrane profiling). Tryptic peptides were labeled with TMT reagents (time course experiment only), subjected to off-line High pH Reversed-Phase (HpRP)-HPLC fractionation and analysed using an Orbitrap Fusion Tribrid mass spectrometer (Thermo Scientific, Waltham, MA, USA) coupled to a Dionex UltiMate 3000 UHPLC (Thermo Scientific, Waltham, MA, USA). Details of sample processing and data analysis have been previously described [53] and time course proteomic data are available from the ProteomeX-change Consortium using dataset identifier PXD002934 (http://proteomecentral.proteomexchange.org).

*3.2.7. Determining Surface Levels of EWI-2 by Microscopy*

To compare EWI-2 surface expression between infected and uninfected cells, CEM-SS, CEM2n cells, and primary $CD4^+$ T cells were infected with VSV-G-pseudotyped NL-sfGI as described above. Two to three days post infection, $3 \times 10^5$ infected cells were plated onto each well of 8-well glass-bottom plates coated with 1:10 poly-L-Lysine in $ddH_2O$. Two additional wells were used for uninfected controls. After 2 h of incubation at 37 ˚C, the medium was replaced with ice cold RPMI/10% FBS containing mouse anti-EWI-2 mAb at 1:200 dilution for surface labeling, and incubated for 45 min at 4 ˚C. Following the primary antibody incubation, cells were washed with RPMI/10% FBS and fixed with 4% PFA in PBS for 10 min at 4 ˚C, blocked and permeabilized with PBS containing 1% BSA and 100 µg/mL digitonin for 10 min, and

incubated with the indicated secondary antibody in block for 45 min at room temperature. Cells were washed with block and imaged in PBS. At least 50 fields containing infected cells were selected for each biological replicate and imaged, deconvolved, and cropped using the DeltaVision microscope and Softworx software described above. After deconvolution, Fiji was used to manually select the cell surface at the midline of each cell and the mean intensity of EWI-2-associated signal was quantified and subsequently subtracted by the mean intensity of an area that did not contain cells. Cell–cell contact sites were excluded from the quantification. Background subtracted intensity values of all cells were normalized to the average surface associated intensity of the entire uninfected cell population, internal controls contained in the same wells as infected cells, contained within respective biological replicates. This normalization allowed for the direct comparison of surface expression trends between biological replicates that accounts for potential variation in protein labeling efficiency between replicates. The virus-associated fluorescent reporter channel was used to segregate measurements into uninfected and infected. The data shown in Figure 3B are pooled from 2–3 independent biological replicates, each consisting of two technical replicates, all of which were sampled randomly until a minimum of 50 infected cells were quantified.

To compare EWI-2 surface expression levels between mononucleated infected cells and HIV-1-induced syncytia, primary $CD4^+$ T cells were infected with VSV-G-pseudotyped virus as described above. Three days post infection, $3 \times 10^5$ infected cells were plated onto each well of 8-well glass-bottom plates coated with 1:10 poly-L-Lysine in $ddH_2O$ alongside two wells of uninfected cells as controls. Cells were incubated at 37 °C for 2 h and surface labeled as described above using either mouse anti-EWI-2 or mouse

anti-CD81 mAb at 1:200 or 1:100, respectively. Samples were fixed, permeabilized, and labeled with appropriate AlexaFluor conjugated antibodies and DAPI as described above. Cells were imaged in PBS and at least 50 fields containing 10–20 cells each and containing at least some infected cells with multinucleated appearance (determined by DAPI and GFP signal) were selected for each biological replicate and imaged, deconvolved, and cropped as described above. Fiji was then used to analyze the surface expression of each protein of interest as described above. The virus-associated fluorescent reporter channel (GFP) was used to segregate measurements into infected and uninfected populations, and nuclear staining (DAPI) was used to further segregate infected cells into mononucleated and multinucleated infected cells. The EWI-2/CD81 channel was not viewed at all during imaging and field selection, or throughout image processing. The data shown in Figure 6 are pooled from 2–3 biological replicates, with two technical replicates each, all of which were sampled randomly until a minimum of 15 syncytia per biological replicate were quantified.

*3.3.8. Determining Surface EWI-2 Signal on Infected Cells by Flow Cytometry*

CEM2n cells infected as described above were harvested after three days and incubated in cold PBS with 5 mM EDTA for 15 min ($3.0 \times 10^5$ cells/tube). Cells were pelleted at 400 rcf for 7 min at 4 ˚C and resuspended in cold RMPI/10% FBS containing mouse anti-EWI-2 mAb at 1:200 dilution. After a 45 min incubation at 4 ˚C, cells were washed with cold RPMI/10% FBS and resuspended in ice cold PBS with 5 mM EDTA. To fix, an equal volume of PBS with 8% PFA was added and samples were incubated on ice for 10 min. Cells were washed and stained with Alexa Fluor 594-conjugated secondary

antibody at 1:500 in block for 45 min at room temperature, before being washed, resuspended in PBS, and analyzed using a BD LSRII flow cytometer. Data were analyzed using FlowJo V10 (Becton, Dickinson & Company, Franklin Lakes, NJ, USA). Samples were gated for infected and uninfected populations by GFP expression. EWI-$2^{high}$ and EWI-$2^{low}$ gates were set based in part on controls lacking primary antibody, and in part by adjusting the gates to reflect the number of uninfected EWI-$2^{high}$ cells as measured by microscopy. The data shown are the collection of three independent biological replicates, each consisting of two technical replicates.

*3.3.9. HeLa-based HIV-1-Induced Cell-Cell Fusion Assay*

First, 50,000 HeLa cells were plated in each well of a 24-well plate and, the next day, transfected (using FuGENE6; see Section 2.5) in duplicate with 100 ng of either pNL-sfGI or pNL-sfGI ΔEnv along with 500 ng total expression vector carrying CD81 or EWI-2. L6, a tetraspanin-like protein that does not inhibit cell–cell fusion, was co-transfected instead of CD81 or EWI-2 as a positive control for maximum fusion activity, For dose response assays, 125, 250, or 500 ng of either EWI-2 or CD81 plasmid was ”stuffed” with L6 expression plasmid to maintain 500 ng of total protein expression plasmid in each condition. No cytotoxicity was observed upon transfection for any of the experimental conditions. Then, 24 h post-transfection, producer HeLa cells were co-cultured with $10^6$ TZM-bl target cells (which, upon producer-target cell fusion, express firefly luciferase under control of the HIV-1 LTR) per well for 3 h before unattached target cells were washed off and the medium was refreshed. 14-18 h later, cells were lysed for at least 30 min on ice using 1% Triton X-100, 2 mM EDTA, 50 mM Tris-HCl, 200 mM NaCl, with

1% protease inhibitor cocktail. Lysates were precleared by centrifugation at 20,000 rcf for 5 min at 4 ˚C and stored at –80 ˚C until use for luciferase activity assays. Note that the timepoints used here ensure that there is not enough time for the development of any luciferase signal resulting from productive infection of target TZM-bl cells through virus transmission and that only cell–cell fusion contributes to the luciferase activity measured.

Each lysate was incubated with an equal volume of firefly luciferase reagent (Promega, Madison, WI, USA, Cat. #E1500) for 1 min in a 96-well white-walled plate (ThermoFisher Scientific, Waltham, MA, USA, Cat. #7571) before collecting luminescence signal intensity on a microplate reader (BioTek Synergy 2, BioTek, Winooski, VT, USA). Background luminescence was determined using a lysis buffer blank and subtracted from all experimental samples. Luminescence intensity was used as a quantitative measurement of relative HeLa-TZM syncytium formation against the non-fusogenic (therefore incapable of forming syncytia) ΔEnv control by dividing each value by the Δenv value (which effectively corresponds to any leaky expression of luciferase in TZM-bl cells as no cell–cell fusion occurs at all in this condition). To then determine relative fusion activity of cells transfected with EWI-2 and CD81, those values were normalized to the L6 condition. Normalized fusion is therefore the fold difference of cell–cell fusion activity taking place when cells were co-transfected with the indicated amount of either CD81 or EWI-2 plasmid, compared to the activity taking place when cells were co-transfected with L6. The data shown are the collection of four independent biological replicates.

*3.3.10. Establishment of EWI-2 Knockdown CEM-SS Cells*

The shRNA-encoding sequences targeting either EWI-2 (modified from previously described EWI-2-targeting siRNA [27] or a scrambled control, were introduced to the lentiviral vector FG12 (as described in 2.3) using oligos containing shRNA sequences, a loop sequence, and an AgeI site, flanked by BbsI and XhoI restriction site overhangs, as previously described [24], (EWI-2 sense, 5'-ACCGGGGCTTCGAAAACGGTG ATCTTCAAGAGAGATCACCGTTTTCGAAGCCCTTTTTTACCGGTC-3', and anti-sense, 5'-TCGAGACCGGTAAAAAAGGGCTTCGAAAACGGTGATCTCTCTTGAA GATCACCGTTTTCGAAGCCC-3'; scramble sense, 5'-ACCGGGCAGATGCGTCCA GTTAGATTCAAGAGATCTAACTGGACGCATCT GCCTTTT TTACCGGTC-3', and anti-sense, 5'-TCGAGACCGGTAAAAAAGGCAGATGCGTCCAGTTAGATCTCTT GAATCTAACTGGACGCATCTGCC-3'). A PolII promoter was first obtained by ligating the oligo with PBS-hU6 digested with BbsI and XhoI restriction endonucleases (New England BioLabs, Ipswich, MA, USA). The PolII-shRNA constructs were obtained by digesting the resulting PBS-hU6 vector with XbaI and XhoI, and the insert was subsequently ligated into the FG12 vector digested with the same enzymes.

VSV-G pseudotyped FG12-shRNA lentiviruses were used to transduce CEM-SS cells by spinoculating one million cells with 500 µL of lentiviral supernatant (either shEWI-2 or shScramble). Cells were incubated at 37 ˚C for 2 days in RPMI/10% FBS and positively transduced cells were then selected for puromycin resistance by supplementing the media with 0.5 µg/mL of puromycin for 8 days. Subsequently, shEWI-2 and shScramble CEM-SS cells were maintained in RPMI/10% FBS/0.25 µg/mL puromycin.

EWI-2 knockdown was analyzed by flow cytometry and microscopy. For flow cytometry analysis, $3.0 \times 10^5$ shScramble and shEWI-2 cells, alongside parental CEM-SS controls, were pelleted at 400 rcf for 7 min, resuspended in 1:1000 Live/Dead Fixable Near-IR stain (Invitrogen, Carlsbad, CA, USA, Cat. #L10119) in PBS for 30–45 min, washed with RPMI/10% FBS and fixed for 10 min in 4% PFA in PBS by resuspending the cells in PBS and then adding an equal volume of 8% PFA in PBS. Fixed samples were washed with 1 mL of PBS, blocked and permeabilized in 100 μL of block/perm buffer for 10 min, and washed with PBS containing 1% BSA. EWI-2 was labeled using mAb 8A12 diluted 1:200 in block for 45 min, washed with block, and stained with Alexa Fluor 488-conjugated secondary antibody in block for 45 min. Cells were then washed and resuspended in PBS for flow cytometry analysis using a BD LSRII flow cytometer. Data were analyzed using FlowJo V10. Samples were gated for live cells, and EWI-2 expression was measured by the mean fluorescence intensity of EWI-2 signal in the live cell population and normalized to the parental control expression within each biological replicate. The data are the result of three independent biological replicates with two technical replicates each. For microscopy, $2.5 \times 10^5$ shScramble and shEWI-2 cells, alongside parental CEM-SS controls, were plated on 8-well glass bottom plates coated with 1:10 poly-L-lysine in $ddH_2O$. After 2 h at 37 °C, cells were fixed for 10 min using 4% PFA in PBS, washed, and incubated with block/perm for 10 min. Cells were washed with block and incubated with 1:200 mAb 8A12 for 45 min, washed, and stained with 1:500 Alexa Fluor 647-conjugated secondary antibody and 1:2500 DAPI in block for 45 min. Cells were washed with block and imaged in PBS using a 60× objective as described

above. Images were deconvolved and cropped by DeltaVision microscope and Softworx software described above and imported into Fiji for analysis.

*3.3.11. CEM-luc-based HIV-1-Induced Cell-Cell Fusion Assay*

Two million shScramble or shEWI-2 cells were spinoculated as described above with 1.7 or 2 μL of VSV-G pseudotyped NL4-3, alongside parental CEM-SS cells spinoculated with 25 μL of VSV-G pseudotyped NL4-3 ΔEnv to achieve an infection rate of ~30% for each condition. Cells were incubated at 37 ˚C for 2 days and then co-cultured with uninfected CEM-luc cells in RPMI/10% FBS containing the following drug treatments; 1:1000 DMSO for vehicle control, 1 μM Efavirenz (EFV) (NIH AIDS Reagent Program, Cat. #4624) to inhibit transmission, or 1 μM EFV with 0.5 μM HIV-1 IIIB C34 peptide (C34) (NIH AIDS Reagent Program, Cat. #9824) to inhibit both transmission and cell–cell fusion. After 24 h, the co-culture medium was refreshed, and all conditions were incubated at 37 ˚C in RPMI/10% FBS containing 1 μM EFV and 0.5 μM C34. 24 h later, cells were pelleted at 1000 rcf for 5 min at 4 ˚C and resuspended in luciferase reporter lysis buffer (Promega, Cat. #E4530) with 1% protease inhibitor cocktail (Millipore Sigma, Darmstadt, Germany, Cat. #P8340) to lyse on ice for 15 min. Lysates were cleared by centrifugation at 20,000 rcf for 5 min at 4 ˚C and stored at –80 ˚C until use for luciferase activity assays.

In parallel, infected cells were prepared for flow cytometry analysis alongside uninfected controls, to determine the infection rate across each condition at the start of the co culture with uninfected CEM-luc cells. Cells were pelleted and resuspended in 1:1000 Live/Dead Fixable Near-IR stain in PBS as described above, washed and resuspended in

PBS. An equal volume of 8% PFA in PBS was added to fix the cells in a final concentration of 4% PFA in PBS for 10 min. Cells were washed and resuspended in block/perm, incubated for 10 min, washed with block, and resuspended for an overnight incubation in 1:100 AG3.0 in block. Cells were washed and stained with 1:500 Alexa Fluor 488-conjugated secondary antibody for 45 min followed by a wash with block. Cells were resuspended in PBS and analyzed by flow cytometry using a BD LSRII flow cytometer. Data was analyzed using FlowJo V10. Live cells were gated using the Live/Dead signal, and the percentage of infected cells in the live population was determined by gating on the AG3.0 associated signal.

Each lysate was incubated with an equal volume of firefly luciferase reagent for 1 min in a 96-well white-walled plate before collecting luminescence signal intensity on a microplate reader as described above (2.9). Background luminescence was determined using a lysis buffer blank and subtracted from all experimental samples. Relative luminescence units (RLUs) were normalized based on the infection level of each cell type determined by flow cytometry analysis, and the average RLU value from the ΔEnv infected, DMSO treated condition was subtracted from all conditions. All samples treated with both EFV and C34 had RLU values below that of the ΔEnv DMSO condition (data not shown), validating the efficacy of the inhibitors for complete inhibition of transmission to target CEM-luc cells. To determine the proportion of luciferase expression due to cell–cell fusion, the average RLU value from the EFV-treated condition (syncytium formation-dependent signal) was divided by that of the DMSO-treated (signal from both transmission and syncytium formation) and multiplied by 100. Data represent the percentage of luciferase signal due to syncytium formation between infected shScramble or shEWI-2

cells and uninfected CEM-luc cells from three independent biological replicates each consisting of 1–2 technical replicates.

*3.3.12. Statistical Analysis*

All statistical analyses were carried out in GraphPad Prism 8 (GraphPad Software, San Diego, CA) as indicated in Figure legends.

## 3.4 Results

*3.4.1. EWI-2 Accumulates at the Virological Presynapse in HIV-1-Infected Cells*

Because EWI-2 is known to associate with ezrin and CD81 [25,27], two cellular factors that accumulate at the producer cell side of the virological synapse (VS) [24,54], we first sought to determine whether this protein also localizes to the VS. CEM-SS cells were infected with (VSV-G-pseudotyped) NL4-3 WT or NL4-3 ΔEnv (virus that does not express Env) and mixed with target CEM-SS cells (labeled with a cytoplasmic dye). Upon imaging with a 60× objective, the VS was identified and defined by region selection as clusters of immunolabeled Gag present at producer-target cell contact sites. DIC was used to identify and region-select cell–cell contacts between ΔEnv producers and uninfected target cells as Gag will not accumulate at these contacts in the absence of Env [1]. The EWI-2 channel was not viewed during the process of defining VS/contact regions to eliminate possible bias. To calculate the enrichment at the VS/contact, we divided the EWI-2 signal intensity within the defined VS/contact site by the sum of the EWI-2 surface intensity at non-contact sites on the producer and target cell at each VS/contact. This

unbiased approach prevents potential inflation of the enrichment value that could occur if we assumed that EWI-2 was solely contributed by either the target or producer cell. Similarly to p-ezrin and CD81 [24,54], EWI-2 was observed to co-accumulate with Gag at the VS in an Env-dependent manner (Figure 3.1A). EWI-2 signal intensity was ~4-fold enriched at the VS in CEM-SS cells infected with NL4-3 WT, while no EWI-2 enrichment was seen at cell–cell contacts in cells expressing NL4-3 ΔEnv (Figure 3.1A). EWI-2 signal intensity was also enriched ~1.6-fold at the VS in infected primary $CD4^+$ T cells at Env-dependent VSs and was again not enriched at non-VS contact sites (ΔEnv) (Figure 3.1B).

To determine whether EWI-2 enrichment at the VS takes place within the infected cell, i.e., at the presynaptic terminal (rather than the apposed uninfected target cell), HIV-1-infected CEM-SS cells were co-cultured with uninfected target TZM-bl cells (which have nearly-undetectable levels of EWI-2 on their surface) and imaged as described above. Significant EWI-2 enrichment (~5.3-fold) was observed at the VS as before (Figure 3.2A), demonstrating that the observed EWI-2 accumulation in CEM-SS-CEM-SS co-cultures takes place at least partially within the producer cell. To evaluate the relative contribution of any postsynaptic (i.e., target cell-side) accumulation of EWI-2, HIV-1-producing HeLa cells (which, like TZM-bl cells, also exhibit nearly undetectable levels of EWI-2 on their surface) were cocultured with uninfected target CEM-SS cells. In this case, minimal EWI-2 accumulation was detected at synapses (~1.1-fold; Figure 3.2B), showing that EWI-2 enrichment seen at T cell-T cell VSs takes place (almost) exclusively at the presynaptic terminal of the VS, i.e., in the producer cell. Together, these results conclusively document that EWI-2 is recruited to the virological presynapse during HIV-1 cell-to-cell transmission.

*3.4.2 Overall Surface Levels of EWI-2 Are Decreased upon HIV-1 Infection*

Despite its enrichment at the virological presynapse, the EWI-2 partner protein CD81 (as well as other tetraspanins) is overall downregulated in HIV-1-infected cells [54,56,57]. We previously used Tandem Mass Tag (TMT)-based quantitative proteomics to map global changes in whole cell protein abundances in HIV-infected T cells [50,51]. Like CD81, EWI-2 was decreased in abundance in both CEM-T4 T cells and primary human $CD4^+$ T cells (Figure 3.3A). To confirm these data using an orthogonal approach, we tested whether surface levels of EWI-2 are decreased in lymphocytes infected with HIV-1 NL-sfGI, a strain in which superfolder GFP (sfGFP) replaces the Nef gene and Nef expression is restored using an IRES [10]. We chose to utilize this GFP reporter virus, rather than immunolabeling Gag after fixation, because Gag-negative (or undetectable) cells still in the early phase of infection may exhibit host protein downregulation due to early Nef expression (reviewed in [58]).

HIV-1-infected cells adhered to glass-bottom dishes were surface-labeled with EWI-2 primary antibody on ice and fixed before incubation with fluorescent secondary antibody. Uninfected and HIV-1-infected cells were imaged with a 60× objective and the resulting images were deconvolved. The mean fluorescence intensity (MFI) of EWI-2 on the surface of each cell was determined by measuring the EWI-2-associated signal intensity of manually-selected regions of the cell surface (representative images shown in Figure 3.3B) and normalizing the raw MFI of each cell to the average EWI-2 signal from uninfected cells within the same imaging set. After measuring surface MFI, on average across three independent biological replicates, infected (GFP-expressing) cells had

significantly lower (~2-fold) EWI-2-associated signal than uninfected (GFP-negative) cells, after subtracting background signal (Figure 3.3B). This phenomenon was consistent across CEM-SS, CEM2n, and primary $CD4^+$ T cells.

We also sought to quantify EWI-2 surface expression by flow cytometry as a means of high-throughput analysis. HIV-1 NL-sfGI-infected CEM2n cells, surface-labeled for EWI-2 and analyzed by flow cytometry, were gated for high or low levels of EWI-2 using appropriate controls (representative histogram plots shown in Figure 3.3D). These data showed that a much lower proportion of infected cells (identified as $GFP^+$) had high levels of EWI-2 surface expression than of uninfected cells (identified as $GFP^-$) in the same culture (Figure 3.3E). Additionally, the mean fluorescence intensity of EWI-2-associated signal was lower within the total population of infected cells compared to that of the uninfected cells (Figure 3.3F).

Like other cell surface proteins downregulated by HIV-1, depletion of CD81 (as well as other tetraspanins) is mediated by the accessory proteins Vpu (predominantly) and Nef [56,57]. We have previously shown that substrates of different HIV-1 accessory proteins may be distinguished by their characteristic patterns of temporal regulation in HIV-1-infected T cells [50,51,53]. Accordingly, the temporal expression profile of plasma membrane EWI-2 was strikingly similar to that of BST2 (Tetherin), a canonical Vpu target (Figure 3.4A).

Furthermore, like BST2, depletion of cell surface EWI-2 by HIV-1 infection was abrogated in the presence of reverse transcriptase inhibitors, and when cells were infected with Vpu-deficient HIV-1 (Figure 3.4B). Taken together, our proteomic data therefore strongly suggest that Vpu is primarily responsible for HIV-1-dependent EWI-2

downregulation. As with the tetraspanins however, the incomplete rescue in the presence of Vpu-deficient virus, and relatively modest depletion when Vpu was expressed as a single gene (Figure 3.4B), suggest that Nef may also contribute to the depletion of cell surface EWI-2 in the context of HIV-1 infection.

### *3.4.3. EWI-2 Inhibits HIV-1-Induced Syncytium Formation*

Likely through their accumulation at the producer cell side of the VS, the EWI-2 partner proteins CD81 and ezrin repress the fusion of infected and uninfected cells, i.e., syncytium formation [22–24]. Given that EWI-2 also accumulates at the VS (Figure 3.1), we sought to test whether it also contributes to the inhibition of HIV-1-induced syncytium formation by both overexpressing EWI-2 and reducing its expression using RNA interference.

As we have done previously to examine the fusion-inhibitory capacity of tetraspanins [22,23], we tested whether EWI-2 inhibits HIV-1-induced syncytium formation in a dose-dependent manner by overexpressing EWI-2 in HeLa cells (which have nearly-undetectable endogenous levels of EWI-2). NL-sfGI-producing HeLa cells overexpressing either EWI-2, CD81, or L6 (a tetraspanin-like surface protein that does not repress HIV-1-induced cell–cell fusion; [23,59]) were co-cultured with uninfected target TZM-bl cells. As a negative control for HIV-1-induced cell–cell fusion, Env-deleted (ΔEnv) NL-sfGI-expressing HeLa cells were also co-cultured with target TZM-bl cells. HIV-1-induced HeLa-TZM-bl syncytia express firefly luciferase under control of the HIV-1 LTR [22]. After 3 h of co-culture (and another 14–18 h to allow for reporter expression), cells were lysed, the lysates were incubated with luciferase substrate, and luminescence

was measured using a microplate reader. Overall, the overexpression of increasing amounts of either CD81 or EWI-2 (125, 250, or 500 ng of plasmid) in NL-sfGI-producing cells resulted in a dose-dependent decrease of cell–cell fusion (Figure 3.5A).

In parallel, we established an EWI-2 knockdown CEM-SS cell line by lentiviral transduction using a targeting vector (FG12) that directs expression of a short hairpin RNA (shRNA) targeting EWI-2 (shEWI-2), using the same targeting sequence as in a previous report [32]. As a control, this targeting sequence was scrambled several times, all resulting sequences were tested against the human genome by BLASTn, and the sequence with the least homology to any human transcript was selected (shScramble, or shScr). This modified FG12 vector also carries a puromycin resistance cassette, while the GFP reporter cassette (as used in [24]) was removed to allow use of GFP reporter viruses. The puromycin-resistant shEWI-2 CEM-SS cells were analyzed by microscopy (Figure 3.5B) and by flow cytometry (Figure 3.5C–D) and were found to have ~3-fold reduced EWI-2 surface levels, compared to both the shScramble control and the parental non-transduced CEM-SS cells.

Subsequently, shEWI-2 and shScramble cells were assayed for their ability to support HIV-1-induced cell–cell fusion with CEM-luc cells as target cells, using a previously reported assay that discriminates between the luciferase signal derived from active virus transmission and signal from cell–cell fusion [24,60]. Across three independent biological replicates, HIV-1-infected shEWI-2 cells were found to consistently form syncytia more frequently (between 1.5 and 2.3-fold) than HIV-1-infected shScramble cells (Figure 3.5E).

Taken together, the accumulation of EWI-2 at the presynaptic terminal of the HIV-1 VS (Figures 3.1 and 3.2), the concomitant overall downregulation of EWI-2 in infected T cells (Figure 3.3), and the requirement for high EWI-2 expression for efficient control of Env-induced cell–cell fusion (Figure 3.5) establish EWI-2 as a host fusion-inhibitory protein harnessed by HIV-1 during cell-to-cell virus transmission.

### *3.4.4. EWI-2 and CD81 Surface Expression is Restored on HIV-1-Induced Syncytia*

HIV-1-infected cells have been well documented to have altered surface expression profiles compared to uninfected cells (reviewed in [61]). However, previous analyses (including ours) were performed using bulk populations of HIV-1 infected cells, and thus could not or did not discriminate between mono- and multinucleated HIV-1-infected cells. HIV-1-induced syncytia likely have altered surface expression compared to mononucleated infected cells, as the process of syncytium formation (infected-uninfected cell fusion) provides a sudden influx of yet-to-be downregulated host proteins contributed by the uninfected target cell upon membrane merger and cytoplasm mixing. Therefore, we chose to use microscopy to analyze the surface expression of EWI-2 and CD81 on HIV-1-infected cells in order to, for the first time, confidently discriminate between mononucleated infected cells and multinucleated HIV-1-induced syncytia.

HIV-1-infected primary $CD4^+$ T cells were cultured for three days post infection to allow time for syncytium formation. Infected cells were plated, surface-labeled for EWI-2 or CD81 on ice and fixed prior to incubation with secondary antibody and imaging as before. The surface expression of each cell was quantified, normalized to internal uninfected controls, and data were segregated into populations of uninfected cells,

mononucleated infected cells, and multinucleated infected cells (syncytia, identified as multinucleated by DAPI nuclear staining and positive for the viral reporter (GFP), as shown in representative images; Figure 3.6A). Strikingly, we found that syncytia had restored the surface expression of both EWI-2 and CD81 to nearly the same level as uninfected T cells found within the same wells (Figure 3.6B).

## 3.5 Discussion

The transient alignment of infected (producer) and uninfected (target) cells allows for efficient transmission of virus particles. However, because of the presence of viral Env and CD4/co-receptor at the surface of producer and target cell, respectively, rather than separating after particle transfer, these cells could also easily fuse with each other, thus forming a syncytium. This study now identifies EWI-2 as a host protein that contributes to the maintenance of viral homeostasis through fusion inhibition.

Our investigations were partially prompted by two recent reports. In one of those studies, Rubinstein and colleagues documented a role for EWI-F, a close relative of EWI-2, in myoblast fusion regulation [26]. EWI-F was shown to act as fusion repressor in cooperation with the tetraspanins CD9 and CD81. With the other study, Yáñez-Mó and colleagues [32] showed the presence of EWI-2 at sites of contact between uninfected T cells and T cells stably expressing HIV-1 Env. In separate experiments, HIV-1-infected EWI-2 knockdown cells were also shown to have somewhat increased virus production and the authors mentioned (as data not shown) that this was accompanied by augmented syncytium formation, indicating that EWI-2 could be involved in the regulation of HIV-1-induced membrane fusion. Importantly, however, the study did not address the question

of whether the reported increase in syncytium formation was (potentially) caused by the action of EWI-2 in producer or target cells, nor did it provide a dissection of where EWI-2 accumulates (producer and/or target cells). The authors did speculate that EWI-2, together with α-actinin, might be active in target cells, there possibly contributing to α-actinin's actin bundling activity, thus ultimately inhibiting virus entry/fusion. They also explicitly stated, however, that even if their speculation about where α-actinin acts during virus replication should eventually be confirmed (with subsequent studies), they cannot exclude an involvement of the partner protein EWI-2 in the "subsequent steps of the viral life cycle". Our study now reveals that EWI-2 indeed acts during the late phase of the HIV-1 replication cycle: It accumulates on the producer cell side of the VS (Figures 3.1 and 3.2). Surprisingly, unlike tetraspanins, which have fusion-inhibitory roles at both sides of the VS (and thus are present at both the viral pre- and post-synapse [22,62]), EWI-2 accumulates (and inhibits fusion) only at the presynaptic terminal of the VS. This leads us to speculate whether EWI-2 accumulation at the presynaptic terminal might contribute to unique intracellular signaling events in HIV-1-infected cells [32,63], such as tuning T cell receptor function.

Paralleling what we previously documented for tetraspanins [22], we found that fusion with uninfected target cells was inhibited by EWI-2, and we established that it does so in a dose-dependent manner (Figure 3.5). Also analogous to our findings about tetraspanins [54,56], we demonstrate that while EWI-2 accumulates at the virological presynapse, overall this protein is downregulated in infected cells (Figure 3.3). Our proteomic analysis (Figure 3.4) now shows that EWI-2 depletion from the infected cell surface, as is also the case for tetraspanins [56,57], is primarily mediated by Vpu (Figure

3.4). Since EWI-2 is a known interactor of tetraspanins CD81 and CD9, it is possible that EWI-2 downregulation by Vpu (with or without Nef) is "direct" (e.g., the canonical Vpu "targets" BST2 and CD4, as well as SNAT1 [53]) or "indirect," possibly through its association with tetraspanins. Note, this is also true of CD81/other tetraspanins, which may likewise be "direct" or "indirect" targets (e.g., by their association with EWI-2). Our data do not distinguish these possibilities, and further mechanistic studies would be required to delineate the detailed mechanism of Vpu-mediated depletion. It should also be noted that in Table S1 of [64], EWI-2 depletion in CEM-T4 cells is (somewhat) dependent on the expression of Vpr. The effect size is modest and likely "indirect," and does not contradict the Vpu and Nef data shown here. It does, however, suggest that the mechanism of EWI-2 depletion in HIV-1 infected T cells may be complex.

Overall, the combination of these two features (enrichment during assembly and transmission at the VS, and regulation by HIV-1 accessory proteins in infected cells), together with the fusion-preventing functions, strongly suggests that a particular host factor plays an important role in virus replication.

We expect that EWI-2 also inhibits the fusion of virus particles to target cells, as tetraspanins do [54,56,59], and we are currently testing that hypothesis (within the context of an extensive follow-up analysis aimed at dissecting the molecular determinants responsible for EWI-2's fusion-inhibitory functions). It seems likely that tetraspanins and EWI-2 are not only tolerated but indeed enriched at virus budding sites because the benefit of cell–cell fusion inhibition at the VS is balanced against any negative effect of a reduction in virus infectivity. This is demonstrated by the fact that, in a native (unmanipulated) context, it is simultaneously true that (A) HIV-1-infected T cells

routinely exhibit enrichment of these fusion inhibitors at virus release sites, (B) that cell–cell fusion is relatively infrequent, and (C) that HIV-1 spreads efficiently in those cell cultures.

As mentioned, while fusion inhibition operates at many levels and is orchestrated by HIV-1 proteins during infection, syncytia do nevertheless form, including *in vivo* [7–9] and when using a transmitted/founder (T/F) R5-tropic Env or even full-length replication-competent T/F virus [10,12]. However, these syncytia seem to remain small, at 4 or fewer nuclei and the vast majority having only two nuclei [9]. Very large syncytia (dozens to thousands of nuclei) are only induced by HIV-1 infection of certain T cell lines, especially Sup-T1 cells [65], or *in vivo* but only with the involvement of macrophage or dendritic cells [66–68]. It is therefore possible that T cell–T cell fusion is inhibited not only when a mononucleated infected cell encounters a target cell, but also when a syncytium encounters a target cell. An alternative explanation is that syncytia may be less viable as they grow larger, though some evidence contradicts that [69]. Here, we present evidence that host fusion-inhibitory proteins EWI-2 and CD81 are present at higher levels on the surface of small T cell syncytia when compared to mononucleated infected cells in the same culture. Because we find that the fusion-inhibitory capacity of EWI-2 and CD81 is also dose-dependent, it would therefore be expected that a higher "dose" of EWI-2 and/or CD81 in syncytia would make them less likely to undergo cell–cell fusion a second (or third) time. We are currently formally testing this hypothesis, and also investigating the surface levels on syncytia of other host proteins normally downregulated upon HIV-1 infection. Without implicating any particular fusion-inhibitory protein, we have in the past found evidence that indeed fusion-inhibitory factors may also be acting at syncytium-

target cell VSs [9]: in Movie S7 of that report, we showed an example of a small syncytium containing two nuclei undergoing cell–cell fusion and acquiring a third nucleus. Subsequently, that syncytium encountered uninfected target cells and transferred virus particles to them through close contact but did not undergo further cell–cell fusion and instead fully separated from them despite exhibiting the ability to fuse only hours earlier. We can now speculate that, as a result of the cell–cell fusion event we captured at the beginning of that sequence, this syncytium likely acquired a dose of EWI-2 and/or CD81, which subsequently allowed the syncytium to mediate cell-to-cell virus transfer at the VS without further cell–cell fusion.

Finally, repressing HIV-1 Env-induced cell–cell fusion not only allows for a continued increase in the number of infected cells (as that number doubles each time producer and target cells separate after virus transmission), but keeping Env's fusion activity at bay may also be beneficial for the virus for other reasons. For instance, we and others have recently shown that lowering Env's fusion activity also allows HIV-1 to overcome a restriction factor (APOBEC3G; [60]), and even antiviral drugs [70]. Further, large syncytia, that could form if Env-induced cell–cell fusion is uncontrolled, are likely prone to be attacked by innate immune cells. It is therefore critical that HIV-1 recruits fusion-inhibitory host factors such as EWI-2 to the VS to prevent excess cell–cell fusion and keep T cell syncytia small when they do form.

## 3.6 Author Contributions

E.E.W., N.J.M., M.S., and M.T. conceived and designed the experiments. E.E.W. performed the experiments and analyzed the results, with contributions by M.S. and P.B.M. in Figure 3.1. N.J.M. performed the proteomics and analyzed the results in Figures 3.3A and 3.4. S.P. performed the FG12 vector modification to remove the GFP reporter cassette. E.E.W., N.J.M., and M.S. prepared the figures. E.E.W., N.J.M., M.S., and M.T. wrote and edited the manuscript.

## 3.7 Funding

The work was supported by the National Institutes of Health (R01-GM117839 to M.T., P30-RR032135 and P30-GM103498 for the Neuroscience COBRE Imaging Facility), the University of Vermont Larner College of Medicine (Bridge Support Grant to M.T.), the University of Vermont Department of Microbiology & Molecular Genetics (Nicole J. Ferland Award to S.P.), the Medical Research Council (CSF MR/P008801/1 to N.J.M.), NHS Blood and Transplant (WPA15-02 to N.J.M.), the NIHR Cambridge BRC, and a Wellcome Trust Strategic Award to CIMR. The contents are solely the responsibility of the authors and do not necessarily represent the official views of these funding sources.

## 3.8 Acknowledgments

The flow cytometry data we presented were obtained at the Harry Hood Bassett Flow Cytometry and Cell Sorting Facility, Larner College of Medicine, University of Vermont. The imaging shown in Figure 3.1A was performed at the Imaging/Physiology Core Facility, Neuroscience Center of Biomedical Research Excellence, Larner College of Medicine, University of Vermont.

## 3.9 Conflicts of Interest

The authors declare no conflict of interest.

## 3.10 Figure Legends

**Figure 3.1.** EWI-2 co-accumulates with Gag at the HIV-1 VS in T cells. (A) CEM-SS cells infected with HIV-1 NL4-3 WT or ΔEnv were co cultured with uninfected CEM-SS target cells for 5 h, and subsequently stained for surface EWI-2 (magenta) and Gag (yellow). The EWI-2-associated fluorescence intensity at cell–cell contacts either enriched with Gag (WT) or not Gag-enriched but identified by DIC (ΔEnv) was measured. This value was then divided by the sum of the EWI-2-associated fluorescence intensity on non-contact sites on the producer and target cell in each VS/contact to yield EWI-2 enrichment (i.e., the values shown here). The data quantified are from one biological replicate consisting of two technical replicates. Similar trends were observed in a second dataset; not shown. (B) Primary $CD4^+$ T cells infected with NL-sfGI WT or NL-CI ΔEnv were co-cultured with uninfected target primary cells for 2 h and stained for EWI-2 (magenta) and Gag (yellow), followed by secondary pAbs (Alexa Fluor 647-conjugated for EWI-2, and either Alexa Fluor 594 or Alexa Fluor 488-conjugated for Gag in the case of WT and ΔEnv, respectively). Because different secondary antibodies were used for Gag in either condition, the scaling shown for that channel is not the same across the two conditions and was based on corresponding primary and uninfected controls done alongside each dataset. Enrichment of EWI-2 at Env-dependent (WT) or Env-independent (ΔEnv) infected-uninfected cell contacts was quantified as described in (A). The data quantified are pooled from two independent biological replicates, each consisting of two technical replicates. Scale bars = 10 μm. In both data plots, each data point represents one cell–cell contact site (as opposed to one cell). The dotted horizontal line indicates a theoretical fold enrichment value of 1, which indicates no enrichment. Error bars = standard deviation of the mean (SD). *p*-values are the result of two-tailed non-parametric Mann-Whitney *U* tests.

**Figure 3.2**. EWI-2 accumulation takes place on the producer cell side of the VS. (A) To evaluate presynaptic accumulation of EWI-2, CEM-SS cells infected with HIV-1 NL-CI WT or ΔEnv were co cultured with CMAC (cyan) labeled TZM-bl target cells (which have nearly-undetectable EWI-2 surface levels compared to CEM-SS cells) for 2.5 h, and subsequently stained for surface EWI-2 (magenta) and Gag (yellow). EWI-2 enrichment was quantified as described in Figure 1. Quantification is the result of pooled VS/contacts from two independent biological replicates. (B) To evaluate postsynaptic accumulation of EWI-2, HeLa cells (which, like TZM-bl cells, also have nearly-undetectable EWI-2 surface levels) were transfected with HIV-1 NL-sfGI or

NL-sfGI ΔEnv and cocultured with uninfected CEM-SS target cells (cyan) for 2–2.5 h. Cells were stained for surface EWI-2 (magenta) and Gag (yellow). Note that Gag expression in the ΔEnv condition was quite low, since Gag expression in this virus is already expected to be considerably reduced [55]. EWI-2 enrichment was calculated as described in Figure 1. Quantification is the result of pooled VSs/contacts from two independent biological replicates. Scale bars = 10 μm. In both data plots, each dot represents the EWI-2 enrichment value of one VS/contact. The dotted horizontal line indicates a theoretical fold enrichment of 1, which indicates no enrichment. Error bars = standard deviation of the mean (SD). *p*-values are the result of two-tailed non-parametric Mann-Whitney *U* tests.

**Figure 3.3.** EWI-2 is downregulated from the surface of infected cells. (A) Abundance of EWI-2 in mock-infected (grey) versus WT HIV-infected (yellow) CEM-T4 T cells or primary human $CD4^+$ T cells. Experiments were conducted in triplicate and whole cell lysates subjected to Tandem Mass Tag (TMT)-based quantitative proteomics 48 h after infection (reanalysis of data from [50,51]). Seven (CEM-T4 T cells) or six (primary human CD4+ T cells) unique peptides were used for EWI-2 quantitation. Mean relative abundances (fraction of maximum TMT reporter ion intensity) shown. (B) Cells were infected with NL-sfGI and surface-labeled for EWI-2, fixed, stained with DAPI (shown in cyan) and Alexa Fluor 594-conjugated secondary antibody, and imaged. GFP signal (yellow) was used to identify infected cells, and EWI-2-associated signal is shown pseudocolored in magenta. Representative cells are shown. Scale bars = 10 μm. (C) Cells were prepared as in (B) and EWI-2 levels at the plasma membrane in infected (Inf) and uninfected (Uninf) cells were measured by manually selecting the plasma membrane at the midline of each cell and quantifying the mean EWI-2-associated fluorescence intensity. Fluorescence intensity of each cell was normalized to the average intensity value of uninfected cells within the same imaging set. Data shown are pooled from two to three biological replicates, each consisting of two technical replicates. Only non-contact sites were quantified. Error bars = SD. *p*-values are the result of a two-tailed non-parametric Mann-Whitney *U* test. (C-E) CEM2n cells were infected with NL-sfGI and surface-labeled for EWI-2, fixed, and stained with Alexa Fluor 647-conjugated secondary antibody, and analyzed by flow cytometry. (D) Representative histogram normalized to mode of the EWI-2 signal intensity at the cell surface for unstained controls (black outline), infected cells (yellow), and uninfected cells (cyan). The gates defining EWI-$2^{high}$ and EWI-$2^{low}$ cells are shown. (E) Data represent the percentage of uninfected and infected cells that fell into the EWI-$2^{high}$ gate shown in (d) from 3 independent biological replicates,

averaged across two technical replicates within each. (F) EWI-2 surface expression was measured by mean fluorescence intensity (MFI) of EWI-2-associated signal. In both panels, lines connect paired data points, i.e., infected cells and uninfected cells (within an infected tube) from the same biological replicate.

**Figure 3.4.** Plasma membrane EWI-2 is downregulated by Vpu. (A) Temporal expression profiles of cell surface EWI-2 (red, upper panel) or indicated control proteins (blue/green/gold, lower panels) in WT HIV-1-infected CEM-T4 T cells (reanalysis of data from [53]). Plasma membrane proteins were subjected to TMT-based quantitative proteomics 0 (uninfected), 6, 24, 48, and 72 h after infection, or 72 h after infection in the presence of reverse transcriptase inhibitors (RTi). Twelve unique peptides were used for EWI-2 quantitation. Relative abundances (fraction of maximum TMT reporter ion intensity) are shown. (B) Abundance of EWI-2 (red, upper panel) or indicated control proteins (blue/green/gold, lower panels) in control CEM-T4 T cells or CEM-T4 T cells infected with WT HIV-1 in the presence/absence of RTi, infected with Vpu- or Nef-deficient HIV-1, or transduced with Vpu or Nef as single genes (reanalysis of data from [53]). Plasma membrane proteins were subjected to Stable Isotope Labelling with Amino acids in Cell culture (SILAC)-based quantitative proteomics 72 h after infection (3 × 3-way comparisons). Twelve (WT HIV-1 +/− RTi), nine (ΔVpu/ΔNef HIV-1) or 14 (Vpu/Nef) unique peptides were used for EWI-2 quantitation. Ratios of abundances to mock-infected CEM-T4 T cells (WT HIV-1 +/- RTi and ΔVpu/ΔNef HIV-1) or GFP-transduced CEM-T4 T cells (Vpu/Nef) are shown. Note that (A) and (B) show data from two different quantitative proteomic methods, as described above and in Materials and Methods.

**Figure 3.5.** EWI-2 inhibits infected-uninfected cell fusion. (A) HeLa-TZM-bl fusion assays were performed using producer HeLa cells that were co-transfected with either pNL-sfGI ΔEnv (ΔEnv) or pNL-sfGI (WT) in combination with overexpression plasmid totaling 500 ng (using the indicated amount of CD81 or EWI-2 supplemented with L6). Luminescence readings (across 4 independent biological replicates, each with two technical replicates) were divided by the ΔEnv condition to obtain the fold increase in fusion, and then normalized to the WT co-transfected with only L6 (i.e., 0 ng of CD81 or EWI-2) condition, making it have a value of 1. Deviation from the dashed line at 1 thus indicates an effect on fusion. Values from the same biological replicate are linked by a grey line. (B–D) EWI-2 expression in shScramble (shScr) and shEWI-2 CEM-SS cells was analyzed by microscopy (B) and flow cytometry (C–D). (B) For microscopy, cells were plated onto poly-L-lysine-coated glass, fixed,

permeabilized, labeled for EWI-2, and stained using fluorescent secondary antibody (magenta) and DAPI (cyan). Scale bars = 10 μm. (C–D) For flow cytometry analysis, cells were labeled with Live/Dead Fixable Near-IR, fixed, permeabilized, labeled for EWI-2, and stained with fluorescent secondary antibody. (C) Representative histogram of the EWI-2 signal intensity normalized to mode in live cells for unstained controls (black line), shEWI-2 (blue), and shScr (red) cells. (D) EWI-2 MFI in live shScr (red) and shEWI-2 (blue) cells from three independent biological replicates, normalized to EWI-2-labeled parental CEM-SS cells (represented at a value of 1 with a dashed line). (E) CEM-luc fusion assays were performed using shScr or shEWI-2 producer cells infected with NL4-3, which were co-cultured with CEM-luc target cells in the presence of DMSO (vehicle control, luciferase signal from transmission and cell–cell fusion) or EFV (luciferase signal resulting exclusively from cell–cell fusion). Luminescence readings (across three independent biological replicates) from the EFV-treated condition were divided by the DMSO reading from the same producer cell type and multiplied by 100 to determine the percentage of luciferase expression dependent on cell–cell fusion (syncytium formation) between either shScr or shEWI-2 producer and CEM-luc target cells. Values from the same biological replicate are linked by a black line.

**Figure 3.6.** Syncytia have higher surface expression of EWI-2 and CD81 than mononucleated infected cells. (A) Primary $CD4^+$ T cells were infected with NL-sfGI, surface-labeled for either EWI-2 or CD81 (both shown in magenta), fixed, stained with DAPI (cyan) and AlexaFluor 647-conjugated secondary antibody, and imaged. Infected cells were identified by GFP (yellow) and discriminated as mono- or multinucleated infected cells by DAPI. Representative cells are shown. Scale bars = 5 μm. (B) Cells were prepared as described in (A) and analyzed for EWI-2 or CD81 surface expression on uninfected cells, mononucleated infected cells (Mono) and syncytia (Syn) by manually selecting the plasma membrane at the midline of each cell and quantifying the mean EWI-2 or CD81-associated fluorescence intensity. Raw fluorescence intensity values were background-subtracted using the fluorescence intensity of a cell-free area within the same image and subsequently normalized to the average intensity value of uninfected cells within the same imaging set. Data shown are the pooled normalized intensity values of two independent biological replicates, each with two technical replicates. Each data point represents the normalized surface MFI of an individual cell. Error bars = SD. *p*-values are the result of Kruskal-Wallis tests.

## 3.11 Figures

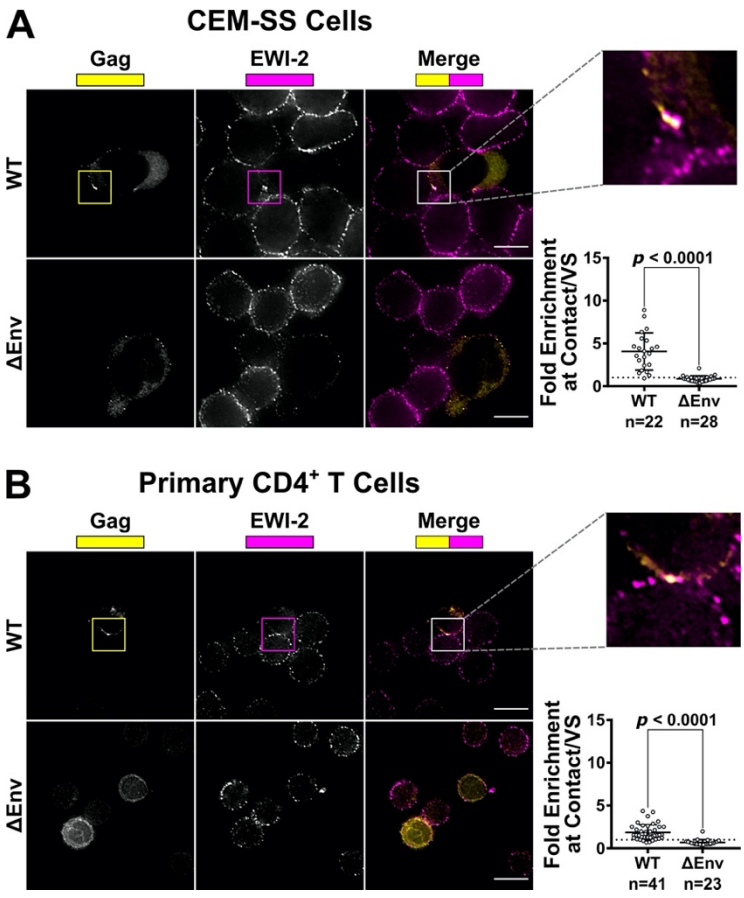


**Figure 3.1. EWI-2 co-accumulates with Gag at the HIV-1 VS in T cells.**

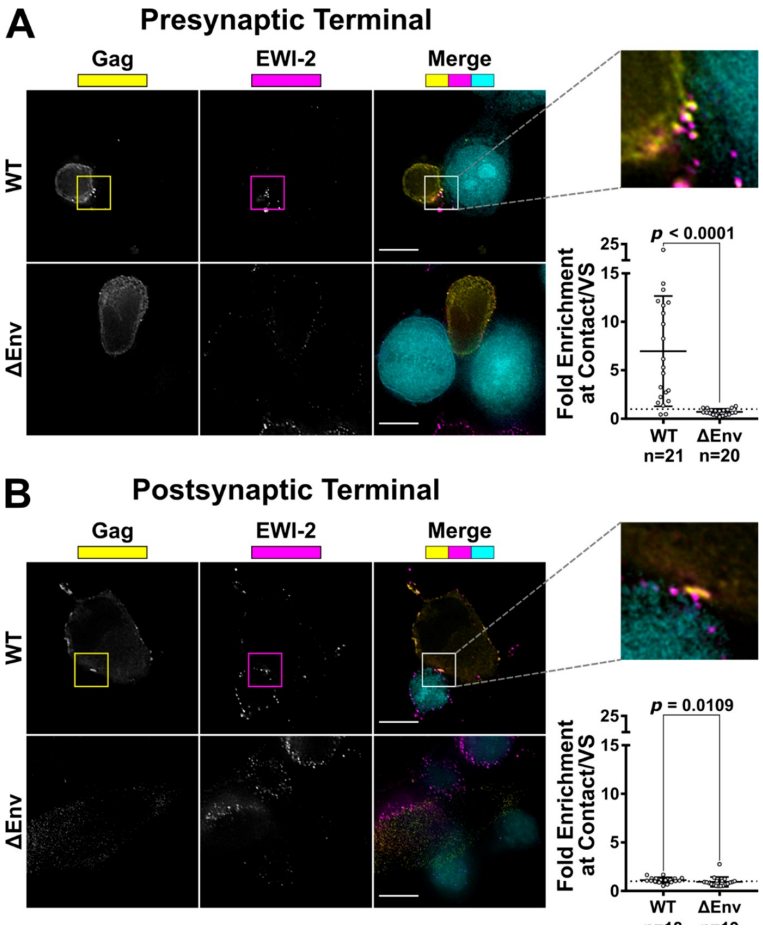


**Figure 3.2. EWI-2 accumulation takes place on the producer cell side of the VS.**

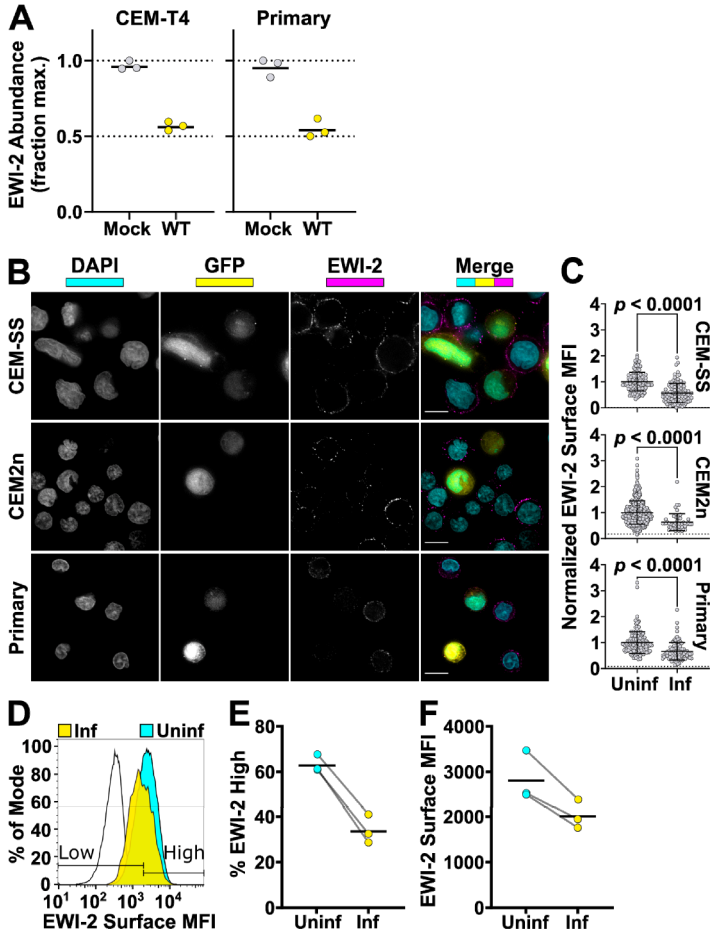


**Figure 3.3. EWI-2 is downregulated from the surface of infected cells.**

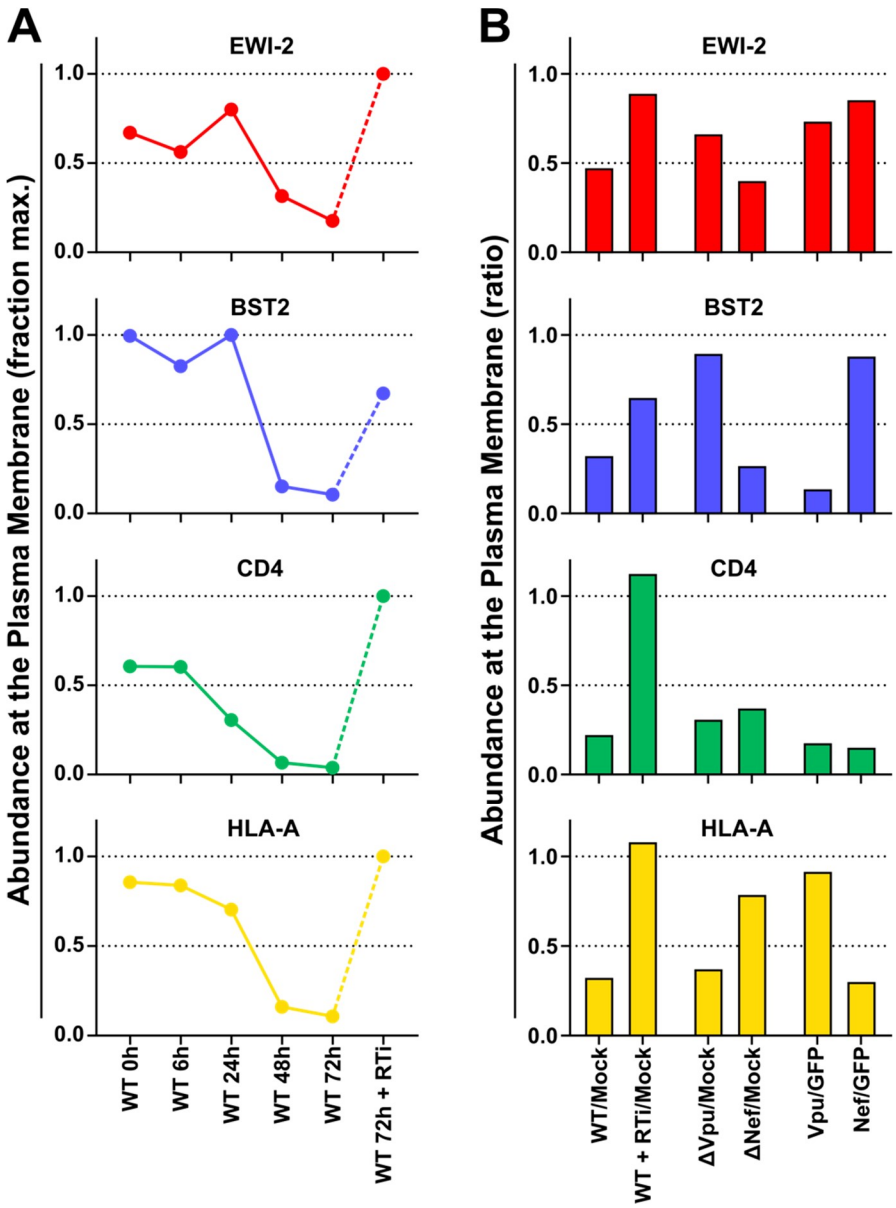


**Figure 3.4. Plasma membrane EWI-2 is downregulated by Vpu.**

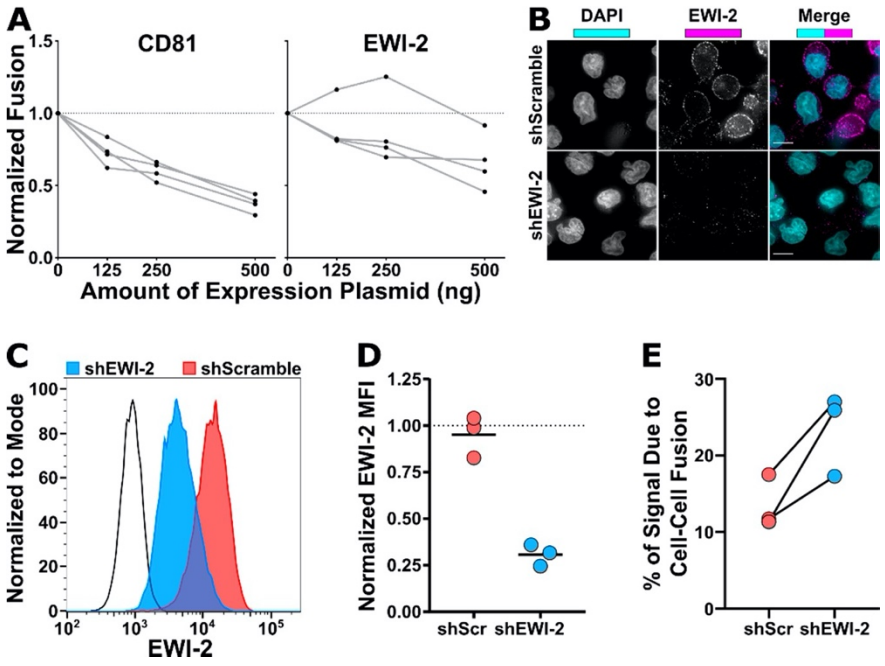


**Figure 3.5. EWI-2 inhibits infected-uninfected cell fusion.**

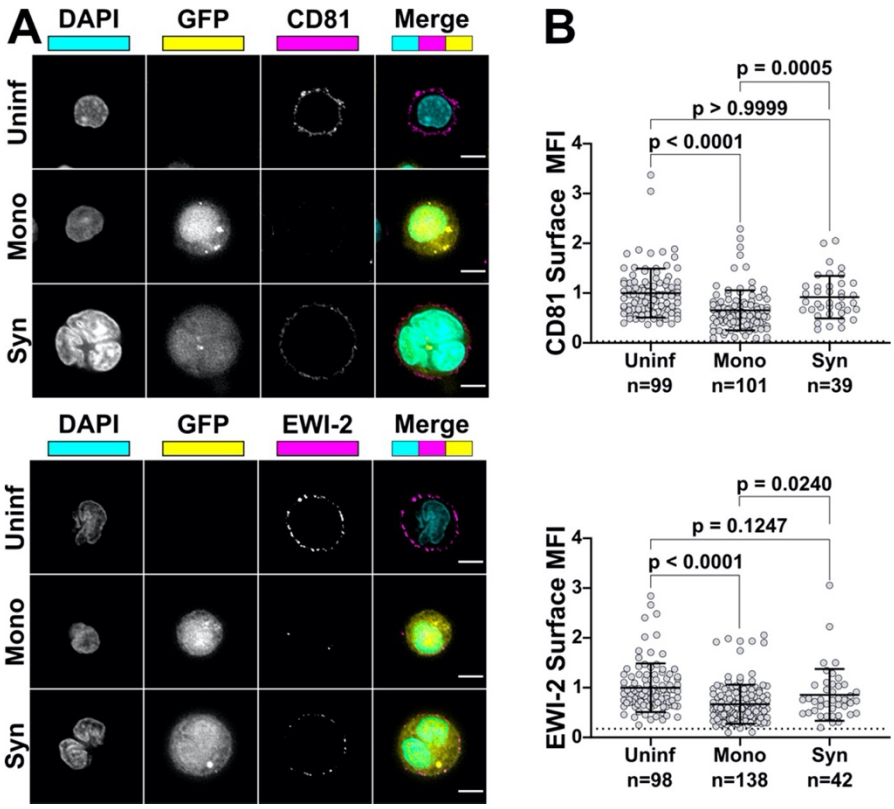


**Figure 3.6. Syncytia have higher surface expression of EWI-2 and CD81 than mononucleated infected cells.**

## 3.12 References


1. Jolly, C.; Kashefi, K.; Hollinshead, M.; Sattentau, Q.J. HIV-1 cell to cell transfer across an Env-induced, actin-dependent synapse. *J. Exp. Med.* 2004, *199*, 283–293. [CrossRef] [PubMed]

2. Hubner, W.; McNerney, G.P.; Chen, P.; Dale, B.M.; Gordon, R.E.; Chuang, F.Y.; Li, X.D.; Asmuth, D.M.; Huser, T.; Chen, B.K. Quantitative 3D video microscopy of HIV transfer across T cell virological synapses. *Science* 2009, *323*, 1743–1747. [CrossRef] [PubMed]

3. Ladinsky, M.S.; Kieffer, C.; Olson, G.; Deruaz, M.; Vrbanac, V.; Tager, A.M.; Kwon, D.S.; Bjorkman, P.J. Electron tomography of HIV-1 infection in gut-associated lymphoid tissue. *PLoS Pathog.* 2014, *10*, e1003899. [CrossRef] [PubMed]

4. Reh, L.; Magnus, C.; Schanz, M.; Weber, J.; Uhr, T.; Rusert, P.; Trkola, A. Capacity of Broadly Neutralizing Antibodies to Inhibit HIV-1 Cell-Cell Transmission Is Strain- and Epitope-Dependent. *PLoS Pathog.* 2015, *11*, e1004966. [CrossRef] [PubMed]

5. Bracq, L.; Xie, M.; Benichou, S.; Bouchet, J. Mechanisms for Cell-to-Cell Transmission of HIV-1. *Front. Immunol.* 2018, *9*, 260. [CrossRef] [PubMed]

6. Imle, A.; Kumberger, P.; Schnellbacher, N.D.; Fehr, J.; Carrillo-Bustamante, P.; Ales, J.; Schmidt, P.; Ritter, C.; Godinez, W.J.; Muller, B.; et al. Experimental and computational analyses reveal that environmental restrictions shape HIV-1 spread in 3D cultures. *Nat. Commun.* 2019, *10*, 2144. [CrossRef]

7. Orenstein, J.M. *In vivo* cytolysis and fusion of human immunodeficiency virus type 1-infected lymphocytes in lymphoid tissue. *J. Infect. Dis.* 2000, *182*, 338–342. [CrossRef]

8. Murooka, T.T.; Deruaz, M.; Marangoni, F.; Vrbanac, V.D.; Seung, E.; von Andrian, U.H.; Tager, A.M.; Luster, A.D.; Mempel, T.R. HIV-infected T cells are migratory vehicles for viral dissemination. *Nature* 2012, *490*, 283–287. [CrossRef]

9. Symeonides, M.; Murooka, T.T.; Bellfy, L.N.; Roy, N.H.; Mempel, T.R.; Thali, M. HIV-1-Induced Small T Cell Syncytia Can Transfer Virus Particles to Target Cells through Transient Contacts. *Viruses* 2015, *7*, 6590–6603. [CrossRef]

10. Law, K.M.; Komarova, N.L.; Yewdall, A.W.; Lee, R.K.; Herrera, O.L.; Wodarz, D.; Chen, B.K. *In Vivo* HIV-1 Cell-to-Cell Transmission Promotes Multicopy Micro-compartmentalized Infection. *Cell Rep.* 2016, *15*, 2771–2783. [CrossRef]

11. Uchil, P.D.; Haugh, K.A.; Pi, R.; Mothes, W. *In Vivo* Imaging-Driven Approaches to Study Virus Dissemination and Pathogenesis. *Annu. Rev. Virol.* 2019, *6*, 501–524. [CrossRef] [PubMed]

12. Ventura, J.D.; Beloor, J.; Allen, E.; Zhang, T.; Haugh, K.A.; Uchil, P.D.; Ochsenbauer, C.; Kieffer, C.; Kumar, P.; Hope, T.J.; et al. Longitudinal bioluminescent imaging of HIV-1 infection during antiretroviral therapy and treatment interruption in humanized mice. *PLoS Pathog.* 2019, *15*, e1008161. [CrossRef] [PubMed]

13. Alvarez, R.A.; Barria, M.I.; Chen, B.K. Unique features of HIV-1 spread through T cell virological synapses. *PLoS Pathog.* 2014, *10*, e1004513. [CrossRef] [PubMed]

14. Compton, A.A.; Schwartz, O. They Might Be Giants: Does Syncytium Formation Sink or Spread HIV Infection? *PLoS Pathog.* 2017, *13*, e1006099. [CrossRef] [PubMed]

15. Rowell, J.F.; Stanhope, P.E.; Siliciano, R.F. Endocytosis of endogenously synthesized HIV-1 envelope protein. Mechanism and role in processing for association with class II MHC. *J. Immunol.* 1995, *155*, 473–488.

16. Egan, M.A.; Carruth, L.M.; Rowell, J.F.; Yu, X.; Siliciano, R.F. Human immunodeficiency virus type 1 envelope protein endocytosis mediated by a highly conserved intrinsic internalization signal in the cytoplasmic domain of gp41 is suppressed in the presence of the Pr55gag precursor protein. *J. Virol.* 1996, *70*, 6547–6556.

17. Roy, N.H.; Chan, J.; Lambele, M.; Thali, M. Clustering and mobility of HIV-1 Env at viral assembly sites predict its propensity to induce cell-cell fusion. *J. Virol.* 2013, *87*, 7516–7525. [CrossRef]

18. Murakami, T.; Ablan, S.; Freed, E.O.; Tanaka, Y. Regulation of human immunodeficiency virus type 1 Env-mediated membrane fusion by viral protease activity. *J. Virol.* 2004, *78*, 1026–1031. [CrossRef]

19. Wyma, D.J.; Jiang, J.; Shi, J.; Zhou, J.; Lineberger, J.E.; Miller, M.D.; Aiken, C. Coupling of human immunodeficiency virus type 1 fusion to virion maturation: A novel role of the gp41 cytoplasmic tail. *J. Virol.* 2004, *78*, 3429–3435. [CrossRef]

20. Jiang, J.; Aiken, C. Maturation-dependent human immunodeficiency virus type 1 particle fusion requires a carboxyl-terminal region of the gp41 cytoplasmic tail. *J. Virol.* 2007, *81*, 9999–10008. [CrossRef]

21. Chojnacki, J.; Staudt, T.; Glass, B.; Bingen, P.; Engelhardt, J.; Anders, M.; Schneider, J.; Muller, B.; Hell, S.W.; Krausslich, H.G. Maturation-dependent HIV-1 surface protein redistribution revealed by fluorescence nanoscopy. *Science* 2012, *338*, 524–528. [CrossRef] [PubMed]

22. Weng, J.; Krementsov, D.N.; Khurana, S.; Roy, N.H.; Thali, M. Formation of syncytia is repressed by tetraspanins in human immunodeficiency virus type 1-producing cells. *J. Virol.* 2009, *83*, 7467–7474. [CrossRef] [PubMed]

23. Symeonides, M.; Lambele, M.; Roy, N.H.; Thali, M. Evidence showing that tetraspanins inhibit HIV-1-induced cell-cell fusion at a post-hemifusion stage. *Viruses* 2014, *6*, 1078–1090. [CrossRef] [PubMed]

24. Roy, N.H.; Lambele, M.; Chan, J.; Symeonides, M.; Thali, M. Ezrin is a component of the HIV-1 virological presynapse and contributes to the inhibition of cell-cell fusion. *J. Virol.* 2014, *88*, 7645–7658. [CrossRef] [PubMed]

25. Charrin, S.; Le Naour, F.; Oualid, M.; Billard, M.; Faure, G.; Hanash, S.M.; Boucheix, C.; Rubinstein, E. The major CD9 and CD81 molecular partner. Identification and characterization of the complexes. *J. Biol. Chem.* 2001, *276*, 14329–14337. [CrossRef] [PubMed]

26. Charrin, S.; Latil, M.; Soave, S.; Polesskaya, A.; Chretien, F.; Boucheix, C.; Rubinstein, E. Normal muscle regeneration requires tight control of muscle cell fusion by tetraspanins CD9 and CD81. *Nat. Commun.* 2013, *4*, 1674. [CrossRef]

27. Sala-Valdes, M.; Ursa, A.; Charrin, S.; Rubinstein, E.; Hemler, M.E.; Sanchez-Madrid, F.; Yanez-Mo, M. EWI-2 and EWI-F link the tetraspanin web to the actin cytoskeleton through their direct association with ezrin-radixin-moesin proteins. *J. Biol. Chem.* 2006, *281*, 19665–19675. [CrossRef]

28. Stipp, C.S.; Kolesnikova, T.V.; Hemler, M.E. EWI-2 is a major CD9 and CD81 partner and member of a novel Ig protein subfamily. *J. Biol. Chem.* 2001, *276*, 40545–40554. [CrossRef]

29. Charrin, S.; Le Naour, F.; Labas, V.; Billard, M.; Le Caer, J.P.; Emile, J.F.; Petit, M.A.; Boucheix, C.; Rubinstein, E. EWI-2 is a new component of the tetraspanin web in hepatocytes and lymphoid cells. *Biochem. J.* 2003, *373*, 409–421. [CrossRef]

30. Rocha-Perugini, V.; Montpellier, C.; Delgrange, D.; Wychowski, C.; Helle, F.; Pillez, A.; Drobecq, H.; Le Naour, F.; Charrin, S.; Levy, S.; et al. The CD81 partner EWI-2wint inhibits hepatitis C virus entry. *PLoS ONE* 2008, *3*, e1866. [CrossRef]

31. Montpellier, C.; Tews, B.A.; Poitrimole, J.; Rocha-Perugini, V.; D'Arienzo, V.; Potel, J.; Zhang, X.A.; Rubinstein, E.; Dubuisson, J.; Cocquerel, L. Interacting regions of CD81 and two of its partners, EWI-2 and EWI-2wint, and their effect on hepatitis C virus infection. *J. Biol. Chem.* 2011, *286*, 13954–13965. [CrossRef] [PubMed]

32. Gordon-Alonso, M.; Sala-Valdes, M.; Rocha-Perugini, V.; Perez-Hernandez, D.; Lopez-Martin, S.; Ursa, A.; Alvarez, S.; Kolesnikova, T.V.; Vazquez, J.; Sanchez-Madrid, F.; et al. EWI-2 association with alpha-actinin regulates T cell immune synapses and HIV viral infection. *J. Immunol.* 2012, *189*, 689–700. [CrossRef] [PubMed]

33. Chen, A.; Leikina, E.; Melikov, K.; Podbilewicz, B.; Kozlov, M.M.; Chernomordik, L.V. Fusion-pore expansion during syncytium formation is restricted by an actin network. *J. Cell Sci.* 2008, *121*, 3619–3628. [CrossRef] [PubMed]

34. Maddon, P.J.; Dalgleish, A.G.; Mcdougal, J.S.; Clapham, P.R.; Weiss, R.A.; Axel, R. The T4 Gene Encodes the Aids Virus Receptor and Is Expressed in the Immune-System and the Brain. *Cell* 1986, *47*, 333–348. [CrossRef]

35. Platt, E.J.; Wehrly, K.; Kuhmann, S.E.; Chesebro, B.; Kabat, D. Effects of CCR5 and CD4 cell surface concentrations on infections by macrophagetropic isolates of human immunodeficiency virus type 1. *J. Virol.* 1998, *72*, 2855–2864.

36. Derdeyn, C.A.; Decker, J.M.; Sfakianos, J.N.; Wu, X.; O'Brien, W.A.; Ratner, L.; Kappes, J.C.; Shaw, G.M.; Hunter, E. Sensitivity of human immunodeficiency virus type 1 to the fusion inhibitor T-20 is modulated by coreceptor specificity defined by the V3 loop of gp120. *J. Virol.* 2000, *74*, 8358–8367. [CrossRef]

37. Wei, X.; Decker, J.M.; Liu, H.; Zhang, Z.; Arani, R.B.; Kilby, J.M.; Saag, M.S.; Wu, X.; Shaw, G.M.; Kappes, J.C. Emergence of resistant human immunodeficiency virus type 1 in patients receiving fusion inhibitor (T-20) monotherapy. *Antimicrob. Agents Chemother.* 2002, *46*, 1896–1905. [CrossRef]

38. Takeuchi, Y.; McClure, M.O.; Pizzato, M. Identification of gammaretroviruses constitutively released from cell lines used for human immunodeficiency virus research. *J. Virol.* 2008, *82*, 12585–12588. [CrossRef]

39. Platt, E.J.; Bilska, M.; Kozak, S.L.; Kabat, D.; Montefiori, D.C. Evidence that ecotropic murine leukemia virus contamination in TZM-bl cells does not affect the outcome of neutralizing antibody assays with human immunodeficiency virus type 1. *J. Virol.* 2009, *83*, 8289–8292. [CrossRef]

40. Trkola, A.; Matthews, J.; Gordon, C.; Ketas, T.; Moore, J.P. A cell line-based neutralization assay for primary human immunodeficiency virus type 1 isolates that use either the CCR5 or the CXCR4 coreceptor. *J. Virol.* 1999, *73*, 8966–8974.

41. Spenlehauer, C.; Gordon, C.A.; Trkola, A.; Moore, J.P. A luciferase-reporter gene-expressing T-cell line facilitates neutralization and drug-sensitivity assays that use either R5 or X4 strains of human immunodeficiency virus type 1. *Virology* 2001, *280*, 292–300. [CrossRef]

42. Foley, G.E.; Lazarus, H.; Farber, S.; Uzman, B.G.; Boone, B.A.; McCarthy, R.E. Continuous Culture of Human Lymphoblasts from Peripheral Blood of a Child with Acute Leukemia. *Cancer* 1965, *18*, 522–529. [CrossRef]

43. Nara, P.L.; Hatch, W.C.; Dunlop, N.M.; Robey, W.G.; Arthur, L.O.; Gonda, M.A.; Fischinger, P.J. Simple, rapid, quantitative, syncytium-forming microassay for the

detection of human immunodeficiency virus neutralizing antibody. *AIDS Res. Hum. Retrovir.* 1987, *3*, 283–302. [CrossRef]

44. Nara, P.L.; Fischinger, P.J. Quantitative infectivity assay for HIV-1 and-2. *Nature* 1988, *332*, 469–470. [CrossRef]

45. Refsland, E.W.; Hultquist, J.F.; Harris, R.S. Endogenous origins of HIV-1 G-to-A hypermutation and restriction in the nonpermissive T cell line CEM2n. *PLoS Pathog.* 2012, *8*, e1002800. [CrossRef]

46. Simm, M.; Shahabuddin, M.; Chao, W.; Allan, J.S.; Volsky, D.J. Aberrant Gag protein composition of a human immunodeficiency virus type 1 vif mutant produced in primary lymphocytes. *J. Virol.* 1995, *69*, 4582–4586.

47. Freed, E.O.; Martin, M.A. Virion incorporation of envelope glycoproteins with long but not short cytoplasmic tails is blocked by specific, single amino acid substitutions in the human immunodeficiency virus type 1 matrix. *J. Virol.* 1995, *69*, 1984–1989.

48. Qin, X.F.; An, D.S.; Chen, I.S.; Baltimore, D. Inhibiting HIV-1 infection in human T cells by lentiviral-mediated delivery of small interfering RNA against CCR5. *Proc. Natl. Acad. Sci. USA* 2003, *100*, 183–188. [CrossRef]

49. Schindelin, J.; Arganda-Carreras, I.; Frise, E.; Kaynig, V.; Longair, M.; Pietzsch, T.; Preibisch, S.; Rueden, C.; Saalfeld, S.; Schmid, B.; et al. Fiji: An open-source platform for biological-image analysis. *Nat. Methods* 2012, *9*, 676–682. [CrossRef]

50. Greenwood, E.J.; Matheson, N.J.; Wals, K.; van den Boomen, D.J.; Antrobus, R.; Williamson, J.C.; Lehner, P.J. Temporal proteomic analysis of HIV infection reveals remodelling of the host phosphoproteome by lentiviral Vif variants. *Elife* 2016, *5*, e18296. [CrossRef]

51. Naamati, A.; Williamson, J.C.; Greenwood, E.J.; Marelli, S.; Lehner, P.J.; Matheson, N.J. Functional proteomic atlas of HIV infection in primary human CD4+ T cells. *Elife* 2019, *8*, e41431. [CrossRef] [PubMed]

52. Matheson, N.J.; Peden, A.A.; Lehner, P.J. Antibody-free magnetic cell sorting of genetically modified primary human CD4+ T cells by one-step streptavidin affinity purification. *PLoS ONE* 2014, *9*, e111437. [CrossRef] [PubMed]

53. Matheson, N.J.; Sumner, J.; Wals, K.; Rapiteanu, R.; Weekes, M.P.; Vigan, R.; Weinelt, J.; Schindler, M.; Antrobus, R.; Costa, A.S.; et al. Cell Surface Proteomic Map of HIV Infection Reveals Antagonism of Amino Acid Metabolism by Vpu and Nef. *Cell Host Microbe* 2015, *18*, 409–423. [CrossRef] [PubMed]

54. Krementsov, D.N.; Weng, J.; Lambele, M.; Roy, N.H.; Thali, M. Tetraspanins regulate cell-to-cell transmission of HIV-1. *Retrovirology* 2009, *6*, 64. [CrossRef]

55. Durham, N.D.; Chen, B.K. HIV-1 Cell-Free and Cell-to-Cell Infections Are Differentially Regulated by Distinct Determinants in the Env gp41 Cytoplasmic Tail. *J. Virol.* 2015, *89*, 9324–9337. [CrossRef]

56. Lambele, M.; Koppensteiner, H.; Symeonides, M.; Roy, N.H.; Chan, J.; Schindler, M.; Thali, M. Vpu is the main determinant for tetraspanin downregulation in HIV-1-infected cells. *J. Virol.* 2015, *89*, 3247–3255. [CrossRef]

57. Haller, C.; Muller, B.; Fritz, J.V.; Lamas-Murua, M.; Stolp, B.; Pujol, F.M.; Keppler, O.T.; Fackler, O.T. HIV-1 Nef and Vpu are functionally redundant broad-spectrum modulators of cell surface receptors, including tetraspanins. *J. Virol.* 2014, *88*, 14241–14257. [CrossRef]

58. Karn, J.; Stoltzfus, C.M. Transcriptional and posttranscriptional regulation of HIV-1 gene expression. *Cold Spring Harb. Perspect. Med.* 2012, *2*, a006916. [CrossRef]

59. Sato, K.; Aoki, J.; Misawa, N.; Daikoku, E.; Sano, K.; Tanaka, Y.; Koyanagi, Y. Modulation of human immunodeficiency virus type 1 infectivity through incorporation of tetraspanin proteins. *J. Virol.* 2008, *82*, 1021–1033. [CrossRef]

60. Ikeda, T.; Symeonides, M.; Albin, J.S.; Li, M.; Thali, M.; Harris, R.S. HIV-1 adaptation studies reveal a novel Env-mediated homeostasis mechanism for evading lethal hypermutation by APOBEC3G. *PLoS Pathog.* 2018, *14*, e1007010. [CrossRef]

61. Sugden, S.M.; Bego, M.G.; Pham, T.N.; Cohen, E.A. Remodeling of the Host Cell Plasma Membrane by HIV-1 Nef and Vpu: A Strategy to Ensure Viral Fitness and Persistence. *Viruses* 2016, *8*, 67. [CrossRef] [PubMed]

62. Gordon-Alonso,M.; Yanez-Mo,M.; Barreiro,O.; Alvarez,S.; Munoz-Fernandez,M.A.; Valenzuela-Fernandez,A.; Sanchez-Madrid, F. Tetraspanins CD9 and CD81 modulate HIV-1-induced membrane fusion. *J. Immunol.* 2006, *177*, 5129–5137. [CrossRef] [PubMed]

63. Len, A.C.L.; Starling, S.; Shivkumar, M.; Jolly, C. HIV-1 Activates T Cell Signaling Independently of Antigen to Drive Viral Spread. *Cell Rep.* 2017, *18*, 1062–1074. [CrossRef] [PubMed]

64. Greenwood, E.J.D.; Williamson, J.C.; Sienkiewicz, A.; Naamati, A.; Matheson, N.J.; Lehner, P.J. Promiscuous Targeting of Cellular Proteins by Vpr Drives Systems-Level Proteomic Remodeling in HIV-1 Infection. *Cell Rep.* 2019, *27*, 1579–1596.e7. [CrossRef] [PubMed]

65. Sylwester, A.; Murphy, S.; Shutt, D.; Soll, D.R. HIV-induced T cell syncytia are self-perpetuating and the primary cause of T cell death in culture. *J. Immunol.* 1997, *158*, 3996–4007.

66. Rinfret, A.; Latendresse, H.; Lefebvre, R.; St-Louis, G.; Jolicoeur, P.; Lamarre, L. Human immunodeficiency virus-infected multinucleated histiocytes in oropharyngeal

lymphoid tissues from two asymptomatic patients. *Am. J. Pathol.* 1991, *138*, 421–426.

67. Frankel, S.S.; Wenig, B.M.; Burke, A.P.; Mannan, P.; Thompson, L.D.; Abbondanzo, S.L.; Nelson, A.M.; Pope, M.; Steinman, R.M. Replication of HIV-1 in dendritic cell-derived syncytia at the mucosal surface of the adenoid. *Science* 1996, *272*, 115–117. [CrossRef]

68. Murooka, T.T.; Sharaf, R.R.; Mempel, T.R. Large Syncytia in Lymph Nodes Induced by CCR5-Tropic HIV-1. *AIDS Res. Hum. Retrovir.* 2015, *31*, 471–472. [CrossRef]

69. Sylwester, A.; Daniels, K.; Soll, D.R. The invasive and destructive behavior of HIV-induced T cell syncytia on collagen and endothelium. *J. Leukoc. Biol.* 1998, *63*, 233–244. [CrossRef]

70. Van Duyne, R.; Kuo, L.S.; Pham, P.; Fujii, K.; Freed, E.O. Mutations in the HIV-1 envelope glycoprotein can broadly rescue blocks at multiple steps in the virus replication cycle. *Proc. Natl. Acad. Sci. USA* 2019, *116*, 9040–9049. [CrossRef]

# CHAPTER 4 : CD4+ T CELLS TRANSIENTLY INFLUENCE EWI-2 SURFACE LEVELS ON HIV-1 INFECTED CELLS UPON HIV-1-INDUCED CELL-CELL FUSION

## 4.1. Abstract

HIV-1 cell-to-cell transmission occurs at the virological synapse (VS) which is formed upon Env at the surface an infected cell binding CD4 on an uninfected cell. While the VS typically resolves with complete separation of the two cells, Env can also facilitate fusion of the infected and uninfected cell membranes, leading to the formation of a multinucleated HIV-1 infected cell (syncytium). T cell-based syncytia can be detected during early infection in humanized mice and can transfer virus to uninfected cells, which overall suggests that these infected entities likely play a role in viral spread. A feature of T cell-based syncytia present during early infection is that they are limited in size (2-4 nuclei) suggesting that they are likely restricted from fusing indefinitely, possibly by previously defined viral and host fusion inhibitory proteins.

We recently demonstrated that syncytia have partially restored levels of fusion inhibitory host proteins CD81 and EWI-2. However, the factors influencing the syncytia surface profile remained unknown. To better understand how the infected cell surface profile is altered upon cell-cell fusion, we used quantitative imaging to investigate the role of uninfected target cells in influencing the EWI-2 levels upon HIV-1-induced syncytium formation and to determine whether the EWI-2 levels on syncytia are fixed or, just as in mononucleated infected cells, downregulated over time over time.

## 4.2. Introduction

Human immunodeficiency virus type 1 (HIV-1), the causative agent for acquired immunodeficiency syndrome (AIDS), can spread through multiple modes of transmission including cell-free and cell-to-cell transmission (reviewed in [1]). Cell-free infection relies on free virus particles encountering an uninfected $CD4^+$ T (target) cell, at which point the viral fusogen (Envelope/Env) can bind its receptor (CD4) and facilitate fusion between the phospholipid bilayer surrounding the viral particle and the plasma membrane of the target cell. Cell-to-cell transmission relies on the formation of a transient infected (producer) to target cell junction known as the virological synapse (VS) [2,3]. The VS forms upon Env present on the surface of a producer cell binding CD4 on target cell [2]. Cell-to-cell transmission at the VS is highly efficient as this junction allows for viral particles to bud from the producer cell in close proximity to the target cell. Although the VS often resolves with transfer of virus particles to the target cell and complete cell separation, formation of a VS can also result in Env-mediated fusion between the producer and target cell membranes to form a multinucleated HIV-1 infected cell (syncytium).

Recently, HIV-1-induced T-cell-based syncytia have been documented *in vivo* in humanized mice by multiple independent groups [4-6]. Syncytia have been detected in humanized mouse models as early as 48 hours post infection [4] and can be induced by virus bearing a transmitted-founder (T/F) virus envelope [5] as well as full-length T/F virus [6], collectively suggesting that HIV-1-induced syncytia may be important for early virus spread. T cell based syncytia seen *in vivo* are migratory and frequently displayed an elongated/multilobed morphology [4,5]. Intriguingly, these syncytia appear limited in size as the majority detected *in vivo* had 2 nuclei while even the largest syncytia contained only

4 nuclei [7]. These small (2-4 nuclei) T cell-based syncytia detected *in vivo* during early infection [7] were clearly distinct from previously described macrophage based multinucleated giant cells (MGCs) in HIV-1 infected patients [8,9] as well as cytopathic syncytia that can grow to be >10 cell volumes in size (therefore likely containing >10 nuclei) observed *in vitro* using highly fusogenic cell lines (ie. SUP-T1 cells, [10])(also discussed in [11]). The distinct phenotype of small T cell-based HIV-1-induced syncytia first documented *in vivo* can be recapitulated *in vitro* by embedding infected T cells in 3D matrices such as those comprised of Collagen or Matrigel [7]. Live-cell imaging of infected cells embedded in a 3D matrix documented an HIV-1-induced syncytium undergoing cell-cell fusion shortly followed by the same syncytium contacting an uninfected target cell, transferring viral particles to the target cell, and ultimately followed by complete separation of the syncytium and target cell [7]. This observation provided additional support for the idea that syncytia may contribute to virus spread. Further, that syncytia are limited in size (2-4 nuclei) and can contact uninfected target cells without inducing cell-cell fusion [7] indicates that syncytia may utilize known viral and host fusion inhibitory proteins to prevent indefinite cell-cell fusion.

Given that Env is fusogenic at neutral pH, both viral (Gag) and host (tetraspanins, Ezrin, and EWI-2) fusion inhibitory proteins are necessary for preventing excessive cell-cell fusion upon Env-CD4 binding at the VS [12-15]. HIV-1-induced cell-cell fusion at the VS is largely prevented by the Gag precursor polyprotein which traps Env at the VS in a non-fusogenic state [12]. Additionally, several host proteins have been shown to co-accumulate with Gag at the VS where they contribute to preventing excessive cell-cell fusion [13-17]. Multiple members of the tetraspanin family (including CD9, CD63, and

CD81) are known to prevent excessive Env-induced cell-cell fusion, and act at a post-hemifusion stage of HIV-1-induced membrane fusion [13,18,19]. Cytoskeletal linker protein Ezrin has also been identified as a fusion inhibitory host protein, likely supporting fusion inhibition at the VS through interactions with the actin cytoskeleton when Ezrin is in an active, phosphorylated (p-ezrin) state [14]. EWI-2 (IGSF8) is an interacting partner of both Ezrin [20] and tetraspanins (CD9 and CD81) [21] and has recently been identified as an inhibitor of HIV-1-induced cell-cell fusion that is enriched specifically on the producer cell side of the VS (the presynapse) [15]. Both tetraspanins and EWI-2 inhibit HIV-1-induced syncytia formation in a dose-dependent manner and, despite being enriched at the VS, are overall downregulated from the surface of HIV-1-infected cells [13,15,17,22-24]. Downregulation of these fusion inhibitory proteins is likely necessary to support optimal viral particle infectivity, as increased incorporation of fusion inhibitory tetraspanins into viral particles is correlated with a decrease in particle infectivity due to tetraspanins inhibiting particle-cell fusion/entry [17,25,26]. Overall, the subcellular localization of fusion inhibitory host proteins is modulated upon infection to balance virus particle infectivity with preventing excessive syncytia formation.

Despite fusion inhibitory tetraspanins and EWI-2 being downregulated from the surface of HIV-1 infected cells, primarily by viral accessory protein Vpu [15,26], it was recently demonstrated that T cell-based syncytia have partially restored surface levels of both EWI-2 and tetraspanin CD81 [15]. Restoration of EWI-2 and CD81 on syncytia challenges not only what is known about regulation of fusion inhibitory host proteins in infected cells, but has potentially broader implications for overall modulation of the surface profile by viral accessory proteins upon infection (reviewed in [27]). As part of our efforts

to better understand the role of HIV-1-induced T cell based syncytia in virus spread and how the surface profile of syncytia is altered compared to mononucleated infected cells, we sought to determine how EWI-2 levels are changed upon cell-cell fusion and whether this altered phenotype is transient or maintained over time.

## 4.3. Materials and Methods

### *4.3.1. Cell Lines and Cell Culture*

The following reagent was obtained through the NIH HIV Reagent Program, Division of AIDS, NIAID, NIH: CEM-SS Cells, ARP-776, contributed by Dr. Peter L. Nara [28-30]. CEM-SS cells were maintained in RPMI 1640 medium (Corning, Corning, NY, Cat. #10-104-CV) supplemented with 10% fetal bovine serum (FBS; Corning, Cat. #35-010-CV) and antibiotics penicillin/streptomycin (P/S; 100 units/mL penicillin and 100 µg/mL streptomycin; Invitrogen) and incubated at 37 ˚C/5% $CO_2$.

CEM-SS cells which were stably transduced with lentiviruses encoding either shRNA targeting EWI-2 (shEWI-2; sequence designed modified from EWI-2 targeting siRNA described previously [20]) or a scrambled control shRNA sequence (shScr) (lentiviral constructs, transduction, and generation of these cell lines described previously [15]) were maintained in RPMI supplemented with 10% FBS and 0.25 µg/ml puromycin to maintain positive selective pressure for transduced cells and incubated at 37 ˚C/5% $CO_2$.

HEK 293 T cells were maintained in Dulbecco's Modification of Eagle's Medium (DMEM) (Corning, Cat. #10-017-CV) supplemented with 10% FBS and P/S and incubated at 37 ˚C/5% $CO_2$.

*4.3.2. Antibodies and Fluorescent Dyes*

Mouse monoclonal antibody (mAb) to human EWI-2 (8A12) [31] was a kind gift from Dr. Eric Rubinstein (Sorbonne Université, Paris, France) and was used at 1:200 for all experiments. Secondary antibody, Alexa Fluor 647-conjugated donkey polyclonal antibody (pAb) to mouse IgG (Invitrogen, Carlsbad, CA, Cat. #A-31571), was used at 1:500 for all experiments. 4'. 6-diamidino-2-phenylindole (DAPI; Roche, Basel, Switzerland, Cat. # 10236276001) prepared in stocks of 5 mg/mL in dd$H_2O$, was used at 2 µg/mL (1:2500) to label double-stranded DNA. CellTracker™ Blue CMAC (CMAC; Invitrogen, Cat. #C2110) prepared in 10 mM stocks in DMSO, was used at 20 µM (1:500) in serum-free RPMI to dye the cytoplasm of uninfected cells as indicated.

*4.3.3. Virus Strains and Virus Stock Preparation*

Proviral plasmid pNL-sfGI was a kind gift from Dr. Benjamin Chen [5] (Mount Sinai School of Medicine, New York, NY) is an NL4-3-derived strain encoding superfolder (sf) green fluorescent protein (GFP) in place of Nef with Nef being reintroduced downstream of an internal ribosome entry site (IRES). VZV-G-pseudotyped NL-sfGI virus stocks were produced in HEK 293 T cells transfected with pVZV-G and pNL-sfGI (at a ratio of 3:17) by calcium phosphate precipitation. Growth medium was refreshed 1 day post transfection. Virus-containing supernatants were harvested 36-48 hr after refreshing the media, centrifuged at 2000 rcf for 10 min and then filtered to remove any cells or cell debris, and stored at -80 ˚C.

*4.3.4. Infections*

To determine the contribution of surface protein on syncytia from target cells upon fusion, 2 million CEM-SS cells were infected by spinoculation with 10 µL of NL-sfGI virus stock. Cells were incubated for 20 min at 37 ˚C/5% $CO_2$ in 500 µL of RPMI/10% FBS containing virus. After the incubation period, cells were centrifuged at 1200 rcf at 37 ˚C for 99 min, followed by a 15 min recovery period at 37 ˚C, followed by an additional centrifugation at 300 rcf for 2 min to pellet the cells. Cells were resuspended in 8 mL of fresh, pre-warmed RPMI/10% FBS and incubated at 37 ˚C/5% $CO_2$ in a 6 well plate.

To determine whether EWI-2 levels on syncytia change over time, 1 million CEM-SS cells were infected by spinoculation using 2 of NL-sfGI virus stock, as described above.

*4.3.5. HIV-1-induced syncytium formation with shRNA expressing target cells*

To determine whether the levels of EWI-2 on previously unfused target cells influence the EWI-2 surface levels on the resulting syncytium, NL-sfGI infected CEM-SS (producer) cells were co-cultured with CMAC-labeled shEWI-2 or shScr CEM-SS (target) cells. To label target cells prior to co-culture, cells were incubated at 2 million cells/mL in pre-warmed, serum-free RPMI containing CMAC (1:500) for 30 minutes at 37 ˚C/5% $CO_2$, washed with 5 mL RPMI/10% FBS, resuspended in 8 mL fresh RPMI/10% FBS, and incubated overnight. 1 day post infection, CMAC-labeled target cells were co-cultured with producer cells (at a ratio of 2:1, $1 \times 10^6 : 5 \times 10^5$, targets:producers) in 4 mL RPMI/10% FBS with 1 µM Efavirenz (EFV) (NIH AIDS Reagent Program, Cat. #4624), and incubated for 17-18 hr at 37 ˚C/5% $CO_2$. Following the co-culture, 2.5-3 $\times 10^5$ cells from each co-culture condition alongside wells containing uninfected (control) cells for each cell type (CEM-SS, shEWI-2, and shScr) and a primary antibody control (CEM-SS) were plated on

8-well glass-bottom plates (Cellvis, Mountain View, CA, Cat. #C8-1.5H-N) coated with 1:10 poly-L-lysine (Newcomer Supply, Middleton, WI, Cat. #3438-100-01) and incubated at 37 ˚C for 2 hr. Plated cells were labeled with 100 µL RPMI/10% FBS with 8A12 (1:200) or RPMI/10% FBS only (primary antibody control) for 45 min at 4 ˚C, followed by two 300 µL washes with RPMI/10% FBS. All samples were fixed with 500 µL phosphate buffered saline (PBS) containing 4% paraformaldehyde for 10 minutes and washed with 500 µL PBS. Fixed samples were permeabilized with 100 µL PBS containing 1% bovine serum albumin (BSA) and 0.1% Triton®X-100 (MilliporeSigma, Burlington, MA, Cat. #TX1568-1) and washed with 300 µL PBS/1% BSA. Fixed and permeabilized samples were labeled with Alexa Fluor 647-conjugated secondary antibody (1:500) in PBS/1% BSA for 45 min, followed by two 300 µL washes with PBS/1% BSA, and kept in 300 µL of PBS for imaging.

*4.3.6. Quantifying EWI-2 surface levels on syncytia over time*

To determine whether EWI-2 is maintained at the syncytium cell surface after HIV-1-induced cell-cell fusion, CEM-SS were infected with NL-sfGI for 3 days to allow for syncytium formation. 3 days post infection, a sample of infected cells prepared for microscopy (0 hr time point). The remaining cells were resuspended in fresh medium containing 1 µM EFV and 0.5 µM HIV-1 IIIB C34 peptide (C34) (NIH AIDS Reagent Program, Cat. #9824) to inhibit continued transmission and HIV-1-induced cell-cell fusion. 6 and 24 hr after the addition of the inhibitors samples of cells were prepared for microscopy (6 and 24 hr time points). The inhibitor containing medium was refreshed and the cells were incubated for an additional 24 hr before cells were harvested and prepared for a 48 hr time point. Upon imaging, there were too few syncytia remaining for analysis

and a striking amount of dying cells were observed (data not shown), thus these samples were not used for analysis.

For each time point, 2.5-3 × $10^5$ cells in 300 µL RPMI/10% FBS (with IL-2 for primary cells) were plated onto glass-bottom plates coated in poly-L-Lysine (as described above, 3.3.5) and incubated for 1 hr at 37 ˚C. Uninfected and primary antibody controls were prepared alongside infected samples for each time point. Plated cells were labeled in 100 µL RPMI/10% FBS with mAb 8A12 (1:200) for 45 min at 4 ˚C or medium only for uninfected primary antibody controls, washed with 2 × 300 µL of RPMI/10% FBS, fixed and permeabilized (as described above). Fixed and permeabilized samples were labeled with 647-conjugated secondary antibody (1:500) and DAPI (1:2500) in 100 µL PBS/1% BSA for 45 min, washed with 2 × 300 µL of PBS/1% BSA, and kept in 300 µL PBS for imaging.

*4.3.7. Image Acquisition*

Imaging was completed using a DeltaVision epifluorescence microscope (GE/Applied Precision, Issaquah, WA, USA) with an Olympus IX-70 base using an Olympus 60× PlanApo 1.42 NA objective and equipped with a CoolSNAP HQ CCD camera (Photometrics, Tucson, AZ). Images were processed by deconvolution and cropping (to remove edge artifacts of deconvolution) and imported into Fiji Version 2.1.0/1.53c for analysis.

*4.3.8. Quantifying EWI-2 Surface Density*

Prior to quantifying the relative EWI-2-associated signal at the cell surface, all images were copied and the copies were relabeled with unique 10 digit IDs (“deidentified”

images). Deidentified images were used to measure the 647-associated fluorescence intensity at the cell surface, as described previously [15]. Briefly, the cell surface was manually outlined to generate a region of interest (ROI), and the mean 647-associated fluorescence intensity (MFI) contained within each ROI was calculated. Only areas that were in focus at the midline of each cell, and not in contact with another cell, were included to calculate the 647 MFI for each cell. All individual MFI values were background subtracted by subtracting both the signal contained in a cell-free area of each cell's associated image frame and the average MFI of the unlabeled/no primary control uninfected CEM-SS cells for the associated biological replicate.

To compare syncytia that formed upon fusion with an shScr compared to an shEWI-2 target cell (3.3.5), CMAC-positive ($CMAC^+$) infected ($GFP^+$) cells were identified as syncytia that formed upon HIV-1-induced fusion with an shRNA expressing target cell. Uninfected CEM-SS cells were identified as CMAC/GFP-negative cells, while uninfected shRNA expressing cells were identified as $CMAC^+$/GFP-negative. After acquiring 647 MFIs and assigning identities (syncytium, uninfected CEM-SS, or uninfected shRNA expressing) to each cell the unique IDs were matched to their associated biological replicate and experimental condition (unlabeled control, uninfected control, infected co-culture with shScr or shEWI-2 target cells). Background subtracted MFIs were then normalized to the average MFI of associated uninfected, non-shRNA expressing CEM-SS cells prepared in parallel for each biological replicate. Background subtracted, normalized 647-MFI from an ROI was interpreted as the relative EWI-2 surface density of the associated cell.

To compare the EWI-2 surface density between syncytia from the 0, 6, and 24 hr time points (3.3.6) the 647-associated fluorescence at the cell surface was measured as

described above. Syncytia were identified as infected ($GFP^+$) cells with 2 or more nuclei (as seen by DAPI). After acquiring 647 MFIs and assigning identities (syncytium, mononucleated infected, or uninfected) to each cell, the unique IDs were matched to their associated biological replicate, time point (0, 6, or 24 hr), and experimental condition (unlabeled control, uninfected control, or infected). Each MFI value was background subtracted as described above, and normalized to the associated uninfected CEM-SS cells present within the infected samples (GFP-negative) for each biological replicate and time point.

All data (background subtracted, normalized 647-associated fluorescence intensity values) were analyzed using GraphPad Prism Version 8.4.3.

## 4.4. Results

### *4.4.1. Uninfected target cells contribute to EWI-2 surface density on syncytia upon HIV-1-induced cell-cell fusion.*

Given that HIV-1-induced syncytia have increased levels of EWI-2 and CD81 compared to mononucleated infected cells, such that both proteins are partially restored to the levels of uninfected T cells [15], we sought to determine whether the previously unfused target cell contributes to the altered surface profile of the resulting syncytium upon cell-cell fusion. To analyze the contribution of target cells to the syncytia surface profile, we co-cultured infected cells with either relatively high or low EWI-2 expressing target cells, and analyzed the EWI-2 surface levels on the resulting HIV-1-induced syncytium (Figure 4.1A). Specifically, CEM-SS cells infected with NL-sfGI were co-cultured with CMAC-labeled target cells that were either EWI-2 knockdown (by shRNA, shEWI-2) or control

(shScr) CEM-SS cells (stable shEWI-2 and shScr cells were generated previously [15]) for 17-18 hr to allow for syncytium formation. Co-cultures were completed in the presence of the reverse transcriptase inhibitor Efavirenz (EFV) to prevent infection of CMAC-labeled target cells without inhibiting cell-cell fusion (Figure 4.1A), thus allowing for identification of syncytia that formed upon fusion with an shEWI-2 or shScr-expressing cell as $CMAC^{+}/GFP^{+}$ cells (Figure 4.1B). After the incubation period, cells from the co-cultures were prepared for microscopy alongside uninfected controls by surface-labeling EWI-2, fixed and permeabilized, then stained with 647-conjugated secondary pAb and imaged using a 60× objective. Relative surface densities of EWI-2 were determined by manually outlining the surface associated 647 signal and quantifying the mean fluorescence intensity (MFI) contained within each outline (as described previously [15]). To compare relative EWI-2 levels between syncytia that formed upon fusion with shEWI-2 and those that fused with shScr targets across biological replicates, MFI values of individual cells were normalized to the average uninfected CEM-SS (not expressing shRNA) EWI-2-associated 647 MFI from the respective biological replicate. Additionally, EWI-2 knockdown in shEWI-2 shRNA expressing target cells compared to shScr was also validated by microscopy (Supplementary Figure 4.1).

Syncytia that formed as a result of fusion with EWI-2 knockdown (shEWI-2 expressing) target cells had a 35% reduction in surface levels of EWI-2 compared to those that formed upon fusion with scrambled control (shScr expressing) target cells (Figure 4.1C-D). The corresponding difference in EWI-2 surface levels on syncytia that form as a result of fusion with EWI-2 WT or low expressing target cells demonstrates that the surface

levels of EWI-2 on the surface of syncytia are dependent on the EWI-2 levels of the previously uninfected target cell population.

*4.4.2. EWI-2 is downregulated from the surface of syncytia over time*

Previous analysis of HIV-1 infected cells by mass spectrometry demonstrated that EWI-2 levels decreased for the infected population over time, consistent with the pattern of modulation for other surface proteins that are downregulated upon infection [32], and that EWI-2 downregulation is primarily mediated by the viral accessory protein Vpu [15]. However, these analyses could not differentiate between mononucleated infected cells and HIV-1-induced syncytia. As syncytia have increased surface levels of EWI-2 [15], we therefore sought to determine whether EWI-2 surface levels on syncytia are maintained or modulated over time following cell-cell fusion. To monitor the EWI-2 surface density on populations of recently formed syncytia compared to populations of syncytia where more time had passed following HIV-1-induced cell-cell fusion, we compared EWI-2 levels across populations of syncytia that had been cultured in the presence of fusion inhibitors for varied amounts of time (0, 6 or 24 hours).

CEM-SS cells were infected with NL-sfGI and cultured for 3 days to allow for robust syncytia formation. At 3 days post infection, a sample of infected cells was harvested and prepared for microscopy (Time Point 0 hr) while the remaining cells were cultured in the presence of reverse transcriptase inhibitor EFV and fusion inhibiting peptide C34 to prevent subsequent infection of target cells and HIV-1-induced cell-cell fusion (Figure 4.2A). Additional samples of infected cells were collected and prepared for microscopy at 6 and 24 hours (Time Points 6 and 24 hr, respectively) after the addition of

the inhibitors. For microscopy preparation, all infected samples were prepared in parallel with uninfected CEM-SS controls, surface-labeled for EWI-2, fixed and permeabilized, stained with 647-conjugated secondary pAb and DAPI, and imaged using a 60× objective. HIV-1-induced syncytia from each time point were identified as infected (GFP positive) cells with at least 2 nuclei (Figure 4.2B). Relative surface density of EWI-2 on syncytia collected at each time point were determined by measuring the surface EWI-2-associated MFI for each cell, which was then normalized to respective uninfected CEM-SS cells present within the infected culture for each biological replicate and time point (see Supplementary Figure 4.2 for EWI-2 surface density of syncytia and controls). Further, we attempted to analyze syncytia cultured in the presence of EFV and C34 for 48 hours. However, syncytia were nearly absent from the samples harvested for the 48 hr time point and therefore could not be included in this analysis.

Comparison of syncytia surface EWI-2 levels over time demonstrates that EWI-2 levels on syncytia were highest on the samples collected at the 0 hr time point, and continually decreased for the 6 and 24 hr time points (Figure 4.2 C-D). These data demonstrate that EWI-2 is downregulated from the surface of syncytia after HIV-1-induced cell-cell fusion.

## 4.5. Discussion

HIV-1-induced syncytia are present *in vivo*, as demonstrated both in analysis of patient tissue samples [33] and several independent studies of infected humanized mice [4-6]. T cell-based syncytia remain small (2-4 nuclei) [7] and recent studies demonstrate that syncytia have restored levels of fusion inhibitory host proteins CD81 and EWI-2 [15]. The

unique phenotype of these infected entities prompted us to investigate how cell-cell fusion influences the syncytia surface profile. We now demonstrate that EWI-2 levels on syncytia depend on an influx of protein from the previously uninfected target cell upon HIV-1-induced cell-cell fusion which is then downregulated over time.

The finding that $CD4^+$ T cell based HIV-1-induced syncytia have partially restored surface levels of CD81 and EWI-2 [15], which are typically downregulated by viral accessory proteins [15,17,22,26], is likely the result of impaired viral accessory protein-mediated modulation of the infected cell surface profile upon cell-cell fusion. As the viral accessory proteins responsible for modulating EWI-2 and CD81 surface levels have many host protein targets, it is reasonable to speculate that cell-cell fusion-induced alterations to the infected cell surface profile may extend beyond fusion inhibitory host proteins to other targets of viral accessory protein mediated regulation. Modulating the surface profile upon infection has numerous functional effects for the infected cell including the ability to evade detection by immune cells and enhanced particle infectivity (reviewed in [27]). To better understand how syncytia formation might disrupt well-characterized viral accessory protein-mediated modulation of host proteins, these studies aimed to determine how syncytia develop an altered surface profile compared to mononucleated infected cells upon cell-cell fusion and whether this phenotype is transient or maintained for the lifetime of a syncytium.

We hypothesized that increased levels host surface proteins on syncytia were the result of an influx of protein contributed by protein from target cell upon fusion that would then be modulated by viral accessory proteins over time. Our data overall support our hypothesis as we demonstrate that reducing the surface levels of EWI-2 on target cells

results in a decrease in EWI-2 on syncytia that form upon fusion with these low EWI-2 expressing cells compared to those that fused with cells expressing higher levels of EWI-2 (Figure 4.1). Further, by inhibiting continued HIV-1-induced cell-cell fusion, we were able to compare the EWI-2 surface density of relatively "young" (Time Point 0 hr) syncytia populations to that of "old" (Time Points 6 and 24 hr) syncytia populations (Figure 4.2). However, it should be noted that we did not see the expected increase in overall surface density of EWI-2 on CEM-SS-based syncytia compared to mononucleated infected CEM-SS cells (Supplementary Figure 4.2). This finding suggests that CEM-SS-based syncytia might not fully recapitulate the partially restored EWI-2 phenotype of primary T cell-based syncytia [15]. We suspect that CEM-SS based syncytia may not have as pronounced restoration of EWI-2 as primary T cell-based syncytia [15], but still have overall higher levels of EWI-2 than mononucleated infected cells that our data cannot reflect due to current technical limitations. Specifically, we predict that the nearly equivalent density between syncytia and mononucleated infected cells (Supplementary Figure 4.2, Time Point 0 hr) supports the idea that syncytia have higher *total* amounts of EWI-2 at the surface as an equivalent density of protein (syncytia versus mononucleated) multiplied over a greater area of plasma membrane (syncytia) would yield more total protein on the cell surface. Future analysis using purified populations of syncytia compared to purified populations of mononucleated infected cells will allow us to complete more high throughput analysis, such as western blot and flow cytometry analysis, where the total amount of EWI-2 per cell can be determined. Given this potential limitation with CEM-SS cells, our data are interpreted in the context of comparing populations of syncytia to each other, and not to mononucleated infected cells. We demonstrate syncytia populations have progressively

decreasing surface levels of EWI-2 from 0-24 hr after the addition of EFV and C34 (Figure 4.2). Overall, these data support the hypothesis that syncytia downregulate EWI-2 over time, likely as a result of Vpu-mediated downregulation of the surface protein contributed by the previously uninfected target cell.

CD81 and EWI-2 are both primarily downregulated by Vpu [15,26]. In addition to these fusion inhibitors, Vpu has numerous host protein targets for modulation in HIV-1 infected cells including BST-2/tetherin, NTB-A, and CCR-7 [34-36]. Data demonstrating that syncytia EWI-2 surface levels depend on the levels of the previously unfused target cell (Figure 4.1) and is downregulated over time (Figure 4.2), indicates that the altered surface levels of EWI-2 on syncytia are not a result of non-functional Vpu in syncytia, but rather that newly formed syncytia have an influx of yet-to-be downregulated EWI-2 that Vpu can subsequently target for downregulation after fusion. We expect that other Vpu-targeted host proteins are also differentially expressed on the surface of "young" HIV-1-induced syncytia, and that this phenomenon extends to host protein modulation mediated by viral accessory protein Nef as well. Further, it is intriguing to speculate that HIV-1-induced cell-cell fusion events might trigger reprogramming in the resulting syncytium that is not dependent on viral accessory protein activity as it was recently demonstrated that plasma membrane modulation upon VSV-G-mediated cell-cell fusion induced transcriptional reprogramming in fused cells [37]. Unbiased analyses of the HIV-1-induced syncytia surface profile compared to mononucleated infected cells using high throughput analysis such as mass spectrometry and flow cytometry are necessary to thoroughly understand how syncytia differ from mononucleated infected cells and to begin

investigating the functional implications for an altered surface profile on these multinucleated HIV-1 infected cells.

Although viral Gag is largely responsible for efficiently inhibiting excessive syncytia formation [12], host proteins including tetraspanins and EWI-2 also support fusion inhibition at the virological synapse (VS) [13,15]. Indeed, overexpression of tetraspanin CD81 and EWI-2 in HIV-1 producer cells demonstrated that both host proteins inhibit HIV-1-induced cell-cell fusion at the virological synapse (VS) in a dose-dependent manner [13,15]. Given that CD81 and EWI-2 inhibit fusion in a dose-dependent manner, transiently increased levels of these fusion inhibitors in recently formed HIV-1-induced syncytia may result in these entities being *less* fusogenic than mononucleated infected cells as more of these fusion inhibitory host proteins are available for recruitment to the presynapse (Figure 4.3) (as also suggested previously [15]). It has already been shown that syncytia are capable of transferring virus to uninfected target cells upon contact without undergoing subsequent cell-cell fusion and are limited in size (2-4 nuclei) [7], which indicates that syncytia likely utilize similar fusion inhibitory mechanisms previously demonstrated to prevent fusion at the VS for mononucleated infected cells. Further, we observed striking depletion of syncytia from the infected cultures 48 hr after the addition of EFV and C34 (data not shown), which suggest that syncytia have limited lifespan, consistent with what has been previously reported for infected cells [38]. The altered levels of fusion inhibitory proteins and a limited cell lifespan may collectively prevent syncytia from fusing indefinitely, therefore allowing them to remain small (2-4 nuclei) rather than becoming large, cytopathic infected entities [39].

Altered levels of fusion inhibitory proteins on the surface of HIV-1-induced syncytia compared to mononucleated infected cells may allow these entities have a unique contribution to viral spread. Increased levels of fusion inhibitory host proteins on relatively "young" syncytia may support syncytia contributing to cell-to-cell spread by transferring viral particles to target cells at the VS while efficiently preventing continued cell-cell fusion (Figure 4.3 and suggested in [15]). Simultaneously, increased levels of fusion inhibitory proteins might have a detrimental effect on syncytia contribution cell-free viral spread by reducing particle infectivity. Previous studies documented that increased expression of tetraspanins in HIV-1 producing cells resulted in greater incorporation of fusion inhibitory tetraspanins into viral particles which correlated with a decrease in particle infectivity [17,25,26], thus an increase in fusion inhibitory proteins on syncytia may decrease the infectivity of the particles produced from these cells (Figure 4.3). However, it is not currently known whether EWI-2 influences HIV-1 particle infectivity. Thus, syncytia may have enhanced abilities to contribute to cell-to-cell spread at the VS, but an impaired ability to contribute to cell-free transmission (Figure 4.3).

Whether syncytia can contribute to viral spread, and if so how efficiently compared to mononucleated infected cells, has yet to be determined. As syncytia are a subpopulation of HIV-1 infected cells they would need to be separated from mononucleated infected cells to determine their functional abilities and particle infectivity relative to mononucleated infected cells. Should syncytia have an altered ability to contribute to virus spread compared to mononucleated infected cells, it would be interesting to "age" syncytia as we have done here (Figure 4.2) to determine whether this altered phenotype may correlate with changes of host protein levels on "young" versus "old" syncytia.

Altogether, we have determined that the levels of EWI-2 on the surface of HIV-1-induced syncytia depend on the levels present in the target cell population and can be downregulated over time after cell-cell fusion. Future work aimed to purify of these infected entities is necessary to determine whether altered levels of fusion inhibitory proteins has any functional consequence for HIV-1-induced syncytia and will greatly enhance our understanding of this subpopulation of HIV-1-infected cells.

## 4.6. Figure Legends

**Figure 4.1.** EWI-2 knockdown in uninfected target cells leads to reduced EWI-2 on the surface of a syncytia upon HIV-1-induced cell-cell fusion. CEM-SS cells infected with NL-sfGI were co-cultured for 17-18 h with CMAC-labeled target cells (CEM-SS cells expressing either shRNA targeting EWI-2, shEWI-2, or a non-targeting shRNA control sequence, shScr [15]) in the presence of Efavirenz (EFV; 1 μM). Following co-culture, the cells were labeled for surface EWI-2, fixed and permeabilized, labeled with Alexa Fluor 647-conjugated pAb, and imaged (60×). A) Schematic representation of the experimental approach. Relative levels of EWI-2 for each cell population (uninfected CEM-SS = blue; infected CEM-SS = red; CMAC-labeled shRNA expressing target cells = purple) are represented by EWI-2 icons (green) at the cell surface. It should be noted that infected cells still retain low levels of EWI-2 at the surface, which was represented here by the absence of EWI-2 icons for simplicity. Image created in BioRender.com. B) Representative images of EWI-2 (magenta in merge) on the surface of syncytia. Syncytia used for analysis were identified as infected (GFP reporter shown in yellow in merge) CMAC-positive (cyan in merge) cells ($GFP^+/CMAC^+$) as these syncytia formed as the result of fusion between an infected CEM-SS cell and a CMAC-labeled shEWI-2 or shScr expressing target cell. Scale bar = 10 μm. C) Cell surfaces were selected to measure relative EWI-2-associated signal intensity. Values were normalized to the mean signal intensity of the associated uninfected control population within each biological replicate. Individual $GFP^+/CMAC^+$ syncytium EWI-2 levels are represented by small, open data points. Cells within the same biological replicate share the same shape and color (magenta diamond, gray triangle, or cyan square). Average EWI-2 associated signal intensities for each biological replicate are represented by large, closed symbols (matched to individual cell data points by shape and color). D) The mean EWI-2 associated signal intensity values shown in C) shown with lines to connect means from the same biological replicate. Note that the scale of the y-axis has changed from the data shown in C) to better visualize the slope of each line.

**Figure 4.2.** EWI-2 levels on HIV-1-induced syncytia decrease over time. A sample of CEM-SS cells 3 days post infection with NL-sfGI were labeled for surface EWI-2 (Time point 0 hr), fixed and permeabilized, labeled with Alexa Fluor-647 conjugated secondary pAb and DAPI, and imaged (60×) as described in Figure 1 while inhibitors EFV (1 μM) and C34 (0.5 μM) were added to the remaining culture of infected cells. Samples were collected 6, and 24 hr (Time points 6, and 24 hr) after adding the inhibitors and labeled for surface EWI-2 as described for the 0 hr sample. A) Schematic representation of the experimental approach; Uninfected CEM-SS cells (blue), infected mononucleated cells (red), HIV-1-induced syncytium (purple), and EWI-2 (green icon) present on the plasma membrane. Image created in BioRender.com. B) Representative images of syncytia from each time point (0, 6, or 24 hr) are shown; DAPI (cyan in merge), GFP (yellow in merge), and EWI-2 associated signal (magenta in merge). Scale bar = 10 μM. C) Cell surfaces were selected to measure relative EWI-2-associated signal intensity on syncytia harvested at each time point. Values were normalized to the mean signal intensity of the uninfected control population prepared and imaged in parallel for each time point. Small, open data

points represent individual syncytium collected at each time point (magenta diamonds, gray triangles, or cyan squares). The median EWI-2 associated intensity for each biological replicate at each time point are represented by large, closed symbols (matched by shape and color to respective individual syncytium data points within each biological replicate). D) Median values of EWI-2 associated signal intensity on the surface of syncytia shown in C) are connected by a line over time for each biological replicate. Note that the y-axis scale has changed to better visualize the pattern between the median values over time.

**Figure 4.3.** Model for how altered levels of fusion inhibitors may impact syncytia-mediated virus spread. Schematic representation depicting how increased levels of EWI-2 and CD81 on the surface of HIV-1-induced syncytia may alter the infectivity of viral particles produced by syncytia and fusogenicity of syncytia upon VS formation for cell-to-cell spread. A) Increased levels of fusion inhibitors on HIV-1-induced syncytia are expected to decrease the infectivity of particles produced from these cells, consistent with previous reports documenting that increased expression of tetraspanins in virus producing cells correlates with increased incorporation of these fusion inhibitory proteins into viral particles and decreased particle infectivity [17,25]. Note that it has yet to be determined whether EWI-2 can be incorporated into viral particles and if so, whether increased incorporation of EWI-2 decreases particle infectivity. B) Increased levels of these fusion inhibitors on syncytia [15] likely allow for increased recruitment of CD81 and EWI-2 to the producer cell side of the VS (presynapse) and thus decreased fusogenicity of these infected entities given that both EWI-2 and CD81 inhibit HIV-1-induced cell-cell fusion in a dose-dependent manner [13,15]. C) The effects of increased fusion inhibitors on syncytia-produced particle infectivity and syncytia fusogenicity are expected to decrease over time after HIV-1-induced cell-cell fusion as EWI-2 is downregulated from the surface of syncytia over time. Note that it has yet to be determined whether CD81 is also downregulated from the surface of syncytia over time. Image created in BioRender.com.

## 4.7. Figures

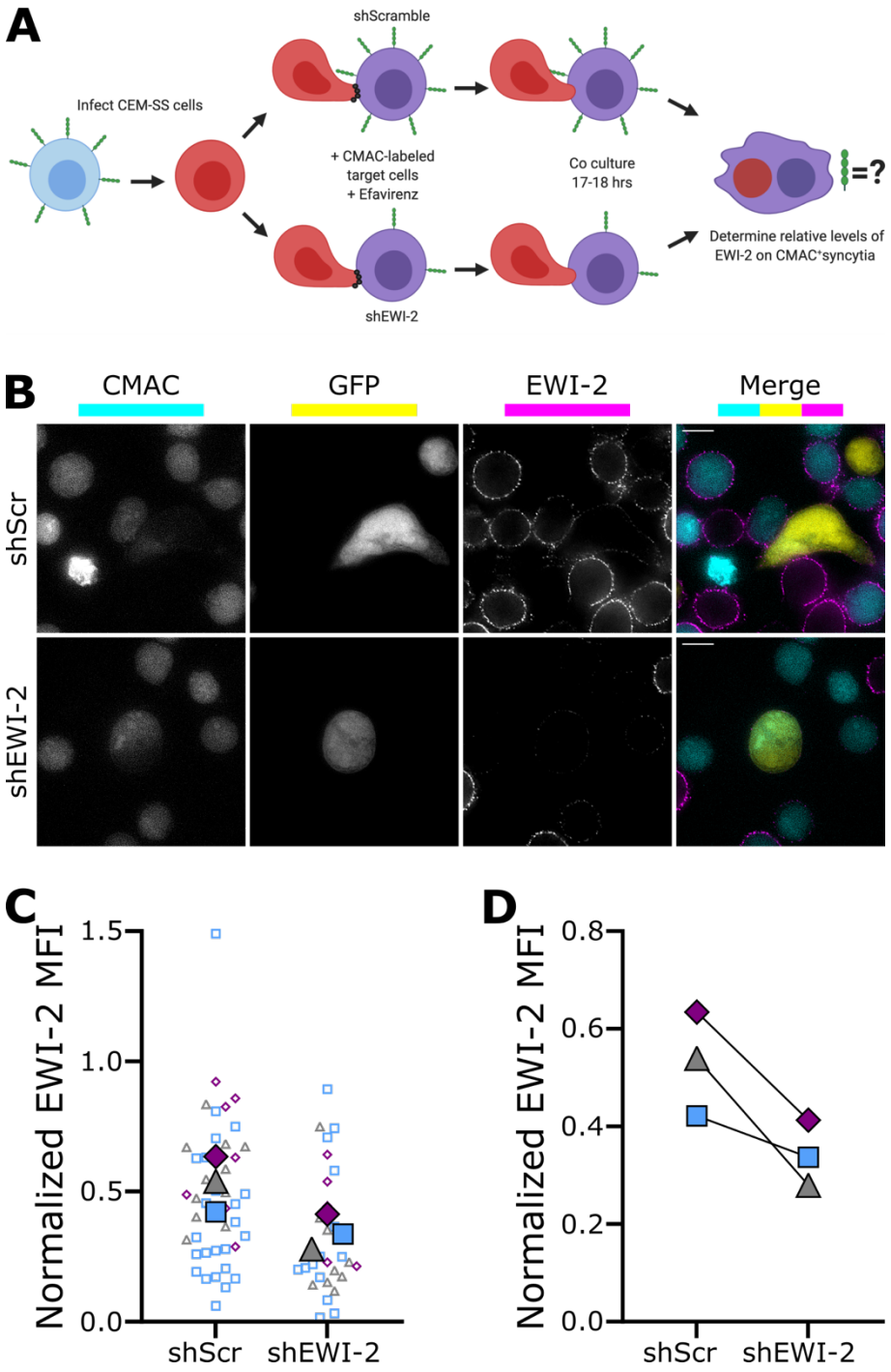


**Figure 4.1. EWI-2 knockdown in uninfected target cells leads to reduced EWI-2 on the surface of syncytia upon HIV-1-induced cell-cell fusion.**

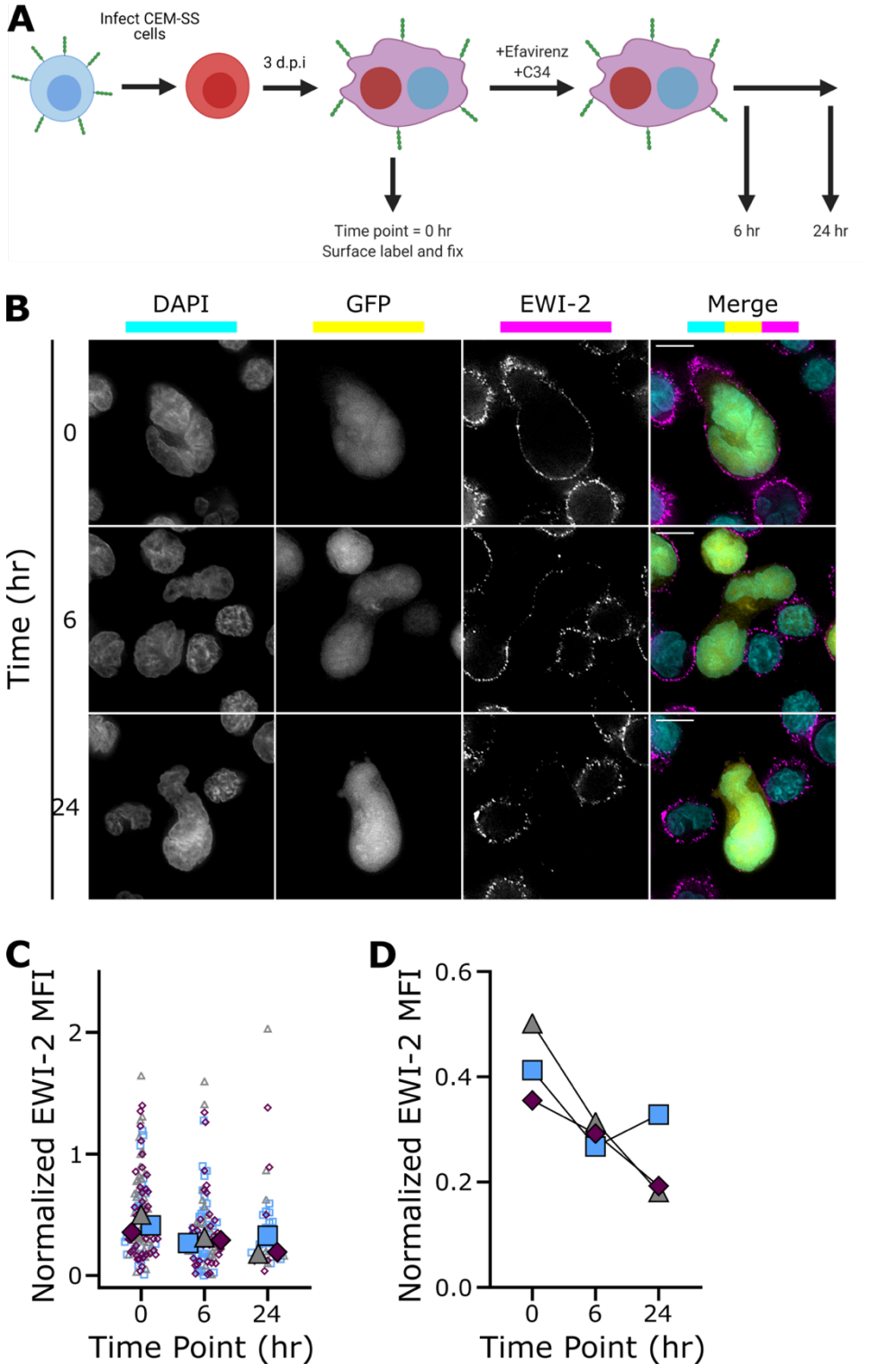


**Figure 4.2. EWI-2 levels on HIV-1-induced syncytia decrease over time.**

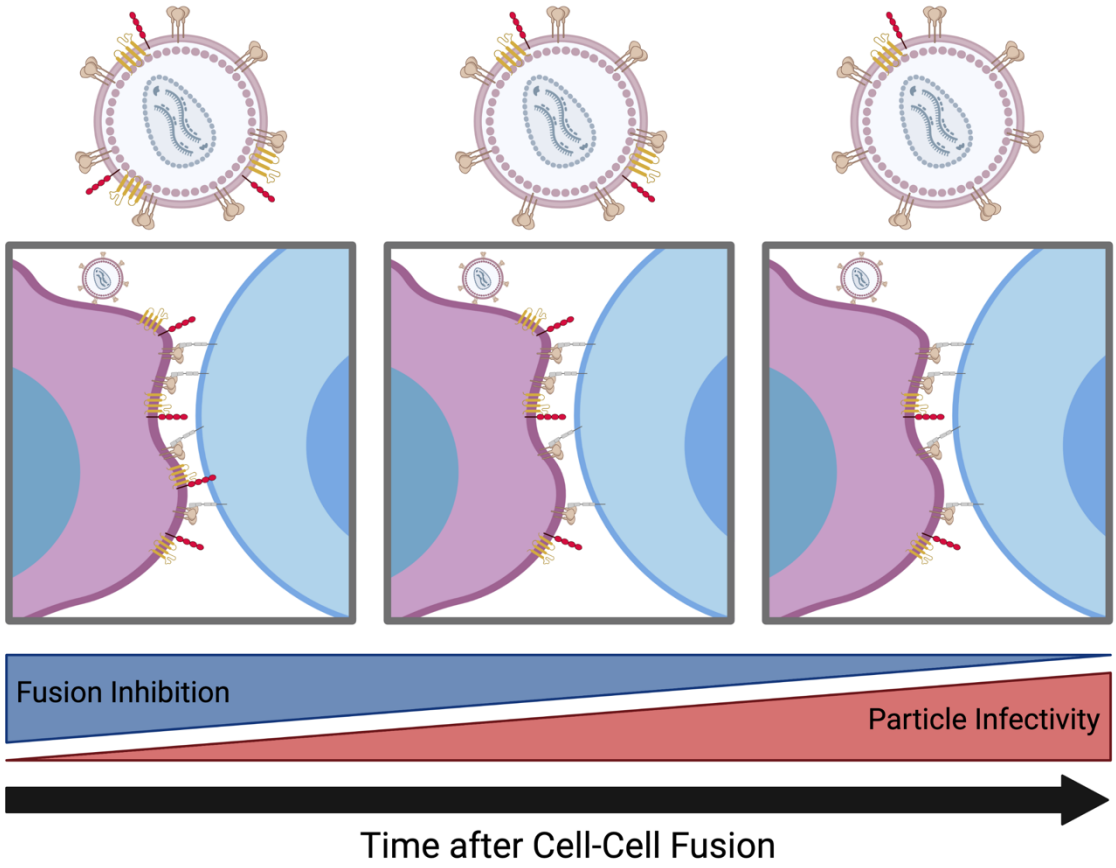


**Figure 4.3. Model for how altered levels of fusion inhibitors may impact syncytia-mediated virus spread.**

## 4.8. Supplementary Figure Legends

**Supplementary Figure 4.1.** shEWI-2 RNA expressing CEM-SS target cells have reduced EWI-2 at the plasma membrane. CEM-SS cells stably expressing shRNA targeting EWI-2 (shEWI-2, interfering RNA sequence based on previously described EWI-2-targeting siRNA [20]) or a scrambled, non-targeting shRNA sequence (shScr) described previously [15] were labeled with cytoplasmic dye CMAC and used as target cells for HIV-1-induced cell-cell fusion. To validate that the shEWI-2 expressing target cells had reduced levels of EWI-2 compared to shScr expressing and non-shRNA expressing (parental) CEM-SS control cells, EWI-2 surface levels on shRNA expressing target cells were quantified in parallel with the resulting HIV-1-induced syncytia (Figure 4.1). A) shRNA expressing uninfected target cells present within the infected population were identified as CMAC-positive/GFP-negative cells. The EWI-2 surface density on CMAC-labeled target cells was quantified by manually outlining the surface of each cell and calculating the mean EWI-2-associated 647 signal intensity (MFI) contained within each outline. All EWI-2-associated MFI values were normalized to the average MFI of uninfected, parental CEM-SS controls. Small, open data points represent normalized MFI values of individual shRNA expressing target cells (shScr or shEWI-2) and data from the same biological replicate (3 total) are distinguished by shape and color (blue square, gray triangle, or magenta diamond). Large, filled data points represent the mean of the individual data points for each biological replicate and are matched to the individual data points from the same replicate by shape and color. B) Black lines connect mean values from A) for the two target cell types from the same biological replicate. Note that the scale for the y-axis has changed from A) to clearly represent the slope of each line.

**Supplementary Figure 4.2.** CEM-SS based HIV-1-induced syncytia do not have increased EWI-2 surface density compared to mononucleated infected cells. CEM-SS cells infected with GFP reporter virus NL-sfGI were prepared as described in Figure 4.2. Uninfected and mononucleated infected cells were prepared and analyzed in parallel with syncytia for each biological replicate at each time point (0, 6 and 24 hr). Each data point represents the density of EWI-2-associated signal on the surface of individual cells (MFI). All data points were normalized to the mean MFI of the uninfected cells from within the infected culture for respective biological replicates and time points. Small open data points represent the normalized EWI-2 associated signal for an individual cell and large, filled data points represent the median for each biological replicate. Data from the same biological replicate are indicated by data points sharing the same shape and color (blue square, gray triangle, or magenta diamond) and include data points representing syncytia for each replicate (data also shown in Figure 4.2). Shown are data for uninfected CEM-SS cells that had never been exposed to infected cells nor the EFV and C34 inhibitor treatment (Uninfected control; UC), uninfected cells (identified as GFP negative) from the same culture as the infected cells (U), mononucleated infected cells (M), and syncytia (S).

## 4.9. Supplementary Figures

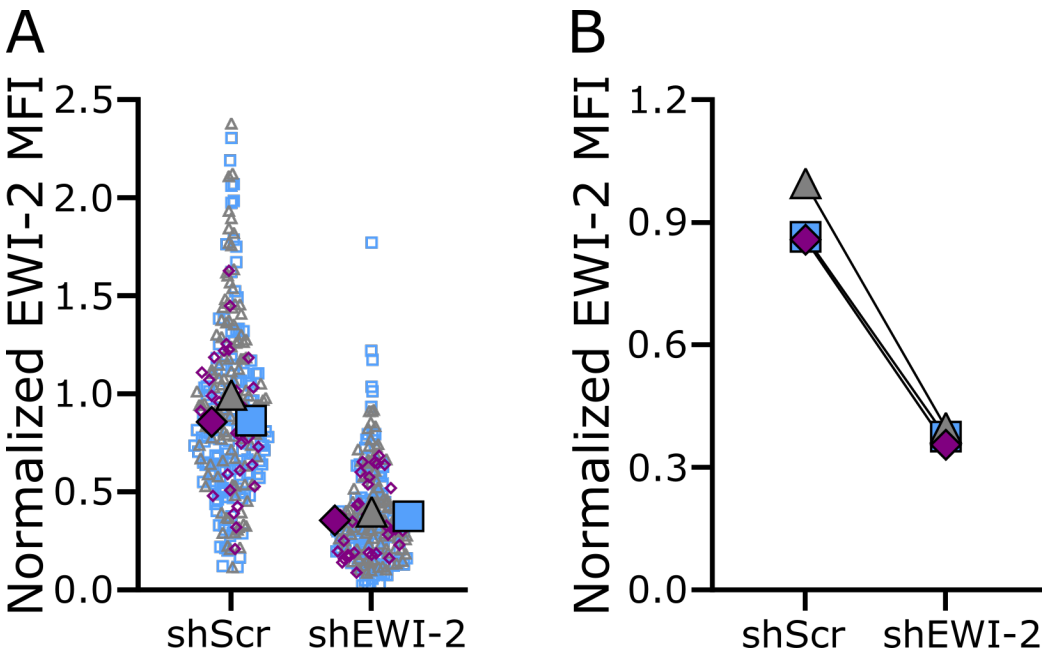


**Supplementary Figure 4.1. shEWI-2 RNA expressing CEM-SS target cells have reduced EWI-2 at the plasma membrane.**

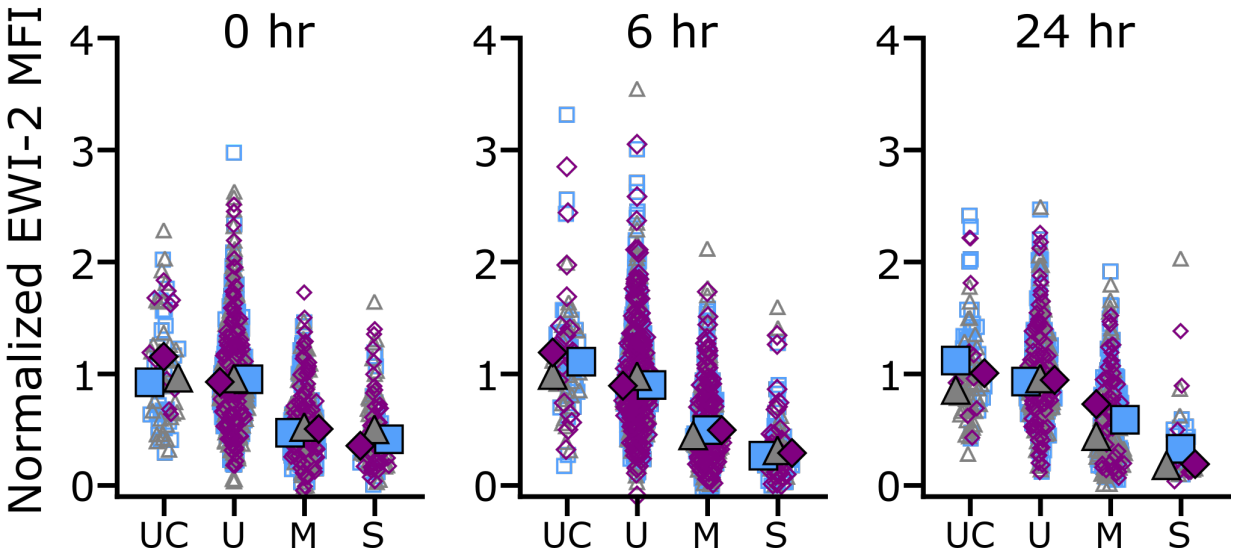


**Supplementary Figure 4.2. CEM-SS based HIV-1-induced syncytia do not have increased EWI-2 surface density compared to mononucleated infected cells.**

## 4.10. References


1. Law, K.M.; Satija, N.; Esposito, A.M.; Chen, B.K. Cell-to-Cell Spread of HIV and Viral Pathogenesis. *Adv Virus Res* **2016**, *95*, 43-85, doi:10.1016/bs.aivir.2016.03.001.

2. Jolly, C.; Kashefi, K.; Hollinshead, M.; Sattentau, Q.J. HIV-1 cell to cell transfer across an Env-induced, actin-dependent synapse. *J Exp Med* **2004**, *199*, 283-293, doi:10.1084/jem.20030648.

3. Jolly, C.; Sattentau, Q.J. Retroviral spread by induction of virological synapses. *Traffic* **2004**, *5*, 643-650, doi:10.1111/j.1600-0854.2004.00209.x.

4. Murooka, T.T.; Deruaz, M.; Marangoni, F.; Vrbanac, V.D.; Seung, E.; von Andrian, U.H.; Tager, A.M.; Luster, A.D.; Mempel, T.R. HIV-infected T cells are migratory vehicles for viral dissemination. *Nature* **2012**, *490*, 283-287, doi:10.1038/nature11398.

5. Law, K.M.; Komarova, N.L.; Yewdall, A.W.; Lee, R.K.; Herrera, O.L.; Wodarz, D.; Chen, B.K. In Vivo HIV-1 Cell-to-Cell Transmission Promotes Multicopy Micro-compartmentalized Infection. *Cell Rep* **2016**, *15*, 2771-2783, doi:10.1016/j.celrep.2016.05.059.

6. Ventura, J.D.; Beloor, J.; Allen, E.; Zhang, T.; Haugh, K.A.; Uchil, P.D.; Ochsenbauer, C.; Kieffer, C.; Kumar, P.; Hope, T.J., et al. Longitudinal bioluminescent imaging of HIV-1 infection during antiretroviral therapy and treatment interruption in humanized mice. *PLoS Pathog* **2019**, *15*, e1008161, doi:10.1371/journal.ppat.1008161.

7. Symeonides, M.; Murooka, T.T.; Bellfy, L.N.; Roy, N.H.; Mempel, T.R.; Thali, M. HIV-1-Induced Small T Cell Syncytia Can Transfer Virus Particles to Target Cells through Transient Contacts. *Viruses* **2015**, *7*, 6590-6603, doi:10.3390/v7122959.

8. Dargent, J.L.; Lespagnard, L.; Kornreich, A.; Hermans, P.; Clumeck, N.; Verhest, A. HIV-associated multinucleated giant cells in lymphoid tissue of the Waldeyer's ring: a detailed study. *Mod Pathol* **2000**, *13*, 1293-1299, doi:10.1038/modpathol.3880237.

9. Orenstein, J.M.; Wahl, S.M. The macrophage origin of the HIV-expressing multinucleated giant cells in hyperplastic tonsils and adenoids. *Ultrastruct Pathol* **1999**, *23*, 79-91, doi:10.1080/019131299281734.

10. Sylwester, A.; Murphy, S.; Shutt, D.; Soll, D.R. HIV-induced T cell syncytia are self-perpetuating and the primary cause of T cell death in culture. *J Immunol* **1997**, *158*, 3996-4007.

11. Compton, A.A.; Schwartz, O. They Might Be Giants: Does Syncytium Formation Sink or Spread HIV Infection? *PLoS Pathog* **2017**, *13*, e1006099, doi:10.1371/journal.ppat.1006099.

12. Roy, N.H.; Chan, J.; Lambelé, M.; Thali, M. Clustering and mobility of HIV-1 Env at viral assembly sites predict its propensity to induce cell-cell fusion. *Journal of virology* **2013**, *87*, 7516-7525, doi:10.1128/jvi.00790-13.

13. Weng, J.; Krementsov, D.N.; Khurana, S.; Roy, N.H.; Thali, M. Formation of syncytia is repressed by tetraspanins in human immunodeficiency virus type 1-producing cells. *Journal of virology* **2009**, *83*, 7467-7474, doi:10.1128/jvi.00163-09.

14. Roy, N.H.; Lambelé, M.; Chan, J.; Symeonides, M.; Thali, M. Ezrin is a component of the HIV-1 virological presynapse and contributes to the inhibition of cell-cell fusion. *Journal of virology* **2014**, *88*, 7645-7658, doi:10.1128/jvi.00550-14.

15. Whitaker, E.E.; Matheson, N.J.; Perlee, S.; Munson, P.B.; Symeonides, M.; Thali, M. EWI-2 Inhibits Cell-Cell Fusion at the HIV-1 Virological Presynapse. *Viruses* **2019**, *11*, doi:10.3390/v11121082.

16. Jolly, C.; Sattentau, Q.J. Human immunodeficiency virus type 1 assembly, budding, and cell-cell spread in T cells take place in tetraspanin-enriched plasma membrane domains. *Journal of virology* **2007**, *81*, 7873-7884, doi:10.1128/jvi.01845-06.

17. Krementsov, D.N.; Weng, J.; Lambele, M.; Roy, N.H.; Thali, M. Tetraspanins regulate cell-to-cell transmission of HIV-1. *Retrovirology* **2009**, *6*, 64, doi:10.1186/1742-4690-6-64.

18. Gordón-Alonso, M.; Yañez-Mó, M.; Barreiro, O.; Alvarez, S.; Muñoz-Fernández, M.A.; Valenzuela-Fernández, A.; Sánchez-Madrid, F. Tetraspanins CD9 and CD81 modulate HIV-1-induced membrane fusion. *J Immunol* **2006**, *177*, 5129-5137, doi:10.4049/jimmunol.177.8.5129.

19. Symeonides, M.; Lambele, M.; Roy, N.H.; Thali, M. Evidence showing that tetraspanins inhibit HIV-1-induced cell-cell fusion at a post-hemifusion stage. *Viruses* **2014**, *6*, 1078-1090, doi:10.3390/v6031078.

20. Sala-Valdés, M.; Ursa, A.; Charrin, S.; Rubinstein, E.; Hemler, M.E.; Sánchez-Madrid, F.; Yáñez-Mó, M. EWI-2 and EWI-F link the tetraspanin web to the actin cytoskeleton through their direct association with ezrin-radixin-moesin proteins. *J Biol Chem* **2006**, *281*, 19665-19675, doi:10.1074/jbc.M602116200.

21. Charrin, S.; Le Naour, F.; Labas, V.; Billard, M.; Le Caer, J.P.; Emile, J.F.; Petit, M.A.; Boucheix, C.; Rubinstein, E. EWI-2 is a new component of the tetraspanin

web in hepatocytes and lymphoid cells. *Biochem J* **2003**, *373*, 409-421, doi:10.1042/bj20030343.

22. Haller, C.; Müller, B.; Fritz, J.V.; Lamas-Murua, M.; Stolp, B.; Pujol, F.M.; Keppler, O.T.; Fackler, O.T. HIV-1 Nef and Vpu are functionally redundant broad-spectrum modulators of cell surface receptors, including tetraspanins. *Journal of virology* **2014**, *88*, 14241-14257, doi:10.1128/jvi.02333-14.

23. Greenwood, E.J.; Matheson, N.J.; Wals, K.; van den Boomen, D.J.; Antrobus, R.; Williamson, J.C.; Lehner, P.J. Temporal proteomic analysis of HIV infection reveals remodelling of the host phosphoproteome by lentiviral Vif variants. *Elife* **2016**, *5*, doi:10.7554/eLife.18296.

24. Naamati, A.; Williamson, J.C.; Greenwood, E.J.; Marelli, S.; Lehner, P.J.; Matheson, N.J. Functional proteomic atlas of HIV infection in primary human CD4+ T cells. *Elife* **2019**, *8*, doi:10.7554/eLife.41431.

25. Sato, K.; Aoki, J.; Misawa, N.; Daikoku, E.; Sano, K.; Tanaka, Y.; Koyanagi, Y. Modulation of human immunodeficiency virus type 1 infectivity through incorporation of tetraspanin proteins. *Journal of virology* **2008**, *82*, 1021-1033, doi:10.1128/jvi.01044-07.

26. Lambelé, M.; Koppensteiner, H.; Symeonides, M.; Roy, N.H.; Chan, J.; Schindler, M.; Thali, M. Vpu is the main determinant for tetraspanin downregulation in HIV-1-infected cells. *Journal of virology* **2015**, *89*, 3247-3255, doi:10.1128/jvi.03719-14.

27. Sugden, S.M.; Bego, M.G.; Pham, T.N.; Cohen É, A. Remodeling of the Host Cell Plasma Membrane by HIV-1 Nef and Vpu: A Strategy to Ensure Viral Fitness and Persistence. *Viruses* **2016**, *8*, 67, doi:10.3390/v8030067.

28. Foley, G.E.; Lazarus, H.; Farber, S.; Uzman, B.G.; Boone, B.A.; McCarthy, R.E. CONTINUOUS CULTURE OF HUMAN LYMPHOBLASTS FROM PERIPHERAL BLOOD OF A CHILD WITH ACUTE LEUKEMIA. *Cancer* **1965**, *18*, 522-529, doi:10.1002/1097-0142(196504)18:4<522::aid-cncr2820180418>3.0.co;2-j.

29. Nara, P.L.; Hatch, W.C.; Dunlop, N.M.; Robey, W.G.; Arthur, L.O.; Gonda, M.A.; Fischinger, P.J. Simple, rapid, quantitative, syncytium-forming microassay for the detection of human immunodeficiency virus neutralizing antibody. *AIDS Res Hum Retroviruses* **1987**, *3*, 283-302, doi:10.1089/aid.1987.3.283.

30. Nara, P.L.; Fischinger, P.J. Quantitative infectivity assay for HIV-1 and-2. *Nature* **1988**, *332*, 469-470, doi:10.1038/332469a0.

31. Charrin, S.; Le Naour, F.; Oualid, M.; Billard, M.; Faure, G.; Hanash, S.M.; Boucheix, C.; Rubinstein, E. The major CD9 and CD81 molecular partner.

Identification and characterization of the complexes. *J Biol Chem* **2001**, *276*, 14329-14337, doi:10.1074/jbc.M011297200.

32. Matheson, N.J.; Sumner, J.; Wals, K.; Rapiteanu, R.; Weekes, M.P.; Vigan, R.; Weinelt, J.; Schindler, M.; Antrobus, R.; Costa, A.S., et al. Cell Surface Proteomic Map of HIV Infection Reveals Antagonism of Amino Acid Metabolism by Vpu and Nef. *Cell Host Microbe* **2015**, *18*, 409-423, doi:10.1016/j.chom.2015.09.003.

33. Orenstein, J.M. In vivo cytolysis and fusion of human immunodeficiency virus type 1-infected lymphocytes in lymphoid tissue. *J Infect Dis* **2000**, *182*, 338-342, doi:10.1086/315640.

34. Van Damme, N.; Goff, D.; Katsura, C.; Jorgenson, R.L.; Mitchell, R.; Johnson, M.C.; Stephens, E.B.; Guatelli, J. The interferon-induced protein BST-2 restricts HIV-1 release and is downregulated from the cell surface by the viral Vpu protein. *Cell Host Microbe* **2008**, *3*, 245-252, doi:10.1016/j.chom.2008.03.001.

35. Shah, A.H.; Sowrirajan, B.; Davis, Z.B.; Ward, J.P.; Campbell, E.M.; Planelles, V.; Barker, E. Degranulation of natural killer cells following interaction with HIV-1-infected cells is hindered by downmodulation of NTB-A by Vpu. *Cell Host Microbe* **2010**, *8*, 397-409, doi:10.1016/j.chom.2010.10.008.

36. Ramirez, P.W.; Famiglietti, M.; Sowrirajan, B.; DePaula-Silva, A.B.; Rodesch, C.; Barker, E.; Bosque, A.; Planelles, V. Downmodulation of CCR7 by HIV-1 Vpu results in impaired migration and chemotactic signaling within $CD4^+$ T cells. *Cell Rep* **2014**, *7*, 2019-2030, doi:10.1016/j.celrep.2014.05.015.

37. Feliciano, D.; Espinosa-Medina, I.; Weigel, A.; Milano, K.M.; Tang, Z.; Lee, T.; Kliman, H.J.; Guller, S.M.; Ott, C.M.; Lippincott-Schwartz, J. Transcriptional reprogramming in fused cells is triggered by plasma-membrane diminution. *bioRxiv* **2019**, 10.1101/832378, 832378, doi:10.1101/832378.

38. Perelson, A.S.; Neumann, A.U.; Markowitz, M.; Leonard, J.M.; Ho, D.D. HIV-1 dynamics in vivo: virion clearance rate, infected cell life-span, and viral generation time. *Science* **1996**, *271*, 1582-1586, doi:10.1126/science.271.5255.1582.

39. Montefiori, D.C.; Mitchell, W.M. Persistent coinfection of T lymphocytes with HTLV-II and HIV and the role of syncytium formation in HIV-induced cytopathic effect. *Virology* **1987**, *160*, 372-378, doi:10.1016/0042-6822(87)90008-0.

# CHAPTER 5 : DISCUSSION & FUTURE DIRECTIONS

Cell-to-cell transmission of HIV-1 is a highly efficient mode of virus spread as it allows virus particles to be released in close proximity to an uninfected $CD4^+$ T (target) cell at a cellular junction called the virological synapse (VS). Given that the VS forms upon binding of the viral fusogen (Env) on the surface of an infected cell (producer) to its receptor CD4 on a target cell, there is a need for fusion inhibitory factors to prevent Env-induced cell-cell fusion (syncytia formation) at this site to support continued virus spread. Over the last decade, our lab has begun identifying viral and host factors involved in preventing excessive cell-cell fusion at the HIV-1 VS and we have recently begun spatio-temporal analyses to investigate how these factors cooperate. The work completed within the context of this thesis contributes to our ongoing efforts to understand mechanisms that ensure efficient virus transmission and spread.

Previous work by our group had identified tetraspanins and ezrin as host factors that contribute to the inhibition of HIV-1-induced cell-cell fusion at the VS alongside viral Gag [1-3], though we suspected that additional host proteins likely also contributed to cell-cell fusion inhibition. We have now identified EWI-2 (IGSF8), an interacting partner of *both* ezrin and tetraspanins CD9 (TSPAN29/MIC3) and CD81 (TSPAN28) [4-6], as a host protein that inhibits HIV-1-induced syncytia formation upon recruitment to the producer cell side of the VS (the presynapse) (Chapter 3, [7]). Despite these studies demonstrating that viral and host factors collectively contribute to efficient fusion inhibition at the VS, it has becoming increasingly apparent that HIV-1-induced cell-cell fusion still occurs as small (2-4 nuclei) HIV-1-induced T-cell based syncytia can be readily detected *in vitro* and

have even been documented *in vivo* [8-11]. While these multinucleated infected entities are present *in vivo*, it remained unclear whether syncytia had any unique properties from mononucleated infected cells and how syncytia were prevented from fusing indefinitely. We have now demonstrated that primary T cell-based syncytia have increased levels of fusion inhibitory host proteins EWI-2 and CD81 compared to mononucleated infected cells [7] where they are typically downregulated upon infection [12-14], thus distinguishing the syncytia surface profile from that of mononucleated infected cells. Further, we also demonstrated that the EWI-2 levels on syncytia are dependent on the expression levels of the previously unfused target cell and that EWI-2 is downregulated from the surface of syncytia over time following cell-cell fusion (Chapter 4).

We have begun investigating how EWI-2 contributes to fusion inhibition at the VS and plan to determine whether the altered syncytia surface profile has any functional impact on these infected entities compared to mononucleated infected cells. Specifically, we propose that increased levels of CD81 and EWI-2 on the syncytia surface prevent syncytia from fusing indefinitely, as has been demonstrated previously using bulk populations of infected cells [1,7] (ie. both mononucleated and syncytia) and that syncytia may have unique properties that impact their ability to contribute to virus spread.

### 5.1. EWI-2 at the presynapse: predicted molecular determinants for fusion inhibition and contributions to protein organization.

We identified EWI-2 as a host protein that inhibits HIV-1-induced cell-cell fusion at the virological presynapse in a dose-dependent manner [7] alongside fusion inhibitory tetraspanins [1] which include EWI-2 interacting partners CD9 and CD81 [4]. However,

mechanism and molecular determinants necessary for EWI-2-mediated fusion inhibition remain unknown. An earlier study which documented that EWI-2 is involved in the HIV-1 replication cycle, which we now know is at least partially due to EWI-2 fusion inhibition at the VS [7], further demonstrated a yet-do-be determined role for the short (10 AA) EWI-2 cytoplasmic tail (CT) [15]. Therefore, we hypothesize that the EWI-2-CT is necessary for EWI-2-mediated fusion inhibition at the VS. Given that the EWI-2 CT contains palmitoylation sites required for interactions with CD9 and CD81 and that related EWI family member (EWI-F) has already been implicated to interact with tetraspanins to efficiently prevent excessive myoblast cell-cell fusion during myotube formation [16], we predict that EWI-2-mediated fusion inhibition at the HIV-1 VS is likely *at least* partially dependent on EWI-2-tetraspanin interactions.

We also demonstrated that EWI-2 is downregulated from the surface of HIV-1-infected cells [7]. Further we showed that viral accessory protein Vpu is primarily responsible for EWI-2 modulation upon infection [7] similar to what has been previously reported for tetraspanins [13,14]. Intriguingly, it has been suggested that targeted regulation of tetraspanins by viral proteins during infection might lead to indirect targeting of tetraspanin interacting partners (such as EWI-2), or alternatively that direct targeting of tetraspanin interacting partners might lead to indirect regulation of tetraspanins [7,17]. As both tetraspanins and EWI-2 share a distinct subcellular localization pattern upon HIV-1 infection, we suspect that interactions between these fusion inhibitory factors may influence their localization within an infected cell including recruitment to the VS and downregulation from the plasma membrane.

We have already determined that EWI-2 knockdown did not alter tetraspanin CD81 recruitment to the presynapse (Figure 5.1), unlike what was previously demonstrated for ezrin where ezrin knockdown did lead to reduced CD81 enrichment to the presynapse [2]. Therefore, we have concluded that tetraspanins are not recruited indirectly to the presynapse as a result of targeted EWI-2 recruitment, nor signaling dependent on the presence of EWI-2. However, we have yet to determine whether EWI-2 recruitment to the presynapse is dependent on tetraspanins. Investigations aimed to address possible tetraspanin-dependent EWI-2 downregulation and/or recruitment to the presynapse EWI-2-CD81 interactions at this site are currently underway (project is supported by an MMG Distinguished Undergraduate Summer Research Award to Elise A. Courtney in 2021). Additionally, we're also interested in investigating whether EWI-2 might influence tetraspanin organization at the HIV-1 presynapse, even if EWI-2 is not involved in tetraspanin recruitment to this site.

*5.1.1. Follow-up Studies.*

For EWI-2 enrichment to the presynapse, we propose that EWI-2 recruitment is dependent on protein-protein interactions with tetraspanins CD9 and CD81, fusion inhibitory host proteins also enriched at the VS [1,12,18]. We will explore this possible regulatory network for host fusion inhibitory proteins in HIV-1-infected cells by knocking down CD81 and CD9 expression in infected producer cells by small interfering RNA and quantifying EWI-2 recruitment to the VS compared to scrambled RNA controls. Further, we are also currently investigating whether palmitoylation of the EWI-2 CT is involved in EWI-2 recruitment to the presynapse as this posttranslational modification is not required

for EWI-2 localization to the plasma membrane, but is essential for EWI-2 interactions with CD9 and CD81 [19] and also enhances interactions with phosphatidylinositol - 4, 5 biphosphate ($PIP_2$) [20]. Analysis of EWI-2 palmitoylation in EWI-2 localization will be completed using previously described palmitoylation-deficient EWI-2 constructs [19] and T cells transduced to stably express EWI-2 palmitoylation-mutants from a CS-II lentiviral construct (cloning to generate lentiviral constructs currently being completed by E. A. Courtney). We expect that tetraspanin knockdown and abrogation of the two palmitoylation sites in the EWI-2 cytoplasmic tail will both reduce EWI-2 enrichment to the VS (compared to scrambled siRNA controls and palmitoylation-competent/shRNA-resistant/FLAG-tagged EWI-2, respectively), leading us to conclude that EWI-2 recruitment to the presynapse is dependent on interactions with tetraspanins CD81 and CD9. However, if EWI-2 enrichment at the VS is only reduced for the palmitoylation-deficient mutants and not upon tetraspanin knockdown, we would be interested in exploring the potential impact of EWI-2 interactions with $PIP_2$. Given that Gag depends on $PIP_2$ for proper localization to the plasma membrane and that this phospholipid is enriched at virus budding sites [21,22], it is interesting to speculate that EWI-2-$PIP_2$ interactions may also support EWI-2 co-accumulation with Gag at the HIV-1 presynapse. Finally, we also propose to complete kinetic analyses (allowing synapses to form for discrete periods of time and analyzing protein enrichment as described previously [23]) of EWI-2, ezrin, and tetraspanins CD9 and CD81 to the VS. Collectively, these studies will enhance our understanding of how these host proteins are recruited to the HIV-1 VS provide insight as to how they and function as a regulatory network to efficiently prevent syncytia formation.

EWI-2-mediated fusion inhibition is naturally tied to its recruitment to the HIV-1 presynapse, as this is the cellular contact site where Env-induced cell-cell fusion would need to be prevented. Similar to what was described above, we expect that EWI-2-mediated fusion inhibition is dependent on tetraspanins. To distinguish between tetraspanin-dependent recruitment to the presynapse from tetraspanin-dependent fusion inhibition, we propose to knockdown CD9 and CD81 while overexpressing EWI-2 in HIV-1 producer cells, analogous to previous experiments documenting that EWI-2 inhibits HIV-1-induced cell-cell fusion in a dose-dependent manner [7]. If EWI-2 contributions to fusion inhibition at the presynapse are dependent on tetraspanins, we would expect to observe reduced fusion inhibition upon EWI-2 overexpression in tetraspanin deficient producer cells compared to controls where tetraspanin have not been knocked down. This finding would be further investigated by analyzing tetraspanin distribution at the presynapse relative to EWI-2 (in WT or EWI-2 knockdown cells) to determine whether the presence of EWI-2 at the presynapse influences tetraspanin organization at this site, possibly explaining how EWI-2 contributes to fusion inhibition.

Indeed, EWI-2-mediated modulation of tetraspanin clusters have been implicated in other membrane processes including glioblastoma migration and growth [24], melanoma development [25], and hepatitis C virus (HCV) entry. For example, a truncated form of EWI-2 (EWI-2wint) restricts HCV infection by influencing CD81 cluster organization in a manner that reduces the efficiency of HCV entry into host cells and appears to be dependent on physical interactions between EWI-2wint and CD81 [19,26,27]. To determine whether the presence of EWI-2 also influences tetraspanin organization at the HIV-1 presynapse, we propose to analyze tetraspanin distribution by super-resolution

microscopy using direct stochastic optical reconstruction microscopy (dSTORM), as super-resolution microscopy has already been shown to be a useful approach for analyzing TEMs within the plasma membrane [28] and tetraspanin localization during virus (or virus-like particle) assembly/budding [29,30]. To induce formation of the HIV-1 presynapse, we will plate infected cells onto coverslips coated with CD4, similar to what has already been described for analyzing protein distribution at the postsynapse by TIRF using coverslips coated with minimal "producer cell" lipid bilayers containing only gp120 and ICAM-1 [31,32]. To visualize CD81 and EWI-2 distribution at the presynapse, we will use a 3-color system where Gag is labeled with TexasRed-conjugated secondary antibodies to identify the presynapse, and this Gag-associated signal will be bleached prior to acquiring 2-color dSTORM data for labeled CD81 and EWI-2. We are interested in analyzing TEM cluster size, composition, and distribution in the absence of EWI-2 to determine whether EWI-2 does indeed influence tetraspanin cluster organization in HIV-1-infected cells and at the presynapse, as has been demonstrated in other cellular contexts [24,33,34].

EWI-2 may also have fusion inhibitory functions that are not dependent on tetraspanins. We predict that EWI-2 may inhibit cell-cell fusion by steric hinderance and possible engagement with a yet-to-be-determined receptor in trans across the synapse. To investigate the contribution of the EWI-2 extracellular Ig domains to cell-cell fusion inhibition in HIV-1-infected cells, we can first screen EWI-2 mutants where the Ig domains have been sequentially deleted (for Ig1-3) [19] in the absence of fully infectious virus (and thus can be completed in a BSL-2 environment). We have generated HeLa and TZM-bl cells which stably express complementary portions of a split-nanoluciferase construct (completed by Danielle G. Allen and supported by a Distinguished Undergraduate

Research Award to DGA in 2019). The split-nanoluciferase can assemble upon Env-mediated Hela-TZM-bl fusion, allowing us to measure relative nanoluciferase activity to rapidly determine relative levels of cell-cell fusion under various conditions. Truncated mutants that impact EWI-2-mediated fusion inhibition compared to WT EWI-2 will be confirmed in fusion assays using fully-infectious virus. Together, these approaches will help us thoroughly characterize the molecular determinants necessary for EWI-2-mediated fusion inhibition at the HIV-1 presynapse.

Finally, we expect that inhibiting the direct tetraspanin-EWI-2 interactions may prevent EWI-2 downregulation upon HIV-1 infection. We plan to analyze the contribution of tetraspanins interactions to EWI-2 downregulation by abrogating EWI-2-tetraspanin interactions as described above, while also investigating the molecular determinants necessary for Vpu-mediated modulation of EWI-2 in parallel. Indeed, we have preliminary data demonstrating pronounced colocalization of EWI-2 and Vpu (E.A. Courtney, data not shown), similar to what has been previously documented for Vpu and tetraspanins [14], providing further support that these host interacting partners may be targeted for modulation upon HIV-1 infection through a similar mechanism.

### *5.1.2 Perspectives for the roles of EWI-2 in viral spread beyond cell-cell fusion inhibition.*

So far, our investigations have shown that EWI-2 appears to have a very similar role as tetraspanins in the HIV-1 replication cycle. However, tetraspanins have also been shown to be influence additional stages in the virus replication cycle as excessive incorporation of tetraspanins into virus particles decreases infectivity [12,14,35]. Therefore, a still unanswered question regarding the role of EWI-2 in virus spread, is

whether EWI-2 also impacts virus particle infectivity. We predict that EWI-2, like tetraspanins [12,35], is incorporated into virus particles and that incorporated EWI-2 likely inhibits particle-cell fusion in a similar manner to how this host protein inhibits cell-cell fusion at the VS. Thus, excessive incorporation of EWI-2 into viral particles (i.e by passive incorporation as the virus buds from the membrane or if particles are budding in EWI-2 enriched microdomains) would be expected to decrease particle infectivity by inhibiting the fusion/entry step of infection. Should EWI-2 incorporation into virus particles inhibit particle-cell fusion, this would explain the role of HIV-1 accessory protein-mediated downregulation of EWI-2 from the cell surface upon infection, and would parallel what has already been shown for fusion inhibitory tetraspanins [14]. However, it also possible that EWI-2 does not impact virus particle infectivity and is perhaps only downregulated indirectly as a result of direct downregulation of tetraspanins by viral accessory proteins (as described above).

Beyond fusion inhibition, we have also begun to speculate that EWI-2 likely has an additional role in supporting optimal cell-to-cell transmission. Recently, HIV-1 VS formation was shown to induce CD3 accumulation at the contact site and also induces TCR-mediated signaling in an antigen-independent manner which promotes efficient virus spread [36,37]. Given that EWI-2 co-accumulates with CD3 at the immunological synapse (IS) where it regulates T cell activation [15], it is interesting to speculate that co-accumulation of these host proteins at the VS might also modulate the T cell response to CD3 signaling within HIV-1-infected cells. EWI-2 may influence CD3-mediated signaling events by inhibiting excessive activation or cytokine secretion (as shown in [15]) or through another currently unknown mechanism, and thus impact virus spread.

## 5.2. Transient "mutants": A unique opportunity for syncytia to contribute to virus transmission?

Although HIV-1-induced T cell-based syncytia have a strikingly different morphology than mononucleated infected cells, as they have multiple nuclei and can be multi-lobed [9,38], little was known about whether syncytia had any other unique characteristics that may distinguish them from other HIV-1-infected cells. Syncytia are challenging to characterize as it is not currently technically feasible to separate them from a mixed population of HIV-1-infected cells (mononucleated and syncytia) nor distinguish them from cell aggregates/clumps generated during even rigorous flow cytometry preparations (Menelaos Symeonides, Ethan Mattice, Emily E. Whitaker, Evan T. Hoffman, M. Thali, unpublished/data not shown). Previous studies have therefore either included syncytia with mononucleated infected cells during bulk/high-throughput analyses or excluded syncytia entirely. However, given their distinct physical appearance, syncytia can be distinguished from mononucleated infected cells by microscopy. We used wide-field fluorescence microscopy to complete single cell analysis of the surface density of proteins typically downmodulated upon HIV-1 infection. This approach allowed us to compare the relative surface density of host proteins between mononucleated infected cells and HIV-1-induced syncytia.

We determined that $CD4^+$ primary T cell-based syncytia have partially restored levels of both EWI-2 and CD81 compared to mononucleated infected cells (Figure 3.6) [7]. Preliminary data suggests that the levels of other host proteins are likely also altered on the surface of syncytia compared to mononucleated infected cells (Figures 5.2-5.4). Further,

we determined that EWI-2 levels on syncytia are dependent on the expression levels of the uninfected target cell population and that EWI-2 is downregulated from the surface of syncytia over time (Figures 4.1 and 4.2). We propose that the transiently altered surface levels documented for EWI-2 on syncytia is representative of a broader phenomenon for an altered host protein profile in infected cells upon HIV-1-induced cell-cell fusion that applies to additional host proteins that are typically modulated by viral accessory proteins (including CD81 which is also restored on the surface of syncytia [7]). Collectively, these data suggest that upon cell-cell fusion, the previously unfused target cell contributes an influx of host proteins such that the resulting HIV-1-induced syncytium has a viral mutant-like phenotype where host protein modulation by viral accessory proteins is temporarily reduced *without* any genetic changes to the virus. A transiently altered proteome could temporarily equip syncytia with unique functional abilities compared to mononucleated infected cells.

Given that both EWI-2 and CD81 inhibit fusion in a dose-dependent manner [1,7], restored levels of fusion inhibitory host proteins CD81 and EWI-2 on the surface of HIV-1-induced syncytia suggests that these entities are less fusogenic than mononucleated infected cells. We hypothesize that the small size of T cell based syncytia, including those observed *in vivo* [38], is the result of transiently increased levels of fusion inhibitors on syncytia for a limited period after fusion with an uninfected target cell ("young" syncytia). However, as EWI-2 is downregulated from the surface of syncytia over time (and likely also CD81), syncytia which have not recently undergone cell-cell fusion with an uninfected target cell ("old" syncytia) might be similarly prone to HIV-1-induced cell-cell fusion as mononucleated infected cells (Figure 4.3). We predict that this rise and fall in the levels of

fusion inhibitors at the cell surface negatively correlates with susceptibility to cell-cell fusion, and would continue over the lifetime of a syncytium as it "grows" in size upon each fusion event until the cell eventually dies. We have observed severe depletion of infected cells, including syncytia, from infected cultures 48-72 hr after the addition of fusion inhibitors to prevent infection and continued cell-cell fusion (unpublished observation). This observation suggests that syncytia have a similar half-life as what has been previously reported for certain HIV-1-infected cells (~1.5 days [39]) and therefore do not live indefinitely. Collectively, we expect that the combination of transiently restored levels of fusion inhibitors CD81 and EWI-2 after cell-cell fusion combined with the limited lifespan of HIV-1-induced syncytia restricts the number of fusion events these cells can undergo, thus addressing the question of how these infected entities remain small (Figure 5.2).

### *5.2.1. Future investigations to address direct contributions of syncytia to virus transmission.*

Whether young syncytia are indeed less fusogenic than mononucleated infected cells, and therefore the effect this might have on their ability to contribute to virus spread, has yet to be determined. It is interesting to speculate that if syncytia are indeed less fusogenic than mononucleated infected cells that they might contribute to cell-to-cell transmission more efficiently, as has been shown for virus encoding less-fusogenic Env variants (unpublished data, M. Symeonides). However, this should be simultaneously considered with the likely event that virus particles produced by HIV-1-induced syncytia may be less infectious than those produced by mononucleated infected cells with low surface levels of fusion inhibitory host proteins (Figure 4.3).

To address whether syncytia are less fusogenic and have altered abilities to contribute to virus transmission than mononucleated infected cells, we plan to prepare purified populations of both mononucleated infected cells and syncytia from heterogenous cultures (uninfected cells, mononucleated infected cells, and syncytia). Purification of syncytia will be achieved by engineering cell lines which that bear a syncytia-specific surface marker upon HIV-1-induced cell-cell fusion. Specifically, we are currently developing an isolation platform that utilizes split-GFP complementation combined with magnetic activated cell sorting (MACS) to isolate syncytia by positive selection for whole GFP (M. Symeonides and E.E. Whitaker). Each split-GFP portion (GFP1 and GFP2) has been fused to a plasma membrane-spanning protein and will be stably expressed in either the producer or target cell population (ex. GFP1 in producer, GFP2 in target). Upon HIV-1-induced cell-cell fusion between GFP1 and GFP2 expressing producer and target cells, the split-GFP portions can associate with each other to form whole GFP. Whole GFP will be used as a syncytia-specific surface marker, and a monoclonal nanobody against whole GFP [40] will be used to label and isolate HIV-1-induced syncytia from the heterogenous culture. Following syncytia purification, a marker specific to the remaining HIV-1-infected cells will be used to isolate mononucleated infected cells from the remaining mixed infected and uninfected culture. Each population of cells (purified mononucleated infected cells or syncytia) will then be used as producer cell populations to analyze their relative fusogenicity and transmission efficiency (as described previously [2,7,41]), as well as relative particle infectivity and efficiency of particle transfer to target cells upon cell-cell contact [42].

We will also determine whether the altered surface profile of syncytia, which we predict impacts host proteins typically modulated upon infection beyond CD81 and EWI-2, has any impact on particle release by measuring ratio of total cellular Gag by labeling p24 to p24 present in the supernatant for syncytia compared to mononucleated infected cells. Additionally, we will measure the relative incorporation of tetraspanins into syncytia-produced particles compared to those produced from mononucleated infected cells to determine whether differences in infectivity do indeed correlate with altered particle composition. Together, these *in vitro* analyses will provide a comprehensive understanding of syncytia contribution to virus transmission. These studies will rigorously investigate the functional consequences of restored levels of EWI-2 and CD81 on syncytia and address whether syncytia contribute differently to virus transmission than mononucleated infected cells. Data generated from these analyses will be included with the data presented in Chapter 4 in a future manuscript.

### 5.3. Implications for altered protein profile/organization beyond fusion inhibitors.

While the immediate follow up studies for our finding that cell-cell fusion temporarily alters the level of fusion inhibitory host proteins on the resulting syncytium include determining how increased levels of CD81 and EWI-2 influence the ability of young syncytia to directly contribute to virus spread – we are also planning to pursue additional ways syncytia may break the mold of what are considered typical traits of infected cells. Specifically, we predict that upon HIV-1-inducd cell-cell fusion, viral accessory protein-mediated modulation of the host cell environment is temporarily disrupted by the influx of host proteins from the previously unfused target cell (Figure 5.3),

beyond what has already been demonstrated for fusion inhibitory host proteins CD81 and EWI-2 [7]. Our preliminary data already suggests that targets of Nef and Vpu-mediated modulation - immune regulatory ligands such as BST-2 (tetherin) [43,44] and NTB-A [45] as well as Env receptor CD4 [46,47] - are altered on the infected cell surface upon cell-cell fusion. Therefore, we plan to investigate the functional consequences of differential modulation of these proteins on the surface of syncytia. Further, as Nef is also responsible for altered actin regulation in infected cells that leads to impaired motile and migratory abilities ([48-50] and reviewed in [51]), we are also interested in investigating whether Nef-mediated modulation of actin organization is altered/disrupted upon HIV-1-induced syncytia to temporarily restore uninfected cell-like motile and migratory abilities in these infected entities.

*5.3.1. Altered modulation of immune stimulatory ligands BST-2 and NTBA on syncytia.*

Altered levels and/or distribution of host proteins BST-2 and NTB-A on the surface of syncytia could influence immune cell responses to these infected entities by direct-cell sensing. An enhanced immune response induced by direct-cell sensing *in vivo* could lead to targeted elimination of syncytia, and potentially increase recruitment of the HIV-1 target cell population to sites of infection, thus acting indirectly as a catalyst for virus spread. Additionally, this could partially explain the prominent immune activation observed during early HIV-1 infection [52] despite the well-documented downregulation of immune stimulatory ligands from the surface of mononucleated infected cells [17].

BST-2 is an interferon (IFN)-inducible host protein that can tether virus particles to the cell surface thus preventing their release from producer cells. However, BST-2 that

is not tethering virus particles to the cell surface ("free" BST-2) and can engage with inhibitory receptor ILT-7 on the surface of plasmacytoid dendritic cells (pDCs; the primary driver if IFN production during HIV-1 infection [53]) to suppress pDC IFN production. Thus BST-2 subcellular localization is tightly regulated by viral accessory protein Vpu to decrease overall levels of BST-2 [43,44], yet retain some BST-2 at the cell surface (sequestered away from virus budding sites) to dampen pDC IFN production in response to infected cells [17,54]. We quantified the relative surface density of BST-2 and co-accumulation of BST-2 with mature virus particles between syncytia and mononucleated infected cells (Figure 5.4). Although we did not see a difference in overall BST-2 surface density between syncytia and mononucleated infected cells (Figure 5.4A), syncytia do have a larger proportion of BST-2 co-accumulating with p17 (interpreted as BST-2 occluded by tethered mature virus particles) and therefore a smaller proportion of total "free" BST-2 (Figure 5.4B). While an increased proportion of occluded BST-2 on syncytia compared to mononucleated infected cells might suggest that direct cell sensing of syncytia by pDCs could elicit a stronger immune response, enthusiasm for this difference is tempered by data demonstrating that the total area of "free" BST-2 on syncytia is still greater than that of mononucleated infected cells (Figure 5.4C). Collectively, these preliminary data suggest that syncytia *might* elicit a stronger IFN response from pDCs than mononucleated infected cells.

Similarly, we have also demonstrated that syncytia have differentially modulated proteins that could influence sensing by natural killer (NK) cells. Specifically, our data show that while syncytia and mononucleated infected cells have similarly low surface levels of NK inhibitory HLA-1, syncytia have increased levels of NK co-activating ligand

NTB-A (Figure 5.5). NTB-A is typically downregulated upon HIV-1 infection by Vpu, inhibiting NK cell degranulation in response to infected cells and lysis of infected cells [45]. Overall, our preliminary data suggests that syncytia might also elicit an increased response from natural killer (NK) cells upon direct cell sensing compared to mononucleated infected cells. Further investigation will be required to determine whether there is any difference in the pDC or NK cell response to syncytia versus mononucleated infected cells.

*5.3.1.1. Future Directions: Analyzing the immune cell response to syncytia upon direct-cell sensing.*

We are currently preparing to investigate both the pDC and NK cell response to syncytia versus mononucleated infected cells (2020 R21 awarded to M. Thali) using purified populations of syncytia and mononucleated infected cells that will be prepared as described in 5.2.1. To determine whether syncytia are differentially sensed by pDCs, we will co-culture purified populations of syncytia with pDC containing PBMCs and analyze IFN production as compared to co-cultures using purified mononucleated infected cells. Similarly, we will also complete co-cultures of syncytia or mononucleated infected cells with NK cells to measure the NK cell response (i.e. screening NK cells for markers of degranulation and monitoring cultures for infected cell depletion at the end of co-culture as described previously [45]) to each of these infected populations. Should we find differences in the pDC and/or NK cell responses to syncytia compared to mononucleated infected cells, we will still need to investigate whether these differences are indeed due to altered levels/distribution of BST-2 and NTB-A. This would be addressed by analyzing the

immune responses as described above upon targeted manipulation of BST-2 and NTB-A levels by knocking down expression of these proteins in infected producer and/or infecting cells with viral strains bearing Vpu mutants that can no longer downregulate BST-2 or NTB-A (i.e. β-Trcp binding-deficient Vpu or a scrambled transmembrane domain Vpu mutant to prevent BST-2 [43] or NTB-A [45] downregulation, respectively).

Should we find that syncytia elicit a stronger response, we would conclude that these infected entities are more sensitive to direct cell-sensing by pDCs and/or NK cells than mononucleated infected cells.

*5.3.2. Potential restoration of HIV-1 Env receptor CD4 on syncytia.*

Preliminary data from ImageStream analysis demonstrate that syncytia have higher levels of surface CD4 than mononucleated infected cells (M. Symeonides, unpublished data), though we have yet to detect differences in CD4 levels on the surface of syncytia compared to mononucleated infected cells by quantitative microscopy (Figure 5.6A). However, we have observed VS-like structures between syncytia and mononucleated infected cells (Figure 5.6B). Given the robust downregulation of CD4 upon infection in mononucleated infected cells, this led us to speculate that there may still be some CD4 present on the surface of syncytia (contributed by the previously uninfected target cell) triggering VS formation with a mononucleated infected cell.

Intriguingly, the formation of a VS between a mononucleated infected cell and a syncytium with partially restored CD4 could provide a unique opportunity for potential viral recombination upon superinfection of the already infected syncytium "target" cell. Viral recombination in a syncytium could contribute to the heterogeneity and evolution of

the virus population within a host, as has previously been predicted to occur upon multicopy infection by cell-to-cell transmission [10,55-57]. Alternatively, superinfection could lead to death of the affected syncytium as superinfection has previously been correlated with increased apoptosis [58]. Further, an influx of yet-to-be downregulated CD4 into a productively infected cell could lead to Env-CD4 interactions in cis within the infected cell. Such Env-CD4 could inhibit efficient release of virus particles and/or expose CD4-binding-induced Env epitopes (CD4i) [17]. Further, syncytia with partially restored CD4 may be susceptible to CD4i antibody-mediated antibody-dependent cell cytotoxicity (ADCC) as has been previously shown for infected cells that do not sufficiently downregulate CD4 [59-61].

We propose to further analyze the total amount of CD4 on syncytia compared to mononucleated infected cells by mass spectrometry and flow cytometry (described below in 5.4) to carefully determine whether there are indeed differences in surface expression that were not detectable by fluorescence microscopy. Should we find that syncytia do indeed have partially restored CD4, we would then aim to determine whether syncytia are indeed susceptible to superinfection and ADCC. Increased syncytia susceptibility to ADCC would be particularly intriguing as enhancing ADCC response to infected cells is of interest as a strategy for treating infection [62].

### *5.3.3. Could altered Nef-modulation lead to restored migratory abilities for syncytia?*

*In vivo* analysis of a Nef mutant which restored normal migratory abilities for infected cells compared to WT Nef (initial infection completed using a combination of mutant:WT virus at a 1:1) revealed that although the Nef mutant initially predominated and

thus seemed to have an enhanced ability drive initial virus spread, WT strains emerged as the dominant species over time [50]. The authors propose that the virus balances a defect in migration, thus rapid establishment of systemic spread, with a yet to be determined benefit to virus spread over the course of infection [50] – possibly enhanced cell-to-cell transmission as the decreased speed may enable the infected cell to form more stable contacts with uninfected target cells (as was observed for 3D cultures of infected cells [63]). However, we predict that transiently altered protein modulation by viral accessory proteins upon cell-cell fusion (ie. EWI-2) is not restricted to surface protein targets but extends to additional host proteins including actin regulators targeted by Nef. In turn, we hypothesize that syncytia have partially restored migratory abilities after cell-cell fusion and analysis of HIV-1-infected cultures embedded in 3D matrices to compare the relative migratory abilities of syncytia to mononucleated infected cells is currently underway (M. Symeonides). Should we determine that syncytia do indeed have enhanced migratory abilities, it is interesting to speculate that syncytia present during early stages of infection (as shown previously [9-11]) may help drive efficient establishment of systemic infection (like what has been previously shown migration modulation-deficient Nef mutants [50]) even when mononucleated infected cell migration is impaired.

### 5.4. Characterizing the proteome of HIV-1-induced syncytia.

We have demonstrated that two host proteins, CD81 and EWI-2, which are typically downregulated from the surface of HIV-1-infected cells are partially restored on syncytia [7]. That syncytia have higher levels of CD81 and EWI-2 on their surface than mononucleated infected cells is exciting as it was the first study that documented distinct

differences in protein profiles between syncytia and mononucleated infected cells, suggesting that syncytia might contribute uniquely to virus spread. The syncytia surface profile was analyzed by quantitative microscopy as this approach allows for clear discrimination between mono and multinucleated HIV-1-infected cells. However, single cell analysis by quantitative microscopy is not a feasible approach for thoroughly characterizing the syncytia surface profile as it is completed by labeling only 1-2 surface proteins of interest at a time and then manually outlining each individual cell to measure the relative surface density of each protein at the cell surface. This approach is also limited to quantifying the relative surface density of proteins of interest (rather than total amounts of protein within the cell) and is also potentially susceptible to bias during analysis. Given these limitations, syncytia should be analyzed using high throughput approaches, including flow cytometry and mass spectrometry analysis, to thoroughly characterize the surface profile and increase our understanding of how syncytia compare to mononucleated infected cells. We plan to implement these approaches by separating syncytia from a heterogenous population of uninfected, mononucleated infected, and multinucleated infected cells using MACs as described above (5.2.1).

Protein surface expression and the whole cell proteome of each purified cell population, mononucleated infected cells and syncytia, could then be directly compared by flow cytometry and mass spectrometry. For flow cytometry, we propose to use a BD lyoplate panel to screen surface proteins typically modulated upon HIV-1 infection by viral accessory proteins Nef and Vpu (as described previously [13]). The ability to use flow cytometry to analyze purified populations of HIV-1-infected cells will also provide an additional approach for analyzing the influence of the target cell population on the syncytia

surface profile beyond EWI-2 and to determine whether other surface proteins (such as CD81) are similarly modulated over time following cell-cell fusion. Further, we will use mass spectrometry to analyze both the surface profile and total proteome of HIV-1-induced syncytia compared to mononucleated HIV-1-infected cells (in collaboration with N.J. Matheson). These high throughput analysis will allow us to thoroughly characterize the syncytia surface profile and determine whether additional proteins are differentially modulated in HIV-1-infected cells upon cell-cell fusion would allow us to address our proposed model of broad host protein modulation upon HIV-1-induced syncytium formation (Figure 5.3).

### 5.5. *In vivo* analysis of syncytia contribution to virus spread.

The *in vitro* studies described above are necessary to determine whether syncytia might have any functional differences between mononucleated infected cells in terms of their ability to directly and/or indirectly contribute to virus spread. To assess the impact of syncytia on early virus spread *in vivo*, we propose to develop a modified approach for the cell-associated infection of humanized mice, previously used to compare cell-free to cell-associated acute transmission [10]. We will work with our colleagues (T. Mempel and T. Murooka), who have expertise in studies using HIV-1-infected humanized mice (immune deficient mice where immune system has been reconstituted with human immune tissues and are thus susceptible to HIV-1 infection, recently reviewed in [64]), to study infected mice which were inoculated with either purified mononucleated infected cells or purified HIV-1-induced syncytia (using the purification approach described above). This acute transmission model was previously used to compare viremia in the blood, infection in lung

and spleen, as well as $CD4^+$ T cell depletion for cell-free versus cell-associated infection [10] and could be useful for analyzing the same metrics to compare how syncytia and mononucleated infected cells each contribute to acute virus spread. As it is currently unknown whether/how syncytia contribute to virus spread, it could be beneficial to implement a recently developed Nanoluciferase/GFP dual-reporter T/F viral strain [11] for this acute transmission assay. Using this viral strain would allow us to monitor infection in live humanized mice [11], allowing for efficient optimization of experimental parameters (i.e. day of peak infection, tissues predominantly susceptible to syncytia-mediated virus spread) necessary for analyzing syncytia contribution to virus spread versus that of mononucleated infected cells. Developing an *in vivo* model for syncytia-mediated virus transmission would greatly enhance our understanding of the role of this subpopulation of infected cells in virus spread.

## 5.6. Conclusions

The work presented in this dissertation has contributed to the field of HIV-1 cell-to-cell transmission by 1) identifying a new host factor (EWI-2) in the network of fusion regulatory proteins which collectively support continued virus transmission at the VS, 2) by taking the first steps toward characterizing HIV-1-induced T cell based syncytia which are a relatively unappreciated group of infected cells, and 3) determining how cell-cell fusion impacts modulation of EWI-2 in HIV-1-infected cells.

By demonstrating that EWI-2 inhibits HIV-1-induced cell-cell fusion at the presynapse, we're closer to understanding how proteins functions are coordinated at the presynapse to inhibit fusion. Previous studies that revealed the molecular determinants for

EWI-2-tetraspanin interactions and the role of EWI-2 on membrane processes (which are largely related to EWI-2 influence on tetraspanins) will help fuel future investigations as to how EWI-2 contributes to efficient fusion inhibition at the presynapse.

Showing that HIV-1-induced syncytia have an altered surface profile compared to mononucleated infected cells, by documenting partially restored levels of CD81 and EWI-2 at the syncytia surface, has cracked open many questions regarding the potential role syncytia may have in overall virus spread. The pressing question we hope to address in the near future is whether syncytia have altered abilities to contribute directly (virus transmission) and indirectly (inducing an immune response that recruits target cells to a site of infection) to virus spread.

Indeed, it is becoming more appreciated that the mononucleated HIV-1-infected T cell population is quite diverse (i.e. a recent multiomics analysis of mononucleated infected cells from humanized mice [65]) and likely collectively contribute to virus spread. We believe that syncytia should be included as another infected subpopulation, and suspect that the syncytia have a yet-to-be determined role in promoting virus spread *in vivo*. As such, targeting syncytia formation by tuning the extent of HIV-1-induced cell-cell fusion could disrupt the homeostasis of the diverse group of infected cells driving spread, and thus may cripple infection. It would be intriguing to see whether this approach of disrupting fusion homeostasis to impede virus spread might be applicable in other viral infections as well – specifically those that produce virus-induced syncytia (such herpesviruses and coronaviruses) or viruses that depend on cell-to-cell transmission at a virological synapse such as human T-cell lymphotropic virus (HTLV) [66,67].

Overall, we're optimistic that these data demonstrating that syncytia are distinct from mononucleated infected cells will encourage continued characterization of the syncytia and spark analyses aimed at understanding whether/how these entities are functionally distinct from other HIV-1-infected cells.

## 5.7. Figure Legends

**Figure 5.1.** EWI-2 is not required for CD81 enrichment at the VS. CEM-SS cells stably expressing either shRNA targeting EWI-2 (shEWI-2) or a non-targeting shRNA control (shScr) [7] were infected with HIV-1 NL4-3 (WT) or Env-deficient NL4-3 (ΔEnv). 48 hours post infection infected (producer) cells were mixed with CMAC-labeled uninfected (target) non-shRNA expressing CEM-SS (CEM-SS) cells and plated on poly-L-lysine coated 8-well plates at 250,000 cells per well (producers:target, 1:1). Producer:target samples were prepared in parallel with uninfected controls; shEWI-2, shScr, CEM-SS, and CEM-SS cells not labeled with primary antibodies (No1 controls). Plated samples were incubated at 37 ˚C for 2.5 hr to allow for VS formation. All samples were then surface labeled for either EWI-2 or CD81 (except for the No1 controls), fixed and permeabilized, labeled for HIV-1 Gag, and stained with AlexaFlour-conjugated (647-conjugated for EWI-2 and CD81, 488-conjugated for Gag) secondary antibodies. Samples were imaged using a 60× objective, deconvolved using SoftWorx, and imported into FIJI for analysis. VSs were identified as areas of Gag-enrichment at a cell-cell contact between a producer and CMAC-labeled target cell. Fold-enrichment of either EWI-2 or CD81 at the VS was calculated by dividing the protein signal contained within the VS (or infected to uninfected cell contact for ΔEnv) by the sum of the surface-associated protein signal at non-contact sites on the producer and target cell. EWI-2 and CD81 were considered enriched at the contact/VS if the fold-enrichment value was greater than 1 (represented as a dashed line).

**Figure 5.2.** Model for HIV-1-induced syncytia contribution to cell-to-cell transmission. Mononucleated HIV-1 infected cells (red) can spread virus through cell-to-cell transmission at a transient junction between infected and uninfected (blue) cells known as a virological synapse (VS) [23]. Typically, the VS resolves with transfer of virus particles to the target cell complete cell separation, which can ultimately lead to production of a new infected cell. Env-mediated fusion at this site is largely prevented by viral (Gag) and host (tetraspanins, ezrin, and EWI-2; EWI-2 surface protein shown in green) fusion inhibitory factors [1-3,7]. However, Env-mediated fusion at the VS does still occur thus resulting in the formation of a multinucleated HIV-1 infected cell (syncytium), which have even been detected *in vivo* [8-11]. Syncytia have been shown to form VSs with uninfected target cells which also result in either transfer of virus particles and complete cell separation or an additional cell-cell fusion event [38]. We have shown that syncytia have partially restored levels of tetraspanin CD81 and EWI-2 (represented as 5 EWI-2 icons) compared to mononucleated infected cells (for simplicity of this schematic, no EWI-2 is present on the cell surface) [4]. Further we have demonstrated that EWI-2 levels on syncytia are the result of an influx of protein from the recently fused target cell (Figure 4.1) and can be downregulated over time (Figure 4.2). Therefore, we suggest that syncytia which have recently undergone a cell-cell fusion event are more likely to form synapses that resolve with transfer of virus particles and complete cell separation and likely production of a newly infected cell. In parallel, we suggest that "older" syncytia are more susceptible to additional cell-cell fusion events than those that recently formed upon cell-cell fusion. We predict that this cycle of cell-cell fusion at the VS will continue for a syncytium until it eventually dies, thus the combination of an influx of fusion inhibitory host proteins and

cell death contribute to the restricted size (2-4 nuclei) of syncytia observed *in vivo* [38]. Image created with BioRender.com.

**Figure 5.3.** Model for fluctuating host protein modulation upon HIV-1-induced cell-cell fusion. HIV-1 (virus particle shown in green) infection of an uninfected (target) cell (shown in blue) leads to substantial modulation of the host cell environment by viral accessory proteins. For simplicity, host protein modulation is represented by downregulation of a host surface protein (represented by pink icon) from the surface of an infected mononucleated cell (shown in red). Upon HIV-1-induced cell-cell fusion, we expect that viral accessory protein-mediated modulation of the infected cell will be disrupted by an influx of proteins from the previously unfused target cell. Therefore the environment/protein profile of a recently formed HIV-1-induced syncytium (syncytium with 2 nuclei shown in purple) will be (at least partially) restored to reflect that of the previously unfused target cell, as shown previously for restored EWI-2 on syncytia [7]. We predict that viral accessory proteins will modulate the yet-to-be-targeted host proteins contributed by the previously unfused target cell over time (as discussed for EWI-2 in Chapter 4) such that the syncytium protein profile and cellular environment reflects what is typically observed for infected mononucleated cells. Should a syncytium undergo further cell-cell fusion (represented as the syncytium with 3 nuclei), we would expect another influx of host protein from the previously unfused target cell followed by viral accessory protein-mediated modulation of these host proteins. This cycle of HIV-1-induced syncytium formation, host protein restoration, and subsequent modulation by viral accessory proteins over time would continue until the eventual death of the syncytium. Image created with BioRender.com.

**Figure 5.4.** BST-2 on the surface of HIV-1 syncytia co-accumulates with mature virus particles more frequently than on mononucleated infected cells. A. CEM-SS cells were infected with NL-sfGI for 3 days to allow for syncytia formation, then plated on poly-L-lysine coated plates for microscopy preparation. Cells were surface labeled for BST-2, fixed, permeabilized, and stained with DAPI and AlexaFlour-conjugated secondary antibody. The relative BST-2 surface density between uninfected (Uninf; GFP negative), mononucleated infected (Mono; GFP positive, 1 nucleus), and HIV-1-induced syncytia (Syn; GFP positive, $\geq$2 nuclei) were determined by manually outlining the surface BST-2 signal at the midline of the cell and calculating the mean fluorescence intensity (MFI) of the signal contained within the outline for each cell (as described previously [7]). All MFI values were background subtracted and normalized to the average MFI of the uninfected cells within their respective biological replicate. Small open data points represent the BST-2 MFI of an individual cell while large filled data points represent the average MFI of each cell type. Black bars represent the mean of the average BST-2 MFI values. Data from the same biological replicate are indicated by shape and color (cyan circles, orange triangles, or magenta squares). B-C. CEM-SS cells were infected as described for (A) and prepared for microscopy by labeling both BST-2 and p17 (to label mature virus particles). Images were acquired and deconvolved as described for (A) and analyzed to determine the relative distribution of BST-2 and p17 for Uninf (black), Mono (gray), and Syn (purple). B) Surface BST-2 that was not co-accumulating with p17-associated signal is identified as "free" surface BST-2. Data points represent the percentage of p17-free BST-2 for individual cells

and n = the number of cells analyzed (left). Dashed line represents 50% of the total cell surface BST-2 signal. Cells p17-free BST-2 comprising less than 50% of the total surface BST-2 were determined to be cells when surface BST-2 is primarily occluded by mature virus particles. Shown are the percentage each cell population (Mono and Syn) with primarily occluded BST-2 (right). C) The size of the area containing p17-free BST-2 signal from (B) was measured to estimate the relative amount of free BST-2 on the surface of each cell type. Data points represent the free BST-2 area of individual cells. Black bars represent the mean size of the area containing free BST-2 for each cell type. All images (A-C) were acquired using a 60× objective, deconvolved using SoftWorx, and imported into FIJI for analysis.

**Figure 5.5.** HIV-1-induced syncytia have increased surface NTBA but equal levels of HLA-1 compared to mononucleated infected cells. CEM-SS cells were infected with NL-sfGI for 3 days and then prepared for microscopy. Cells were plated on poly-L-lysine coated plates, surface labeled for NTB-A (A) or HLA-1 (B), fixed and permeabilized, stained with DAPI and AlexaFluor-conjugated secondary antibodies, and imaged using a 60× objective. Images were processed by deconvolution in SoftWorx and imported into FIJI for analysis. Shown are representative images of syncytia (*) and mononucleated infected cells (Δ) labeled for NTB-A (A) and HLA-1 (B). Scale bars = 10 μm. To measure the relative surface density of NTB-A (A) or HLA-1 (B) on uninfected cells (GFP negative), mononucleated infected cells (GFP positive/1 nucleus), and syncytia (GFP positive ≥2 nuclei) the surface of each cell was manually outlined and used to calculate the mean fluorescence intensity (MFI) of the surface-associated signal (as described previously [7]). MFI values were background subtracted and normalized to the average MFI of the uninfected controls. Each data point represents the normalized MFI of an individual cell (uninfected; Uninf/black, mononucleated infected; mono/gray, syncytia; syn/magenta) and n = the number of cells analyzed. Black bars represent the mean MFI of each cell population.

**Figure 5.6.** HIV-1-induced syncytia have unique properties that allow them to form Gag-enriched synapses with other infected cells. A) $CD4^+$ primary T cells were infected with NL-sfGI for 3 days and then plated on poly-L-lysine coated plates for microscopy preparation. Cells were surface labeled for CD4, fixed and permeabilized, labeled with DAPI and AlexaFluor-conjugated secondary antibody. Samples were then imaged using a 60× objective, processed by deconvolution in SoftWorx, and imported into FIJI for analysis. Relative CD4 density on the surface for uninfected cells (GFP negative), mononucleated infected cells (GFP positive, 1 nucleus) and syncytia (GFP positive, ≥2 nuclei) was determined by manually outlining the cell surface at the midline of each cell and calculating the mean fluorescence intensity (MFI) of that site (as described previously [7]). The MFI for each cell was background subtracted and normalized to the average MFI of the uninfected cell population within the biological replicate. Small open data points represent the normalized MFI for individual cells (uninfected; Uni, mononucleated infected; Mono, and syncytia; Syn) while large filled data points represent the average MFI of the cell population for each biological replicate. Data points within the same biological replicate are organized by shape and color (cyan circles, orange triangles, and magenta

squares). Black bars represent the mean of the average MFI for each population. B) CEM-SS cells were infected with NL4-3 and cultured in the presence of fusion inhibitor AMD3100 starting 7 hours post infection. 2 days post infection, cells were plated on poly-L-lysine coated plates and prepared for microscopy. Cells were fixed, permeabilized, labeled for Gag (yellow) and stained with DAPI (cyan). Images were acquired using a 60X objective, processed by deconvolution using SoftWorx, and imported into FIJI for analysis. Scale bar = 10 μm.

## 5.8. Figures

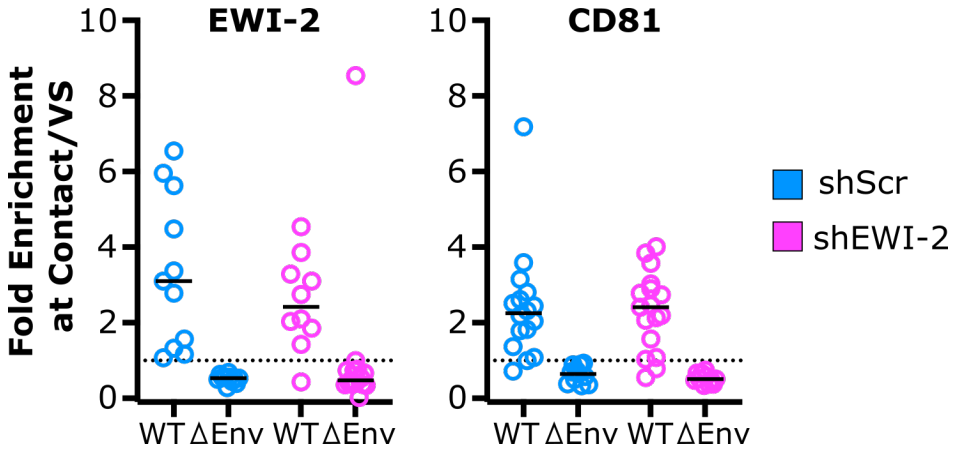


**Figure 5.1. EWI-2 is not required for CD81 enrichment at the VS.**

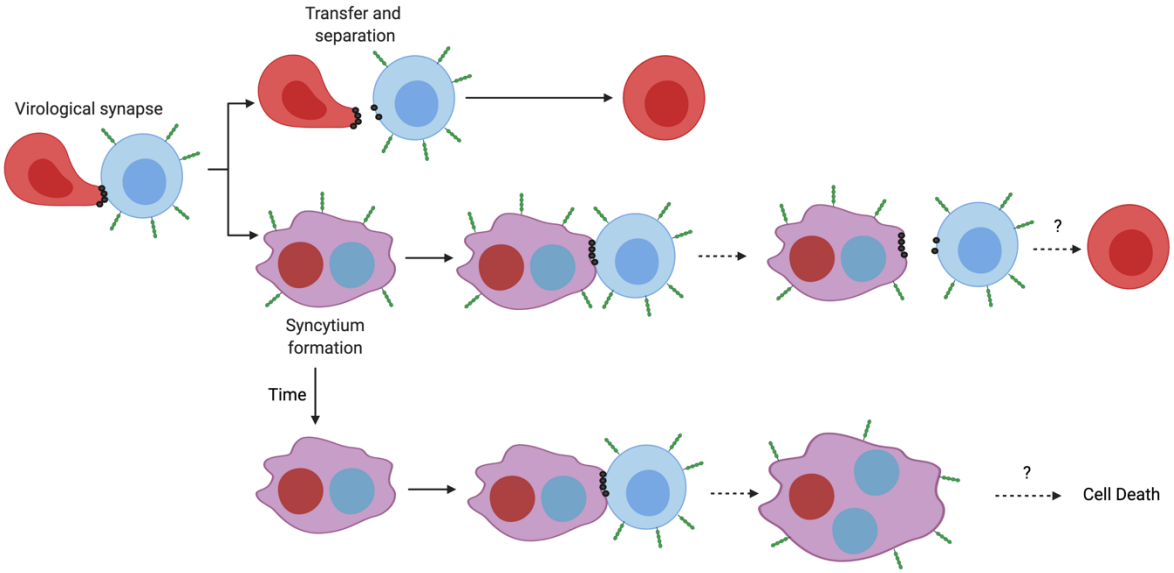


**Figure 5.2. Model for HIV-1-induced syncytia contribution to cell-to-cell transmission.**

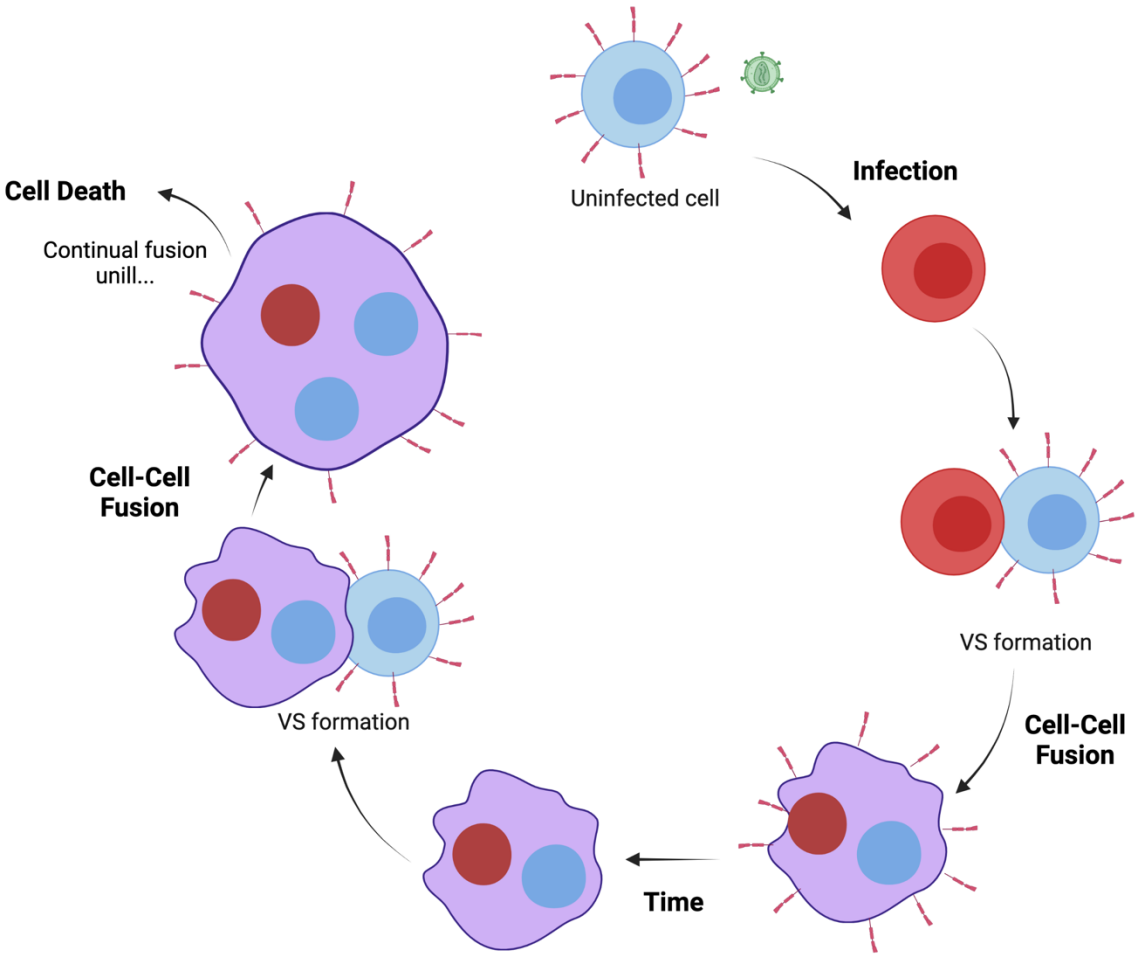


**Figure 5.3. Model for fluctuating host protein modulation upon HIV-1-induced cell-cell fusion.**

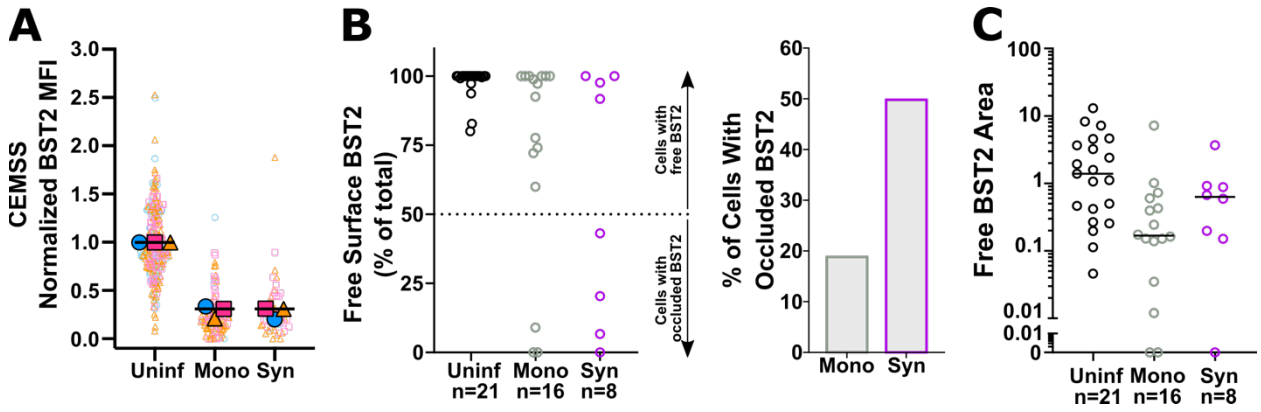


**Figure 5.4. BST-2 on the surface of HIV-1 syncytia co-accumulates with mature virus particles more frequently than on mononucleated infected cells.**

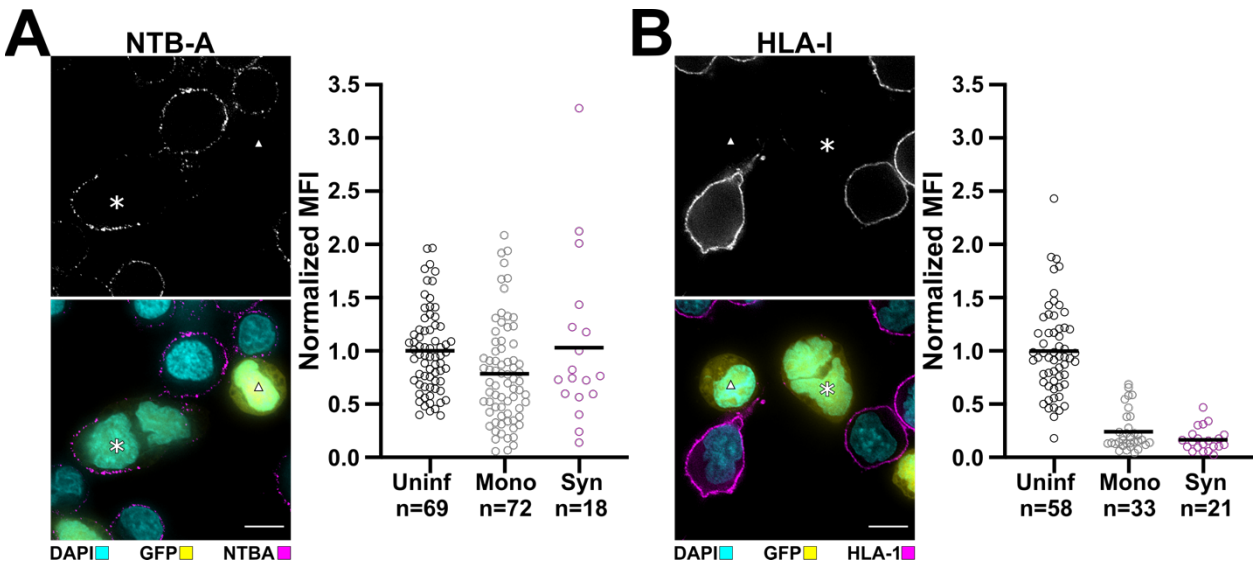


**Figure 5.5. HIV-1-induced syncytia have increased surface NTBA but equal levels of HLA-1 compared to mononucleated infected cells.**

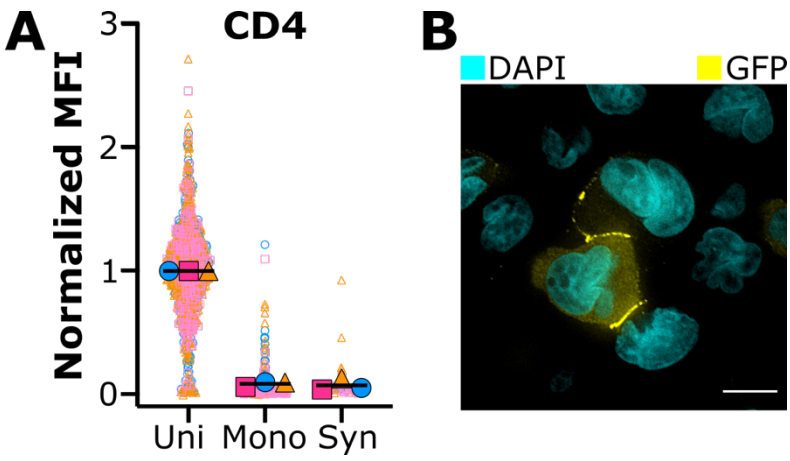


**Figure 5.6. HIV-1-induced syncytia have unique properties that allow them to form Gag-enriched synapses with other infected cells.**

## 5.9. References


1. Weng, J.; Krementsov, D.N.; Khurana, S.; Roy, N.H.; Thali, M. Formation of syncytia is repressed by tetraspanins in human immunodeficiency virus type 1-producing cells. *Journal of virology* **2009**, *83*, 7467-7474, doi:10.1128/jvi.00163-09.

2. Roy, N.H.; Lambelé, M.; Chan, J.; Symeonides, M.; Thali, M. Ezrin is a component of the HIV-1 virological presynapse and contributes to the inhibition of cell-cell fusion. *Journal of virology* **2014**, *88*, 7645-7658, doi:10.1128/jvi.00550-14.

3. Roy, N.H.; Chan, J.; Lambelé, M.; Thali, M. Clustering and mobility of HIV-1 Env at viral assembly sites predict its propensity to induce cell-cell fusion. *Journal of virology* **2013**, *87*, 7516-7525, doi:10.1128/jvi.00790-13.

4. Stipp, C.S.; Kolesnikova, T.V.; Hemler, M.E. EWI-2 is a major CD9 and CD81 partner and member of a novel Ig protein subfamily. *J Biol Chem* **2001**, *276*, 40545-40554, doi:10.1074/jbc.M107338200.

5. Charrin, S.; Le Naour, F.; Labas, V.; Billard, M.; Le Caer, J.P.; Emile, J.F.; Petit, M.A.; Boucheix, C.; Rubinstein, E. EWI-2 is a new component of the tetraspanin web in hepatocytes and lymphoid cells. *Biochem J* **2003**, *373*, 409-421, doi:10.1042/bj20030343.

6. Sala-Valdés, M.; Ursa, A.; Charrin, S.; Rubinstein, E.; Hemler, M.E.; Sánchez-Madrid, F.; Yáñez-Mó, M. EWI-2 and EWI-F link the tetraspanin web to the actin cytoskeleton through their direct association with ezrin-radixin-moesin proteins. *J Biol Chem* **2006**, *281*, 19665-19675, doi:10.1074/jbc.M602116200.

7. Whitaker, E.E.; Matheson, N.J.; Perlee, S.; Munson, P.B.; Symeonides, M.; Thali, M. EWI-2 Inhibits Cell-Cell Fusion at the HIV-1 Virological Presynapse. *Viruses* **2019**, *11*, doi:10.3390/v11121082.

8. Orenstein, J.M. In vivo cytolysis and fusion of human immunodeficiency virus type 1-infected lymphocytes in lymphoid tissue. *J Infect Dis* **2000**, *182*, 338-342, doi:10.1086/315640.

9. Murooka, T.T.; Deruaz, M.; Marangoni, F.; Vrbanac, V.D.; Seung, E.; von Andrian, U.H.; Tager, A.M.; Luster, A.D.; Mempel, T.R. HIV-infected T cells are migratory vehicles for viral dissemination. *Nature* **2012**, *490*, 283-287, doi:10.1038/nature11398.

10. Law, K.M.; Komarova, N.L.; Yewdall, A.W.; Lee, R.K.; Herrera, O.L.; Wodarz, D.; Chen, B.K. In Vivo HIV-1 Cell-to-Cell Transmission Promotes Multicopy Micro-compartmentalized Infection. *Cell Rep* **2016**, *15*, 2771-2783, doi:10.1016/j.celrep.2016.05.059.

11. Ventura, J.D.; Beloor, J.; Allen, E.; Zhang, T.; Haugh, K.A.; Uchil, P.D.; Ochsenbauer, C.; Kieffer, C.; Kumar, P.; Hope, T.J., et al. Longitudinal bioluminescent imaging of HIV-1 infection during antiretroviral therapy and treatment interruption in humanized mice. *PLoS Pathog* **2019**, *15*, e1008161, doi:10.1371/journal.ppat.1008161.

12. Krementsov, D.N.; Weng, J.; Lambele, M.; Roy, N.H.; Thali, M. Tetraspanins regulate cell-to-cell transmission of HIV-1. *Retrovirology* **2009**, *6*, 64, doi:10.1186/1742-4690-6-64.

13. Haller, C.; Müller, B.; Fritz, J.V.; Lamas-Murua, M.; Stolp, B.; Pujol, F.M.; Keppler, O.T.; Fackler, O.T. HIV-1 Nef and Vpu are functionally redundant broad-spectrum modulators of cell surface receptors, including tetraspanins. *Journal of virology* **2014**, *88*, 14241-14257, doi:10.1128/jvi.02333-14.

14. Lambelé, M.; Koppensteiner, H.; Symeonides, M.; Roy, N.H.; Chan, J.; Schindler, M.; Thali, M. Vpu is the main determinant for tetraspanin downregulation in HIV-1-infected cells. *Journal of virology* **2015**, *89*, 3247-3255, doi:10.1128/jvi.03719-14.

15. Gordon-Alonso, M.; Sala-Valdes, M.; Rocha-Perugini, V.; Perez-Hernandez, D.; Lopez-Martin, S.; Ursa, A.; Alvarez, S.; Kolesnikova, T.V.; Vazquez, J.; Sanchez-Madrid, F., et al. EWI-2 association with alpha-actinin regulates T cell immune synapses and HIV viral infection. *J Immunol* **2012**, *189*, 689-700, doi:10.4049/jimmunol.1103708.

16. Charrin, S.; Latil, M.; Soave, S.; Polesskaya, A.; Chrétien, F.; Boucheix, C.; Rubinstein, E. Normal muscle regeneration requires tight control of muscle cell fusion by tetraspanins CD9 and CD81. *Nat Commun* **2013**, *4*, 1674, doi:10.1038/ncomms2675.

17. Sugden, S.M.; Bego, M.G.; Pham, T.N.; Cohen É, A. Remodeling of the Host Cell Plasma Membrane by HIV-1 Nef and Vpu: A Strategy to Ensure Viral Fitness and Persistence. *Viruses* **2016**, *8*, 67, doi:10.3390/v8030067.

18. Jolly, C.; Sattentau, Q.J. Human immunodeficiency virus type 1 assembly, budding, and cell-cell spread in T cells take place in tetraspanin-enriched plasma membrane domains. *Journal of virology* **2007**, *81*, 7873-7884, doi:10.1128/jvi.01845-06.

19. Montpellier, C.; Tews, B.A.; Poitrimole, J.; Rocha-Perugini, V.; D'Arienzo, V.; Potel, J.; Zhang, X.A.; Rubinstein, E.; Dubuisson, J.; Cocquerel, L. Interacting regions of CD81 and two of its partners, EWI-2 and EWI-2wint, and their effect on hepatitis C virus infection. *J Biol Chem* **2011**, *286*, 13954-13965, doi:10.1074/jbc.M111.220103.

20. He, B.; Zhang, Y.H.; Richardson, M.M.; Zhang, J.S.; Rubinstein, E.; Zhang, X.A. Differential functions of phospholipid binding and palmitoylation of tumour suppressor EWI2/PGRL. *Biochem J* **2011**, *437*, 399-411, doi:10.1042/bj20101381.

21. Freed, E.O. HIV-1 assembly, release and maturation. *Nat Rev Microbiol* **2015**, *13*, 484-496, doi:10.1038/nrmicro3490.

22. Wen, Y.; Feigenson, G.W.; Vogt, V.M.; Dick, R.A. Mechanisms of PI(4,5)P2 Enrichment in HIV-1 Viral Membranes. *J Mol Biol* **2020**, *432*, 5343-5364, doi:10.1016/j.jmb.2020.07.018.

23. Jolly, C.; Kashefi, K.; Hollinshead, M.; Sattentau, Q.J. HIV-1 cell to cell transfer across an Env-induced, actin-dependent synapse. *J Exp Med* **2004**, *199*, 283-293, doi:10.1084/jem.20030648.

24. Kolesnikova, T.V.; Kazarov, A.R.; Lemieux, M.E.; Lafleur, M.A.; Kesari, S.; Kung, A.L.; Hemler, M.E. Glioblastoma inhibition by cell surface immunoglobulin protein EWI-2, in vitro and in vivo. *Neoplasia* **2009**, *11*, 77-86, 74p following 86, doi:10.1593/neo.81180.

25. Wang, H.X.; Sharma, C.; Knoblich, K.; Granter, S.R.; Hemler, M.E. EWI-2 negatively regulates TGF-β signaling leading to altered melanoma growth and metastasis. *Cell Res* **2015**, *25*, 370-385, doi:10.1038/cr.2015.17.

26. Rocha-Perugini, V.; Montpellier, C.; Delgrange, D.; Wychowski, C.; Helle, F.; Pillez, A.; Drobecq, H.; Le Naour, F.; Charrin, S.; Levy, S., et al. The CD81 partner EWI-2wint inhibits hepatitis C virus entry. *PLoS One* **2008**, *3*, e1866, doi:10.1371/journal.pone.0001866.

27. Potel, J.; Rassam, P.; Montpellier, C.; Kaestner, L.; Werkmeister, E.; Tews, B.A.; Couturier, C.; Popescu, C.I.; Baumert, T.F.; Rubinstein, E., et al. EWI-2wint promotes CD81 clustering that abrogates Hepatitis C Virus entry. *Cellular microbiology* **2013**, *15*, 1234-1252, doi:10.1111/cmi.12112.

28. Zuidscherwoude, M.; Göttfert, F.; Dunlock, V.M.; Figdor, C.G.; van den Bogaart, G.; van Spriel, A.B. The tetraspanin web revisited by super-resolution microscopy. *Sci Rep* **2015**, *5*, 12201, doi:10.1038/srep12201.

29. He, J.; Sun, E.; Bujny, M.V.; Kim, D.; Davidson, M.W.; Zhuang, X. Dual function of CD81 in influenza virus uncoating and budding. *PLoS Pathog* **2013**, *9*, e1003701, doi:10.1371/journal.ppat.1003701.

30. Dahmane, S.; Doucet, C.; Le Gall, A.; Chamontin, C.; Dosset, P.; Murcy, F.; Fernandez, L.; Salas, D.; Rubinstein, E.; Mougel, M., et al. Nanoscale organization of tetraspanins during HIV-1 budding by correlative dSTORM/AFM. *Nanoscale* **2019**, *11*, 6036-6044, doi:10.1039/c8nr07269h.

31. Vasiliver-Shamis, G.; Cho, M.W.; Hioe, C.E.; Dustin, M.L. Human immunodeficiency virus type 1 envelope gp120-induced partial T-cell receptor signaling creates an F-actin-depleted zone in the virological synapse. *Journal of virology* **2009**, *83*, 11341-11355, doi:10.1128/jvi.01440-09.

32. Prins, K.C.; Vasiliver-Shamis, G.; Cammer, M.; Depoil, D.; Dustin, M.L.; Hioe, C.E. Imaging of HIV-1 envelope-induced virological synapse and signaling on synthetic lipid bilayers. *J Vis Exp* **2012**, 10.3791/3757, doi:10.3791/3757.

33. Yang, X.H.; Kovalenko, O.V.; Kolesnikova, T.V.; Andzelm, M.M.; Rubinstein, E.; Strominger, J.L.; Hemler, M.E. Contrasting effects of EWI proteins, integrins, and protein palmitoylation on cell surface CD9 organization. *J Biol Chem* **2006**, *281*, 12976-12985, doi:10.1074/jbc.M510617200.

34. Wang, H.X.; Hemler, M.E. Novel impact of EWI-2, CD9, and CD81 on TGF-β signaling in melanoma. *Mol Cell Oncol* **2015**, *2*, doi:10.1080/23723556.2015.1030536.

35. Sato, K.; Aoki, J.; Misawa, N.; Daikoku, E.; Sano, K.; Tanaka, Y.; Koyanagi, Y. Modulation of human immunodeficiency virus type 1 infectivity through incorporation of tetraspanin proteins. *Journal of virology* **2008**, *82*, 1021-1033, doi:10.1128/jvi.01044-07.

36. Len, A.C.L.; Starling, S.; Shivkumar, M.; Jolly, C. HIV-1 Activates T Cell Signaling Independently of Antigen to Drive Viral Spread. *Cell Rep* **2017**, *18*, 1062-1074, doi:10.1016/j.celrep.2016.12.057.

37. Mesner, D.; Hotter, D.; Kirchhoff, F.; Jolly, C. Loss of Nef-mediated CD3 down-regulation in the HIV-1 lineage increases viral infectivity and spread. *Proc Natl Acad Sci U S A* **2020**, *117*, 7382-7391, doi:10.1073/pnas.1921135117.

38. Symeonides, M.; Murooka, T.T.; Bellfy, L.N.; Roy, N.H.; Mempel, T.R.; Thali, M. HIV-1-Induced Small T Cell Syncytia Can Transfer Virus Particles to Target Cells through Transient Contacts. *Viruses* **2015**, *7*, 6590-6603, doi:10.3390/v7122959.

39. Perelson, A.S.; Neumann, A.U.; Markowitz, M.; Leonard, J.M.; Ho, D.D. HIV-1 dynamics in vivo: virion clearance rate, infected cell life-span, and viral generation time. *Science* **1996**, *271*, 1582-1586, doi:10.1126/science.271.5255.1582.

40. Croucher, D.R.; Iconomou, M.; Hastings, J.F.; Kennedy, S.P.; Han, J.Z.; Shearer, R.F.; McKenna, J.; Wan, A.; Lau, J.; Aparicio, S., et al. Bimolecular complementation affinity purification (BiCAP) reveals dimer-specific protein interactions for ERBB2 dimers. *Sci Signal* **2016**, *9*, ra69, doi:10.1126/scisignal.aaf0793.

41. Ikeda, T.; Symeonides, M.; Albin, J.S.; Li, M.; Thali, M.; Harris, R.S. HIV-1 adaptation studies reveal a novel Env-mediated homeostasis mechanism for

evading lethal hypermutation by APOBEC3G. *PLoS Pathog* **2018**, *14*, e1007010, doi:10.1371/journal.ppat.1007010.

42. Durham, N.D.; Chen, B.K. Measuring T Cell-to-T Cell HIV-1 Transfer, Viral Fusion, and Infection Using Flow Cytometry. *Methods Mol Biol* **2016**, *1354*, 21-38, doi:10.1007/978-1-4939-3046-3_2.

43. Van Damme, N.; Goff, D.; Katsura, C.; Jorgenson, R.L.; Mitchell, R.; Johnson, M.C.; Stephens, E.B.; Guatelli, J. The interferon-induced protein BST-2 restricts HIV-1 release and is downregulated from the cell surface by the viral Vpu protein. *Cell Host Microbe* **2008**, *3*, 245-252, doi:10.1016/j.chom.2008.03.001.

44. Neil, S.J.; Zang, T.; Bieniasz, P.D. Tetherin inhibits retrovirus release and is antagonized by HIV-1 Vpu. *Nature* **2008**, *451*, 425-430, doi:10.1038/nature06553.

45. Shah, A.H.; Sowrirajan, B.; Davis, Z.B.; Ward, J.P.; Campbell, E.M.; Planelles, V.; Barker, E. Degranulation of natural killer cells following interaction with HIV-1-infected cells is hindered by downmodulation of NTB-A by Vpu. *Cell Host Microbe* **2010**, *8*, 397-409, doi:10.1016/j.chom.2010.10.008.

46. Guy, B.; Kieny, M.P.; Riviere, Y.; Le Peuch, C.; Dott, K.; Girard, M.; Montagnier, L.; Lecocq, J.P. HIV F/3' orf encodes a phosphorylated GTP-binding protein resembling an oncogene product. *Nature* **1987**, *330*, 266-269, doi:10.1038/330266a0.

47. Willey, R.L.; Maldarelli, F.; Martin, M.A.; Strebel, K. Human immunodeficiency virus type 1 Vpu protein induces rapid degradation of CD4. *Journal of virology* **1992**, *66*, 7193-7200, doi:10.1128/jvi.66.12.7193-7200.1992.

48. Nobile, C.; Rudnicka, D.; Hasan, M.; Aulner, N.; Porrot, F.; Machu, C.; Renaud, O.; Prévost, M.C.; Hivroz, C.; Schwartz, O., et al. HIV-1 Nef inhibits ruffles, induces filopodia, and modulates migration of infected lymphocytes. *Journal of virology* **2010**, *84*, 2282-2293, doi:10.1128/jvi.02230-09.

49. Stolp, B.; Imle, A.; Coelho, F.M.; Hons, M.; Gorina, R.; Lyck, R.; Stein, J.V.; Fackler, O.T. HIV-1 Nef interferes with T-lymphocyte circulation through confined environments in vivo. *Proc Natl Acad Sci U S A* **2012**, *109*, 18541-18546, doi:10.1073/pnas.1204322109.

50. Usmani, S.M.; Murooka, T.T.; Deruaz, M.; Koh, W.H.; Sharaf, R.R.; Di Pilato, M.; Power, K.A.; Lopez, P.; Hnatiuk, R.; Vrbanac, V.D., et al. HIV-1 Balances the Fitness Costs and Benefits of Disrupting the Host Cell Actin Cytoskeleton Early after Mucosal Transmission. *Cell Host Microbe* **2019**, *25*, 73-86.e75, doi:10.1016/j.chom.2018.12.008.

51. Ospina Stella, A.; Turville, S. All-Round Manipulation of the Actin Cytoskeleton by HIV. *Viruses* **2018**, *10*, doi:10.3390/v10020063.

52. McMichael, A.J.; Borrow, P.; Tomaras, G.D.; Goonetilleke, N.; Haynes, B.F. The immune response during acute HIV-1 infection: clues for vaccine development. *Nat Rev Immunol* **2010**, *10*, 11-23, doi:10.1038/nri2674.

53. Lepelley, A.; Louis, S.; Sourisseau, M.; Law, H.K.; Pothlichet, J.; Schilte, C.; Chaperot, L.; Plumas, J.; Randall, R.E.; Si-Tahar, M., et al. Innate sensing of HIV-infected cells. *PLoS Pathog* **2011**, *7*, e1001284, doi:10.1371/journal.ppat.1001284.

54. Bego, M.G.; Côté, É.; Aschman, N.; Mercier, J.; Weissenhorn, W.; Cohen É, A. Vpu Exploits the Cross-Talk between BST2 and the ILT7 Receptor to Suppress Anti-HIV-1 Responses by Plasmacytoid Dendritic Cells. *PLoS Pathog* **2015**, *11*, e1005024, doi:10.1371/journal.ppat.1005024.

55. Del Portillo, A.; Tripodi, J.; Najfeld, V.; Wodarz, D.; Levy, D.N.; Chen, B.K. Multiploid inheritance of HIV-1 during cell-to-cell infection. *Journal of virology* **2011**, *85*, 7169-7176, doi:10.1128/jvi.00231-11.

56. Kreger, J.; Komarova, N.L.; Wodarz, D. Effect of synaptic cell-to-cell transmission and recombination on the evolution of double mutants in HIV. *J R Soc Interface* **2020**, *17*, 20190832, doi:10.1098/rsif.2019.0832.

57. Kreger, J.; Garcia, J.; Zhang, H.; Komarova, N.L.; Wodarz, D.; Levy, D.N. Quantifying the dynamics of viral recombination during free virus and cell-to-cell transmission in HIV-1 infection. *Virus Evol* **2021**, *7*, veab026, doi:10.1093/ve/veab026.

58. Wildum, S.; Schindler, M.; Münch, J.; Kirchhoff, F. Contribution of Vpu, Env, and Nef to CD4 down-modulation and resistance of human immunodeficiency virus type 1-infected T cells to superinfection. *Journal of virology* **2006**, *80*, 8047-8059, doi:10.1128/jvi.00252-06.

59. Veillette, M.; Désormeaux, A.; Medjahed, H.; Gharsallah, N.E.; Coutu, M.; Baalwa, J.; Guan, Y.; Lewis, G.; Ferrari, G.; Hahn, B.H., et al. Interaction with cellular CD4 exposes HIV-1 envelope epitopes targeted by antibody-dependent cell-mediated cytotoxicity. *Journal of virology* **2014**, *88*, 2633-2644, doi:10.1128/jvi.03230-13.

60. Veillette, M.; Coutu, M.; Richard, J.; Batraville, L.A.; Dagher, O.; Bernard, N.; Tremblay, C.; Kaufmann, D.E.; Roger, M.; Finzi, A. The HIV-1 gp120 CD4-bound conformation is preferentially targeted by antibody-dependent cellular cytotoxicity-mediating antibodies in sera from HIV-1-infected individuals. *Journal of virology* **2015**, *89*, 545-551, doi:10.1128/jvi.02868-14.

61. Prévost, J.; Richard, J.; Medjahed, H.; Alexander, A.; Jones, J.; Kappes, J.C.; Ochsenbauer, C.; Finzi, A. Incomplete Downregulation of CD4 Expression Affects HIV-1 Env Conformation and Antibody-Dependent Cellular Cytotoxicity Responses. *Journal of virology* **2018**, *92*, doi:10.1128/jvi.00484-18.

62. Richard, J.; Ding, S.; Finzi, A. Unlocking HIV-1 Env: implications for antibody attack. *AIDS Res Ther* **2017**, *14*, 42, doi:10.1186/s12981-017-0168-5.

63. Imle, A.; Kumberger, P.; Schnellbächer, N.D.; Fehr, J.; Carrillo-Bustamante, P.; Ales, J.; Schmidt, P.; Ritter, C.; Godinez, W.J.; Müller, B., et al. Experimental and computational analyses reveal that environmental restrictions shape HIV-1 spread in 3D cultures. *Nat Commun* **2019**, *10*, 2144, doi:10.1038/s41467-019-09879-3.

64. Weichseldorfer, M.; Heredia, A.; Reitz, M.; Bryant, J.L.; Latinovic, O.S. Use of Humanized Mouse Models for Studying HIV-1 Infection, Pathogenesis and Persistence. *J AIDS HIV Treat* **2020**, *2*, 23-29.

65. Aso, H.; Nagaoka, S.; Kawakami, E.; Ito, J.; Islam, S.; Tan, B.J.Y.; Nakaoka, S.; Ashizaki, K.; Shiroguchi, K.; Suzuki, Y., et al. Multiomics Investigation Revealing the Characteristics of HIV-1-Infected Cells In Vivo. *Cell Rep* **2020**, *32*, 107887, doi:10.1016/j.celrep.2020.107887.

66. Bangham, C.R.M. The immune control and cell-to-cell spread of human T-lymphotropic virus type 1. *J Gen Virol* **2003**, *84*, 3177-3189, doi:10.1099/vir.0.19334-0.

67. Jolly, C.; Sattentau, Q.J. Retroviral spread by induction of virological synapses. *Traffic* **2004**, *5*, 643-650, doi:10.1111/j.1600-0854.2004.00209.x.

## BIBLIOGRAPHY


1. Achuthan, V.; Perreira, J.M.; Sowd, G.A.; Puray-Chavez, M.; McDougall, W.M.; Paulucci-Holthauzen, A.; Wu, X.; Fadel, H.J.; Poeschla, E.M.; Multani, A.S., et al. Capsid-CPSF6 Interaction Licenses Nuclear HIV-1 Trafficking to Sites of Viral DNA Integration. *Cell Host Microbe* **2018**, *24*, 392-404.e398, doi:10.1016/j.chom.2018.08.002.

2. Agosto, L.M.; Herring, M.B.; Mothes, W.; Henderson, A.J. HIV-1-Infected CD4+ T Cells Facilitate Latent Infection of Resting CD4+ T Cells through Cell-Cell Contact. *Cell Rep* **2018**, *24*, 2088-2100, doi:10.1016/j.celrep.2018.07.079.

3. Alfadhli, A.; Staubus, A.O.; Tedbury, P.R.; Novikova, M.; Freed, E.O.; Barklis, E. Analysis of HIV-1 Matrix-Envelope Cytoplasmic Tail Interactions. *J Virol* **2019**, *93*, doi:10.1128/jvi.01079-19.

4. Alvarez, R.A.; Barría, M.I.; Chen, B.K. Unique features of HIV-1 spread through T cell virological synapses. *PLoS Pathog* **2014**, *10*, e1004513, doi:10.1371/journal.ppat.1004513.

5. Andre, M.; Chambrion, C.; Charrin, S.; Soave, S.; Chaker, J.; Boucheix, C.; Rubinstein, E.; Le Naour, F. In situ chemical cross-linking on living cells reveals CD9P-1 cis-oligomer at cell surface. *Journal of proteomics* **2009**, *73*, 93-102, doi:10.1016/j.jprot.2009.08.005.

6. Andre, M.; Morelle, W.; Planchon, S.; Milhiet, P.E.; Rubinstein, E.; Mollicone, R.; Chamot-Rooke, J.; Le Naour, F. Glycosylation status of the membrane protein CD9P-1. *Proteomics* **2007**, *7*, 3880-3895, doi:10.1002/pmic.200700355.

7. Arhel, N. Revisiting HIV-1 uncoating. *Retrovirology* **2010**, *7*, 96, doi:10.1186/1742-4690-7-96.

8. Bangham, C.R.M. The immune control and cell-to-cell spread of human T-lymphotropic virus type 1. *J Gen Virol* **2003**, *84*, 3177-3189, doi:10.1099/vir.0.19334-0.

9. Bedwell, G.J.; Engelman, A.N. You can keep your coat on. *Elife* **2021**, *10*, doi:10.7554/eLife.69887.

10. Bego, M.G.; Côté, É.; Aschman, N.; Mercier, J.; Weissenhorn, W.; Cohen É, A. Vpu Exploits the Cross-Talk between BST2 and the ILT7 Receptor to Suppress Anti-HIV-1 Responses by Plasmacytoid Dendritic Cells. *PLoS Pathog* **2015**, *11*, e1005024, doi:10.1371/journal.ppat.1005024.

11. Berlioz-Torrent, C.; Shacklett, B.L.; Erdtmann, L.; Delamarre, L.; Bouchaert, I.; Sonigo, P.; Dokhelar, M.C.; Benarous, R. Interactions of the cytoplasmic domains of human and simian retroviral transmembrane proteins with components of the clathrin adaptor complexes modulate intracellular and cell surface expression of envelope glycoproteins. *J Virol* **1999**, *73*, 1350-1361, doi:10.1128/jvi.73.2.1350-1361.1999.

12. Bracq, L.; Xie, M.; Benichou, S.; Bouchet, J. Mechanisms for Cell-to-Cell Transmission of HIV-1. *Front Immunol* **2018**, *9*, 260, doi:10.3389/fimmu.2018.00260.

13. Briggs, J.A.; Kräusslich, H.G. The molecular architecture of HIV. *J Mol Biol* **2011**, *410*, 491-500, doi:10.1016/j.jmb.2011.04.021.

14. Burdick, R.C.; Li, C.; Munshi, M.; Rawson, J.M.O.; Nagashima, K.; Hu, W.S.; Pathak, V.K. HIV-1 uncoats in the nucleus near sites of integration. *Proc Natl Acad Sci U S A* **2020**, *117*, 5486-5493, doi:10.1073/pnas.1920631117.

15. Bussienne, C.; Marquet, R.; Paillart, J.C.; Bernacchi, S. Post-Translational Modifications of Retroviral HIV-1 Gag Precursors: An Overview of Their Biological Role. *Int J Mol Sci* **2021**, *22*, doi:10.3390/ijms22062871.

16. Charrin, S.; Latil, M.; Soave, S.; Polesskaya, A.; Chrétien, F.; Boucheix, C.; Rubinstein, E. Normal muscle regeneration requires tight control of muscle cell fusion by tetraspanins CD9 and CD81. *Nat Commun* **2013**, *4*, 1674, doi:10.1038/ncomms2675.

17. Charrin, S.; Le Naour, F.; Labas, V.; Billard, M.; Le Caer, J.P.; Emile, J.F.; Petit, M.A.; Boucheix, C.; Rubinstein, E. EWI-2 is a new component of the tetraspanin web in hepatocytes and lymphoid cells. *Biochem J* **2003**, *373*, 409-421, doi:10.1042/bj20030343.

18. Charrin, S.; Le Naour, F.; Oualid, M.; Billard, M.; Faure, G.; Hanash, S.M.; Boucheix, C.; Rubinstein, E. The major CD9 and CD81 molecular partner. Identification and characterization of the complexes. *J Biol Chem* **2001**, *276*, 14329-14337, doi:10.1074/jbc.M011297200.

19. Charrin, S.; Yalaoui, S.; Bartosch, B.; Cocquerel, L.; Franetich, J.F.; Boucheix, C.; Mazier, D.; Rubinstein, E.; Silvie, O. The Ig domain protein CD9P-1 down-regulates CD81 ability to support Plasmodium yoelii infection. *J Biol Chem* **2009**, *284*, 31572-31578, doi:10.1074/jbc.M109.057927.

20. Checkley, M.A.; Luttge, B.G.; Freed, E.O. HIV-1 envelope glycoprotein biosynthesis, trafficking, and incorporation. *J Mol Biol* **2011**, *410*, 582-608, doi:10.1016/j.jmb.2011.04.042.

21. Chen, A.; Leikina, E.; Melikov, K.; Podbilewicz, B.; Kozlov, M.M.; Chernomordik, L.V. Fusion-pore expansion during syncytium formation is restricted by an actin network. *J Cell Sci* **2008**, *121*, 3619-3628, doi:10.1242/jcs.032169.

22. Chen, B. Molecular Mechanism of HIV-1 Entry. *Trends Microbiol* **2019**, *27*, 878-891, doi:10.1016/j.tim.2019.06.002.

23. Chen, P.; Hübner, W.; Spinelli, M.A.; Chen, B.K. Predominant mode of human immunodeficiency virus transfer between T cells is mediated by sustained Env-dependent neutralization-resistant virological synapses. *J Virol* **2007**, *81*, 12582-12595, doi:10.1128/jvi.00381-07.

24. Chojnacki, J.; Staudt, T.; Glass, B.; Bingen, P.; Engelhardt, J.; Anders, M.; Schneider, J.; Müller, B.; Hell, S.W.; Kräusslich, H.G. Maturation-dependent HIV-1 surface protein redistribution revealed by fluorescence nanoscopy. *Science* **2012**, *338*, 524-528, doi:10.1126/science.1226359.

25. Chojnacki, J.; Waithe, D.; Carravilla, P.; Huarte, N.; Galiani, S.; Enderlein, J.; Eggeling, C. Envelope glycoprotein mobility on HIV-1 particles depends on the virus maturation state. *Nat Commun* **2017**, *8*, 545, doi:10.1038/s41467-017-00515-6.

26. Chukkapalli, V.; Ono, A. Molecular determinants that regulate plasma membrane association of HIV-1 Gag. *J Mol Biol* **2011**, *410*, 512-524, doi:10.1016/j.jmb.2011.04.015.

27. Cohen, M.S.; Shaw, G.M.; McMichael, A.J.; Haynes, B.F. Acute HIV-1 Infection. *N Engl J Med* **2011**, *364*, 1943-1954, doi:10.1056/NEJMra1011874.

28. Compton, A.A.; Schwartz, O. They Might Be Giants: Does Syncytium Formation Sink or Spread HIV Infection? *PLoS Pathog* **2017**, *13*, e1006099, doi:10.1371/journal.ppat.1006099.

29. Croucher, D.R.; Iconomou, M.; Hastings, J.F.; Kennedy, S.P.; Han, J.Z.; Shearer, R.F.; McKenna, J.; Wan, A.; Lau, J.; Aparicio, S., et al. Bimolecular complementation affinity purification (BiCAP) reveals dimer-specific protein interactions for ERBB2 dimers. *Sci Signal* **2016**, *9*, ra69, doi:10.1126/scisignal.aaf0793.

30. Cuevas, J.M.; Geller, R.; Garijo, R.; López-Aldeguer, J.; Sanjuán, R. Extremely High Mutation Rate of HIV-1 In Vivo. *PLoS Biol* **2015**, *13*, e1002251, doi:10.1371/journal.pbio.1002251.

31. Dahmane, S.; Rubinstein, E.; Milhiet, P.E. Viruses and tetraspanins: lessons from single molecule approaches. *Viruses* **2014**, *6*, 1992-2011, doi:10.3390/v6051992.

32. Dale, B.M.; Alvarez, R.A.; Chen, B.K. Mechanisms of enhanced HIV spread through T-cell virological synapses. *Immunol Rev* **2013**, *251*, 113-124, doi:10.1111/imr.12022.

33. Dale, B.M.; McNerney, G.P.; Hübner, W.; Huser, T.R.; Chen, B.K. Tracking and quantitation of fluorescent HIV during cell-to-cell transmission. *Methods* **2011**, *53*, 20-26, doi:10.1016/j.ymeth.2010.06.018.

34. Dargent, J.L.; Lespagnard, L.; Kornreich, A.; Hermans, P.; Clumeck, N.; Verhest, A. HIV-associated multinucleated giant cells in lymphoid tissue of the Waldeyer's ring: a detailed study. *Mod Pathol* **2000**, *13*, 1293-1299, doi:10.1038/modpathol.3880237.

35. Debouck, C.; Gorniak, J.G.; Strickler, J.E.; Meek, T.D.; Metcalf, B.W.; Rosenberg, M. Human immunodeficiency virus protease expressed in Escherichia coli exhibits autoprocessing and specific maturation of the gag precursor. *Proc Natl Acad Sci U S A* **1987**, *84*, 8903-8906, doi:10.1073/pnas.84.24.8903.

36. Del Portillo, A.; Tripodi, J.; Najfeld, V.; Wodarz, D.; Levy, D.N.; Chen, B.K. Multiploid inheritance of HIV-1 during cell-to-cell infection. *J Virol* **2011**, *85*, 7169-7176, doi:10.1128/jvi.00231-11.

37. Derdeyn, C.A.; Decker, J.M.; Sfakianos, J.N.; Wu, X.; O'Brien, W.A.; Ratner, L.; Kappes, J.C.; Shaw, G.M.; Hunter, E. Sensitivity of human immunodeficiency virus type 1 to the fusion inhibitor T-20 is modulated by coreceptor specificity defined by the V3 loop of gp120. *J Virol* **2000**, *74*, 8358-8367.

38. Deruaz, M.; Murooka, T.T.; Ji, S.; Gavin, M.A.; Vrbanac, V.D.; Lieberman, J.; Tager, A.M.; Mempel, T.R.; Luster, A.D. Chemoattractant-mediated leukocyte trafficking enables HIV dissemination from the genital mucosa. *JCI Insight* **2017**, *2*, e88533, doi:10.1172/jci.insight.88533.

39. Dharan, A.; Bachmann, N.; Talley, S.; Zwikelmaier, V.; Campbell, E.M. Nuclear pore blockade reveals that HIV-1 completes reverse transcription and uncoating in the nucleus. *Nat Microbiol* **2020**, *5*, 1088-1095, doi:10.1038/s41564-020-0735-8.

40. Dimitrov, D.S.; Willey, R.L.; Sato, H.; Chang, L.J.; Blumenthal, R.; Martin, M.A. Quantitation of human immunodeficiency virus type 1 infection kinetics. *J Virol* **1993**, *67*, 2182-2190, doi:10.1128/jvi.67.4.2182-2190.1993.

41. Do, T.; Murphy, G.; Earl, L.A.; Del Prete, G.Q.; Grandinetti, G.; Li, G.H.; Estes, J.D.; Rao, P.; Trubey, C.M.; Thomas, J., et al. Three-dimensional imaging of HIV-1 virological synapses reveals membrane architectures involved in virus transmission. *J Virol* **2014**, *88*, 10327-10339, doi:10.1128/jvi.00788-14.

42. Dubuisson, J.; Helle, F.; Cocquerel, L. Early steps of the hepatitis C virus life cycle. *Cellular microbiology* **2008**, *10*, 821-827, doi:10.1111/j.1462-5822.2007.01107.x.

43. Durham, N.D.; Chen, B.K. HIV-1 Cell-Free and Cell-to-Cell Infections Are Differentially Regulated by Distinct Determinants in the Env gp41 Cytoplasmic Tail. *J Virol* **2015**, *89*, 9324-9337, doi:10.1128/JVI.00655-15.

44. Durham, N.D.; Chen, B.K. Measuring T Cell-to-T Cell HIV-1 Transfer, Viral Fusion, and Infection Using Flow Cytometry. *Methods Mol Biol* **2016**, *1354*, 21-38, doi:10.1007/978-1-4939-3046-3_2.

45. Dustin, M.L. Cell adhesion molecules and actin cytoskeleton at immune synapses and kinapses. *Curr Opin Cell Biol* **2007**, *19*, 529-533, doi:10.1016/j.ceb.2007.08.003.

46. Dustin, M.L. T-cell activation through immunological synapses and kinapses. *Immunol Rev* **2008**, *221*, 77-89, doi:10.1111/j.1600-065X.2008.00589.x.

47. Egan, M.A.; Carruth, L.M.; Rowell, J.F.; Yu, X.; Siliciano, R.F. Human immunodeficiency virus type 1 envelope protein endocytosis mediated by a highly conserved intrinsic internalization signal in the cytoplasmic domain of gp41 is suppressed in the presence of the Pr55gag precursor protein. *J Virol* **1996**, *70*, 6547-6556.

48. Elliott, J.L.; Kutluay, S.B. Going beyond Integration: The Emerging Role of HIV-1 Integrase in Virion Morphogenesis. *Viruses* **2020**, *12*, doi:10.3390/v12091005.

49. Engelman, A.N.; Singh, P.K. Cellular and molecular mechanisms of HIV-1 integration targeting. *Cellular and molecular life sciences : CMLS* **2018**, *75*, 2491-2507, doi:10.1007/s00018-018-2772-5.

50. Etienne, L.; Nerrienet, E.; LeBreton, M.; Bibila, G.T.; Foupouapouognigni, Y.; Rousset, D.; Nana, A.; Djoko, C.F.; Tamoufe, U.; Aghokeng, A.F., et al. Characterization of a new simian immunodeficiency virus strain in a naturally infected Pan troglodytes troglodytes chimpanzee with AIDS related symptoms. *Retrovirology* **2011**, *8*, 4, doi:10.1186/1742-4690-8-4.

51. Feliciano, D.; Espinosa-Medina, I.; Weigel, A.; Milano, K.M.; Tang, Z.; Lee, T.; Kliman, H.J.; Guller, S.M.; Ott, C.M.; Lippincott-Schwartz, J. Transcriptional reprogramming in fused cells is triggered by plasma-membrane diminution. *bioRxiv* **2019**, 10.1101/832378, 832378, doi:10.1101/832378.

52. Foley, G.E.; Lazarus, H.; Farber, S.; Uzman, B.G.; Boone, B.A.; McCarthy, R.E. CONTINUOUS CULTURE OF HUMAN LYMPHOBLASTS FROM PERIPHERAL BLOOD OF A CHILD WITH ACUTE LEUKEMIA. *Cancer*

**1965**, *18*, 522-529, doi:10.1002/1097-0142(196504)18:4<522::aid-cncr2820180418>3.0.co;2-j.

53. Francis, A.C.; Marin, M.; Prellberg, M.J.; Palermino-Rowland, K.; Melikyan, G.B. HIV-1 Uncoating and Nuclear Import Precede the Completion of Reverse Transcription in Cell Lines and in Primary Macrophages. *Viruses* **2020**, *12*, doi:10.3390/v12111234.

54. Frankel, S.S.; Wenig, B.M.; Burke, A.P.; Mannan, P.; Thompson, L.D.; Abbondanzo, S.L.; Nelson, A.M.; Pope, M.; Steinman, R.M. Replication of HIV-1 in dendritic cell-derived syncytia at the mucosal surface of the adenoid. *Science* **1996**, *272*, 115-117, doi:10.1126/science.272.5258.115.

55. Freed, E.O. HIV-1 assembly, release and maturation. *Nat Rev Microbiol* **2015**, *13*, 484-496, doi:10.1038/nrmicro3490.

56. Freed, E.O.; Martin, M.A. Virion incorporation of envelope glycoproteins with long but not short cytoplasmic tails is blocked by specific, single amino acid substitutions in the human immunodeficiency virus type 1 matrix. *J Virol* **1995**, *69*, 1984-1989.

57. Freed, E.O.; Martin, M.A. Domains of the human immunodeficiency virus type 1 matrix and gp41 cytoplasmic tail required for envelope incorporation into virions. *J Virol* **1996**, *70*, 341-351, doi:10.1128/jvi.70.1.341-351.1996.

58. Friedman, R.S.; Beemiller, P.; Sorensen, C.M.; Jacobelli, J.; Krummel, M.F. Real-time analysis of T cell receptors in naive cells in vitro and in vivo reveals flexibility in synapse and signaling dynamics. *J Exp Med* **2010**, *207*, 2733-2749, doi:10.1084/jem.20091201.

59. Gao, F.; Bailes, E.; Robertson, D.L.; Chen, Y.; Rodenburg, C.M.; Michael, S.F.; Cummins, L.B.; Arthur, L.O.; Peeters, M.; Shaw, G.M., et al. Origin of HIV-1 in the chimpanzee Pan troglodytes troglodytes. *Nature* **1999**, *397*, 436-441, doi:10.1038/17130.

60. Gardiner, J.C.; Mauer, E.J.; Sherer, N.M. HIV-1 Gag, Envelope, and Extracellular Determinants Cooperate To Regulate the Stability and Turnover of Virological Synapses. *J Virol* **2016**, *90*, 6583-6597, doi:10.1128/jvi.00600-16.

61. Gordon-Alonso, M.; Sala-Valdes, M.; Rocha-Perugini, V.; Perez-Hernandez, D.; Lopez-Martin, S.; Ursa, A.; Alvarez, S.; Kolesnikova, T.V.; Vazquez, J.; Sanchez-Madrid, F., et al. EWI-2 association with alpha-actinin regulates T cell immune synapses and HIV viral infection. *J Immunol* **2012**, *189*, 689-700, doi:10.4049/jimmunol.1103708.

62. Gordón-Alonso, M.; Yañez-Mó, M.; Barreiro, O.; Alvarez, S.; Muñoz-Fernández, M.A.; Valenzuela-Fernández, A.; Sánchez-Madrid, F. Tetraspanins CD9 and

CD81 modulate HIV-1-induced membrane fusion. *J Immunol* **2006**, *177*, 5129-5137, doi:10.4049/jimmunol.177.8.5129.

63. Göttlinger, H.G.; Dorfman, T.; Sodroski, J.G.; Haseltine, W.A. Effect of mutations affecting the p6 gag protein on human immunodeficiency virus particle release. *Proc Natl Acad Sci U S A* **1991**, *88*, 3195-3199, doi:10.1073/pnas.88.8.3195.

64. Greenwood, E.J.; Matheson, N.J.; Wals, K.; van den Boomen, D.J.; Antrobus, R.; Williamson, J.C.; Lehner, P.J. Temporal proteomic analysis of HIV infection reveals remodelling of the host phosphoproteome by lentiviral Vif variants. *Elife* **2016**, *5*, doi:10.7554/eLife.18296.

65. Greenwood, E.J.D.; Williamson, J.C.; Sienkiewicz, A.; Naamati, A.; Matheson, N.J.; Lehner, P.J. Promiscuous Targeting of Cellular Proteins by Vpr Drives Systems-Level Proteomic Remodeling in HIV-1 Infection. *Cell Rep* **2019**, *27*, 1579-1596 e1577, doi:10.1016/j.celrep.2019.04.025.

66. Groppelli, E.; Starling, S.; Jolly, C. Contact-induced mitochondrial polarization supports HIV-1 virological synapse formation. *J Virol* **2015**, *89*, 14-24, doi:10.1128/jvi.02425-14.

67. Guy, B.; Kieny, M.P.; Riviere, Y.; Le Peuch, C.; Dott, K.; Girard, M.; Montagnier, L.; Lecocq, J.P. HIV F/3' orf encodes a phosphorylated GTP-binding protein resembling an oncogene product. *Nature* **1987**, *330*, 266-269, doi:10.1038/330266a0.

68. Haller, C.; Müller, B.; Fritz, J.V.; Lamas-Murua, M.; Stolp, B.; Pujol, F.M.; Keppler, O.T.; Fackler, O.T. HIV-1 Nef and Vpu are functionally redundant broad-spectrum modulators of cell surface receptors, including tetraspanins. *J Virol* **2014**, *88*, 14241-14257, doi:10.1128/jvi.02333-14.

69. He, B.; Zhang, Y.H.; Richardson, M.M.; Zhang, J.S.; Rubinstein, E.; Zhang, X.A. Differential functions of phospholipid binding and palmitoylation of tumour suppressor EWI2/PGRL. *Biochem J* **2011**, *437*, 399-411, doi:10.1042/bj20101381.

70. He, J.; Choe, S.; Walker, R.; Di Marzio, P.; Morgan, D.O.; Landau, N.R. Human immunodeficiency virus type 1 viral protein R (Vpr) arrests cells in the G2 phase of the cell cycle by inhibiting p34cdc2 activity. *J Virol* **1995**, *69*, 6705-6711, doi:10.1128/jvi.69.11.6705-6711.1995.

71. Helle, F.; Dubuisson, J. Hepatitis C virus entry into host cells. *Cellular and molecular life sciences : CMLS* **2008**, *65*, 100-112, doi:10.1007/s00018-007-7291-8.

72. Hemler, M.E. Tetraspanin functions and associated microdomains. *Nat Rev Mol Cell Biol* **2005**, *6*, 801-811, doi:10.1038/nrm1736.

73. Hikichi, Y.; Freed, E.O. Maturation of HIV-1. *Science* **2021**, *373*, 621-622, doi:10.1126/science.abj9075.

74. Huang, M.; Orenstein, J.M.; Martin, M.A.; Freed, E.O. p6Gag is required for particle production from full-length human immunodeficiency virus type 1 molecular clones expressing protease. *J Virol* **1995**, *69*, 6810-6818, doi:10.1128/jvi.69.11.6810-6818.1995.

75. Hübner, W.; McNerney, G.P.; Chen, P.; Dale, B.M.; Gordon, R.E.; Chuang, F.Y.; Li, X.D.; Asmuth, D.M.; Huser, T.; Chen, B.K. Quantitative 3D video microscopy of HIV transfer across T cell virological synapses. *Science* **2009**, *323*, 1743-1747, doi:10.1126/science.1167525.

76. Ikeda, T.; Symeonides, M.; Albin, J.S.; Li, M.; Thali, M.; Harris, R.S. HIV-1 adaptation studies reveal a novel Env-mediated homeostasis mechanism for evading lethal hypermutation by APOBEC3G. *PLoS Pathog* **2018**, *14*, e1007010, doi:10.1371/journal.ppat.1007010.

77. Imle, A.; Kumberger, P.; Schnellbächer, N.D.; Fehr, J.; Carrillo-Bustamante, P.; Ales, J.; Schmidt, P.; Ritter, C.; Godinez, W.J.; Müller, B., et al. Experimental and computational analyses reveal that environmental restrictions shape HIV-1 spread in 3D cultures. *Nat Commun* **2019**, *10*, 2144, doi:10.1038/s41467-019-09879-3.

78. Ivanusic, D.; Madela, K.; Bannert, N.; Denner, J. The large extracellular loop of CD63 interacts with gp41 of HIV-1 and is essential for establishing the virological synapse. *Sci Rep* **2021**, *11*, 10011, doi:10.1038/s41598-021-89523-7.

79. Jacks, T.; Power, M.D.; Masiarz, F.R.; Luciw, P.A.; Barr, P.J.; Varmus, H.E. Characterization of ribosomal frameshifting in HIV-1 gag-pol expression. *Nature* **1988**, *331*, 280-283, doi:10.1038/331280a0.

80. Jiang, J.; Aiken, C. Maturation-dependent human immunodeficiency virus type 1 particle fusion requires a carboxyl-terminal region of the gp41 cytoplasmic tail. *J Virol* **2007**, *81*, 9999-10008, doi:10.1128/jvi.00592-07.

81. Jolly, C. T cell polarization at the virological synapse. *Viruses* **2010**, *2*, 1261-1278, doi:10.3390/v2061261.

82. Jolly, C.; Booth, N.J.; Neil, S.J. Cell-cell spread of human immunodeficiency virus type 1 overcomes tetherin/BST-2-mediated restriction in T cells. *J Virol* **2010**, *84*, 12185-12199, doi:10.1128/jvi.01447-10.

83. Jolly, C.; Kashefi, K.; Hollinshead, M.; Sattentau, Q.J. HIV-1 cell to cell transfer across an Env-induced, actin-dependent synapse. *J Exp Med* **2004**, *199*, 283-293, doi:10.1084/jem.20030648.

84. Jolly, C.; Mitar, I.; Sattentau, Q.J. Adhesion molecule interactions facilitate human immunodeficiency virus type 1-induced virological synapse formation between T cells. *J Virol* **2007**, *81*, 13916-13921, doi:10.1128/jvi.01585-07.

85. Jolly, C.; Sattentau, Q.J. Retroviral spread by induction of virological synapses. *Traffic* **2004**, *5*, 643-650, doi:10.1111/j.1600-0854.2004.00209.x.

86. Jolly, C.; Sattentau, Q.J. Human immunodeficiency virus type 1 assembly, budding, and cell-cell spread in T cells take place in tetraspanin-enriched plasma membrane domains. *J Virol* **2007**, *81*, 7873-7884, doi:10.1128/jvi.01845-06.

87. Jolly, C.; Welsch, S.; Michor, S.; Sattentau, Q.J. The regulated secretory pathway in CD4(+) T cells contributes to human immunodeficiency virus type-1 cell-to-cell spread at the virological synapse. *PLoS Pathog* **2011**, *7*, e1002226, doi:10.1371/journal.ppat.1002226.

88. Joseph, S.B.; Swanstrom, R.; Kashuba, A.D.; Cohen, M.S. Bottlenecks in HIV-1 transmission: insights from the study of founder viruses. *Nat Rev Microbiol* **2015**, *13*, 414-425, doi:10.1038/nrmicro3471.

89. Kariuki, S.M.; Selhorst, P.; Ariën, K.K.; Dorfman, J.R. The HIV-1 transmission bottleneck. *Retrovirology* **2017**, *14*, 22, doi:10.1186/s12977-017-0343-8.

90. Karn, J.; Stoltzfus, C.M. Transcriptional and posttranscriptional regulation of HIV-1 gene expression. *Cold Spring Harb Perspect Med* **2012**, *2*, a006916, doi:10.1101/cshperspect.a006916.

91. Keele, B.F.; Jones, J.H.; Terio, K.A.; Estes, J.D.; Rudicell, R.S.; Wilson, M.L.; Li, Y.; Learn, G.H.; Beasley, T.M.; Schumacher-Stankey, J., et al. Increased mortality and AIDS-like immunopathology in wild chimpanzees infected with SIVcpz. *Nature* **2009**, *460*, 515-519, doi:10.1038/nature08200.

92. Keele, B.F.; Van Heuverswyn, F.; Li, Y.; Bailes, E.; Takehisa, J.; Santiago, M.L.; Bibollet-Ruche, F.; Chen, Y.; Wain, L.V.; Liegeois, F., et al. Chimpanzee reservoirs of pandemic and nonpandemic HIV-1. *Science* **2006**, *313*, 523-526, doi:10.1126/science.1126531.

93. Kettner, S.; Kalthoff, F.; Graf, P.; Priller, E.; Kricek, F.; Lindley, I.; Schweighoffer, T. EWI-2/CD316 is an inducible receptor of HSPA8 on human dendritic cells. *Mol Cell Biol* **2007**, *27*, 7718-7726, doi:10.1128/mcb.00180-07.

94. Khan, M.A.; Aberham, C.; Kao, S.; Akari, H.; Gorelick, R.; Bour, S.; Strebel, K. Human immunodeficiency virus type 1 Vif protein is packaged into the

nucleoprotein complex through an interaction with viral genomic RNA. *J Virol* **2001**, *75*, 7252-7265, doi:10.1128/jvi.75.16.7252-7265.2001.

95. Kieffer, C.; Ladinsky, M.S.; Ninh, A.; Galimidi, R.P.; Bjorkman, P.J. Longitudinal imaging of HIV-1 spread in humanized mice with parallel 3D immunofluorescence and electron tomography. *Elife* **2017**, *6*, doi:10.7554/eLife.23282.

96. Kirschman, J.; Qi, M.; Ding, L.; Hammonds, J.; Dienger-Stambaugh, K.; Wang, J.J.; Lapierre, L.A.; Goldenring, J.R.; Spearman, P. HIV-1 Envelope Glycoprotein Trafficking through the Endosomal Recycling Compartment Is Required for Particle Incorporation. *J Virol* **2018**, *92*, doi:10.1128/jvi.01893-17.

97. Kogan, M.; Rappaport, J. HIV-1 accessory protein Vpr: relevance in the pathogenesis of HIV and potential for therapeutic intervention. *Retrovirology* **2011**, *8*, 25, doi:10.1186/1742-4690-8-25.

98. Kolesnikova, T.V.; Kazarov, A.R.; Lemieux, M.E.; Lafleur, M.A.; Kesari, S.; Kung, A.L.; Hemler, M.E. Glioblastoma inhibition by cell surface immunoglobulin protein EWI-2, in vitro and in vivo. *Neoplasia* **2009**, *11*, 77-86, 74p following 86, doi:10.1593/neo.81180.

99. Komarova, N.L.; Anghelina, D.; Voznesensky, I.; Trinité, B.; Levy, D.N.; Wodarz, D. Relative contribution of free-virus and synaptic transmission to the spread of HIV-1 through target cell populations. *Biol Lett* **2013**, *9*, 20121049, doi:10.1098/rsbl.2012.1049.

100. Konvalinka, J.; Kräusslich, H.G.; Müller, B. Retroviral proteases and their roles in virion maturation. *Virology* **2015**, *479-480*, 403-417, doi:10.1016/j.virol.2015.03.021.

101. Kowalski, M.; Potz, J.; Basiripour, L.; Dorfman, T.; Goh, W.C.; Terwilliger, E.; Dayton, A.; Rosen, C.; Haseltine, W.; Sodroski, J. Functional regions of the envelope glycoprotein of human immunodeficiency virus type 1. *Science* **1987**, *237*, 1351-1355, doi:10.1126/science.3629244.

102. Kreger, J.; Garcia, J.; Zhang, H.; Komarova, N.L.; Wodarz, D.; Levy, D.N. Quantifying the dynamics of viral recombination during free virus and cell-to-cell transmission in HIV-1 infection. *Virus Evol* **2021**, *7*, veab026, doi:10.1093/ve/veab026.

103. Kreger, J.; Komarova, N.L.; Wodarz, D. Effect of synaptic cell-to-cell transmission and recombination on the evolution of double mutants in HIV. *J R Soc Interface* **2020**, *17*, 20190832, doi:10.1098/rsif.2019.0832.

104. Krementsov, D.N.; Rassam, P.; Margeat, E.; Roy, N.H.; Schneider-Schaulies, J.; Milhiet, P.E.; Thali, M. HIV-1 assembly differentially alters dynamics and

partitioning of tetraspanins and raft components. *Traffic* **2010**, *11*, 1401-1414, doi:10.1111/j.1600-0854.2010.01111.x.

105. Krementsov, D.N.; Weng, J.; Lambele, M.; Roy, N.H.; Thali, M. Tetraspanins regulate cell-to-cell transmission of HIV-1. *Retrovirology* **2009**, *6*, 64, doi:10.1186/1742-4690-6-64.

106. Ladinsky, M.S.; Kieffer, C.; Olson, G.; Deruaz, M.; Vrbanac, V.; Tager, A.M.; Kwon, D.S.; Bjorkman, P.J. Electron tomography of HIV-1 infection in gut-associated lymphoid tissue. *PLoS Pathog* **2014**, *10*, e1003899, doi:10.1371/journal.ppat.1003899.

107. Lambelé, M.; Koppensteiner, H.; Symeonides, M.; Roy, N.H.; Chan, J.; Schindler, M.; Thali, M. Vpu is the main determinant for tetraspanin downregulation in HIV-1-infected cells. *J Virol* **2015**, *89*, 3247-3255, doi:10.1128/jvi.03719-14.

108. Law, K.M.; Komarova, N.L.; Yewdall, A.W.; Lee, R.K.; Herrera, O.L.; Wodarz, D.; Chen, B.K. In Vivo HIV-1 Cell-to-Cell Transmission Promotes Multicopy Micro-compartmentalized Infection. *Cell Rep* **2016**, *15*, 2771-2783, doi:10.1016/j.celrep.2016.05.059.

109. Law, K.M.; Satija, N.; Esposito, A.M.; Chen, B.K. Cell-to-Cell Spread of HIV and Viral Pathogenesis. *Adv Virus Res* **2016**, *95*, 43-85, doi:10.1016/bs.aivir.2016.03.001.

110. Le Naour, F.; André, M.; Boucheix, C.; Rubinstein, E. Membrane microdomains and proteomics: lessons from tetraspanin microdomains and comparison with lipid rafts. *Proteomics* **2006**, *6*, 6447-6454, doi:10.1002/pmic.200600282.

111. Len, A.C.L.; Starling, S.; Shivkumar, M.; Jolly, C. HIV-1 Activates T Cell Signaling Independently of Antigen to Drive Viral Spread. *Cell Rep* **2017**, *18*, 1062-1074, doi:10.1016/j.celrep.2016.12.057.

112. Lepelley, A.; Louis, S.; Sourisseau, M.; Law, H.K.; Pothlichet, J.; Schilte, C.; Chaperot, L.; Plumas, J.; Randall, R.E.; Si-Tahar, M., et al. Innate sensing of HIV-infected cells. *PLoS Pathog* **2011**, *7*, e1001284, doi:10.1371/journal.ppat.1001284.

113. Levin, J.G.; Mitra, M.; Mascarenhas, A.; Musier-Forsyth, K. Role of HIV-1 nucleocapsid protein in HIV-1 reverse transcription. *RNA Biol* **2010**, *7*, 754-774, doi:10.4161/rna.7.6.14115.

114. Liu, H.; Wu, X.; Newman, M.; Shaw, G.M.; Hahn, B.H.; Kappes, J.C. The Vif protein of human and simian immunodeficiency viruses is packaged into virions and associates with viral core structures. *J Virol* **1995**, *69*, 7630-7638, doi:10.1128/jvi.69.12.7630-7638.1995.

115. Lusic, M.; Siliciano, R.F. Nuclear landscape of HIV-1 infection and integration. *Nat Rev Microbiol* **2017**, *15*, 69-82, doi:10.1038/nrmicro.2016.162.

116. Maddon, P.J.; Dalgleish, A.G.; Mcdougal, J.S.; Clapham, P.R.; Weiss, R.A.; Axel, R. The T4 Gene Encodes the Aids Virus Receptor and Is Expressed in the Immune-System and the Brain. *Cell* **1986**, *47*, 333-348, doi:Doi 10.1016/0092-8674(86)90590-8.

117. Malim, M.H.; Emerman, M. HIV-1 accessory proteins--ensuring viral survival in a hostile environment. *Cell Host Microbe* **2008**, *3*, 388-398, doi:10.1016/j.chom.2008.04.008.

118. Martin, N.; Welsch, S.; Jolly, C.; Briggs, J.A.; Vaux, D.; Sattentau, Q.J. Virological synapse-mediated spread of human immunodeficiency virus type 1 between T cells is sensitive to entry inhibition. *J Virol* **2010**, *84*, 3516-3527, doi:10.1128/jvi.02651-09.

119. Martin-Serrano, J.; Zang, T.; Bieniasz, P.D. HIV-1 and Ebola virus encode small peptide motifs that recruit Tsg101 to sites of particle assembly to facilitate egress. *Nat Med* **2001**, *7*, 1313-1319, doi:10.1038/nm1201-1313.

120. Matheson, N.J.; Peden, A.A.; Lehner, P.J. Antibody-free magnetic cell sorting of genetically modified primary human CD4+ T cells by one-step streptavidin affinity purification. *PloS one* **2014**, *9*, e111437, doi:10.1371/journal.pone.0111437.

121. Matheson, N.J.; Sumner, J.; Wals, K.; Rapiteanu, R.; Weekes, M.P.; Vigan, R.; Weinelt, J.; Schindler, M.; Antrobus, R.; Costa, A.S., et al. Cell Surface Proteomic Map of HIV Infection Reveals Antagonism of Amino Acid Metabolism by Vpu and Nef. *Cell Host Microbe* **2015**, *18*, 409-423, doi:10.1016/j.chom.2015.09.003.

122. Mayya, V.; Judokusumo, E.; Abu Shah, E.; Peel, C.G.; Neiswanger, W.; Depoil, D.; Blair, D.A.; Wiggins, C.H.; Kam, L.C.; Dustin, M.L. Durable Interactions of T Cells with T Cell Receptor Stimuli in the Absence of a Stable Immunological Synapse. *Cell Rep* **2018**, *22*, 340-349, doi:10.1016/j.celrep.2017.12.052.

123. McDonald, D.; Wu, L.; Bohks, S.M.; KewalRamani, V.N.; Unutmaz, D.; Hope, T.J. Recruitment of HIV and its receptors to dendritic cell-T cell junctions. *Science* **2003**, *300*, 1295-1297, doi:10.1126/science.1084238.

124. McMichael, A.J.; Borrow, P.; Tomaras, G.D.; Goonetilleke, N.; Haynes, B.F. The immune response during acute HIV-1 infection: clues for vaccine development. *Nat Rev Immunol* **2010**, *10*, 11-23, doi:10.1038/nri2674.

125. Mesner, D.; Hotter, D.; Kirchhoff, F.; Jolly, C. Loss of Nef-mediated CD3 down-regulation in the HIV-1 lineage increases viral infectivity and spread. *Proc Natl Acad Sci U S A* **2020**, *117*, 7382-7391, doi:10.1073/pnas.1921135117.

126. Montefiori, D.C.; Mitchell, W.M. Persistent coinfection of T lymphocytes with HTLV-II and HIV and the role of syncytium formation in HIV-induced cytopathic effect. *Virology* **1987**, *160*, 372-378, doi:10.1016/0042-6822(87)90008-0.

127. Montpellier, C.; Tews, B.A.; Poitrimole, J.; Rocha-Perugini, V.; D'Arienzo, V.; Potel, J.; Zhang, X.A.; Rubinstein, E.; Dubuisson, J.; Cocquerel, L. Interacting regions of CD81 and two of its partners, EWI-2 and EWI-2wint, and their effect on hepatitis C virus infection. *J Biol Chem* **2011**, *286*, 13954-13965, doi:10.1074/jbc.M111.220103.

128. Mouhand, A.; Pasi, M.; Catala, M.; Zargarian, L.; Belfetmi, A.; Barraud, P.; Mauffret, O.; Tisné, C. Overview of the Nucleic-Acid Binding Properties of the HIV-1 Nucleocapsid Protein in Its Different Maturation States. *Viruses* **2020**, *12*, doi:10.3390/v12101109.

129. Müller, T.G.; Zila, V.; Peters, K.; Schifferdecker, S.; Stanic, M.; Lucic, B.; Laketa, V.; Lusic, M.; Müller, B.; Kräusslich, H.G. HIV-1 uncoating by release of viral cDNA from capsid-like structures in the nucleus of infected cells. *Elife* **2021**, *10*, doi:10.7554/eLife.64776.

130. Munro, J.B.; Mothes, W. Structure and Dynamics of the Native HIV-1 Env Trimer. *J Virol* **2015**, *89*, 5752-5755, doi:10.1128/jvi.03187-14.

131. Murakami, T.; Ablan, S.; Freed, E.O.; Tanaka, Y. Regulation of human immunodeficiency virus type 1 Env-mediated membrane fusion by viral protease activity. *J Virol* **2004**, *78*, 1026-1031, doi:10.1128/jvi.78.2.1026-1031.2004.

132. Murakami, T.; Carmona, N.; Ono, A. Virion-incorporated PSGL-1 and CD43 inhibit both cell-free infection and transinfection of HIV-1 by preventing virus-cell binding. *Proc Natl Acad Sci U S A* **2020**, *117*, 8055-8063, doi:10.1073/pnas.1916055117.

133. Murakami, T.; Freed, E.O. Genetic evidence for an interaction between human immunodeficiency virus type 1 matrix and alpha-helix 2 of the gp41 cytoplasmic tail. *J Virol* **2000**, *74*, 3548-3554, doi:10.1128/jvi.74.8.3548-3554.2000.

134. Murooka, T.T.; Deruaz, M.; Marangoni, F.; Vrbanac, V.D.; Seung, E.; von Andrian, U.H.; Tager, A.M.; Luster, A.D.; Mempel, T.R. HIV-infected T cells are migratory vehicles for viral dissemination. *Nature* **2012**, *490*, 283-287, doi:10.1038/nature11398.

135. Murooka, T.T.; Sharaf, R.R.; Mempel, T.R. Large Syncytia in Lymph Nodes Induced by CCR5-Tropic HIV-1. *AIDS Res Hum Retroviruses* **2015**, *31*, 471-472, doi:10.1089/aid.2014.0378.

136. Naamati, A.; Williamson, J.C.; Greenwood, E.J.; Marelli, S.; Lehner, P.J.; Matheson, N.J. Functional proteomic atlas of HIV infection in primary human CD4+ T cells. *Elife* **2019**, *8*, doi:10.7554/eLife.41431.

137. Naghavi, M.H. HIV-1 capsid exploitation of the host microtubule cytoskeleton during early infection. *Retrovirology* **2021**, *18*, 19, doi:10.1186/s12977-021-00563-3.

138. Nara, P.L.; Fischinger, P.J. Quantitative infectivity assay for HIV-1 and-2. *Nature* **1988**, *332*, 469-470, doi:10.1038/332469a0.

139. Nara, P.L.; Hatch, W.C.; Dunlop, N.M.; Robey, W.G.; Arthur, L.O.; Gonda, M.A.; Fischinger, P.J. Simple, rapid, quantitative, syncytium-forming microassay for the detection of human immunodeficiency virus neutralizing antibody. *AIDS Res Hum Retroviruses* **1987**, *3*, 283-302, doi:10.1089/aid.1987.3.283.

140. Neil, S.J.; Zang, T.; Bieniasz, P.D. Tetherin inhibits retrovirus release and is antagonized by HIV-1 Vpu. *Nature* **2008**, *451*, 425-430, doi:10.1038/nature06553.

141. Okoye, A.A.; Picker, L.J. CD4(+) T-cell depletion in HIV infection: mechanisms of immunological failure. *Immunol Rev* **2013**, *254*, 54-64, doi:10.1111/imr.12066.

142. Orenstein, J.M. In vivo cytolysis and fusion of human immunodeficiency virus type 1-infected lymphocytes in lymphoid tissue. *J Infect Dis* **2000**, *182*, 338-342, doi:10.1086/315640.

143. Orenstein, J.M.; Wahl, S.M. The macrophage origin of the HIV-expressing multinucleated giant cells in hyperplastic tonsils and adenoids. *Ultrastruct Pathol* **1999**, *23*, 79-91, doi:10.1080/019131299281734.

144. Ospina Stella, A.; Turville, S. All-Round Manipulation of the Actin Cytoskeleton by HIV. *Viruses* **2018**, *10*, doi:10.3390/v10020063.

145. Pedro, K.D.; Henderson, A.J.; Agosto, L.M. Mechanisms of HIV-1 cell-to-cell transmission and the establishment of the latent reservoir. *Virus Res* **2019**, *265*, 115-121, doi:10.1016/j.virusres.2019.03.014.

146. Perelson, A.S.; Neumann, A.U.; Markowitz, M.; Leonard, J.M.; Ho, D.D. HIV-1 dynamics in vivo: virion clearance rate, infected cell life-span, and viral generation time. *Science* **1996**, *271*, 1582-1586, doi:10.1126/science.271.5255.1582.

147. Pezeshkian, N.; Groves, N.S.; van Engelenburg, S.B. Single-molecule imaging of HIV-1 envelope glycoprotein dynamics and Gag lattice association exposes determinants responsible for virus incorporation. *Proc Natl Acad Sci U S A* **2019**, *116*, 25269-25277, doi:10.1073/pnas.1910008116.

148. Phillips, D.M. The role of cell-to-cell transmission in HIV infection. *Aids* **1994**, *8*, 719-731, doi:10.1097/00002030-199406000-00001.

149. Platt, E.J.; Bilska, M.; Kozak, S.L.; Kabat, D.; Montefiori, D.C. Evidence that ecotropic murine leukemia virus contamination in TZM-bl cells does not affect the outcome of neutralizing antibody assays with human immunodeficiency virus type 1. *J Virol* **2009**, *83*, 8289-8292, doi:10.1128/JVI.00709-09.

150. Platt, E.J.; Wehrly, K.; Kuhmann, S.E.; Chesebro, B.; Kabat, D. Effects of CCR5 and CD4 cell surface concentrations on infections by macrophagetropic isolates of human immunodeficiency virus type 1. *J Virol* **1998**, *72*, 2855-2864.

151. Pontow, S.E.; Heyden, N.V.; Wei, S.; Ratner, L. Actin cytoskeletal reorganizations and coreceptor-mediated activation of rac during human immunodeficiency virus-induced cell fusion. *J Virol* **2004**, *78*, 7138-7147, doi:10.1128/jvi.78.13.7138-7147.2004.

152. Potel, J.; Rassam, P.; Montpellier, C.; Kaestner, L.; Werkmeister, E.; Tews, B.A.; Couturier, C.; Popescu, C.I.; Baumert, T.F.; Rubinstein, E., et al. EWI-2wint promotes CD81 clustering that abrogates Hepatitis C Virus entry. *Cellular microbiology* **2013**, *15*, 1234-1252, doi:10.1111/cmi.12112.

153. Prins, K.C.; Vasiliver-Shamis, G.; Cammer, M.; Depoil, D.; Dustin, M.L.; Hioe, C.E. Imaging of HIV-1 envelope-induced virological synapse and signaling on synthetic lipid bilayers. *J Vis Exp* **2012**, 10.3791/3757, doi:10.3791/3757.

154. Qin, X.F.; An, D.S.; Chen, I.S.; Baltimore, D. Inhibiting HIV-1 infection in human T cells by lentiviral-mediated delivery of small interfering RNA against CCR5. *Proc Natl Acad Sci U S A* **2003**, *100*, 183-188, doi:10.1073/pnas.232688199.

155. Qu, K.; Ke, Z.; Zila, V.; Anders-Osswein, M.; Glass, B.; Mucksch, F.; Muller, R.; Schultz, C.; Muller, B.; Krausslich, H.G., et al. Maturation of the matrix and viral membrane of HIV-1. *Science* **2021**, *373*, 700-704, doi:10.1126/science.abe6821.

156. Quintana, A.; Schwindling, C.; Wenning, A.S.; Becherer, U.; Rettig, J.; Schwarz, E.C.; Hoth, M. T cell activation requires mitochondrial translocation to the immunological synapse. *Proc Natl Acad Sci U S A* **2007**, *104*, 14418-14423, doi:10.1073/pnas.0703126104.

157. Ramirez, P.W.; Famiglietti, M.; Sowrirajan, B.; DePaula-Silva, A.B.; Rodesch, C.; Barker, E.; Bosque, A.; Planelles, V. Downmodulation of CCR7 by HIV-1

Vpu results in impaired migration and chemotactic signaling within CD4$^+$ T cells. *Cell Rep* **2014**, *7*, 2019-2030, doi:10.1016/j.celrep.2014.05.015.

158. Re, F.; Braaten, D.; Franke, E.K.; Luban, J. Human immunodeficiency virus type 1 Vpr arrests the cell cycle in G2 by inhibiting the activation of p34cdc2-cyclin B. *J Virol* **1995**, *69*, 6859-6864, doi:10.1128/jvi.69.11.6859-6864.1995.

159. Refsland, E.W.; Hultquist, J.F.; Harris, R.S. Endogenous origins of HIV-1 G-to-A hypermutation and restriction in the nonpermissive T cell line CEM2n. *PLoS Pathog* **2012**, *8*, e1002800, doi:10.1371/journal.ppat.1002800.

160. Reh, L.; Magnus, C.; Schanz, M.; Weber, J.; Uhr, T.; Rusert, P.; Trkola, A. Capacity of Broadly Neutralizing Antibodies to Inhibit HIV-1 Cell-Cell Transmission Is Strain- and Epitope-Dependent. *PLoS Pathog* **2015**, *11*, e1004966, doi:10.1371/journal.ppat.1004966.

161. Rinfret, A.; Latendresse, H.; Lefebvre, R.; St-Louis, G.; Jolicoeur, P.; Lamarre, L. Human immunodeficiency virus-infected multinucleated histiocytes in oropharyngeal lymphoid tissues from two asymptomatic patients. *Am J Pathol* **1991**, *138*, 421-426.

162. Rocha-Perugini, V.; Montpellier, C.; Delgrange, D.; Wychowski, C.; Helle, F.; Pillez, A.; Drobecq, H.; Le Naour, F.; Charrin, S.; Levy, S., et al. The CD81 partner EWI-2wint inhibits hepatitis C virus entry. *PloS one* **2008**, *3*, e1866, doi:10.1371/journal.pone.0001866.

163. Rodriguez-Plata, M.T.; Puigdomènech, I.; Izquierdo-Useros, N.; Puertas, M.C.; Carrillo, J.; Erkizia, I.; Clotet, B.; Blanco, J.; Martinez-Picado, J. The infectious synapse formed between mature dendritic cells and CD4(+) T cells is independent of the presence of the HIV-1 envelope glycoprotein. *Retrovirology* **2013**, *10*, 42, doi:10.1186/1742-4690-10-42.

164. Rose, K.M. When in Need of an ESCRT: The Nature of Virus Assembly Sites Suggests Mechanistic Parallels between Nuclear Virus Egress and Retroviral Budding. *Viruses* **2021**, *13*, doi:10.3390/v13061138.

165. Rowell, J.F.; Stanhope, P.E.; Siliciano, R.F. Endocytosis of endogenously synthesized HIV-1 envelope protein. Mechanism and role in processing for association with class II MHC. *J Immunol* **1995**, *155*, 473-488.

166. Roy, N.H.; Chan, J.; Lambelé, M.; Thali, M. Clustering and mobility of HIV-1 Env at viral assembly sites predict its propensity to induce cell-cell fusion. *J Virol* **2013**, *87*, 7516-7525, doi:10.1128/jvi.00790-13.

167. Roy, N.H.; Lambelé, M.; Chan, J.; Symeonides, M.; Thali, M. Ezrin is a component of the HIV-1 virological presynapse and contributes to the inhibition of cell-cell fusion. *J Virol* **2014**, *88*, 7645-7658, doi:10.1128/jvi.00550-14.

168. Rudnicka, D.; Feldmann, J.; Porrot, F.; Wietgrefe, S.; Guadagnini, S.; Prévost, M.C.; Estaquier, J.; Haase, A.T.; Sol-Foulon, N.; Schwartz, O. Simultaneous cell-to-cell transmission of human immunodeficiency virus to multiple targets through polysynapses. *J Virol* **2009**, *83*, 6234-6246, doi:10.1128/jvi.00282-09.

169. Sala-Valdés, M.; Ursa, A.; Charrin, S.; Rubinstein, E.; Hemler, M.E.; Sánchez-Madrid, F.; Yáñez-Mó, M. EWI-2 and EWI-F link the tetraspanin web to the actin cytoskeleton through their direct association with ezrin-radixin-moesin proteins. *J Biol Chem* **2006**, *281*, 19665-19675, doi:10.1074/jbc.M602116200.

170. Samreen, B.; Khaliq, S.; Ashfaq, U.A.; Khan, M.; Afzal, N.; Shahzad, M.A.; Riaz, S.; Jahan, S. Hepatitis C virus entry: role of host and viral factors. *Infection, genetics and evolution : journal of molecular epidemiology and evolutionary genetics in infectious diseases* **2012**, *12*, 1699-1709, doi:10.1016/j.meegid.2012.07.010.

171. Sato, K.; Aoki, J.; Misawa, N.; Daikoku, E.; Sano, K.; Tanaka, Y.; Koyanagi, Y. Modulation of human immunodeficiency virus type 1 infectivity through incorporation of tetraspanin proteins. *J Virol* **2008**, *82*, 1021-1033, doi:10.1128/jvi.01044-07.

172. Schindelin, J.; Arganda-Carreras, I.; Frise, E.; Kaynig, V.; Longair, M.; Pietzsch, T.; Preibisch, S.; Rueden, C.; Saalfeld, S.; Schmid, B., et al. Fiji: an open-source platform for biological-image analysis. *Nat Methods* **2012**, *9*, 676-682, doi:10.1038/nmeth.2019.

173. Schindler, M.; Münch, J.; Kutsch, O.; Li, H.; Santiago, M.L.; Bibollet-Ruche, F.; Müller-Trutwin, M.C.; Novembre, F.J.; Peeters, M.; Courgnaud, V., et al. Nef-mediated suppression of T cell activation was lost in a lentiviral lineage that gave rise to HIV-1. *Cell* **2006**, *125*, 1055-1067, doi:10.1016/j.cell.2006.04.033.

174. Schröder, A.R.; Shinn, P.; Chen, H.; Berry, C.; Ecker, J.R.; Bushman, F. HIV-1 integration in the human genome favors active genes and local hotspots. *Cell* **2002**, *110*, 521-529, doi:10.1016/s0092-8674(02)00864-4.

175. Schuster, C.; Baumert, T.F. EWI-2wint--a host cell factor inhibiting hepatitis C virus entry. *Journal of hepatology* **2009**, *50*, 222-224, doi:10.1016/j.jhep.2008.10.009.

176. Shah, A.H.; Sowrirajan, B.; Davis, Z.B.; Ward, J.P.; Campbell, E.M.; Planelles, V.; Barker, E. Degranulation of natural killer cells following interaction with HIV-1-infected cells is hindered by downmodulation of NTB-A by Vpu. *Cell Host Microbe* **2010**, *8*, 397-409, doi:10.1016/j.chom.2010.10.008.

177. Sharp, P.M.; Hahn, B.H. The evolution of HIV-1 and the origin of AIDS. *Philos Trans R Soc Lond B Biol Sci* **2010**, *365*, 2487-2494, doi:10.1098/rstb.2010.0031.

178. Shaw, G.M.; Hunter, E. HIV transmission. *Cold Spring Harb Perspect Med* **2012**, *2*, doi:10.1101/cshperspect.a006965.

179. Silvestri, G. Immunity in natural SIV infections. *J Intern Med* **2009**, *265*, 97-109, doi:10.1111/j.1365-2796.2008.02049.x.

180. Simm, M.; Shahabuddin, M.; Chao, W.; Allan, J.S.; Volsky, D.J. Aberrant Gag protein composition of a human immunodeficiency virus type 1 vif mutant produced in primary lymphocytes. *J Virol* **1995**, *69*, 4582-4586.

181. Sodora, D.L.; Silvestri, G. Immune activation and AIDS pathogenesis. *Aids* **2008**, *22*, 439-446, doi:10.1097/QAD.0b013e3282f2dbe7.

182. Sol-Foulon, N.; Sourisseau, M.; Porrot, F.; Thoulouze, M.I.; Trouillet, C.; Nobile, C.; Blanchet, F.; di Bartolo, V.; Noraz, N.; Taylor, N., et al. ZAP-70 kinase regulates HIV cell-to-cell spread and virological synapse formation. *Embo j* **2007**, *26*, 516-526, doi:10.1038/sj.emboj.7601509.

183. Sourisseau, M.; Sol-Foulon, N.; Porrot, F.; Blanchet, F.; Schwartz, O. Inefficient human immunodeficiency virus replication in mobile lymphocytes. *J Virol* **2007**, *81*, 1000-1012, doi:10.1128/jvi.01629-06.

184. Spenlehauer, C.; Gordon, C.A.; Trkola, A.; Moore, J.P. A luciferase-reporter gene-expressing T-cell line facilitates neutralization and drug-sensitivity assays that use either R5 or X4 strains of human immunodeficiency virus type 1. *Virology* **2001**, *280*, 292-300, doi:10.1006/viro.2000.0780.

185. Starling, S.; Jolly, C. LFA-1 Engagement Triggers T Cell Polarization at the HIV-1 Virological Synapse. *J Virol* **2016**, *90*, 9841-9854, doi:10.1128/jvi.01152-16.

186. Stipp, C.S.; Kolesnikova, T.V.; Hemler, M.E. EWI-2 is a major CD9 and CD81 partner and member of a novel Ig protein subfamily. *J Biol Chem* **2001**, *276*, 40545-40554, doi:10.1074/jbc.M107338200.

187. Stipp, C.S.; Orlicky, D.; Hemler, M.E. FPRP, a major, highly stoichiometric, highly specific CD81- and CD9-associated protein. *J Biol Chem* **2001**, *276*, 4853-4862, doi:10.1074/jbc.M009859200.

188. Stolp, B.; Imle, A.; Coelho, F.M.; Hons, M.; Gorina, R.; Lyck, R.; Stein, J.V.; Fackler, O.T. HIV-1 Nef interferes with T-lymphocyte circulation through confined environments in vivo. *Proc Natl Acad Sci U S A* **2012**, *109*, 18541-18546, doi:10.1073/pnas.1204322109.

189. Strack, B.; Calistri, A.; Craig, S.; Popova, E.; Göttlinger, H.G. AIP1/ALIX is a binding partner for HIV-1 p6 and EIAV p9 functioning in virus budding. *Cell* **2003**, *114*, 689-699, doi:10.1016/s0092-8674(03)00653-6.

190. Sugden, S.M.; Bego, M.G.; Pham, T.N.; Cohen, E.A. Remodeling of the Host Cell Plasma Membrane by HIV-1 Nef and Vpu: A Strategy to Ensure Viral Fitness and Persistence. *Viruses* **2016**, *8*, 67, doi:10.3390/v8030067.

191. Swanstrom, R.; Coffin, J. HIV-1 pathogenesis: the virus. *Cold Spring Harb Perspect Med* **2012**, *2*, a007443, doi:10.1101/cshperspect.a007443.

192. Sylwester, A.; Daniels, K.; Soll, D.R. The invasive and destructive behavior of HIV-induced T cell syncytia on collagen and endothelium. *J Leukoc Biol* **1998**, *63*, 233-244, doi:10.1002/jlb.63.2.233.

193. Sylwester, A.; Murphy, S.; Shutt, D.; Soll, D.R. HIV-induced T cell syncytia are self-perpetuating and the primary cause of T cell death in culture. *J Immunol* **1997**, *158*, 3996-4007.

194. Symeonides, M.; Lambele, M.; Roy, N.H.; Thali, M. Evidence showing that tetraspanins inhibit HIV-1-induced cell-cell fusion at a post-hemifusion stage. *Viruses* **2014**, *6*, 1078-1090, doi:10.3390/v6031078.

195. Symeonides, M.; Murooka, T.T.; Bellfy, L.N.; Roy, N.H.; Mempel, T.R.; Thali, M. HIV-1-Induced Small T Cell Syncytia Can Transfer Virus Particles to Target Cells through Transient Contacts. *Viruses* **2015**, *7*, 6590-6603, doi:10.3390/v7122959.

196. Takeuchi, Y.; McClure, M.O.; Pizzato, M. Identification of gammaretroviruses constitutively released from cell lines used for human immunodeficiency virus research. *J Virol* **2008**, *82*, 12585-12588, doi:10.1128/jvi.01726-08.

197. Tedbury, P.R.; Freed, E.O. The cytoplasmic tail of retroviral envelope glycoproteins. *Prog Mol Biol Transl Sci* **2015**, *129*, 253-284, doi:10.1016/bs.pmbts.2014.10.009.

198. Toccafondi, E.; Lener, D.; Negroni, M. HIV-1 Capsid Core: A Bullet to the Heart of the Target Cell. *Front Microbiol* **2021**, *12*, 652486, doi:10.3389/fmicb.2021.652486.

199. Trebak, M.; Kinet, J.P. Calcium signalling in T cells. *Nat Rev Immunol* **2019**, *19*, 154-169, doi:10.1038/s41577-018-0110-7.

200. Trkola, A.; Matthews, J.; Gordon, C.; Ketas, T.; Moore, J.P. A cell line-based neutralization assay for primary human immunodeficiency virus type 1 isolates that use either the CCR5 or the CXCR4 coreceptor. *J Virol* **1999**, *73*, 8966-8974.

201. Uchil, P.D.; Haugh, K.A.; Pi, R.; Mothes, W. In Vivo Imaging-Driven Approaches to Study Virus Dissemination and Pathogenesis. *Annu Rev Virol* **2019**, *6*, 501-524, doi:10.1146/annurev-virology-101416-041429.

202. Umeda, R.; Satouh, Y.; Takemoto, M.; Nakada-Nakura, Y.; Liu, K.; Yokoyama, T.; Shirouzu, M.; Iwata, S.; Nomura, N.; Sato, K., et al. Structural insights into tetraspanin CD9 function. *Nat Commun* **2020**, *11*, 1606, doi:10.1038/s41467-020-15459-7.

203. Usardi, A.; Iyer, K.; Sigoillot, S.M.; Dusonchet, A.; Selimi, F. The immunoglobulin-like superfamily member IGSF3 is a developmentally regulated protein that controls neuronal morphogenesis. *Dev Neurobiol* **2017**, *77*, 75-92, doi:10.1002/dneu.22412.

204. Usmani, S.M.; Murooka, T.T.; Deruaz, M.; Koh, W.H.; Sharaf, R.R.; Di Pilato, M.; Power, K.A.; Lopez, P.; Hnatiuk, R.; Vrbanac, V.D., et al. HIV-1 Balances the Fitness Costs and Benefits of Disrupting the Host Cell Actin Cytoskeleton Early after Mucosal Transmission. *Cell Host Microbe* **2019**, *25*, 73-86.e75, doi:10.1016/j.chom.2018.12.008.

205. Van Damme, N.; Goff, D.; Katsura, C.; Jorgenson, R.L.; Mitchell, R.; Johnson, M.C.; Stephens, E.B.; Guatelli, J. The interferon-induced protein BST-2 restricts HIV-1 release and is downregulated from the cell surface by the viral Vpu protein. *Cell Host Microbe* **2008**, *3*, 245-252, doi:10.1016/j.chom.2008.03.001.

206. Van Duyne, R.; Kuo, L.S.; Pham, P.; Fujii, K.; Freed, E.O. Mutations in the HIV-1 envelope glycoprotein can broadly rescue blocks at multiple steps in the virus replication cycle. *Proc Natl Acad Sci U S A* **2019**, *116*, 9040-9049, doi:10.1073/pnas.1820333116.

207. Vanhamel, J.; Bruggemans, A.; Debyser, Z. Establishment of latent HIV-1 reservoirs: what do we really know? *J Virus Erad* **2019**, *5*, 3-9.

208. Vasiliver-Shamis, G.; Cho, M.W.; Hioe, C.E.; Dustin, M.L. Human immunodeficiency virus type 1 envelope gp120-induced partial T-cell receptor signaling creates an F-actin-depleted zone in the virological synapse. *J Virol* **2009**, *83*, 11341-11355, doi:10.1128/jvi.01440-09.

209. Ventura, J.D.; Beloor, J.; Allen, E.; Zhang, T.; Haugh, K.A.; Uchil, P.D.; Ochsenbauer, C.; Kieffer, C.; Kumar, P.; Hope, T.J., et al. Longitudinal bioluminescent imaging of HIV-1 infection during antiretroviral therapy and treatment interruption in humanized mice. *PLoS Pathog* **2019**, *15*, e1008161, doi:10.1371/journal.ppat.1008161.

210. VerPlank, L.; Bouamr, F.; LaGrassa, T.J.; Agresta, B.; Kikonyogo, A.; Leis, J.; Carter, C.A. Tsg101, a homologue of ubiquitin-conjugating (E2) enzymes, binds the L domain in HIV type 1 Pr55(Gag). *Proc Natl Acad Sci U S A* **2001**, *98*, 7724-7729, doi:10.1073/pnas.131059198.

211. Vidya Vijayan, K.K.; Karthigeyan, K.P.; Tripathi, S.P.; Hanna, L.E. Pathophysiology of CD4+ T-Cell Depletion in HIV-1 and HIV-2 Infections. *Front Immunol* **2017**, *8*, 580, doi:10.3389/fimmu.2017.00580.

212. Votteler, J.; Sundquist, W.I. Virus budding and the ESCRT pathway. *Cell Host Microbe* **2013**, *14*, 232-241, doi:10.1016/j.chom.2013.08.012.

213. Wang, H.X.; Hemler, M.E. Novel impact of EWI-2, CD9, and CD81 on TGF-beta signaling in melanoma. *Molecular & cellular oncology* **2015**, *2*, doi:10.1080/23723556.2015.1030536.

214. Wang, H.X.; Hemler, M.E. Novel impact of EWI-2, CD9, and CD81 on TGF-β signaling in melanoma. *Molecular & cellular oncology* **2015**, *2*, doi:10.1080/23723556.2015.1030536.

215. Wang, H.X.; Li, Q.; Sharma, C.; Knoblich, K.; Hemler, M.E. Tetraspanin protein contributions to cancer. *Biochemical Society transactions* **2011**, *39*, 547-552, doi:10.1042/bst0390547.

216. Wang, H.X.; Sharma, C.; Knoblich, K.; Granter, S.R.; Hemler, M.E. EWI-2 negatively regulates TGF-β signaling leading to altered melanoma growth and metastasis. *Cell research* **2015**, *25*, 370-385, doi:10.1038/cr.2015.17.

217. Wang, L.; Eng, E.T.; Law, K.; Gordon, R.E.; Rice, W.J.; Chen, B.K. Visualization of HIV T Cell Virological Synapses and Virus-Containing Compartments by Three-Dimensional Correlative Light and Electron Microscopy. *J Virol* **2017**, *91*, doi:10.1128/jvi.01605-16.

218. Wang, L.; Izadmehr, S.; Kamau, E.; Kong, X.P.; Chen, B.K. Sequential trafficking of Env and Gag to HIV-1 T cell virological synapses revealed by live imaging. *Retrovirology* **2019**, *16*, 2, doi:10.1186/s12977-019-0464-3.

219. Wei, X.; Decker, J.M.; Liu, H.; Zhang, Z.; Arani, R.B.; Kilby, J.M.; Saag, M.S.; Wu, X.; Shaw, G.M.; Kappes, J.C. Emergence of resistant human immunodeficiency virus type 1 in patients receiving fusion inhibitor (T-20) monotherapy. *Antimicrobial agents and chemotherapy* **2002**, *46*, 1896-1905.

220. Weichseldorfer, M.; Heredia, A.; Reitz, M.; Bryant, J.L.; Latinovic, O.S. Use of Humanized Mouse Models for Studying HIV-1 Infection, Pathogenesis and Persistence. *J AIDS HIV Treat* **2020**, *2*, 23-29.

221. Wen, Y.; Feigenson, G.W.; Vogt, V.M.; Dick, R.A. Mechanisms of PI(4,5)P2 Enrichment in HIV-1 Viral Membranes. *J Mol Biol* **2020**, *432*, 5343-5364, doi:10.1016/j.jmb.2020.07.018.

222. Weng, J.; Krementsov, D.N.; Khurana, S.; Roy, N.H.; Thali, M. Formation of syncytia is repressed by tetraspanins in human immunodeficiency virus type 1-producing cells. *J Virol* **2009**, *83*, 7467-7474, doi:10.1128/jvi.00163-09.

223. Whitaker, E.E.; Matheson, N.J.; Perlee, S.; Munson, P.B.; Symeonides, M.; Thali, M. EWI-2 Inhibits Cell-Cell Fusion at the HIV-1 Virological Presynapse. *Viruses* **2019**, *11*, doi:10.3390/v11121082.

224. Wildum, S.; Schindler, M.; Münch, J.; Kirchhoff, F. Contribution of Vpu, Env, and Nef to CD4 down-modulation and resistance of human immunodeficiency virus type 1-infected T cells to superinfection. *J Virol* **2006**, *80*, 8047-8059, doi:10.1128/jvi.00252-06.

225. Wiley, C.A.; Schrier, R.D.; Nelson, J.A.; Lampert, P.W.; Oldstone, M.B. Cellular localization of human immunodeficiency virus infection within the brains of acquired immune deficiency syndrome patients. *Proc Natl Acad Sci U S A* **1986**, *83*, 7089-7093, doi:10.1073/pnas.83.18.7089.

226. Willey, R.L.; Maldarelli, F.; Martin, M.A.; Strebel, K. Human immunodeficiency virus type 1 Vpu protein induces rapid degradation of CD4. *J Virol* **1992**, *66*, 7193-7200, doi:10.1128/jvi.66.12.7193-7200.1992.

227. Wu, Y. HIV-1 gene expression: lessons from provirus and non-integrated DNA. *Retrovirology* **2004**, *1*, 13, doi:10.1186/1742-4690-1-13.

228. Wurth, M.A.; Schowalter, R.M.; Smith, E.C.; Moncman, C.L.; Dutch, R.E.; McCann, R.O. The actin cytoskeleton inhibits pore expansion during PIV5 fusion protein-promoted cell-cell fusion. *Virology* **2010**, *404*, 117-126, doi:10.1016/j.virol.2010.04.024.

229. Wyma, D.J.; Jiang, J.; Shi, J.; Zhou, J.; Lineberger, J.E.; Miller, M.D.; Aiken, C. Coupling of human immunodeficiency virus type 1 fusion to virion maturation: a novel role of the gp41 cytoplasmic tail. *J Virol* **2004**, *78*, 3429-3435, doi:10.1128/jvi.78.7.3429-3435.2004.

230. Wyma, D.J.; Kotov, A.; Aiken, C. Evidence for a stable interaction of gp41 with Pr55(Gag) in immature human immunodeficiency virus type 1 particles. *J Virol* **2000**, *74*, 9381-9387, doi:10.1128/jvi.74.20.9381-9387.2000.

231. Xiao, T.; Cai, Y.; Chen, B. HIV-1 Entry and Membrane Fusion Inhibitors. *Viruses* **2021**, *13*, doi:10.3390/v13050735.

232. Yáñez-Mó, M.; Barreiro, O.; Gordon-Alonso, M.; Sala-Valdés, M.; Sánchez-Madrid, F. Tetraspanin-enriched microdomains: a functional unit in cell plasma membranes. *Trends Cell Biol* **2009**, *19*, 434-446, doi:10.1016/j.tcb.2009.06.004.

233. Yang, X.H.; Kovalenko, O.V.; Kolesnikova, T.V.; Andzelm, M.M.; Rubinstein, E.; Strominger, J.L.; Hemler, M.E. Contrasting effects of EWI proteins, integrins, and protein palmitoylation on cell surface CD9 organization. *J Biol Chem* **2006**, *281*, 12976-12985, doi:10.1074/jbc.M510617200.

234. Yeo, J.Y.; Goh, G.R.; Su, C.T.; Gan, S.K. The Determination of HIV-1 RT Mutation Rate, Its Possible Allosteric Effects, and Its Implications on Drug Resistance. *Viruses* **2020**, *12*, doi:10.3390/v12030297.

235. Zhang, C.; Zhou, S.; Groppelli, E.; Pellegrino, P.; Williams, I.; Borrow, P.; Chain, B.M.; Jolly, C. Hybrid spreading mechanisms and T cell activation shape the dynamics of HIV-1 infection. *PLoS Comput Biol* **2015**, *11*, e1004179, doi:10.1371/journal.pcbi.1004179.

236. Zhong, P.; Agosto, L.M.; Ilinskaya, A.; Dorjbal, B.; Truong, R.; Derse, D.; Uchil, P.D.; Heidecker, G.; Mothes, W. Cell-to-cell transmission can overcome multiple donor and target cell barriers imposed on cell-free HIV. *PloS one* **2013**, *8*, e53138, doi:10.1371/journal.pone.0053138.

237. Zhong, P.; Agosto, L.M.; Munro, J.B.; Mothes, W. Cell-to-cell transmission of viruses. *Curr Opin Virol* **2013**, *3*, 44-50, doi:10.1016/j.coviro.2012.11.004.

238. Zila, V.; Margiotta, E.; Turoňová, B.; Müller, T.G.; Zimmerli, C.E.; Mattei, S.; Allegretti, M.; Börner, K.; Rada, J.; Müller, B., et al. Cone-shaped HIV-1 capsids are transported through intact nuclear pores. *Cell* **2021**, *184*, 1032-1046.e1018, doi:10.1016/j.cell.2021.01.025.